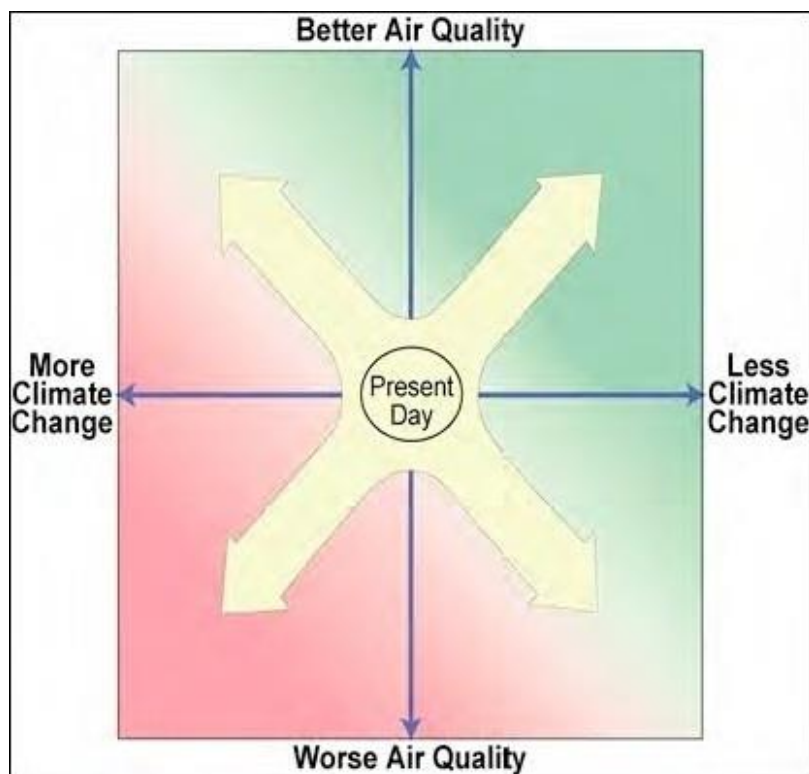


1 **Synthesis of Policy Relevant Findings**
2 **from the CalNex 2010 Field Study**
3

4 **(California Research at the Nexus of**
5 **Air Quality and Climate Change)**
6
7



8
9
10 **Final Report to the**
11 **Research Division of the California Air Resources Board**
12

13 Prepared by **David D. Parrish**
14 Tropospheric Chemistry Group
15 NOAA/ESRL/Chemical Sciences Division
16 325 Broadway R/CSD7
17 Boulder, CO 80305-3337
18

19
20
21 ARB Agreement No. 10-326
22

23 **13 November 2013**

24

Table of Contents

25	Executive Summary	3
26	Introduction	12
27	CalNex 2010 Science Questions	15
28	Glossary of Symbols and Acronyms	19
29	Summary of Platforms and Sites deployed for CalNex	23
30	Synthesis of Results - Meteorology and Atmospheric Climatology	24
31	Question A	24
32	Question B	28
33	Question C	31
34	Question D	34
35	Synthesis of Results - Emissions	41
36	Question E	41
37	Question F	44
38	Question G	53
39	Question H	58
40	Question I	60
41	Question J	63
42	Question K	67
43	Question L	69
44	Synthesis of Results - Climate Processes/Transformations	74
45	Question M	74
46	Question N	79
47	Question O	86
48	Question P	90
49	Question Q	95
50	Synthesis of Results - Atmospheric Transport	99
51	Question R	99
52	Question S	105
53	Question T	110
54	Synthesis of Results - Modeling	115
55	Question U	115
56	Synthesis of Results - Climate and Air Quality Nexus	119
57	Question V	119
58	Question W	122
59	Acknowledgments	125
60	Appendix A - Sites, Platforms and Instruments deployed during	
61	the CalNex 2010 Field Study	129

62

63

64

Executive Summary

65 This Synthesis is intended to address 23 policy-relevant Science Questions formulated by the
66 California Air Resources Board (CARB) in consultation with the National Oceanic and
67 Atmospheric Administration (NOAA). Answers to these questions are needed by CARB and
68 other stakeholders in California to help fulfill the Board's responsibility to formulate
69 scientifically sound policies to simultaneously address concerns regarding air quality degradation
70 and increasing climate change.

71 This Preliminary Report provides statements of Findings in response to each of CARB's policy-
72 relevant Science Questions. These Questions and Findings address six general areas:

- 73 1) Meteorology during the CalNex field study period and atmospheric climatology,
- 74 2) An assessment of emission inventories of air pollutants and climate forcing agents,
75 including greenhouse gases,
- 76 3) An assessment of climate processes and atmospheric transformations,
- 77 4) An overview of important atmospheric transport processes,
- 78 5) An assessment of the skill of current air quality modeling and forecasting systems and
79 recommendations for improvement of these systems, and
- 80 6) A discussion of the areas where it is particularly important to simultaneously consider the
81 air quality and climate impacts of policy decisions.

82 The Executive Summary collects the scientific Findings from the CalNex research for use by
83 CARB managers and other air-quality decision makers and stakeholders in California. It
84 comprises a list of the 23 policy-relevant Science Questions and a series of Findings that have
85 been developed in response to each of these questions. We emphasize that these Findings are
86 based on analysis and interpretation of results that have so far emerged; additional analyses are
87 continuing, and will yield additional important information in the future. Furthermore, the
88 Responses to many of the Questions are incomplete in this Preliminary Report. During the
89 coming months more complete Responses will be developed.

90 Each section of this report is structured as a Response to address one of the Science Questions,
91 including a numbered sequence of succinctly stated Findings in response to that question. Where
92 useful, the policy relevance on the Science Question is briefly summarized in a text box.
93 Important references are given for publications upon which the Finding is based, and following
94 some Findings is an acknowledgment of the individual(s) whose analyses and data contributed to
95 that Finding, particularly if the analysis has not yet been published. A brief discussion of
96 background and the evidence that supports each Finding is given.

97 A brief summary of platforms and sites deployed for CalNex is included in the body of the
98 report, and Appendix A gives extensive details.

99 The institutional affiliations of the scientists responsible for the field measurements and the
100 analyses leading to these Findings are given in the Acknowledgments section, which follows the
101 discussion of the Science Questions and Findings.

102

103 **Findings**

104 **QUESTION A**

105 **How did the meteorology during CalNex compare to historical norms?**

106 *Finding A1:* May 2010 was cooler and wetter than normal, followed by more seasonal warm
107 temperatures in June. In May deep upper level troughs moved into California bringing
108 stratospheric intrusions that affected ozone concentrations in the state.

109 **QUESTION B**

110 **How did the CalNex air quality measurements fit in the context of historical** 111 **measurements?**

112 *Finding B1:* While nearly all atmospheric pollutants have decreased in California, ethanol is an
113 exception because its use in gasoline has recently increased markedly. During CalNex ethanol
114 was the VOC with the highest ambient concentrations in SoCAB. Acetaldehyde (an air toxic) is
115 a secondary product of the atmospheric oxidation of ethanol, but its concentration has continued
116 to decrease.

117 **QUESTION C**

118 **How do the CalNex air quality measurements in late spring and early summer relate to the** 119 **peak ozone concentrations in summer and the peak PM_{2.5} concentrations in winter?**

120 *Finding C1:* The CalNex fieldwork was conducted primarily in May and June, 2010, but
121 included some aircraft flights through mid-July. The measurements provide characterization of
122 the photochemical environment in southern California, particularly in the SoCAB during its most
123 active period.

124 *Finding C2:* The CalNex measurements cannot be used to characterize the peak PM_{2.5}
125 concentrations observed in the Central Valley in winter. However, they do provide a guide for
126 further studies of this important phenomenon.

127 **QUESTION D**

128 **What were the global “background” concentrations observed during CalNex and how did** 129 **they vary spatially and temporally?**

130 *Finding D1:* Baseline concentrations of air quality relevant species have such large variability
131 on time scales of days that average vertical profiles of baseline concentrations provide only poor
132 quantification of boundary conditions for regional air quality modeling.

133 *Finding D2:* Along the west U.S. coast there is little indication of significant latitudinal gradient
134 in average baseline concentrations.

135 *Finding D3:* Global chemical climate models (GCMs) capture a significant fraction of the
136 variability of the baseline concentrations, and hence can provide improved boundary conditions
137 for regional air quality modeling.

138 **QUESTION E**

139 **How effective have historical air pollution control efforts been? How effective have specific**
 140 **emission control measures been?**

141 **Finding E1:** The five decades of air pollution controls implemented in the SoCAB have
 142 produced remarkable improvement in air quality, with substantial reductions in both primary and
 143 secondary air pollutants.

144 **Finding E2:** Compliance of marine vessels with the California fuel quality regulation and
 145 participation in the vessel speed reduction program yields the expected reduction in emissions of
 146 SO₂, and also provides substantial reductions in emissions of carbon dioxide and primary PM.

147 **QUESTION F**

148 **Are current emission inventory estimates for air pollutants and climate-forcing agents**
 149 **accurate? Are there under- or over-estimated emissions or even missing emission sources**
 150 **in the current emission inventories?**

151 **Finding F1:** CO₂ emissions for the SoCAB estimated by an observation-based mesoscale
 152 inverse modeling technique agree with emission estimates by CARB. Both of these estimates
 153 are higher by 15 to 38% than that in the Vulcan inventory of North American CO₂ emissions.

154 **Finding F2a:** Total methane emissions for the SoCAB have been consistently underestimated by
 155 inventories. CalNex analyses implicate larger-than-expected CH₄ emissions from the oil and gas
 156 sector in Los Angeles as the emissions missing from current inventories.

157 **Finding F2b:** Methane emissions from landfills and dairies in the SoCAB are accurately
 158 estimated in the inventories developed by CARB.

159 **Finding F2c:** Annual average methane emissions from rice agriculture are factors of 2 to 3
 160 greater than in the CARB inventory.

161 **Finding F3:** Analyses of CalNex nitrous oxide measurements suggest that inventory
 162 improvements are needed to correct a potential low bias and improve the spatial and seasonal
 163 patterns of emissions.

164 **Finding F4:** Top-down assessments of anthropogenic halocarbon emissions are generally
 165 consistent with the CARB emission inventory.

166 **Finding F5:** Top-down assessments of the CO emissions in 2010 are within 15% of the CARB
 167 2008 emission inventory.

168 **Finding F6:** Top-down assessments of NO_x emissions are in good agreement with the CARB
 169 emission inventory.

170 **Finding F7:** Top-down assessments of VOC emissions indicate some discrepancies with
 171 inventories, but they are not sufficiently large to appreciably affect results of air quality
 172 modeling.

173 **QUESTION G**174 **Do the VOC measurements provide any new insights into emission sources?**

175 **Finding G1:** Ambient VOC concentrations in the SoCAB have decreased by a factor of
 176 approximately 50 in the past five decades, but the ambient relative concentrations have remained
 177 remarkably constant, indicating that mobile emissions have remained the predominant source
 178 over this entire period.

179 **Finding G2:** The individual VOC to CO emission ratios observed in the SoCAB can disagree by
 180 a factor of four or more with the ratios derived from NEI 2005 and CARB 2008 emission
 181 inventories. The agreement is particularly poor for oxygenated VOCs. Nevertheless, the
 182 difference between measurements and inventory in terms of the overall OH reactivity is within
 183 15% of that from the CARB inventory, and the potential to form secondary organic aerosols
 184 (SOA) agrees within 35%.

186 **Finding G3:** Ambient benzene concentrations in the SoCAB have decreased more rapidly than
 187 concentrations of other VOCs, which is primarily attributed to efforts to remove benzene from
 188 gasoline due to its recognized toxicity.

189 **QUESTION H**190 **Can emission estimates from area sources be improved with the CalNex measurements?**

191 **Finding H1:** Gaseous elemental mercury emissions from a variety of California sources were
 192 estimated, and these estimates generally agreed with inventoried emissions. An exception is that
 193 emissions from the Los Angeles urban area were much larger than those in the inventory;
 194 reemission of mercury accumulated over the industrialized history of Los Angeles could account
 195 for this discrepancy.

196 **QUESTION I**197 **What are the relative roles and impacts of NH₃ emissions from motor vehicles and dairy farms?**

199 **Finding I1:** Within the SoCAB, conditions observed downwind of the dairy facilities were
 200 always thermodynamically favorable for NH₄NO₃ formation due to high NH₃ mixing ratios from
 201 those concentrated sources. Although automobile emissions of NH₃ were of approximately the
 202 same magnitude as the dairies, they were more dispersed and thus generated lower NH₃ mixing
 203 ratios. However, they are sufficiently high that they can thermodynamically favor NH₄NO₃
 204 formation. Reducing the dairy NH₃ emissions would have a larger impact on reducing SoCAB
 205 NH₄NO₃ formation than would reducing automobile NH₃ emissions.

206 **Finding I2a:** Within the San Joaquin Valley, despite large concentrations of NH₃ (often many
 207 100's of ppbv) associated with dairies, measured NH₄NO₃ concentrations were relatively low (\leq
 208 1 ppbv) due to low HNO₃ concentrations resulting from low NO_x emissions.

209 **Finding I2b:** Within the San Joaquin Valley NH₃ emissions are underestimated in the
 210 inventories by about a factor of three.

211 **QUESTION J**212 **Are there significant differences between emissions in the San Joaquin Valley Air Basin**
213 **(SJVAB) and the South Coast Air Basin (SoCAB)?**

214 **Finding J1:** NO_x emissions from the on-road vehicle fleet have decreased more rapidly in the
215 SoCAB than in the SJVAB.

216 **Finding J2:** There is evidence that temperature dependent VOC emissions from an unidentified
217 source, perhaps associated with agricultural activities and petroleum operations, are important in
218 the SJVAB but absent in the SoCAB.

219 **Finding J3:** The relative amounts of ammonia and NO_x emissions are such that formation of
220 ammonium nitrate aerosol (the major component of PM_{2.5} during many exceedance episodes) is
221 ammonia-limited in the SoCAB and NO_x-limited in the SJVAB.

222 **QUESTION K**223 **What are the significant sources of sulfur in southern California that contribute to**
224 **enhanced sulfate (SO₄²⁻) concentrations in the SoCAB?**

225 **Finding K1:** No significant sources of sulfur beyond those included in the CARB inventory can
226 be identified from the CalNex 2010 data.

227 **QUESTION L**228 **What is the impact of biogenic emissions, especially in foothills of the Sierra Nevada?**

229 **Finding L1a:** Photochemical O₃ formation in the SoCAB is dominated by anthropogenic VOCs
230 rather than biogenic VOCs; this was true in 2010 despite very substantial reductions in
231 anthropogenic VOC emissions over past decades.

232 **Finding L1b:** Considering only the individually measured VOCs, photochemical O₃ formation in
233 the SJVAB is also dominated by anthropogenic VOCs. However, on the hotter days in the
234 SJVAB there is evidence that unmeasured VOCs make an important contribution to O₃
235 formation, and this contribution well may be of biogenic origin.

236 **Finding L2:** Biogenic VOCs play significant roles in SOA formation in the SJVAB during both
237 daytime and nighttime; the different processes important during light and dark periods both
238 involve interactions between biogenic VOCs and anthropogenic emissions.

239 **Finding L3:** Biogenic VOCs play a significant, but minor role in SOA formation in the SoCAB.

240 **QUESTION M**241 **How does the atmospheric chemistry vary with time of day?**

242 **Finding M1:** Nighttime atmospheric chemistry plays multiple important air quality roles
243 including interconversion of reactive oxidized nitrogen species, formation of gas phase chlorine
244 species, and formation of aerosol nitrate. It is important that these processes are accurately
245 included in the air quality models from which air quality policy and regulations are generally
246 developed.

247 **Finding M2:** ClNO₂ and HONO are significant primary radical sources in SoCAB, particularly
248 in early morning when they were the dominant radical source near the surface between sunrise
249 and 09:00 PDT. However, it is important that vertical gradients of radical precursors be taken
250 into account in radical budgets, particularly with respect to HONO.

251 **Finding M3:** The propensity of Cl for radical propagation yielding second-generation OH
252 radicals indicates that the relative contributions of Cl and OH to tropospheric oxidation are not
253 accurately captured through simple radical budgets.

254 QUESTION N

255 **What are the major contributors to secondary organic aerosol (SOA)? What are the**
256 **relative magnitudes of SOA compared with primary organic aerosols in different areas?**

257 **Finding N1:** SOA contributions to OA at Pasadena could be identified from 1) their diurnal
258 cycles and their correlations with photochemical ozone production, and 2) an increase in SOA
259 concentration with increasing photochemical processing of urban air.

260 **Finding N2:** Averaged over the entire CalNex study, the 24-hour average SOA contribution
261 ($\approx 66\%$) to total OA at the Pasadena site was about twice that of primary organic aerosols.

262 **Finding N3:** Analysis of ambient OA measurements in SoCAB indicate that gasoline emissions
263 dominate over diesel in formation of secondary organic aerosol mass; however, an analysis
264 (based on liquid fuel composition) indicated that diesel dominates over gasoline for the
265 formation of SOA in the southern SJV.

266 **Finding N4:** At the Bakersfield site, most nighttime SOA formation is due to the reaction of the
267 NO₃ radical (a product of anthropogenic NO_x emissions) with unsaturated, primarily biogenic
268 VOCs.

269 QUESTION O

270 **How do layers of enhanced ozone concentrations form aloft, and how do they impact**
271 **ground-level ozone concentrations?**

272 **Finding O1:** Layers of enhanced O₃ concentrations aloft over California reflect the interleaving
273 of layers of air affected by differing O₃ sources. Enhanced O₃ concentrations arise from decent
274 of upper tropospheric air with O₃ of stratospheric origin, long-range transport of anthropogenic
275 emissions (e.g., from Asia), and lofted aged regional pollution (e.g., from California urban
276 areas).

277 **Finding O2:** Layers of enhanced ozone concentrations aloft are entrained into the convective
278 boundary layer, thereby enhancing surface level ozone concentrations.

279

280

281 **QUESTION P**

282 **What is the prevalence and spatial extent of the ozone weekend effect? What are the**
283 **contributing factors?**

284 **Finding P1:** In the SoCAB, NO_x emissions are reduced by nearly half on weekends, while VOC
285 emissions remain approximately constant. As a result, weekend hydroxyl radical concentrations
286 are greater, giving 65%–75% faster photochemical processing. In addition, ozone production
287 efficiency is 20%–50% higher. These effects yield 8-16 ppbv higher average midday ozone
288 concentrations on weekends than on weekdays.

289 **Finding P2:** The weekend reduction of NO_x emissions, and the concomitant changes in the
290 photochemical environment in the SoCAB, provides an opportunity to investigate certain aspects
291 of urban photochemistry such as secondary aerosol formation.

292 **Finding P3:** Investigation of the history of the weekend O₃ effect in the San Joaquin Valley
293 suggests that NO_x emissions reductions are already effective for reducing maximum O₃
294 concentrations, or are poised to become so, in the southern and central SJV.

295 **QUESTION Q**

296 **How do the different aerosol compositions in different areas influence radiative balances?**

297 **Finding Q1:** Climate models need more detailed treatment of direct radiative effects related to
298 black carbon absorption enhancements and also of ammonium nitrate partitioning between
299 aerosol and gas phases.

300 **Finding Q2:** The hygroscopicity of particles in the Central Valley is consistent with the
301 emerging global picture of a limited range of hygroscopicities, which may simplify the treatment
302 of indirect aerosol effects in global climate models. However, considerable variability was
303 found in aerosol hygroscopicity in the Los Angeles basin, which may complicate the treatment of
304 this issue in regional climate models.

305 **QUESTION R**

306 **Is there evidence of pollutant recirculation aloft, particularly in the SoCAB?**

307 **Finding R1a:** San Francisco Bay Area pollutants are transported efficiently to the Central
308 Valley. Automotive CO emitted in the Bay Area is a significant fraction of total CO found in the
309 San Joaquin Valley.

310 **Finding R1b:** Agricultural emissions (as well as emissions from other sources) in the Central
311 Valley can be transported aloft to the Southern California Bight.

312 **Finding R1c:** Southern California emissions are typically transported to less-populated areas to
313 the east.

314 **Finding R2:** The primary direction of transport of Mexican emissions in the border area (as
315 exemplified by Tijuana emissions) was to the east or southeast. At least during May and June of
316 2010, the transport of emissions from the Mexican border regions into the San Diego area was
317 not an important influence.

318 **QUESTION S**319 **Is there evidence of pollutant recirculation, particularly in the South Coast Air Basin**
320 **(SoCAB)?**

321 **Finding S1:** Pollutants from the SoCAB can be recirculated within the Catalina Eddy in the
322 boundary layer over the Southern California Bight. In the process, they can be combined with
323 pollutants from the San Francisco Bay Area, which can be transported down the coast.
324 Concentrations from San Francisco Bay Area sources coming onshore in the southern part of the
325 Los Angeles metropolitan area and Orange County are generally small.

326 **Finding S2:** The direction that emissions originating from Los Angeles exit from the basin
327 varies with time of day. From late morning to early evening most emissions exit to the east,
328 while during the rest of the day significant flux exits to the west and south in shallow layers over
329 the ocean. Both the sea-land breeze circulation and the Catalina Eddy flow over the Southern
330 California Bight force emissions that had exited the LA basin to the west and south back into the
331 source region. For NO_y, total inflow from upwind sources and this return flux equals 40% of
332 that emitted within the basin when averaged over May of 2010.

333 **QUESTION T**334 **Is there evidence of long-range transport during CalNex? What were the relative**
335 **contributions of the various sources outside the control of emissions within California (i.e.,**
336 **policy-relevant background ozone)?**

337 **Finding T1:** Transport of baseline O₃ can enhance surface O₃ concentrations to such an extent
338 that the margin for local and regional O₃ production before exceeding the NAAQS is greatly
339 reduced or potentially eliminated, even in California's urban areas.

340 **Finding T2:** Transport of baseline ozone accounts for a majority of surface ozone concentrations
341 in California at urban as well as rural locations, both on average and during many exceedance
342 events. Only in the most intense exceedance events does local and regional photochemical
343 production contribute a majority.

344 **Finding T3:** In addition to being a receptor of long-range pollutant transport, California is also a
345 source of transport to downwind areas.

346 **QUESTION U**347 **How well did the meteorological and air quality forecast models perform during CalNex?**
348 **What weaknesses need attention?**

349 **Finding U1:** Evaluation of different meteorological models against CalNex measurements shows
350 that details of model configuration (physics, initialization, resolution) can impact performance
351 for specific processes and regions. Particular attention needs to be paid to land surface and soil
352 parameters and to clouds offshore. Significant but poorly characterized biases (for example,
353 high wind speeds and weak land breeze) remain in the best available simulations.

354 **Finding U2a:** Evaluation of several different real-time air quality forecasts against O₃ and
355 PM_{2.5} observations show that none of the models perform statistically better than the persistence
356 forecast (i.e., predicting that tomorrow's air quality will be exactly the same as today's air

357 quality). All models show temporal correlations for maximum 8-hr O₃ that beat persistence, but
 358 model biases and poor spatial correlations limit over-all forecast skill.

359 **Finding U2b:** Incorporation of the RAQMS global forecast [*Pierce et al.*, 2003] to modify
 360 lateral boundary conditions improved temporal skill for O₃ forecasts but increased model bias.

361 QUESTION V

362 What pollution control efforts are likely to result in “win-win” or “win-lose” situations?

363 **Finding V1:** Cessation of burning crop residue from rice agriculture (a "win" for air quality)
 364 increased methane emissions (a "lose" for climate).

365 **Finding V2:** Marine vessel emissions changes due to fuel sulfur reductions and speed controls
 366 result in a net warming effect (a "lose" for climate), but have substantial positive impacts on
 367 local sulfur and primary PM emissions (a "win" for air quality).

368 QUESTION W

369 Could the same pollutant control efforts in different air basins (i.e., SJVAB and SoCAB) 370 have different results with respect to changes in air quality and climate (i.e., move toward 371 different nexus quadrants in the figure on the front page of this report)?

372 **Finding W1:** The southern SJVAB has an unidentified, temperature dependent VOC emission
 373 source that dominates O₃ production on the hottest days when the highest O₃ concentrations
 374 occur. As a consequence, NO_x emission controls are expected to be more effective for reducing
 375 O₃ in the southern SJVAB than in the SoCAB.

376 **Finding W2a:** In the SJVAB ammonia is in large excess compared to nitric acid; consequently
 377 NH₄NO₃ PM concentrations in the SJVAB will be more responsive to NO_x emissions reductions
 378 compared to ammonia emissions reductions.

379 **Finding W2b:** In the SoCAB the response of NH₄NO₃ PM concentrations to emission reductions
 380 will depend upon meteorological conditions, other aerosol components, and the regional
 381 distribution of NH₃ and NO_x emissions.

382 **Finding W3a:** In both the SoCAB and the SJVAB, anthropogenic VOCs are believed to be the
 383 primary precursors of secondary organic aerosol; thus in both basins organic aerosol
 384 concentrations will be sensitive to VOC emissions control.

385 **Finding W3b:** Biogenic VOCs oxidized in the presence of NO_x provides additional sources of
 386 secondary organic aerosol that are important for the SJVAB, but less so in the SoCAB. Thus,
 387 NO_x emissions reductions will be effective for controlling this source of organic aerosol in the
 388 SJVAB, but will have less impact in the SoCAB.

389

390 **Introduction**

391 The California Air Resources Board (CARB) and the National Oceanic and Atmospheric
 392 Administration (NOAA) jointly organized an atmospheric field study in the spring and early
 393 summer of 2010 (CalNex) that collected atmospheric composition and meteorological data
 394 pertinent to addressing issues at the nexus between air quality and climate change (see
 395 <http://www.arb.ca.gov/research/calnex2010/calnex2010.htm> and
 396 <http://esrl.noaa.gov/csd/calnex/>). This report is intended to ensure that the results of the analysis
 397 of the field observations are made fully available to California policy makers who must deal with
 398 air quality and climate change issues. Much of the material in this report has been presented in
 399 *Ryerson et al.* [2013] in a different format with a different emphasis.

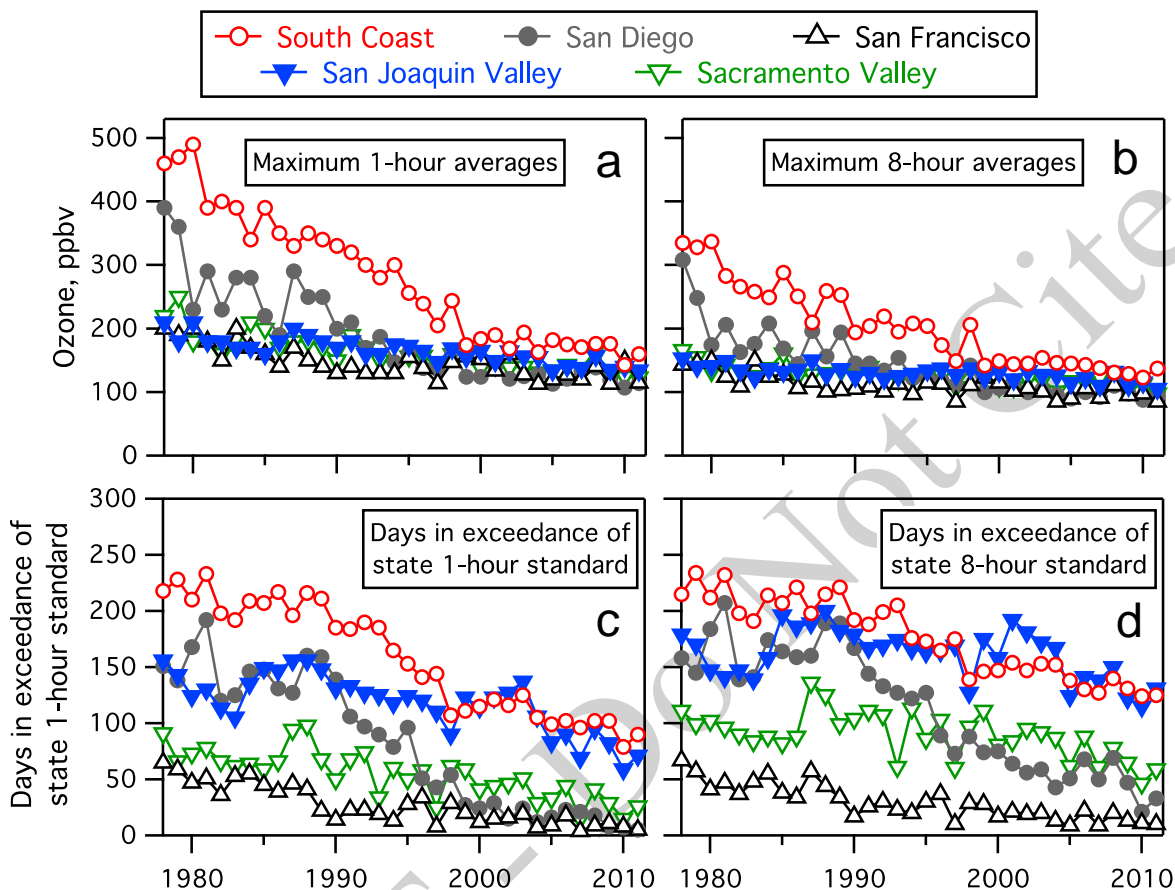
400 *As fully as possible, the findings from the CalNex publications and from additional integrated*
 401 *analysis of the diverse data sets from the CalNex researchers, as well as other historical air*
 402 *quality studies in California, are here synthesized in a timely fashion and in a form useful to*
 403 *policy makers. The goal is to provide a comprehensive and integrated presentation of our*
 404 *current understanding of the interrelated air quality and climate issues in California.*

405 The California Research at the Nexus of Air Quality and Climate Change (CalNex) 2010 field
 406 project was undertaken to provide improved scientific knowledge for emissions control strategies
 407 to simultaneously address the two interrelated issues of air quality and climate change. Air
 408 quality and climate change issues are linked because in many cases the atmospheric agents of
 409 concern are the same, and the sources of the agents are the same or intimately connected.
 410 Examples include tropospheric ozone (O₃), which is both an air pollutant and a greenhouse gas
 411 (GHG), and atmospheric particulate matter (PM), which affects the radiative budget of the
 412 atmosphere as well as human and ecosystem health, visibility degradation, and acidic deposition.
 413 Efforts to address one of these issues can be beneficial to the other, but in some cases policies
 414 addressing one issue without additional consideration can have unintended detrimental impacts
 415 on the other. The goal of CalNex 2010 is to improve and advance the science needed to support
 416 continued and effective air quality and climate management policy for the State of California.

417 Over the past several decades in the U.S., emissions reductions implemented for vehicles and
 418 point sources have significantly improved air quality in most metropolitan areas. In recent years
 419 the rate of improvement in air quality in most regions of the U.S. has slowed, both in terms of
 420 regional ozone concentrations and ozone exceedance days (e.g., Fig. 1 for California). At the
 421 same time, accelerating emissions of greenhouse gases have increased the net radiative forcing of
 422 the climate system. Overall, from 1990 to 2005, total emissions of carbon dioxide (CO₂) in the
 423 US were estimated to have increased by 20% (from 5062 to 6090 Tg per year) [EPA, 2007].

424 California was chosen as the region for this study because it has well-documented air quality
 425 problems and faces the difficult task of managing them with an increasing population and
 426 demand for goods and services. The CalNex study was designed to build upon the knowledge
 427 developed through decades of previous atmospheric research field projects in California.
 428 Consistent themes across the many studies include quantifying anthropogenic emissions and
 429 their changes over time, notably in tunnel studies (e.g., [Harley et al., 2005]) and by roadside
 430 monitoring (e.g., [Bishop and Stedman, 2008]); the role that regional transport plays in shaping
 431 pollutant concentrations, forced either by the sea breeze (e.g., [Boucouvala and Bornstein, 2003;
 432 Cass and Shair, 1984; Shair et al., 1982]), by complex terrain (e.g., [Langford et al., 2010;
 433 Skamarock et al., 2002; Wakimoto and McElroy, 1986]) or both [Lu and Turco, 1996; Rosenthal
 434 et al., 2003]; the roles of chlorine chemistry (e.g., [Finlayson-Pitts, 2003; Knipping and Dabdub,

435 2003] and the weekend effect (e.g., [Blanchard and Tanenbaum, 2003; Marr and Harley, 2002])
 436 in ozone formation; and studies of the sources and chemistry leading to atmospheric haze
 437 formation (e.g., [Hersey et al., 2011; Schauer et al., 1996; Turpin and Huntzicker, 1995]).



438
 439 **Figure 1.** Maximum 1-hour (a) and 8-hour (b) averaged surface O₃ data, and number
 440 of days in exceedance of the state 1-hour (c) and 8-hour (d) O₃ standards, for selected
 441 air basins in California (www.arb.ca.gov/adam/trends/trends1.php).

442 The literature from previous field studies in California is extensive; initial descriptions can be
 443 found in the project overview papers for the Southern California Air Quality Study (SCAQS;
 444 which took place in 1987) [Hering and Blumenthal, 1989], the Southern California Ozone Study
 445 (SCOS, 1997) (www.arb.ca.gov/research/scos/scos.htm), the California Regional Particulate
 446 AirQuality Study (CRPAQS, 1999-2001) [Chow et al., 2006; Qin and Prather, 2006; Rinehart et
 447 al., 2006], the Central California Ozone Study (CCOS, summer 2000) [Bao et al., 2008a; Liang
 448 et al., 2006; Tonse et al., 2008], the Intercontinental Transport and Chemical Transformation of
 449 Anthropogenic Pollution (ITCT, spring 2002) study [Parrish et al., 2004], the Intercontinental
 450 Chemical Transport Experiment - North America (INTEX-NA, summer 2004) study, the Study
 451 of Organic Aerosols at Riverside (SOAR; 2005) [Docherty et al., 2011], the Arctic Research of
 452 the Composition of the Troposphere from Aircraft and Satellites-California Air Resources Board
 453 (ARCTAS-CARB, summer 2008) study [Jacob et al., 2010], the Pre-CalNex (summer 2009)
 454 study [Langford et al., 2010], and the Pasadena Aerosol Characterization Observatory study
 455 (PACO, 2009-2010) study [Hersey et al., 2011].

456 In addition to its long-standing focus on air quality issues, in 2006 California led the nation's
 457 effort to address global climate change by implementing Assembly Bill 32 (AB32;
 458 arb.ca.gov/cc/ab32/ab32.htm) as the Global Warming Solutions Act of 2006, mandating controls
 459 on the emissions of greenhouse gases within, or attributable to, the state. Thus, California is
 460 particularly interested in finding the most effective way to simultaneously manage the two
 461 challenges of air quality and climate change. The CalNex study was organized to address issues
 462 simultaneously relevant to both, including (1) emission inventory assessment, (2) atmospheric
 463 transport and dispersion, (3) atmospheric chemical processing, and (4) cloud-aerosol interactions
 464 and aerosol radiative effects.

465 The CalNex project was loosely coordinated with the U.S. Department of Energy (DOE)-
 466 sponsored Carbonaceous Aerosol and Radiative Effects Study (CARES;
 467 <http://campaign.arm.gov/cares>) in Sacramento and the Central Valley, and the multi-institutional
 468 CalMex study (<http://mce2.org/en/activities/cal-mex-2010>) based in Tijuana, Mexico. CARES
 469 took place in June of 2010 with a focus on the evolution of secondary and black carbon aerosols
 470 and their climate-relevant properties in the Sacramento urban plume. The scientific objectives,
 471 deployment approach, and a summary of initial findings from this project are described in *Zaveri*
 472 *et al.* [2012]. CalMex took place in May and June of 2010 with a focus on characterizing the
 473 sources and processing of emissions in the California-Mexico border regions to better understand
 474 their transport [*Bei et al.*, 2012], transformation, impacts on regional air quality and climate (*e.g.*,
 475 [*Takahama et al.*, 2012]) and to support the design and implementation of emission control
 476 strategies at local, regional and trans-boundary scales.

477 The fieldwork was planned to address twelve general Science Questions (see the CalNex White
 478 Paper at <http://esrl.noaa.gov/csd/calnex/whitepaper.pdf> for a listing) that were formulated to
 479 guide the study planning. Those questions address many specific and general science needs
 480 required to guide policy approaches to effectively address air quality and climate change issues.
 481 The questions addressed pollutant emissions (of greenhouse gases and ozone and aerosol
 482 precursors), important atmospheric transformation and climate processes, and pollutant transport
 483 and meteorology. Instrumentation and platforms (airborne, ship- and ground-based) were
 484 deployed to collect the data sets necessary to address those questions. Analyses of the resulting
 485 data sets have been reported in many science publications (81 published or submitted to date),
 486 and more are expected during coming years. However, most of these publications are intended
 487 to further our understanding of the scientific issues at hand, and not necessarily at directly
 488 addressing the most policy-relevant issues.

489 The general Science Questions that were formulated to guide the CalNex field study are here
 490 revised into twenty-three specific policy-relevant Science Questions (see text box on next pages)
 491 that can be addressed, and ideally fully answered, by CalNex analyses. They provide the
 492 organizational framework of this synthesis for presentation of the scientific results of this
 493 ongoing analysis in a format that is maximally useful to California policy makers responsible for
 494 formulating the state's response to air quality and climate change issues, both at the state and
 495 more regional levels. This report brings together in an organized fashion the most important
 496 policy-relevant findings to date, and is intended to present them as concise but comprehensive
 497 findings. The goals are that: 1) each question/issue be succinctly stated, 2) the policy-relevance
 498 is discussed if appropriate, 3) the historical context is given, 4) the analytical approach (along
 499 with caveats and uncertainties) is summarized, and 4) the findings and recommendations, if any,
 500 are presented succinctly and clearly. Of course, an approximately 6-week sampling program
 501 cannot definitively answer all the questions and issues, but it does effectively address and
 502 advance our understanding of all twenty-three policy-relevant Science Questions.

503 ***CalNex 2010 Science Questions***504 ***Meteorology and Atmospheric Climatology***

- 505 A. How did the meteorology during CalNex compare to historical norms?
 506 B. How did the CalNex air quality measurements fit in the context of historical measurements?
 507 C. How do the CalNex air quality measurements in late spring and early summer relate to the
 508 peak ozone concentrations in summer and the peak PM_{2.5} concentrations in winter?
 509 D. What were the global “background” concentrations observed during CalNex and how did
 510 they vary spatially and temporally?

511 ***Emissions***

- 512 E. How effective have historical air pollution control efforts been? How effective have specific
 513 emission control measures been?
 514 F. Are current emission inventory estimates for air pollutants and climate-forcing agents
 515 accurate? Are there under- or over-estimated emissions or even missing emission sources in
 516 the current emission inventories?
 517 G. Do the VOC measurements provide any new insights into emission sources?
 518 H. Can emission estimates from area sources be improved with the CalNex measurements?
 519 I. What are the relative roles and impacts of NH₃ emissions from motor vehicles and dairy
 520 farms?
 521 J. Are there significant differences between emissions in the San Joaquin Valley Air Basin
 522 (SJVAB) and the South Coast Air Basin (SoCAB)?
 523 K. What are the significant sources of sulfur in southern California that contribute to enhanced
 524 sulfate (SO₄⁻) concentrations in the SoCAB?
 525 L. What is the impact of biogenic emissions, especially in foothills of the Sierra Nevada?

526 ***Climate Processes/Transformations***

- 527 M. How does the atmospheric chemistry vary with time of day?
 528 N. What are the major contributors to secondary organic aerosol (SOA)? What are the relative
 529 magnitudes of SOA compared with primary organic aerosols in different areas?
 530 O. How do layers of enhanced ozone concentrations form aloft, and how do they impact ground-
 531 level ozone concentrations?
 532 P. What is the prevalence and spatial extent of the ozone weekend effect? What are the
 533 contributing factors?
 534 Q. How do the different aerosol compositions in different areas influence radiative balances?

535 ***Atmospheric Transport***

- 536 R. Is there evidence of pollutant transport between air basins or states?
 537 S. Is there evidence of pollutant recirculation, particularly in the South Coast Air Basin
 538 (SoCAB)?
 539 T. Is there evidence of long-range transport during CalNex? What were the relative
 540 contributions of the various sources outside the control of emissions within California (i.e.,
 541 policy-relevant background ozone)?

542

543 ***CalNex 2010 Science Questions (cont.)***544 ***Modeling***

545 U. How well did the meteorological and air quality forecast models perform during CalNex?
546 What weaknesses need attention?

547 ***Climate and Air Quality Nexus***

548 V. What pollution control efforts are likely to result in “win-win” or “win-lose” situations?
549 W. Could the same pollutant control efforts in different air basins (i.e., SJVAB and SoCAB)
550 have different results with respect to changes in air quality and climate (i.e., move toward
551 different nexus quadrants in the figure on the front page of this report)?
552

553 The CalNex fieldwork was conducted during May through July of 2010 through a collaborative,
554 multiagency, intensive effort. Partners in the study included the local air quality districts,
555 universities (both in California and other states), Department of Energy, NASA, National
556 Science Foundation, U.S. Environmental Protection Agency, and the Mexican air quality
557 community. The field measurements were executed by a very large number of scientists from
558 the study partners. Individual scientists from these institutions have formulated and conducted
559 the analyses that they excitedly believe will reinforce foundational air quality and climate change
560 principles and definitively address outstanding issues and uncertainties. For the most part, these
561 research scientists have and will continue to present their analyses and findings in scientific
562 presentations and publications, and generally all will submit final reports to their respective
563 funding agencies. The acknowledgment section contains a reasonably complete listing of the
564 institutions that participated in CalNex.

565 **References**

- 566 Bao, J. W., S. A. Michelson, P. O. G. Persson, I. V. Djalalova, and J. M. Wilczak (2008),
567 Observed and WRF-simulated low-level winds in a high-ozone episode during the Central
568 California Ozone Study, *Journal of Applied Meteorology and Climatology*, 47(9), 2372-
569 2394.
- 570 Bei, N., et al. (2012), Meteorological overview and plume transport patterns during Cal-Mex
571 2010, *Atmospheric Environment*, doi:10.1016/j.atmosenv.2012.01.065.
- 572 Bishop, G. A., and D. H. Stedman (2008), A decade of on-road emissions measurements,
573 *Environmental Science & Technology*, 42(5), 1651-1656, doi:10.1021/es702413b.
- 574 Blanchard, C. L., and S. J. Tanenbaum (2003), Differences between weekday and weekend air
575 pollutant levels in southern California, *Journal of the Air and Waste Management*
576 *Association*, 53(7), 816-828.
- 577 Boucouvala, D., and R. Bornstein (2003), Analysis of transport patterns during an SCOS97-
578 NARSTO episode, *Atmospheric Environment*, 37(Supplement no. 2), S73-S94,
579 doi:10.1016/S1352-2310(03)00383-2.
- 580 Cass, G. R., and F. H. Shair (1984), Sulfate accumulation in a sea breeze/land breeze circulation
581 system, *Journal of Geophysical Research*, 89, 1429-1438.

- 582 Chow, J. C., L. W. A. Chen, J. G. Watson, D. H. Lowenthal, K. A. Magliano, K. Turkiewicz, and
583 D. E. Lehrman (2006), PM_{2.5} chemical composition and spatiotemporal variability during the
584 California Regional PM₁₀/PM_{2.5} Air Quality Study (CRPAQS), *Journal of Geophysical*
585 *Research*, 111(D10S04), doi:10.1029/2005JD006457.
- 586 Docherty, K. S., et al. (2011), The 2005 Study of Organic Aerosols at Riverside (SOAR-1):
587 instrumental intercomparisons and fine particle composition, *Atmospheric Chemistry and*
588 *Physics*, 11, 12387-12420, doi:10.5194/acp-11-12387-2011.
- 589 EPA, U.S. (2007), Inventory of U.S. greenhouse gas emissions and sinks: 1900–2005 Rep. EPA-
590 430-R-07-002, Washington, D.C.
- 591 Finlayson-Pitts, B. J. (2003), The tropospheric chemistry of sea salt: a molecular-level view of
592 the chemistry of NaCl and NaBr, *Chemical Reviews*, 103, 4801-4822.
- 593 Harley, R. A., L. C. Marr, J. K. Lehner, and S. N. Giddings (2005), Changes in motor vehicle
594 emissions on diurnal to decadal time scales and effects on atmospheric composition,
595 *Environmental Science & Technology*, 39(14), 5356-5362, doi:10.1021/es048172+.
- 596 Hering, S. V., and D. L. Blumenthal (1989), Southern California Air Quality Study (SCAQS)
597 description of measurement activities, final report to California Air Resources Board,
598 contract no. A5-157-32.
- 599 Hersey, S. P., J. S. Craven, K. A. Schilling, A. R. Metcalf, A. Sorooshian, M. N. Chan, R. C.
600 Flagan, and J. H. Seinfeld (2011), The Pasadena Aerosol Characterization Observatory
601 (PACO): chemical and physical analysis of the Western Los Angeles Basin aerosol,
602 *Atmospheric Chemistry and Physics*, 11, 7417-7443, doi:10.5194/acp-11-7417-2011.
- 603 Jacob, D. J., et al. (2010), The Arctic Research of the Composition of the Troposphere from
604 Aircraft and Satellites (ARCTAS) mission: design, execution, and first results, *Atmospheric*
605 *Chemistry and Physics*, 10, 5191–5212, doi:10.5194/acp-10-5191-2010.
- 606 Knipping, E., and D. Dabdub (2003), Impact of chlorine emissions from sea-salt aerosol on
607 coastal urban ozone, *Environmental Science & Technology*, 37(2), 275-284,
608 doi:10.1021/es025793z.
- 609 Langford, A. O., C. J. Senff, R. J. I. Alvarez, R. M. Banta, and R. M. Hardesty (2010), Long-
610 range transport of ozone from the Los Angeles Basin: a case study, *Geophysical Research*
611 *Letters*, 37(L06807), doi:10.1029/2010GL042507.
- 612 Liang, J., B. Jackson, and A. Kaduwela (2006), Evaluation of the ability of indicator species
613 ratios to determine the sensitivity of ozone to reductions in emissions of volatile organic
614 compounds and oxides of nitrogen in northern California, *Atmospheric Environment*, 40,
615 5156–5166, doi:10.1016/j.atmosenv.2006.03.060.
- 616 Lu, R., and R. P. Turco (1996), Ozone distributions over the Los Angeles Basin: Three-
617 dimensional simulations with the SMOG model, *Atmospheric Environment*, 30, 4155-4176.
- 618 Marr, L. C., and R. A. Harley (2002), Modeling the effect of weekday-weekend differences in
619 motor vehicle emissions on photochemical air pollution in central California, *Environmental*
620 *Science & Technology*, 36(19), 4099-4106, doi:10.1021/es020629x.
- 621 Parrish, D. D., Y. Kondo, O. R. Cooper, C. A. Brock, D. A. Jaffe, M. Trainer, T. Ogawa, G.
622 Hübner, and F. C. Fehsenfeld (2004), Intercontinental Transport and Chemical
623 Transformation 2002 (ITCT 2K2) and Pacific Exploration of Asian Continental Emission

- 624 (PEACE) experiments: An overview of the 2002 winter and spring intensives, *Journal of*
625 *Geophysical Research*, 109,D23S01,doi:10.1029/2004JD004980
- 626 Qin, X., and K. A. Prather (2006), Impact of biomass emissions on particle chemistry during the
627 California Regional Particulate Air Quality Study, *International Journal of Mass*
628 *Spectrometry*, 258, 142–150, doi:10.1016/j.ijms.2006.09.004.
- 629 Rinehart, L. R., E. M. Fujita, J. C. Chow, K. Magliano, and B. Zeilinska (2006), Spatial
630 distribution of PM_{2.5} associated organic compounds in central California, *Atmospheric*
631 *Environment*, 40, 290–303, doi:10.1016/j.atmosenv.2005.09.035.
- 632 Rosenthal, J. S., R. A. Helvey, T. E. Battalino, C. Fisk, and P. W. Greiman (2003), Ozone
633 transport by mesoscale and diurnal wind circulations across southern California, *Atmospheric*
634 *Environment*, 37(Supplement no. 2), S51-S71.
- 635 Ryerson, T.B., et al. (2013), The 2010 California Research at the Nexus of Air Quality and
636 Climate Change (CalNex) field study. *J. Geophys. Res.-Atmos.*, in press.
- 637 Schauer, J. J., W. G. Rogge, L. M. Hildemann, M. A. Mazurek, and G. R. Cass (1996), Source
638 apportionment of airborne particulate matter using organic compounds as tracers,
639 *Atmospheric Environment*, 30, 3837-3855.
- 640 Shair, F. H., et al. (1982), Transport and dispersion of airborne pollutants associated with the
641 land breeze-sea breeze system, *Atmospheric Environment*, 16, 2043-2053.
- 642 Skamarock, W. C., R. Rotunno, and J. B. Klemp (2002), Catalina eddies and coastally trapped
643 disturbances, *Journal of Atmospheric Sciences*, 59, 2270-2278.
- 644 Takahama, S., S. Liu, and L. M. Russell (2010), Coatings and clusters of carboxylic acids in
645 carbon-containing atmospheric particles from spectromicroscopy and their implications for
646 cloud-nucleating and optical properties, *Journal of Geophysical Research*, 115(D01202),
647 doi:10.1029/2009JD012622.
- 648 Tonse, S. R., N. J. Brown, R. A. Harley, and L. Jin (2008), A process–analysis based study of the
649 ozone weekend effect, *Atmospheric Environment*, 42, 7728–7736,
650 doi:10.1016/j.atmosenv.2008.05.061.
- 651 Turpin, B. J., and J. J. Huntzicker (1995), Identification of secondary organic aerosol episodes
652 and quantitation of primary and secondary organic aerosol concentrations during SCAQS,
653 *Atmospheric Environment*, 29(23), 3527-3544.
- 654 Wakimoto, R. M., and J. L. McElroy (1986), Lidar observation of elevated pollution layers in
655 Los Angeles, *Journal of Climate and Applied Meteorology*, 25, 1583–1599.
- 656 Zaveri, R. A., et al. (2012), Overview of the 2010 Carbonaceous Aerosols and Radiative Effects
657 Study (CARES), *Atmospheric Chemistry and Physics Discussions*, 12, 7647-7687,
658 doi:10.5194/acp-12-7647-2012.
- 659
- 660
- 661

662

Glossary of Terms, Symbols and Acronyms

663	¹⁴ C	carbon 14 isotope
664	8-h	8-hour
665	AB32	Assembly Bill 32: Global Warming Solutions Act
666	AGL	above ground level
667	AIM/IC	ambient ion monitor/ion chromatograph
668	AIRNow	web site providing public access to national air quality information
669	AGU	American Geophysical Union
670	AM3	Atmospheric model developed by NOAA GFDL
671	AMS	aerosol mass spectrometer
672	amu	atomic mass unit
673	APN	acyl peroxy nitrates
674	ARB	Air Resources Board
675	ARCTAS	Arctic Research of the Composition of the Troposphere from Aircraft and
676		Satellites
677	ASL	above sea level
678	BAMS	Baron Advanced Meteorological Services
679	BC	black carbon
680	BEARPEX	Biosphere Effects on AeRosols and Photochemistry EXperiment
681	Bight	The Southern California Bight includes the Channel Islands and that part of the
682		Pacific Ocean bounded by the curved coastline of Southern California from
683		Point Conception to San Diego.
684	BVOC	biogenic volatile organic compound
685	Cal-Mex	2010 US-Mexico collaborative field study of air quality and climate change in
686		the California-Mexico border that was loosely coordinated with CalNex
687	CalNex	California Research at the Nexus of Air Quality and Climate Change
688	CalNex-LA	CalNex super monitoring site in the Los Angeles basin (Pasadena)
689	CalNex-SJV	CalNex super monitoring site in the San Joaquin Valley (Bakersfield)
690	CARB	California Air Resources Board
691	carbonyl	a functional group composed of a carbon atom double-bonded to an oxygen
692	CARES	Carbonaceous Aerosol and Radiative Effects Study
693	CBL	convective boundary layer
694	CCN	cloud condensation nuclei
695	CFC(s)	chlorofluorocarbon(s)
696	Cl ⁻	chloride ion
697	Cl ₂	molecular chlorine
698	CINO ₂	nitryl chloride
699	CIOA	cooking-influenced organic aerosol
700	CIMS	chemical ionization mass spectrometer
701	CIRPAS	the Center for Interdisciplinary Remotely-Piloted Aircraft Studies
702	CMAQ	Community Multi-scale Air Quality model
703	CMB	chemical mass balance
704	CO	carbon monoxide
705	CO ₂	carbon dioxide
706	COAMPS	Coupled Ocean–Atmosphere Mesoscale Prediction System
707	DMS	dimethyl sulfide, a reduced sulfur species released by natural sources
708	DOAS	differential optical absorption spectroscopy

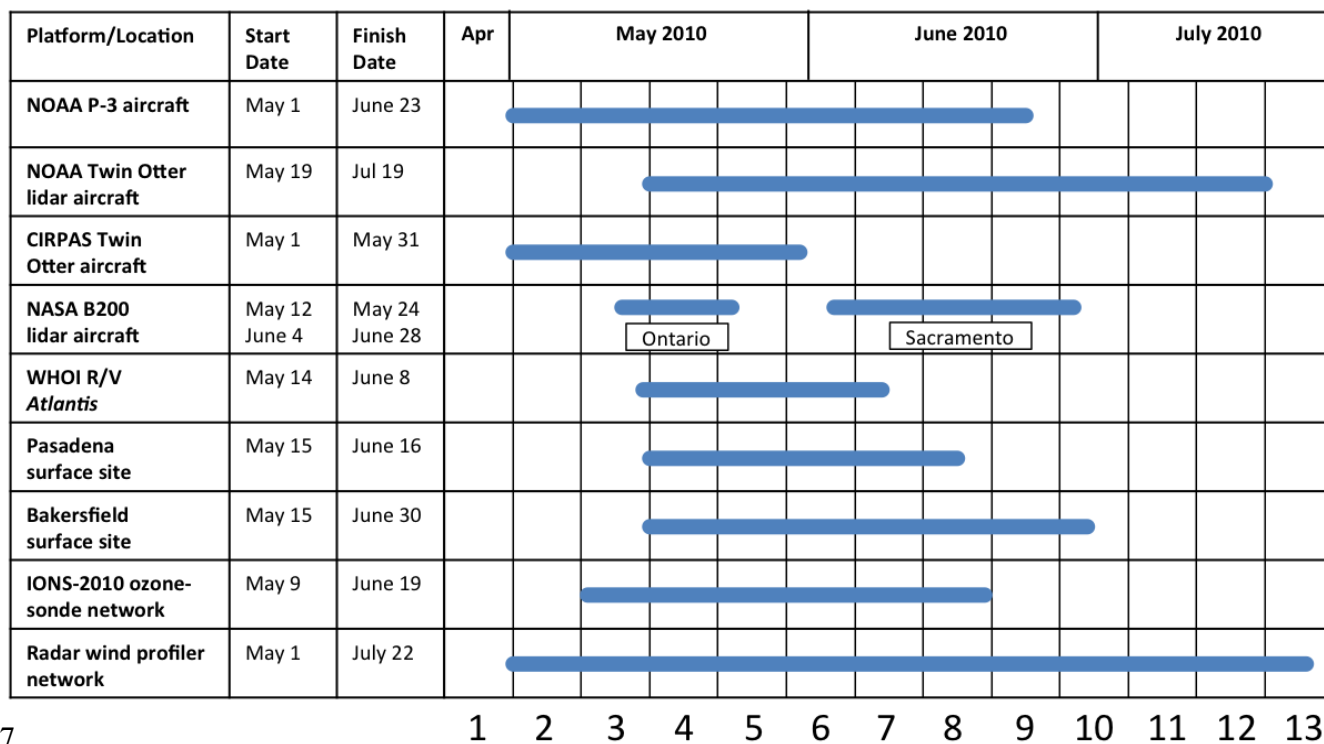
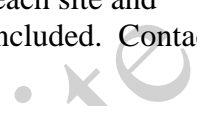
709	EC	elemental carbon
710	ECMWF	European Centre for Medium-Range Weather Forecasts
711	EDGAR	Emission Database for Global Atmospheric Research
712	EMFAC	Emission model used in California to estimate vehicle emissions
713	EPA	U.S. Environmental Protection Agency
714	ER	enhancement ratio or emission ratio
715	FLEXPART	Lagrangian particle dispersion model for describing atmospheric transport
716	FTS	Fourier transform spectrometer
717	GC/MS-FID	Gas Chromatography/Mass Spectrometry-Flame Ionization Detector
718	GEM	gaseous elemental mercury
719	GEOS-Chem	a global 3-D model of atmospheric composition
720	GFDL	NOAA's Geophysical Fluid Dynamics Laboratory
721	GHG	greenhouse gas
722	GOCART	the Goddard Chemistry Aerosol Radiation and Transport model
723	GOME	Global Ozone Monitoring Experiment - a satellite borne instrument
724	GWP	global warming potential (usually based on 100 year period)
725	H ₂ O	water vapor
726	H ₂ O ₂	hydrogen peroxide
727	HCFC(s)	hydrochlorofluorocarbon(s)
728	HCN	hydrogen cyanide
729	HFCs	hydrofluorocarbon(s)
730	HNO ₃	nitric acid
731	HO ₂	hydroperoxy radical
732	HOA	hydrogen-like organic aerosol
733	HONO	nitrous acid
734	HO _x	OH + HO ₂
735	hPa	atmospheric pressure unit - one standard atmosphere equals 1013.25 hPa
736	IC	ion chromatography
737	IMPROVE	Interagency Monitoring of Protected Visual Environments
738	IONS-2010	Intercontinental Chemical Transport Experiment Ozone Sonde Network Study
739		- 2010
740	IPCC	Inter-governmental Panel on Climate Change
741	km	kilometer
742	LAT	latitude
743	LAX	Los Angeles International Airport
744	LOA	local organic aerosol
745	LV-OOA	low-volatility OOA
746	MDA8	daily maximum 8-hour average
747	MODIS	Moderate Resolution Imaging Spectroradiometer
748	molec. cm ⁻³	molecules per cubic centimeter
749	MOZAIC	Measurements of Ozone, water vapor, carbon monoxide and nitrogen oxides
750		by in-service Airbus aircraft)
751	MPAN	methyl peroxy acetyl nitrate
752	MSD	mass selective detector
753	N ₂ O	nitrous oxide
754	N ₂ O ₅	dinitrogen pentoxide
755	NAAQS	national ambient air quality standard
756	NEI	National Emission Inventory

757	NH ₃	ammonia gas
758	NH ₄ ⁺	ammonium ion (also NH ₄)
759	NH ₄ NO ₃	particulate ammonium nitrate
760	nm	nanometer
761	NO	nitric oxide
762	NO ₂	nitrogen dioxide
763	NO ₃	nitrate radical
764	NO ₃ ⁻	nitrate ion (also NO ₃ , depending on context to differentiate from radical)
765	NOAA	National Oceanic and Atmospheric Administration
766	NOAA/ESRL	NOAA/Earth System Research Laboratory
767	NOAA/ESRL/CSD	NOAA/ESRL/Chemical Sciences Division
768	NOAA/ESRL/GSD	NOAA/ESRL/Global Systems Division
769	NOAA/NCEP	NOAA/National Centers for Environmental Prediction
770	NO _x	oxides of nitrogen, NO + NO ₂
771	NO _y	total reactive oxidized nitrogen, i.e., NO + NO ₂ + HONO + HNO ₃ + N ₂ O ₅ + ...
772	NR-PM1	non-refractive particulate matter smaller than 1 micron in aerodynamic
773		diameter
774	N _{TOT}	total particle density (units generally part. cm ⁻³)
775	O(¹ D)	an excited state of atomic oxygen (free radical)
776	O ₃	ozone
777	O _x	total oxidant (often estimated as O ₃ + NO ₂)
778	OA	organic aerosol
779	OH	hydroxyl radical
780	OMI	Ozone Monitoring Instrument - a satellite borne instrument
781	OOA	oxygenated organic aerosol
782	P-3	(aka WP-3, or WP-3D) – Lockheed WP-3D Orion Aircraft operated by NOAA
783	PACO	Pasadena Aerosol Characterization Observatory
784	PAN	peroxy acetylnitrate
785	PBL	planetary boundary layer
786	PDT	Pacific Daylight Time
787	PFA	Perfluoroalkoxy
788	PHO _x	HO _x Production Rate
789	PM	particulate matter
790	PM1	particulate matter smaller than 1 micron in aerodynamic diameter
791	PM2.5	particulate matter less than 2.5 microns aerodynamic diameter
792	PO ₃	Ozone Production Rate
793	POA	primary (directly emitted) organic aerosol
794	POM	particulate organic matter
795	ppbv	parts-per-billion by volume - mixing ratio unit based on mole ratio
796	ppmv	parts-per-million by volume - mixing ratio unit based on mole ratio
797	PPN	peroxy propionyl nitrate
798	PRB	policy-relevant background
799	PST	Pacific Standard Time
800	RACM	Regional Atmospheric Chemistry Mechanism Version 2
801	RAQMS	Regional Air Quality Modeling System
802	RONO ₂	alkyl nitrate
803	R/V	research vessel
804	s	second

805	SCAQS	Southern California Air Quality Study
806	SCIAMACHY	Scanning Imaging Absorption Spectrometer for Atmospheric Cartography- a
807		satellite borne instrument
808	SFBA	San Francisco Bay Area
809	SIP	State Implementation Plan
810	SJV(AB)	San Joaquin Valley (Air Basin)
811	SO ₂	sulfur dioxide
812	SO ₄ ⁼	sulfate ion (also, SO ₄)
813	SO _x	total oxidized sulfur, SO ₂ + SO ₄ ⁼
814	SOA	secondary (formed in the atmosphere, not directly emitted) organic aerosol
815	SoCAB	South Coast Air Basin
816	SST	sea surface temperature
817	STP	standard temperature and pressure
818	STT	stratosphere to troposphere
819	SULEV	super ultra-low emitting vehicle
820	SV-OOA	semi-volatile OOA
821	TD-CIMS	Thermal Dissociation Chemical Ionization Mass Spectrometer
822	TD-LIF	Thermal Dissociation Laser Induced Fluorescence
823	TES	EOS Aura Tropospheric Emissions Spectrometer (satellite borne instrument)
824	Twin Otter	Aircraft operated during CalNex by CIRPAS and NOAA
825	µg m ⁻³	micrograms per cubic meter
826	UT/LS	upper troposphere/lower stratosphere
827	VOC(s)	volatile organic compound
828	VOCR	volatile organic compound reactivity with OH
829	VSR	vessel speed reduction
830	W/m ²	watts per square meter
831	WD	weekday
832	WE	weekend
833	WP-3D	Lockheed WP-3D Orion Aircraft operated by NOAA
834	WRF	Weather Research and Forecasting
835	WSOC	water-soluble organic carbon
836		

837 **Summary of Platforms and Sites deployed for CalNex**

838 For the fieldwork portion of CalNex, four instrumented aircraft and a research vessel were
 839 deployed, two major research sites in Pasadena and Bakersfield were established, networks of
 840 ozonesondes and radar wind profilers were operated, and the measurement program at Mt.
 841 Wilson was enhanced. Data from existing networks of air quality and meteorological
 842 measurements and satellite observations were incorporated into the analysis. Figure 2
 843 summarizes the operation periods of the platforms and sites specifically deployed for CalNex.
 844 Appendix A gives details of these resources, including measurements made at each site and
 845 platform. Figures showing flight and ship tracks for the mobile platforms are included. Contact
 846 information and details for accessing data archives is also included.



847 1 2 3 4 5 6 7 8 9 10 11 12 13

848 **Figure 2.** Operations schedule of CalNex 2010 mobile platforms, ground sites and instrument networks

849

DRAFT

850 **Synthesis of Results - Meteorology and Atmospheric Climatology**851 **Response to Question A**852 **QUESTION A**853 **How did the meteorology during CalNex compare to historical norms?**854 **FINDING**

855 ***Finding A1: May 2010 was cooler and wetter than normal, followed by more seasonal***
 856 ***warm temperatures in June. In May deep upper level troughs moved into California***
 857 ***bringing stratospheric intrusions that affected ozone concentrations in the state.***

858 *Analysis: This material is taken from Ryerson et al. (2013)*

859 Local land-sea breeze and mountain valley circulations drive much of the pollutant transport in
 860 California [Bao et al., 2008; Langford et al., 2010; Lu and Turco, 1996]; however, synoptic-scale
 861 meteorology significantly influences both transport patterns and photochemical processing. Here
 862 we provide an overview of the climate and synoptic weather patterns during CalNex. Fast et al.
 863 [2012] provide an overview of the meteorology and transport during June 2010 when the
 864 Carbonaceous Aerosol and Radiative Effects Study (CARES) was conducted with an emphasis
 865 on the Sacramento Valley.

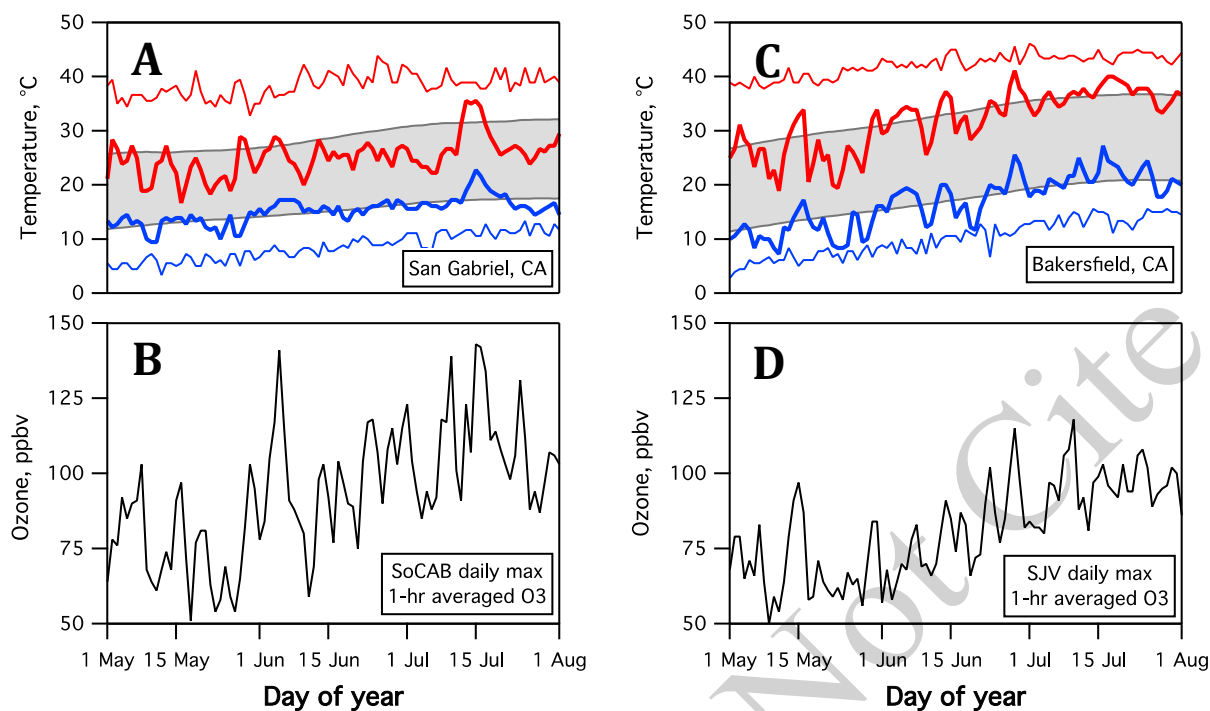
866 Spring 2010 was cooler and wetter than normal over most of California with frequent cold fronts
 867 and upper air disturbances. Fog was present frequently in the coastal areas and western Los
 868 Angeles basin and the monthly average temperature for the State during May was 2.3 °C below
 869 the long-term average of 13.0 °C (Fig. A1; <http://www.wrcc.dri.edu/monitor/cal-mon/>). There
 870 were 62 new record low minimum temperatures and five record high maximum temperatures set
 871 in California during the month. These conditions followed the weakening El Niño, which
 872 dissipated during May as positive sea surface temperature (SST) anomalies decreased across the
 873 equatorial Pacific Ocean and negative SST anomalies emerged across the eastern half of the
 874 Pacific (<http://www.cpc.ncep.noaa.gov>).

875 The synoptic meteorology in May was dominated by a series of deep upper level troughs that
 876 moved off the Pacific Ocean into California on the 9th, 17th, 22nd, and 27th. Cold fronts
 877 associated with these systems brought low temperatures, high winds, and precipitation to many
 878 parts of the State. The first system brought up to 20 cm of snow to the central Sierra Nevada
 879 between Yosemite and Sequoia National Parks. Bishop, CA tied the all-time May low
 880 temperature of -4 °C on 11 May. The second system brought cold and rain to much of the San
 881 Joaquin Valley, with another 8-15 cm of snow to the Sierras. The third system brought more
 882 rain to the southern San Joaquin Valley, and led to record low temperatures at 22 locations
 883 across the State from Redding to Riverside on 23 May; Bishop tied the all-time May record low
 884 of -4 °C once again on that day, and the record lows were tied in both San Francisco and
 885 Sacramento. Storms associated with the 27-29 May trough brought more snow and
 886 thunderstorms to the southern Sierra Nevada and wind gusts in excess of 50 mph to the
 887 Tehachapi Mountains. Deep stratospheric intrusions associated with all four of these troughs
 888 were detected by IONS-2010 ozonesondes [Cooper et al., 2011], and the NOAA WP-3D and
 889 Twin Otter aircraft [Langford et al., 2012; Lin et al., 2012].

890 Conditions became more seasonal in early June, which was slightly drier than average for most
891 of California; the monthly mean temperature was 19.3 °C, only 0.1 °C higher than the long-term
892 average. The weather patterns during the first week of June were dominated by the presence of a
893 low-pressure system over the Gulf of Alaska and an upper-level high-pressure ridge over the
894 southern half of the State. A weak upper level trough over northern California brought record
895 precipitation to Crescent City on both 1 and 2 June (6 cm and 5 cm of rain, respectively) and
896 slightly cooler temperatures to Sacramento and Bakersfield. The warm temperatures and
897 subsiding air associated with the ridge led to the first prolonged ozone episode of the year in the
898 Los Angeles basin, and the highest 8-h ozone concentrations measured in the State during 2010,
899 123 ppbv at Crestline on 5 June. Temperatures warmed to 27 °C (low 80s in °F) in downtown
900 Los Angeles by 5 and 6 June, exceeding 36 °C (high 90s in °F) the central and southern San
901 Joaquin Valley. Warming in the southern Sierras initiated rapid melting of the snowpack and
902 afternoon cumulus formation in the San Joaquin Valley. A series of upper level lows in the
903 Pacific Northwest kept the ridge from growing northward and produced strong winds over much
904 of the State.

905 Temperatures fell over the southern half of the State as another upper-level trough moved into
906 California off the Pacific on 9 June. This system developed into a cutoff low and spawned
907 another tropopause fold with possible influence on surface ozone in southern California on 12
908 June [Lin *et al.*, 2012]. Cooler than normal temperatures persisted through 11 June with light
909 rain over the southern Sierra Nevada and persistent high winds in the Tehachapi Mountains and
910 west side of the San Joaquin Valley. Temperatures rose as high pressure followed the trough
911 with near normal temperatures on 12 June; the first 37.8 °C (100 °F) day in Fresno occurred on
912 14 June, one week later than normal. However, two more upper level troughs on 15-17 and 21-
913 23 June moderated the surface temperatures in the Central Valley through the third week of June,
914 disrupting the local mountain-valley circulation patterns. The final trough brought a few
915 showers to the central San Joaquin Valley and Southern Sierra Nevada during the morning of 25
916 June. A high-pressure ridge built up into California on 26 June as the trough passed through,
917 with 38.3 °C observed in both Bakersfield and Fresno on 27 June, with Fresno tying the record
918 high of 42.2 °C (108 °F) for the date on 28 June.

919 Most of the CalNex field operations had ceased by the end of June, but following its
920 redeployment for a series of flights in the Sacramento and San Joaquin Valleys the NOAA Twin
921 Otter returned to southern California from 30 June through 18 July. Although the July monthly
922 mean temperature for the State was slightly above average, southern California remained cooler
923 than average with frequent coastal fog that persisted into the afternoon. Temperatures were
924 particularly low near the coast and Los Angeles Airport reached monthly record low maximum
925 temperatures twice, with readings of 19 °C on 6 July followed by 18 °C on 8 July. The first six
926 days of July 2010 were cooler than the first six days of January 2010 for Downtown Los
927 Angeles, Los Angeles Airport, Long Beach Airport, Santa Barbara Airport, and Oxnard. San
928 Diego also tied its lowest maximum temperature for July on the 8th with a reading of 64°F. This
929 broke the daily record low maximum temperature of 65°F set in 1902. Temperatures along the
930 coast increased on 13 July and remained several degrees above normal through 18 July.



931
 932 **Figure A1.** A) 2010 daily maximum (thick red line) and daily minimum (thick blue line)
 933 temperature data from a weather station near the CalNex ground site in Pasadena. Also
 934 shown are the record daily maximum (thin red line), record daily minimum (thin blue line)
 935 and average daily maximum and minimum (upper and lower bounds of grey shading)
 936 temperatures for 1979-2010. B) Daily 1-hour averaged ozone maxima in the air basin
 937 containing the Pasadena ground site, obtained from www.arb.ca.gov/aqmis2/aqdselect.php.
 938 C) As in A) using data from a weather station near the CalNex ground site in Bakersfield. D)
 939 As in B) using ozone data in the air basin containing the Bakersfield ground site.

940 **References**

- 941 Bao, J. W., S. A. Michelson, P. O. G. Persson, I. V. Djalalova, and J. M. Wilczak (2008),
 942 Observed and WRF-simulated low-level winds in a high-ozone episode during the Central
 943 California Ozone Study, *J. Appl. Meteorol. Climatol.*, 47(9), 2372–2394.
- 944 Cooper, O. R., et al. (2011), Measurement of western U.S. baseline ozone from the surface to the
 945 tropopause and assessment of downwind impact regions, *J. Geophys. Res.*, 116(D00V03),
 946 doi:10.1029/2011JD016095.
- 947 Fast, J. D., et al. (2012), Transport and mixing patterns over Central California during the
 948 carbonaceous aerosol and radiative effects study (CARES), *Atmos. Chem. Phys.*, 12, 1759–
 949 1783, doi:10.5194/acp-12-1759-2012.
- 950 Langford, A. O., C. J. Senff, R. J. I. Alvarez, R. M. Banta, and R. M. Hardesty (2010), Long-
 951 range transport of ozone from the Los Angeles Basin: A case study, *Geophys. Res. Lett.*,
 952 37(L06807), doi:10.1029/2010GL042507.
- 953 Langford, A. O., J. Brioude, O. R. Cooper, C. J. Senff, R. J. Alvarez II, R. M. Hardesty, B. J.
 954 Johnson, and S. J. Oltmans (2012), Stratospheric influence on surface ozone in the Los
 955 Angeles area during late spring and early summer of 2010, *J. Geophys. Res.*, 117(D00V06),
 956 doi:10.1029/2011JD016766.

- 957 Lin, M., A. M. Fiore, O. R. Cooper, L. W. Horowitz, A. O. Langford, H. Levy II, B. J. Johnson,
958 B. Naik, S. J. Oltmans, and C. J. Senff (2012a), Springtime high surface ozone events over
959 the western United States: Quantifying the role of stratospheric intrusions, *J. Geophys. Res.*,
960 *117* (D00V22), doi:10.1029/2012JD018151.
- 961 Lu, R., and R. P. Turco (1996), Ozone distributions over the Los Angeles Basin: Three-
962 dimensional simulations with the SMOG model, *Atmos. Environ.*, *30*, 4155–4176.
- 963 Ryerson, T. B., et al. (2013), The 2010 California Research at the Nexus of Air Quality and
964 Climate Change (CalNex) field study, *J. Geophys. Res. Atmos.*, *118*, 5830–5866,
965 doi:10.1002/jgrd.50331.
- 966

DRAFT - Do Not Cite

967 **Synthesis of Results - Meteorology and Atmospheric Climatology**

968 **Response to Question B**

969 **QUESTION B**

970 **How did the CalNex air quality measurements fit in the context of historical**
 971 **measurements?**

972 **BACKGROUND**

973 Substantial efforts have been made to improve air quality throughout the U.S. and in California
 974 in particular. Ambient measurements over the past decades demonstrate that these efforts have
 975 resulted in very substantial reductions in a wide spectrum of air pollutants. This is a success that
 976 is perhaps not as widely appreciated as it should be by the general public. The CalNex field
 977 measurements provide a "snapshot" of current air quality, particularly in the South Coast Air
 978 Basin (SoCAB) and the San Joaquin Valley (SJV), that indicates continuing improvement. To
 979 provide a qualitative perspective of the dramatic progress made over the last five decades, Fig.
 980 B1 shows a historical photograph that documents the visibility degradation that often occurred in
 981 the Los Angeles area; such conditions no longer occur. It is perhaps difficult to appreciate



982
 983 **Figure B1.** View of the Los Angeles Civic Center area from January 5, 1948 showing a severe
 984 pollution episode. (Photo: Los Angeles Times; Photographic Archive/UCLA)

985

986 the improvement when it occurs over many decades. The Response to Question E quantifies the
987 improvements in some particular air pollutants of concern.

988 Several CalNex analyses serve to place the CalNex datasets in a historical context, usually as the
989 latest in a series of measurements that define the temporal evolution of air quality in California.
990 *Warneke et al.* [2012] document that the mixing ratios of VOCs and CO have decreased in
991 SoCAB by almost two orders of magnitude during the past five decades at an average annual rate
992 of about 7.5% year⁻¹. This decrease has been accomplished despite approximately a factor of
993 three increase in fuel sales during that time (see Fig. G1 and associated discussion). *Pollack et*
994 *al.* [2013] show that ambient concentrations of NO_x, ozone and other secondary photochemical
995 products in SoCAB have also decreased at varying rates (see Fig. E1 and associated discussion).
996 *Pusede and Cohen* [2012] use sixteen years of observations of ozone, nitrogen oxides, and
997 temperature at sites in SJV to show that as emissions have decreased, photochemical O₃
998 production is transitioning to NO_x-limited chemistry in the southern and central parts of SJV,
999 where O₃ violations are most frequent. *Thompson et al.* [2012] summarize optical properties
1000 measured at the Pasadena site during CalNex, and show that the 2010 aerosol optical densities
1001 were approximately five times lower than measured during the 1987 SCAQS field work [*Adams*
1002 *et al.*, 1990].

1003 These results at least qualitatively demonstrate the major progress in PM control and resulting
1004 visibility improvement in the Los Angeles area in the last two decades, even though there were
1005 substantial differences between the SCAQS and the CalNex measurements. The SCAQS
1006 measurements were from a comparable season (i.e., 10 summer days during four months in
1007 1987), but at a different site in Claremont CA. Most importantly, the sample treatment before
1008 measurement differed from that employed during CalNex [*Thompson et al.*, 2012].

1009 FINDING

1010 ***Finding B1: While nearly all atmospheric pollutants have decreased in California, ethanol***
1011 ***is an exception because its use in gasoline has recently increased markedly. During CalNex***
1012 ***ethanol was the VOC with the highest ambient concentrations in SoCAB. Acetaldehyde***
1013 ***(an air toxic) is a secondary product of the atmospheric oxidation of ethanol, but its***
1014 ***concentration has continued to decrease.***

1015 The use of ethanol as a transportation fuel in the U.S. increased significantly from 2000–2009,
1016 and in 2010 nearly all gasoline contained 10% ethanol. In accordance with this increased use,
1017 atmospheric measurements of VOCs in SoCAB during CalNex were significantly enriched in
1018 ethanol compared to measurements in urban outflow in the Northeast U.S. in 2002 and 2004 [*de*
1019 *Gouw et al.*, 2012]. Mixing ratios of acetaldehyde, an atmospheric oxidation product of ethanol,
1020 decreased between 2002 and 2010 in Los Angeles. Previous work [e.g., *Jacobson*, 2007] has
1021 suggested that large-scale use of ethanol may have detrimental effects on air quality. While no
1022 evidence for this has been identified in the U.S., this study indicates that ethanol has become a
1023 ubiquitous compound in urban air and that better measurements are required to monitor its
1024 increase and effects.

1025

1026

1027

1028 **References**

- 1029 Adams, K.M., Davis, L.I., Japar, S.M., Finley, D.R. (1990) Real-time, in situ measurements of
1030 atmospheric optical absorption in the visible via photoacoustic spectroscopy - IV. Visibility
1031 degradation and aerosol optical properties in Los Angeles. *Atmos. Environ.* 24A, 605-610.
- 1032 de Gouw, J. A., J. B. Gilman, A. Borbon, C. Warneke, W. C. Kuster, P. D. Goldan, J. S.
1033 Holloway, J. Peischl, and T. B. Ryerson (2012), Increasing atmospheric burden of ethanol in
1034 the United States, *Geophys. Res. Lett.*, 39(L15803), doi:10.1029/2012GL052109.
- 1035 Jacobson, M. Z. (2007), Effects of ethanol (E85) versus gasoline vehicles on cancer and
1036 mortality in the United States, *Environ. Sci. Technol.*, 41, 4150–4157,
1037 doi:10.1021/es062085v.
- 1038 Pollack, I. B., T. B. Ryerson, M. Trainer, J. A. Neuman, J. M. Roberts, and D. D. Parrish (2013),
1039 Trends in ozone, its precursors, and related secondary oxidation products in Los Angeles,
1040 California: A synthesis of measurements from 1960 to 2010, *J. Geophys. Res. Atmos.*, 118,
1041 5893–5911, doi:10.1002/jgrd.50472.
- 1042 Pusede, S.E., and R.C. Cohen (2012), On the observed response of ozone to NO_x and VOC
1043 reactivity reductions in San Joaquin Valley California 1995–present, *Atmos. Chem. Phys.*, 12,
1044 8323–8339, www.atmos-chem-phys.net/12/8323/2012/doi:10.5194/acp-12-8323-2012
- 1045 Thompson, J. E., P. L. Hayes, J. L. Jimenez, K. Adachi, X. Zhang, J. Liu, R. J. Weber, and P. R.
1046 Buseck (2012), Aerosol optical properties at Pasadena, CA during CalNex 2010, *Atmos.*
1047 *Environ.*, 55, 190-200, doi:10.1016/j.atmosenv.2012.03.011.
- 1048 Warneke, C., J. A. de Gouw, J. S. Holloway, J. Peischl, T. B. Ryerson, E. Atlas, D. Blake, M.
1049 Trainer, and D. D. Parrish (2012), Multi-year trends in volatile organic compounds in Los
1050 Angeles, California: five decades of improving air quality, *J. Geophys. Res.*, 117(D00V17),
1051 doi:10.1029/2012JD017899.
- 1052
- 1053

1054 **Synthesis of Results - Meteorology and Atmospheric Climatology**

1055 **Response to Question C**

1056 **Question C**

1057 **How do the CalNex air quality measurements in late spring and early summer relate to the**
 1058 **peak ozone concentrations in summer and the peak PM2.5 concentrations in winter?**

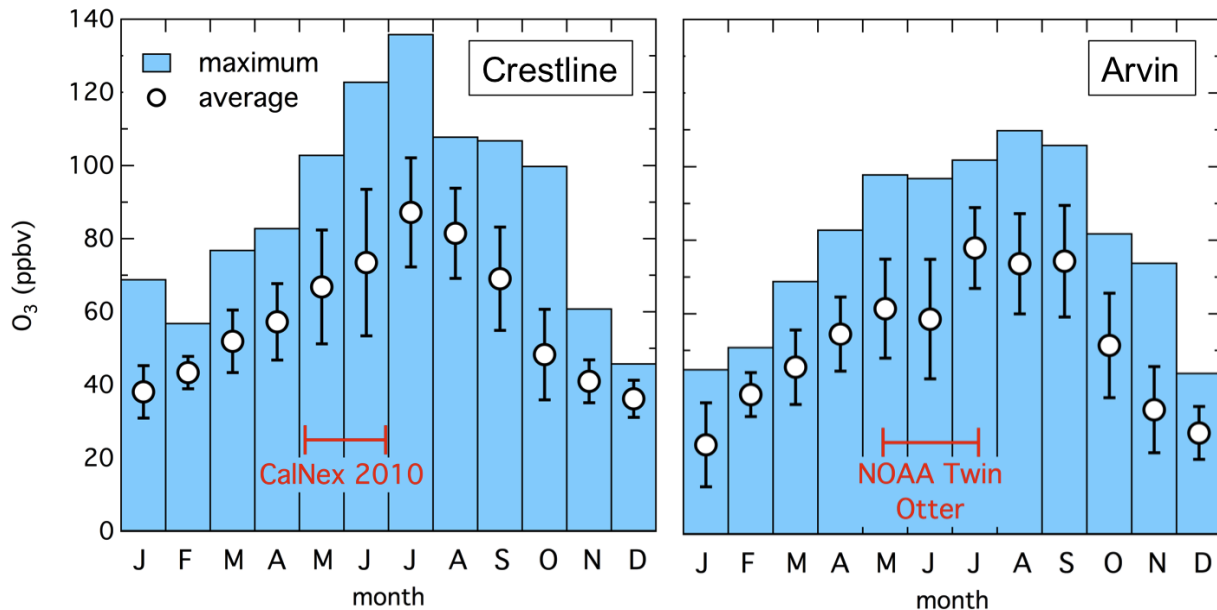
1059 **FINDINGS**

1060 ***Finding C1:* The CalNex fieldwork was conducted primarily in May and June, 2010, but**
 1061 **included some aircraft flights through mid-July. The measurements provide**
 1062 **characterization of the photochemical environment in southern California, particularly in**
 1063 **the SoCAB during its most active period.**

1064 ***Finding C2:* The CalNex measurements cannot be used to characterize the peak PM2.5**
 1065 **concentrations observed in the Central Valley in winter. However, they do provide a guide**
 1066 **for further studies of this important phenomenon.**

1067 *Analysis: D.D. Parrish, unpublished*

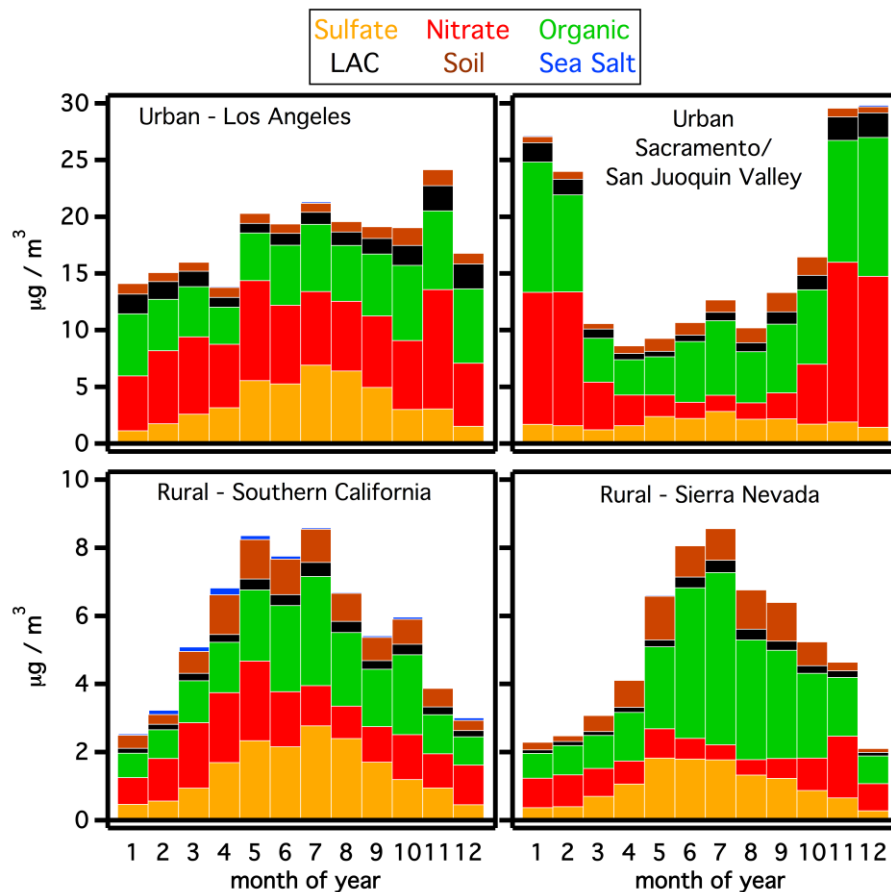
1068 In most urban and rural areas of California maximum ozone and PM2.5 concentrations are
 1069 generally observed in summer (see e.g., Figs. C1 and C2); one major exception to this generality
 1070 is that PM2.5 concentrations are at a maximum in winter in the Central Valley. Figure C1 shows
 1071 O₃ data from Crestline, a monitoring station in the SoCAB that often records the highest
 1072 concentrations in the state, and from Arvin, a monitoring station that often records the highest
 1073 concentrations in the southern in SJV. Figure C2 reports PM2.5 data from 4 California regions.



1074 **Figure C1.** Monthly averages with standard deviations (symbols) and monthly maxima
 (bars) of daily maximum 8-hr ozone concentrations at the Crestline monitoring site in the
 SoCAB and the Arvin monitoring site in SJV for 2009-2011. The red bars indicate the
 time period of the majority of the CalNex fieldwork (left panel) and the NOAA Twin Otter
 deployment (right panel).

1075

1076 On average the highest O₃ in SoCAB was observed in July and August, with June having greater
 1077 variability (and a higher maximum) than August. In the SJV the highest O₃ is shifted to
 1078 somewhat later in the year, with July, August and September exhibiting similar concentrations.
 1079 In Los Angeles and many rural areas of California, maximum PM_{2.5} concentrations occur in
 1080 May through September (with perhaps an anomalous peak in November in SoCAB).



1081 **Figure C2.** Comparison of monthly mean fine aerosol composition in urban and rural
 1082 areas in California for 2005-2008 [Hand *et al.*, 2011]. The urban data are from US
 1083 EPA's Speciated Trend (now Chemical Speciation) Network, and the rural data are from
 1084 the Interagency Monitoring of Protected Visual Environments (IMPROVE) network.
 1085 "LAC" stands for light absorbing carbon.
 1086

1087
 1088 The chosen focus of CalNex was on the photochemically active season; due to availability of
 1089 platforms, most of the measurements on the airborne and ship platforms, as well as at the two
 1090 major sites in Pasadena and Bakersfield were conducted in May and June, 2010, with the NOAA
 1091 Twin Otter continuing operations until July 19 (see CalNex Operations Schedule on pg. 17).

1092 Major photochemical episodes did occur during CalNex. In the SoCAB the maximum daily 8-
 1093 hour O₃ average exceeded 75 ppbv on 5 of 31 days in May and 21 of 30 days in June. The
 1094 highest 8-hour maximum O₃ (123 ppbv) concentration recorded in California during 2010 was at
 1095 the Crestline site on June 5 (a Saturday). The Central Valley experienced lower O₃
 1096 concentrations. At the Arvin-Bear Mountain Blvd site during May and June, maximum daily 8-
 1097 hour O₃ average exceeded 75 ppbv on 2 and 4 days, respectively, with a 90 ppbv maximum. The
 1098 NOAA Twin Otter operated through July 19, and on 9 days in this period the Arvin site recorded

1099 maximum daily 8-hour O₃ average exceeding 75 ppbv, with a 93 ppbv maximum. The CalNex
1100 measurements do provide characterization of the photochemical environment in southern
1101 California, in SoCAB during its most active period, but are perhaps less useful for this purpose in
1102 the San Joaquin Valley (SJV).

1103 Figure C2 shows that PM_{2.5} is at or near its maximum during the CalNex field study period in
1104 most of California, but that a strong PM_{2.5} maximum occurs in winter in the Central Valley.
1105 Hence the CalNex measurements provide characterization of the maximum PM_{2.5} levels in the
1106 SoCAB and much of the rest of California, but not in the Central Valley. However, the CalNex
1107 measurements do provide a guide for future research into PM_{2.5} in the SJV. Figure C2 indicates
1108 that PM in the Central Valley is dominated by organic matter and aerosol nitrate throughout the
1109 year. CalNex provides a detailed characterization of these PM components during May and
1110 June. It will be useful to contrast the wintertime organic character with that measured in CalNex
1111 to determine if it is the same emissions and transformations that are responsible for this organic
1112 matter throughout the year. Aerosol nitrate is believed to be predominately ammonium nitrate
1113 (NH₄NO₃), which was characterized in SJV during CalNex (See Question I Response). The
1114 CalNex measurements demonstrate that there was a large excess of ammonia, and that NH₄NO₃
1115 concentrations were limited by the availability of nitric acid in May and June. A similar
1116 situation is reasonably hypothesized to exist in winter, since the emissions of nitric acid
1117 precursors (i.e. NO_x) are not expected to be significantly larger, and conversion to nitric acid is
1118 not expected to be faster. Hence, the major reason for higher PM in winter is reasonably
1119 hypothesized to be less dilution due to a shallow boundary layer and slower advection in winter,
1120 which allows PM to accumulate the very high observed concentrations. During January and
1121 February 2013 the NASA DISCOVER AQ (<http://discover-aq.larc.nasa.gov/>) field study was
1122 conducted in the Central Valley, and one of the goals of this study was to investigate these
1123 hypotheses.

1124 **References**

1125 Hand, J. L., Copeland, S. A., Day, D. E., Dillner, A. M., Indresand, H, Malm., W. C., McDade,
1126 C. E., Moore, C. T., Pitchford, M. L., Schichtel, B. A., Watson, J. G., 2011. Spatial and
1127 seasonal patterns and temporal variability of haze and its constituents in the United States—
1128 Report V. IMPROVE Reports. Available online:
1129 http://vista.cira.colostate.edu/improve/Publications/improve_reports.htm (accessed 02.15.13).

1130

1131

1132

1133

1134

1135

1136 **Synthesis of Results - Meteorology and Atmospheric Climatology**1137 **Response to Question D**1138 **QUESTION D**

1139 **What were the global “background” concentrations observed during CalNex and how did**
 1140 **they vary spatially and temporally?**

1141 **BACKGROUND**

1142 An important consideration for O₃ and PM air quality is transport of pollutants into a particular
 1143 region from upwind regions or continents [e.g. *Dentener et al.*, 2011]. In California the transport
 1144 issues for O₃ and PM are fundamentally different. For PM the species of concern (see Fig. C2)
 1145 are emitted or produced close to source regions before being transported downwind. Long-range
 1146 transport from Asia and other upwind continents is observed in the form of discrete plumes in the
 1147 free troposphere with pollutant concentrations significantly greater than those usually
 1148 encountered. These plumes often contain dust or smoke from large wild fires. Often such a
 1149 plume can be directly attributed to a particular upwind source, and in favorable cases particular
 1150 plumes can be tracked in satellite data over periods of several days. The concept of a global or
 1151 even regional background is not applicable to PM as many air masses arriving in California carry
 1152 negligible PM concentrations. Nevertheless, plumes of transported PM can potentially affect
 1153 California's air quality; for example *Jaffe et al.* [2003] report an episode when dust transported
 1154 from Asia increased surface PM_{2.5} concentrations by up to 20 µg/m³ over large regions of the
 1155 U.S.

1156 **POLICY RELEVANCE**

1157 Emissions from within California are only partially responsible for exceedances of O₃ and PM
 1158 air quality standards in the state. Transport of "background" (better referred to as "baseline")
 1159 concentrations into California from over the Pacific Ocean can substantially contribute to local
 1160 concentrations, even during exceedance episodes. Reliable and effective air quality modeling of
 1161 O₃ and PM must accurately include the influence of baseline concentrations of PM, O₃, and its
 1162 important precursors transported into the modeling domain.

1163 In contrast, O₃ is a tropospheric species resulting from a complex manifold of sources and sinks.
 1164 Injection from the stratosphere is a direct source. Ozone is also a secondary pollutant produced
 1165 from precursor emissions such as CO, VOCs and NO_x. Production occurs not only close to
 1166 source regions, but also continues during long-range transport due to photochemical production
 1167 from transported precursors. Chemical and physical loss processes (dry and wet deposition, and
 1168 reactions on aerosols) and mixing with air of different composition occur during transport. Air
 1169 transported ashore along the California coast carries a complex mixture of ozone produced over
 1170 time scales ranging from the previous few minutes to more than thirty days earlier, and from
 1171 ozone precursors emitted from nearby ships or distant sources such as Asia or Europe. Thus,
 1172 there are no clear source and receptor relationships. Ozone imported into California will include
 1173 contributions from many anthropogenic and natural sources, importantly including the
 1174 stratosphere. The spectrum of O₃ and its precursor concentrations in the air masses arriving at
 1175 California from over the Pacific generally defines the "background" concentrations that affect O₃
 1176 air quality in the state. However, this "background" is not "global" in the sense that this

1177 "background" is not uniform over the globe, and it is not a "natural background" as these
 1178 concentrations have been strongly perturbed by anthropogenic influences. Here we use the term
 1179 "baseline" to refer to these "background" concentrations, and take it to mean the concentrations
 1180 measured in air masses transported into California that have not been influenced by local
 1181 emissions or loss processes. The Responses to Questions O and T address some additional
 1182 features of baseline O₃ entering California.

1183 Recent studies have demonstrated that baseline O₃ flowing into California has been increasing
 1184 since the 1980s both at the surface [Parrish *et al.*, 2009] and in the free troposphere [Cooper
 1185 *et al.*, 2010], even as California's emissions of O₃ precursors have been decreasing. As a result
 1186 baseline O₃ constitutes an increasing proportion of ambient concentrations when the NAAQS for
 1187 O₃ is exceeded in California [NRC, 2009; Dentener *et al.*, 2011]. Hence, accurate treatment of
 1188 lateral boundary conditions for regional air quality models, which are determined by these
 1189 baseline concentrations, is increasingly important.

1190 Ozone and PM are the two criteria pollutants whose baseline concentrations are of sufficient
 1191 magnitude to have air quality significance in California. In addition, CO and peroxyacetyl
 1192 nitrate (PAN) have sufficiently long lifetimes (at least in the upper troposphere for PAN) that
 1193 transported concentrations can affect downwind photochemistry. CO and PAN are important
 1194 because CO is an O₃ precursor and PAN is a reservoir species for NO_x, another O₃ precursor.
 1195 As air warms during descent into the boundary layer of California, PAN decomposes to release
 1196 NO_x, which can then enter the photochemical O₃ formation process. The variability of the
 1197 baseline concentrations of these four species is great enough that the varying boundary
 1198 conditions for each can significantly affect the results of regional air quality modeling. Methane
 1199 is another important O₃ precursor whose transported concentrations affect photochemical O₃
 1200 formation; however the variability of its baseline concentrations is sufficiently small that
 1201 boundary conditions are well represented by monthly mean concentrations measured at NOAA's
 1202 baseline observatory at Trinidad Head CA; these data are available from
 1203 <http://www.esrl.noaa.gov/gmd/dv/data/>.

1204 Seasonally and interannually varying baseline concentrations entering California cannot be
 1205 quantified based solely on the CalNex data sets. The following discussion relies upon other
 1206 recent work in addition to the CalNex data.

1207 FINDINGS

1208 **Finding D1:** *Baseline concentrations of air quality relevant species have such large*
 1209 *variability on time scales of days that average vertical profiles of baseline concentrations*
 1210 *provide only poor quantification of boundary conditions for regional air quality modeling.*

1211 Cooper *et al.* [2011] report the results from IONS- 2010 (Intercontinental Chemical Transport
 1212 Experiment Ozonesonde Network Study), the seven-site network (one in southern British
 1213 Columbia and six in California) that launched near-daily ozonesondes between May 10 and June
 1214 19 during CalNex. To quantify the baseline ozone impacting California, four of the sites were
 1215 positioned very close to the shore along a 960 km transect. Figure D1 shows vertical O₃ profiles
 1216 measured at Trinidad Head CA during CalNex (white lines), and compares them with data
 1217 collected during the previous years of operation (black lines). A notable feature of Fig. D1 is the
 1218 high variability of measured O₃ at all altitudes. For example, the 5th to 95th percentiles of the
 1219 data span the range from < 20 to > 40 ppbv at the surface, and from ≈ 25 to > 80 ppbv at 2km

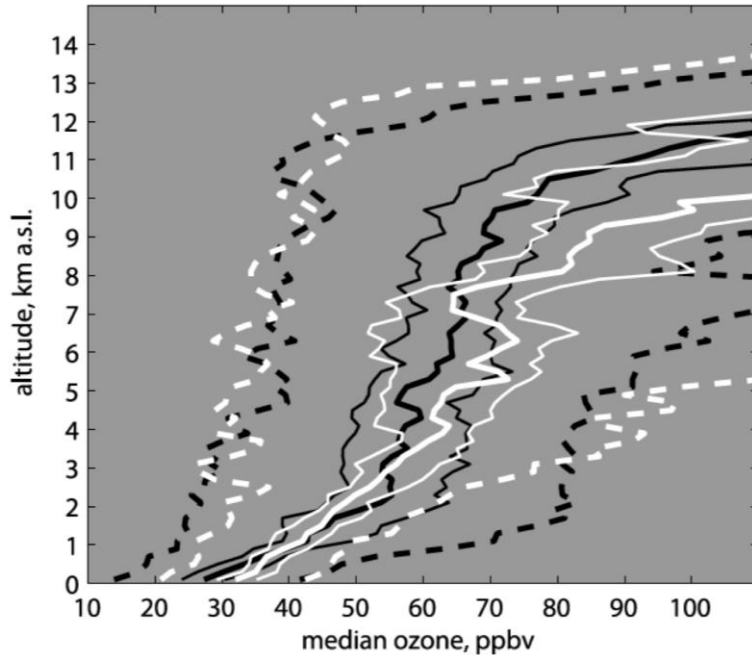
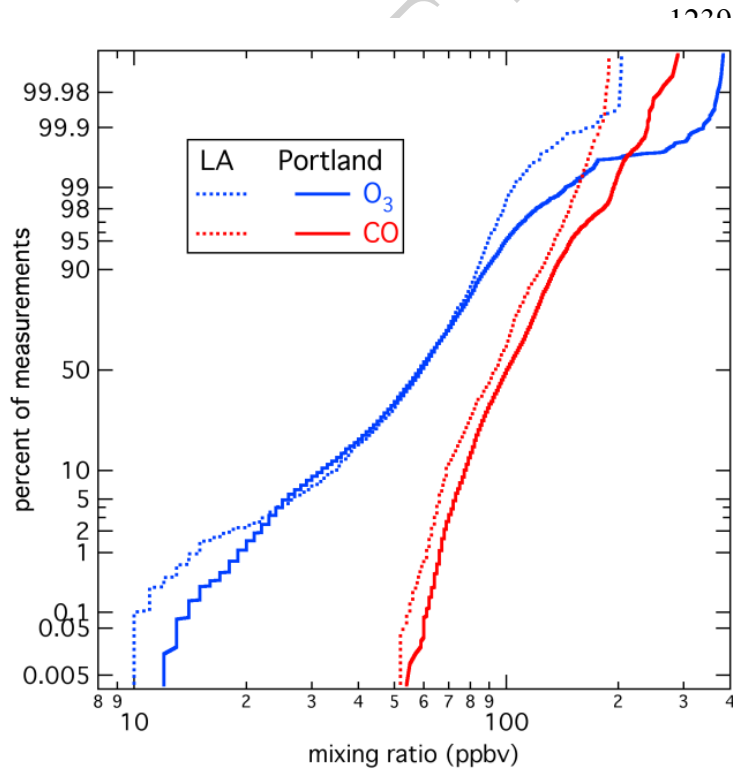


Figure D1. Ozone distributions above Trinidad Head for May–June 2004–2009 (black) and May–June 2010 (white) showing from left to right: 5th, 33rd, 50th, 67th and 95th ozone percentiles. (Reproduced from Cooper *et al.*, 2011).

altitude. Parrish *et al.* [2010] found that baseline O₃ transported in the lowest 2 km does impact the surface of the northern Sacramento Valley, so this variability in baseline O₃ must be incorporated into regional air quality modeling if it is to capture this important source of variability in observed surface ozone measurements.

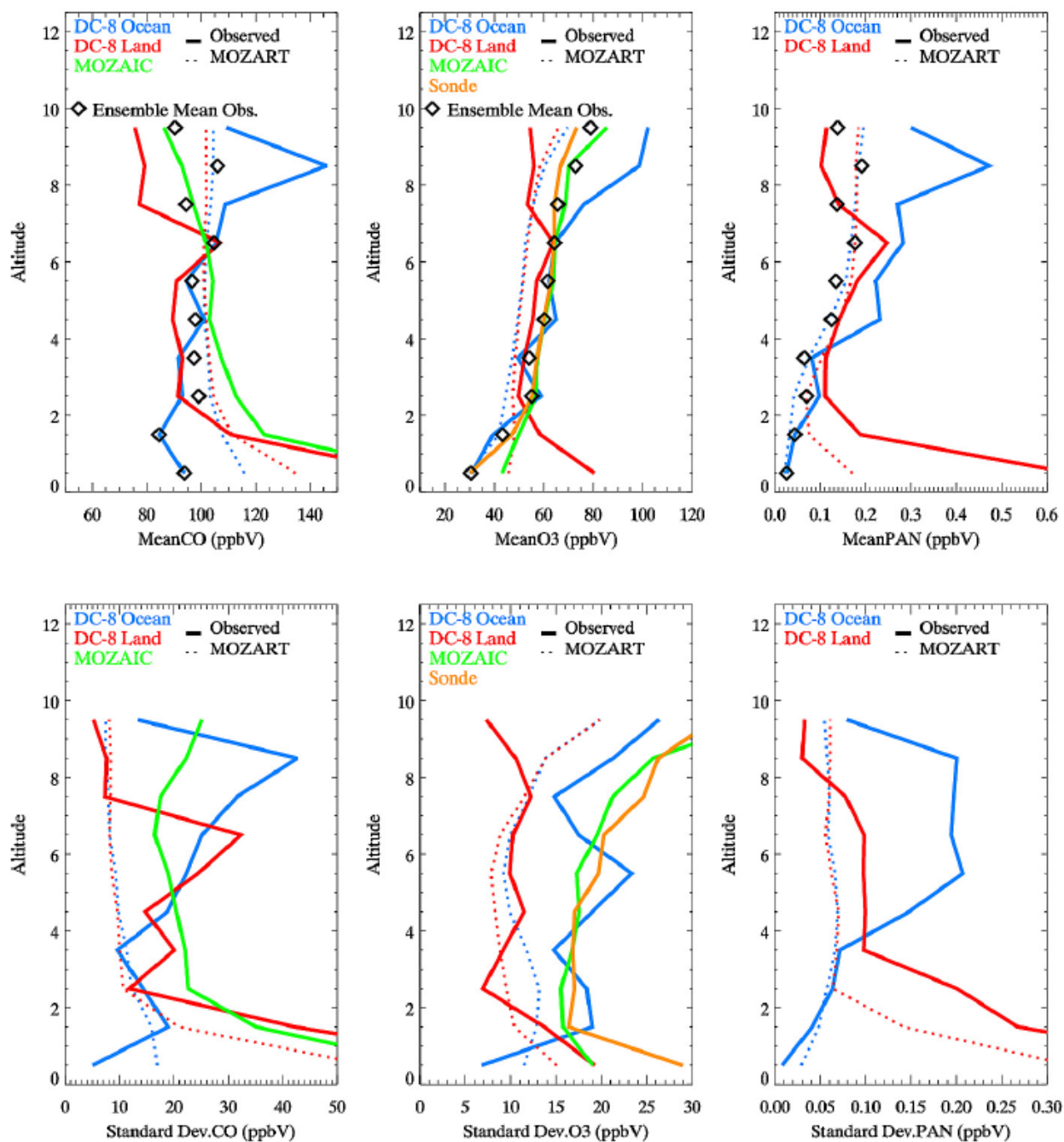
1230 The high variability of baseline O₃ is also reflected in the MOZAIC (Measurements of OZone,
 1231 water vapor, carbon monoxide and nitrogen oxides by in- service Airbus airCRAFT) program
 1232 [Thouret *et al.*, 2006] measurements along the North American west coast. Figure D2 shows
 1233 cumulative probability distribution plots for O₃ and CO measurements on profiles (aircraft
 1234 descents and ascents) over two airports. The variability of O₃ in Fig. D2 is consistent with that
 1235 shown in Fig. D1. The variability of CO is lower with the 5th to 95th percentiles of the data
 1236 between 2 and 10 km above Los Angeles spanning a range of approximately 55 to 135 ppbv in
 1237 summer.
 1238



Pfister et al. [2011] combined in situ measurements collected during the June 2008 ARCTAS-CARB flights of the NASA DC-8 aircraft, data from the MOZAIC program and ozonesondes with satellite retrievals of carbon monoxide and ozone by the EOS Aura Tropospheric Emissions

Figure D2. Summertime probability distribution functions of CO (red lines) and O₃ (blue lines) measured between 2 and 10 km altitude by MOZAIC (<http://mozaic.aero.obs-mip.fr>) aircraft on descents into and ascents out off Portland, Oregon (solid lines) and Los Angeles, California (dotted lines) on the U.S. west coast. (Reproduced from Dentener *et al.*, 2011).

1248 Spectrometer (TES) satellite. They report mean and standard deviation of summertime baseline
 1249 concentrations for O₃, CO and PAN synthesized from these results (Fig. D3). These results also
 1250 indicate large relative variability of these important gas phase species, including PAN.

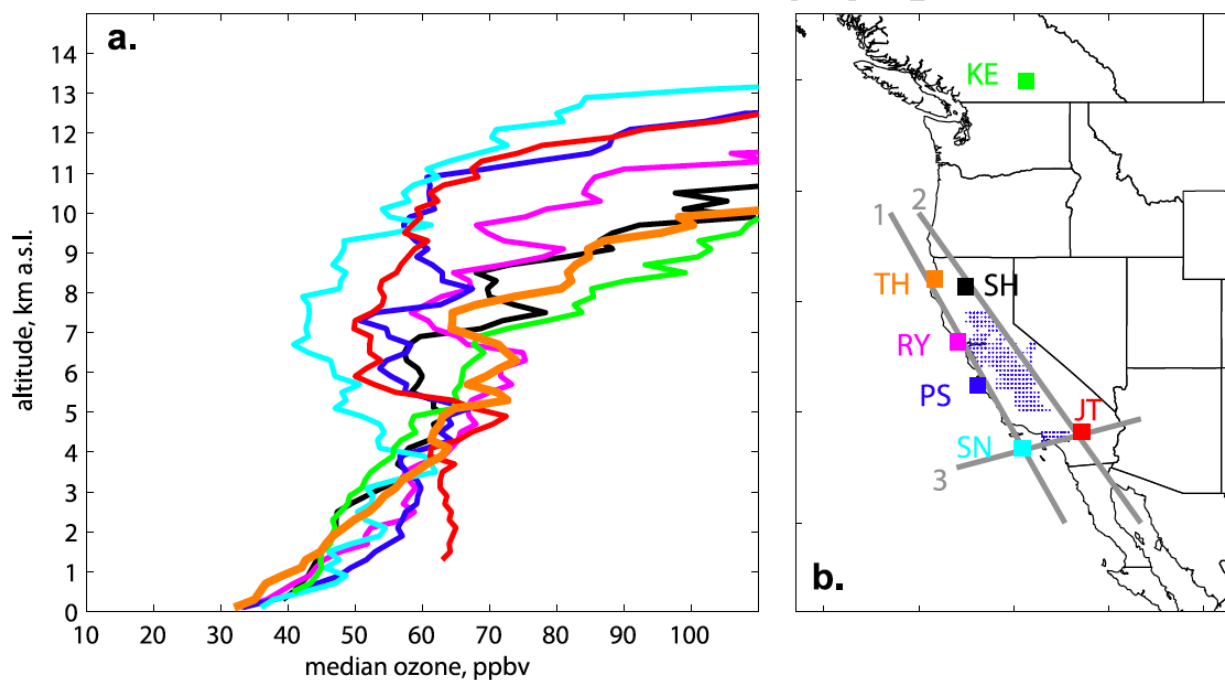


1251

Figure D3. Mean and standard deviation of vertical profiles for CO, O₃ and PAN from the different data sets: DC8 over the ocean (blue), DC-8 over land (red), MOZAIC (green) and ozonesondes (orange). Observations are shown in thick solid lines, and model averages in dotted lines. The ensemble mean observed profile is denoted by symbols. For altitudes <2 km the ensemble mean is derived from DC-8 over ocean and ozonesonde data only. Except for MOZAIC and sonde data, the data have been filtered to exclude California fire influence. (Reproduced from *Pfister et al.*, 2011).

1252 **Finding D2:** *Along the west U.S. coast there is little indication of significant latitudinal*
 1253 *gradient in average baseline concentrations.*

1254 The available evidence indicates that there is little latitudinal gradient in baseline concentrations
 1255 transported ashore along the west coast of California. The IONS- 2010 measurements (Fig. D4)
 1256 indicate similar median ozone profiles below 4 km at the seven sites with only the inland site at
 1257 Joshua Tree (JT) showing strong ozone enhancements above baseline. These enhancements are
 1258 expected since the JT site receives outflow from the Los Angeles basin, and thus measurements
 1259 there do not represent baseline conditions. Among the four coastal sites, there is a small
 1260 latitudinal gradient of ozone below 1 km, with Point Sur (PS) and San Nicolas Island (SN)
 1261 having 13% and 26% more ozone than Trinidad Head (TH), respectively (a statistically
 1262 significant difference based on the total mass of ozone between 1025 and 900 hPa); Point Reyes
 1263 (RY) has more ozone than TH by an insignificant 5%. The large variability in O₃ above 4 km in
 1264 Fig. 4 is likely due to different impacts of transport of stratospheric O₃ the various sites. The
 1265 CalNex period was a particularly active period for such stratospheric input [Cooper *et al.*, 2011].
 1266 The surface impact of these relatively high altitude O₃ enhancements is discussed in the response
 1267 to Question O.



1268 **Figure D4.** (a) Median ozone profiles above the IONS- 2010 ozonesonde sites using all
 1269 available profiles. Line colors correspond to the site label colors in Figure 4b. (b) Locations
 1270 of the seven IONS- 2010 ozone sonde sites. Gray transects indicate locations of the three
 1271 ozone vertical cross sections with 1) representing the coastal baseline transect.

1272
 1273 Figure D2 indicates generally similar O₃ and CO distributions below 10 km at Portland OR and
 1274 Los Angeles CA. Through most of the distribution CO is approximately 5 to 10 ppbv higher at
 1275 Portland, with the upper 2 percentiles of the plumes enhanced by about 40 to 60 ppbv. Through
 1276 most of the distribution, O₃ is nearly identical above the two cities. The O₃ differences at the
 1277 lowest concentrations likely represent stronger local influences at Los Angeles or indicate greater
 1278 tropical influence bringing lower O₃ concentrations to Los Angeles than Portland. The

1279 differences at the highest concentrations likely represent stronger stratospheric input at high
 1280 altitudes above more northerly Portland, where the tropopause is lower; this pattern is consistent
 1281 with the median IONS- 2010 O₃ profiles shown in Fig. 5 of *Cooper et al.* [2011].

1282 **Finding D3: Global chemical climate models (GCMs) capture a significant fraction of the**
 1283 **variability of the baseline concentrations, and hence can provide improved boundary**
 1284 **conditions for regional air quality modeling.**

1285 Pfister et al. [2011] show that global models can calculate time and space varying chemical
 1286 boundary conditions that provide useful input to regional models for O₃, CO and PAN.
 1287 Sensitivity simulations with a regional model with boundary conditions derived from a global
 1288 model show that the temporal variability in the pollution inflow does impact modeled surface
 1289 concentrations in California. However, the global model captured only about half of the
 1290 observed free tropospheric variability, so inclusion of the varying boundary conditions likely still
 1291 underestimate peak surface concentrations and the variability associated with long-range
 1292 pollution transport.

1293 As briefly discussed in the response to Question U, provision of lateral boundary conditions to a
 1294 regional air quality model from a global model that included assimilation of upper-tropospheric
 1295 satellite O₃ data did improve the correlation between observed and predicted ground level ozone,
 1296 but it also significantly increased the positive bias of the model. In contrast, the correlation
 1297 between observed and predicted ground level PM was negatively impacted by use of boundary
 1298 conditions provided by the global model.

1299 In summary, it is recognized that baseline concentrations of PM, O₃ and its precursors vary
 1300 markedly in time and location. Thus, providing spatially varying lateral boundary conditions to
 1301 regional air quality models is important for improving their performance. Some progress has
 1302 been made toward achieving this goal through the use of global models, particularly with the
 1303 incorporation of satellite data assimilation, but much work remains to be done before reliable
 1304 procedures can be implemented to effect this process on a routine basis.

1305 References

- 1306 Cooper, O. R., et al. (2011), Measurement of western U.S. baseline ozone from the surface to the
 1307 tropopause and assessment of downwind impact regions, *J. Geophys. Res.*, 116, D00V03,
 1308 doi:10.1029/2011JD016095.
- 1309 Cooper, O. R., et al. (2010), Increasing springtime ozone mixing ratios in the free troposphere
 1310 over western North America, *Nature*, 463, 344–348, doi:10.1038/nature08708.
- 1311 Dentener, F., T. Keating, and H. Akimoto (Eds.) (2011), *Hemispheric Transport of Air Pollution*
 1312 *2010: Part A: Ozone and Particulate Matter, Air Pollut. Stud.*, vol. 17, United Nations, New
 1313 York.
- 1314 Jaffe, D., et al. (2003), The 2001 Asian Dust Events: Transport and Impact on Surface Aerosol
 1315 Concentrations in the U.S., *EOS, Transactions American Geophysical Union*, 84(46), 501-
 1316 507.
- 1317 National Research Council (NRC) (2009), *Global Sources of Local Pollution: An Assessment of*
 1318 *Long- Range Transport of Key Air Pollutants to and From the United States*, 248 pp., Nat.
 1319 Acad., Washington, D. C.

- 1320 Parrish, D. D., D. B. Millet, and A. H. Goldstein (2009), Increasing ozone in marine boundary
1321 layer inflow at the west coasts of North America and Europe, *Atmos. Chem. Phys.*, *9*, 1303–
1322 1323, doi:10.5194/acp-9-1303-2009.
- 1323 Parrish, D. D., K. C. Aikin, S. J. Oltmans, B. J. Johnson, M. Ives, and C. Sweeny (2010), Impact
1324 of transported background ozone inflow on summertime air quality in a California ozone
1325 exceedance area, *Atmos. Chem. Phys.*, *10*, 10,093–10,109, doi:10.5194/acp-10-10093-2010.
- 1326 Pfister, G. G., D. Parrish, H. Worden, L. K. Emmons, D. P. Edwards, C. Wiedinmyer, G. S.
1327 Diskin, G. Huey, S. J. Oltmans, V. Thouret, A. Weinheimer and A. Wisthaler (2011)
1328 Characterizing summertime chemical boundary conditions for airmasses entering the US
1329 West Coast, *Atmos. Chem. Phys.*, *11*, 1769–1790, 2011, doi:10.5194/acp-11-1769-2011.
- 1330 Thouret, V., J.- P. Cammas, B. Sauvage, G. Athier, R. Zbinden, P. Nédélec, P. Simon, and F.
1331 Karcher (2006), Tropopause referenced ozone climatology and inter- annual variability
1332 (1994–2003) from the MOZAIC programme, *Atmos. Chem. Phys.*, *6*, 1033–1051,
1333 doi:10.5194/acp-6-1033-2006.
1334
1335
1336
1337
1338
1339
1340

1341 **Synthesis of Results - Emissions**1342 **Response to Question E**1343 **QUESTION E**

1344 **How effective have historical air pollution control efforts been? How effective have specific**
 1345 **emission control measures been?**

1346 **BACKGROUND**

1347 Substantial public resources have been expended to improve air quality throughout the U.S., and
 1348 in California in particular. Ambient measurements demonstrate that these resources have
 1349 resulted in very significant reductions in a wide spectrum of air pollutants. The following
 1350 utilizes historical ambient pollutant measurements to document the long-term improvement of air
 1351 quality in the SoCAB, and utilizes a specific CalNex investigation to demonstrate the efficacy of
 1352 a recent pollution control measure.

1353 **POLICY RELEVANCE**

1354 When the public is asked to invest resources in air quality improvement, it is important to
 1355 demonstrate that the policies implemented are effective in achieving their goals. Further,
 1356 examination of long-term pollutant trends can guide us toward effective policy approaches (and
 1357 perhaps help us avoid ineffective policies).

1358 In both California and the U.S., criteria air pollutants (i.e., those subject to regulation setting
 1359 permissible ambient atmospheric levels) include both primary (i.e., directly emitted) and
 1360 secondary (i.e., formed within the atmosphere) pollutants. The former include nitrogen oxides
 1361 (NO_x), carbon monoxide (CO) and sulfur dioxide (SO_2) while the latter includes ozone (O_3).
 1362 Particulate matter is a criteria air pollutant with both primary and secondary sources (see
 1363 Response to Question N). Volatile organic compounds (VOCs) are not criteria pollutants, but
 1364 their emissions from various sources are subject to regulation because they react in the
 1365 atmosphere to create criteria pollutants. Finally, other secondary pollutants are of concern
 1366 although not subject to specific regulation; two examples are peroxyacetyl nitrate (PAN), a
 1367 species first identified as a component of Los Angeles smog that was a particularly important eye
 1368 irritant [Leighton, 1961], and nitric acid (HNO_3), an important contributor to acid precipitation
 1369 and a precursor to ammonium nitrate, which is an important component of PM. Both PAN and
 1370 HNO_3 are atmospheric oxidation products of NO_x , while O_3 is a product of atmospheric
 1371 photochemistry involving NO_x , VOCs and CO.

1372 **FINDINGS**

1373 ***Finding E1:* The five decades of air pollution controls implemented in the SoCAB have**
 1374 **produced remarkable improvement in air quality, with substantial reductions in both**
 1375 **primary and secondary air pollutants.**

1376 *Pollack et al.* [2013] show that decreases in O_3 concentrations observed in SoCAB over the past
 1377 five decades are correlated with decreases in abundances of its precursors, NO_x , CO, and VOCs
 1378 (Fig. E1). Ozone precursors have been widely investigated and well characterized in the SoCAB
 1379 with measurements dating back to 1960. *Pollack et al.* [2013] compiled an extensive SoCAB

1380 data set spanning 1960 to 2010 including ambient measurements from the CARB surface
 1381 monitoring network, mobile roadside monitors, ground-based field studies and chemically-
 1382 instrumented research aircraft.

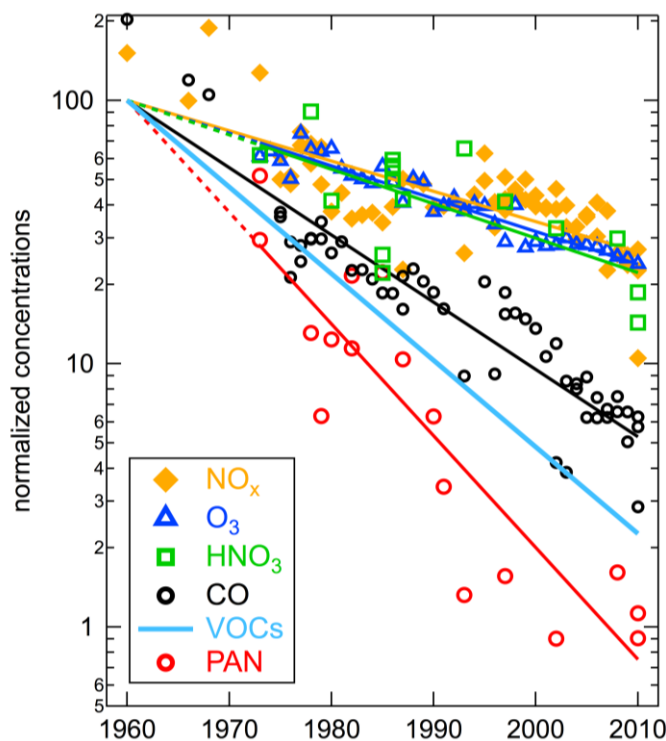
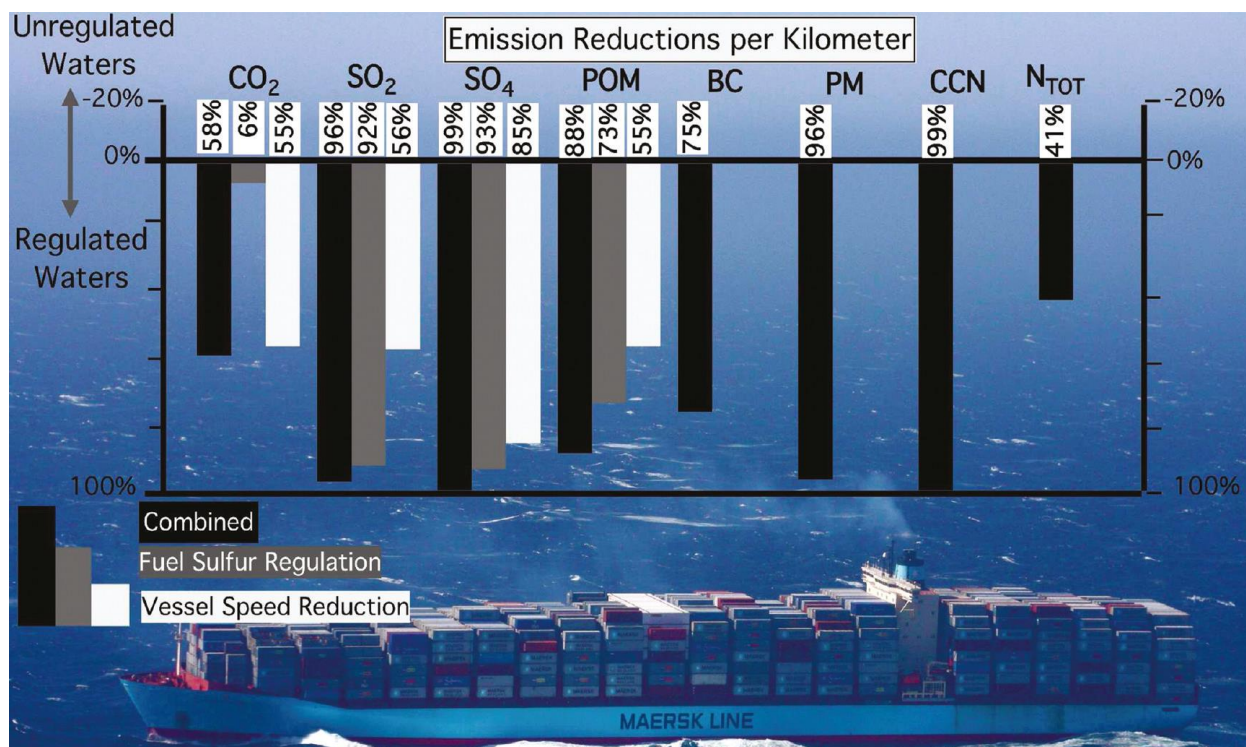


Figure E1. Long-term trends of ambient concentrations of primary (CO, VOCs and NO_x) and secondary (O₃, PAN, and HNO₃) pollutants in SoCAB. The respective lines are linear least-squares fits to log-transformed data; these lines therefore define exponential decreases of the concentrations. The data are normalized so that the linear fits intersect 100 in the year 1960. Ozone data are annual maximum 8-hour averages for each year; other data are average concentrations for summertime weekdays. For clarity, only the linear fit to the VOC data is shown. All analyses and data are from *Pollack et al.* [2013].

1383
 1384 Not all pollutants have decreased at the same rate in SoCAB. Of the primary pollutants, faster
 1385 rates of decrease are observed in abundances of VOCs (-7.3 ± 0.7 % year⁻¹) and CO (-5.7 ± 0.3 %
 1386 year⁻¹) than NO_x (-2.6 ± 0.3 % year⁻¹). The rate of decrease of O₃ (-2.8 ± 0.8 % year⁻¹) and HNO₃
 1387 (-3.0 ± 0.8 % year⁻¹) are statistically equivalent to that of NO_x, while PAN has decreased faster
 1388 (-9.3 ± 1.1 % year⁻¹) than other secondary or primary pollutants. Progress has been much faster in
 1389 reducing concentrations of PAN (a factor of 133 decrease over 50 years) compared to O₃ (a
 1390 factor of 4.2 decrease over 50 years). Since PAN has been a compound of particular concern, air
 1391 quality improvement cannot be measured by the rate of decrease of O₃ concentrations alone.

1392 ***Finding E2: Compliance of marine vessels with the California fuel quality regulation and***
 1393 ***participation in the vessel speed reduction program yields the expected reduction in***
 1394 ***emissions of SO₂, and also provides substantial reductions in emissions of carbon dioxide***
 1395 ***and primary PM.***

1396 CalNex studies have reported the speed dependence of emissions from a vessel burning low-
 1397 sulfur fuel [*Cappa et al.*, 2013] and from a vessel during a switch from high- to low-sulfur fuel
 1398 [*Lack et al.*, 2011]. These analyses showed that speed reductions led to significant reductions in
 1399 primary emissions of all species per kilometer traveled, by a factor of two or more. Further,
 1400 *Lack et al.* [2011] used a wide variety of chemical and aerosol measurements from the NOAA
 1401 WP-3D aircraft and the Research Vessel *Atlantis* to quantify differences in actual emissions from
 1402 a single ship observed underway prior to, during, and after switching between high- and low-
 1403 sulfur fuel. That analysis noted additional reductions in emissions as a result of burning low-
 1404 sulfur fuel: both SO₂ and particulate sulfate decreased by more than 90%, and particulate organic
 1405 matter by decreased by 73% (Fig. E2).



1406

1407 **Figure E2.** Emissions reductions (per km of travel) from the *Margrethe Maersk*
 1408 vessel as a result of the State of California fuel sulfur regulation (gray), vessel speed
 1409 reduction program (white) and combined (black). (Figure from *Lack et al.* [2011])
 1410

1411 References

1412 Cappa, C. D., et al. (2013), The influence of operating speed on gas and particle-phase shipping
 1413 emissions: results from the NOAA Ship *Miller Freeman*, *J. Geophys. Res. Atmos.*, (in
 1414 preparation).

1415 Lack, D. A., et al. (2011), Impact of fuel quality regulation and speed reductions on shipping
 1416 emissions: Implications for climate and air quality, *Environ. Sci. Technol.*, 45, 9052–9060,
 1417 doi:10.1021/es2013424.

1418 Leighton, P. A. (1961), *Photochemistry of Air Pollution*, Academic Press, New York.

1419 Pollack, I.B., T. B. Ryerson, M. Trainer, J.A. Neuman, J.M. Roberts and D.D. Parrish (2013),
 1420 Trends in ozone, its precursors, and related secondary oxidation products in Los Angeles,
 1421 California: A synthesis of measurements from 1960 to 2010, *J. Geophys. Res. Atmos.*, 118,
 1422 5893–5911, doi:10.1002/jgrd.50472.

1423

1424

1425

1426 **Synthesis of Results - Emissions**1427 **Response to Question F**1428 **QUESTION F**

1429 **Are current emission inventory estimates for air pollutants and climate forcing agents**
 1430 **accurate? Are there under- or over-estimated emissions or even missing emission sources**
 1431 **in the current emission inventories?**

1432 **BACKGROUND**

1433 Top-down assessment of emissions inventories is a major focus of analysis of the CalNex data
 1434 sets. Measured atmospheric concentrations in source regions can provide critical assessments of
 1435 the emissions of the measured species. These assessments test the bottom-up approach used in
 1436 inventory tabulations and establish benchmarks for relative emissions changes over time in
 1437 response to control strategies. Several analyses of CalNex data have used top-down emissions
 1438 assessment approaches to help quantify inventories of greenhouse gases and precursors of ozone
 1439 and aerosols.

1440 **POLICY RELEVANCE**

1441 Our ability to understand air quality degradation and changing climate is based upon a wide
 1442 array of atmospheric models that treat transport, composition, chemical transformations and
 1443 other atmospheric processes. Policy decisions are guided by the results of these models.
 1444 Emission inventories are one of the essential components of models, providing the location,
 1445 magnitude, and composition of relevant chemical species. The guidance provided by models can
 1446 be no more reliable than the emission inventories upon which they are based. Further, changing
 1447 emissions (e.g., amount, composition, timing of release, etc.) is the only means available to
 1448 implement policy. To effectively apply this tool requires accurate knowledge of emission
 1449 sources and magnitudes, information provided by the emission inventories.

1450 Emissions of greenhouse gases from California, when averaged over the 2002-2004 period,
 1451 account for 2% of the global total [CARB, 2008]. The provisions in the California Global
 1452 Warming Solutions Act of 2006 call for regulations to reduce emissions by 2020 to levels
 1453 equivalent to those estimated for 1990 (equivalent to a 10 to 15% reduction from the 2002-2004
 1454 average by 2020). Implementation requires the State to establish a GHG inventory and evaluate
 1455 emissions reduction progress against this inventory baseline. Anthropogenic CO₂ is emitted
 1456 primarily from combustion processes; its annually-averaged emissions account for 86% of the
 1457 calculated 100-year global warming potential (GWP) and thus dominate the CARB inventory of
 1458 directly emitted greenhouse gases [CARB, 2011] (Fig. F1). The ubiquity of anthropogenic CO₂
 1459 emission sources, coupled with significant diurnal variability in biospheric CO₂ sources and
 1460 sinks, complicates accurate top-down assessments of CO₂ emissions based on atmospheric
 1461 measurements. CH₄ emissions account for 7% of the total GWP in the 2009 California annual
 1462 inventory [CARB, 2011] (Fig. F1). This inventory apportions total CH₄ emissions as 56% from
 1463 enteric fermentation and manure management, (primarily dairy cattle), 21% from landfills, 11%
 1464 from the combined emissions of wastewater treatment, oil and gas development, rice cultivation,
 1465 and vehicular traffic sources, and 12% from sources listed as “other”. The variety of source

1466 types leads to significant spatial and temporal heterogeneity of CH₄ emissions in California.
 1467 N₂O emissions account for approximately 3% of the total GWP in the California annual
 1468 inventory (Fig. F1); the largest anthropogenic emissions in California are thought to be from
 1469 agriculture, primarily synthetic fertilizer use, and dairy cattle, both predominately located in the
 1470 Central Valley. Halocarbons (the sum of CFCs, HCFCs, HFCs, and other halogenated gases)
 1471 account for 3% of the annual GWP of inventoried California emissions. Emissions of all these
 1472 greenhouse gases have been assessed from the CalNex data.

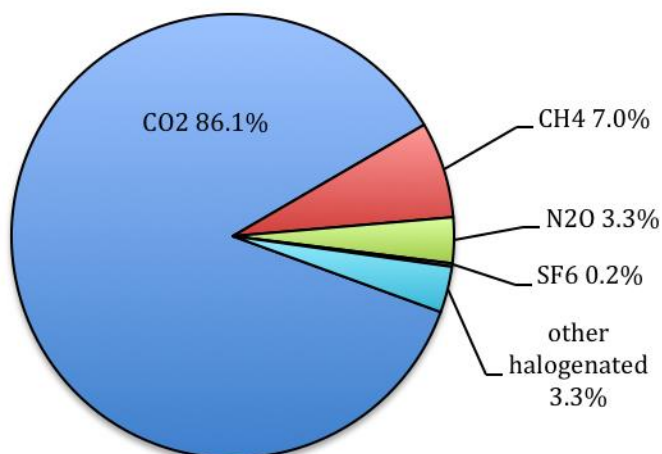


Figure F1. CO₂-equivalent radiative forcing estimated from the 2009 inventory of California greenhouse gas emissions [CARB, 2011]. Figure reproduced from Ryerson *et al.* (2013).

1473
 1474 Ozone precursors include carbon monoxide (CO), volatile organic compounds (VOCs) and
 1475 oxides of nitrogen (NO_x). Other emissions that lead to air quality degradation are particulate
 1476 matter (PM) including black carbon (BC) and PM precursors including ammonia (NH₃) and
 1477 sulfur dioxide (SO₂), as well as VOCs and NO_x. Aspects of the emissions of all of these
 1478 precursor species have also been assessed from the CalNex data.

1479 The CalNex fieldwork was conducted in 2010, so ideally emission inventory assessments would
 1480 be based upon inventories for the year 2010. However, at the time that the assessments were
 1481 conducted, 2008 inventories generally were the most recent available, and therefore were used
 1482 for comparisons. The 2010 inventories are generally slightly different, so for purposes requiring
 1483 very precise comparisons, this difference should be taken into account.

1484 FINDINGS

1485 ***Finding F1:*** CO₂ emissions for the SoCAB estimated by an observation-based mesoscale
 1486 inverse modeling technique agree with emission estimates by CARB. Both of these
 1487 estimates are higher by 15 to 38% than that in the Vulcan inventory of North American
 1488 CO₂ emissions.

1489 Brioude *et al.* [2013] present top-down estimates of anthropogenic CO₂ surface emissions using
 1490 a Lagrangian model in combination with three different WRF model meteorological
 1491 configurations, driven by CO₂ measurements from NOAA WP-3D aircraft flights during
 1492 CalNex, as well as one flight in 2002. Within the uncertainties of these estimates, CO₂ emissions
 1493 in SoCAB did not change significantly with day of week (increase of 7 ± 14% on weekends) or
 1494 between 2002 and 2010 (decrease of 4 ± 10%). Assuming that the CalNex results can be
 1495 extrapolated to total yearly average anthropogenic emissions, 183±18 Tg CO₂ yr⁻¹ is estimated

1496 for the SoCAB. This estimate agrees well with the estimate of 180 Tg yr^{-1} derived by *Peischl et al.* [2013] from the CARB statewide greenhouse gas inventory for 2009, but is 15 to 38% higher
 1497 than the widely used Vulcan inventory [<http://vulcan.project.asu.edu/>, *Gurney et al.*, 2009].
 1498

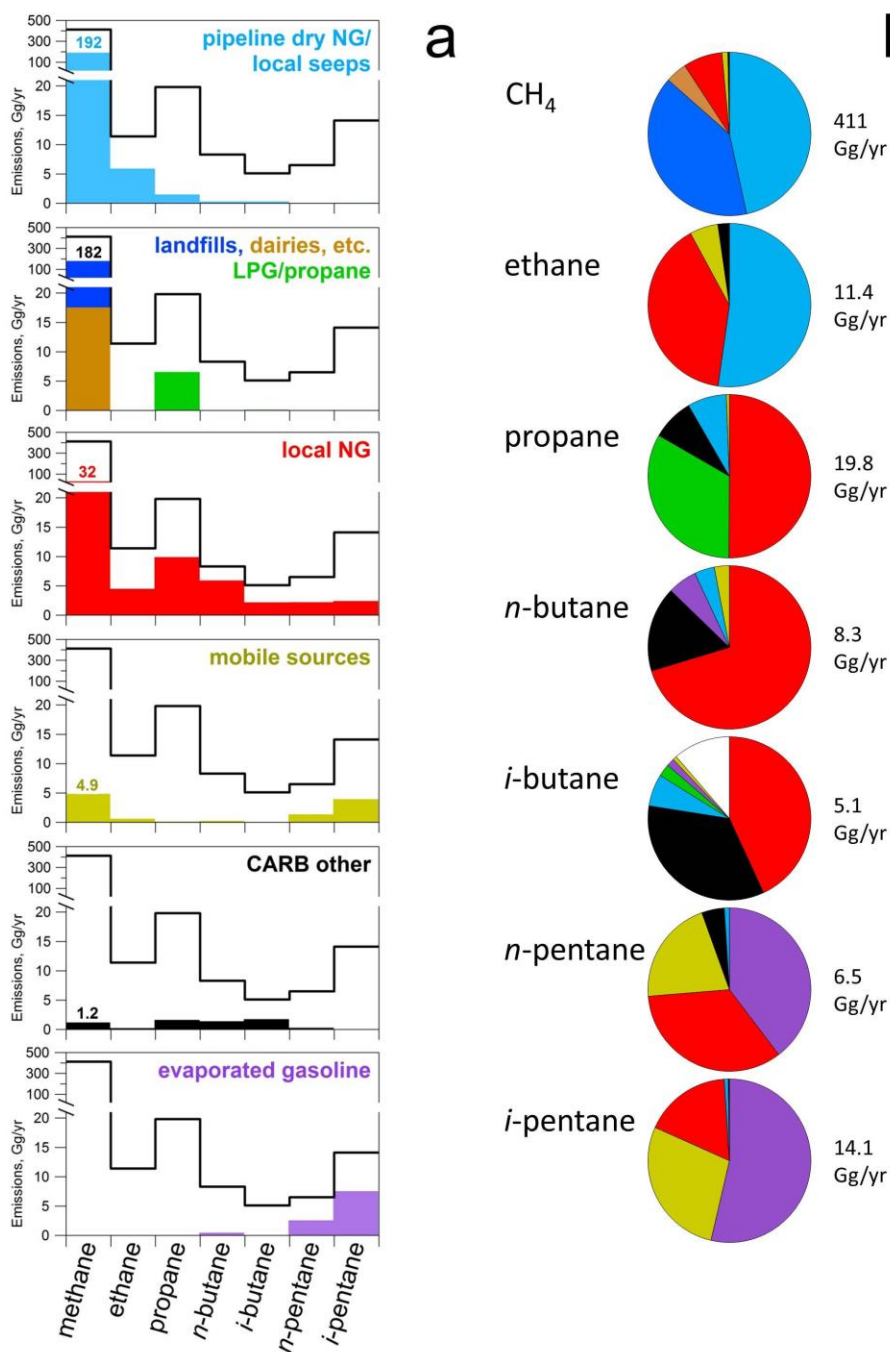
1499 ***Finding F2a: Total methane emissions for the SoCAB have been consistently***
 1500 ***underestimated by inventories. CalNex analyses implicate larger-than-expected CH₄***
 1501 ***emissions from the oil and gas sector in Los Angeles as the emissions missing from current***
 1502 ***inventories.***

1503 *Analysis: This material is taken from Ryerson et al. (2013).*

1504 Ground-based Fourier transform spectrometer (FTS) measurements of atmospheric column
 1505 abundances of CH₄ above Pasadena, CA in 2007 and 2008 [*Wunch et al.*, 2009] had suggested
 1506 that a significant source of CH₄, up to one half of the derived total of 0.6 Tg/yr, was unaccounted
 1507 for in the CARB emission inventory for the heavily urbanized SoCAB. Following these studies
 1508 *Wennberg et al.* [2012], *Santoni et al.* [2013] and *Peischl et al.* [2013] analyzed CalNex ground
 1509 and airborne data and separately concluded that CH₄ sources continue to be significantly
 1510 underestimated in the current inventory for the Los Angeles basin. *Wennberg et al.* [2012] note
 1511 that atmospheric CH₄ enhancement ratios to ethane (C₂H₆) are similar to those in natural gas
 1512 supplied to the basin in both 2008 and in 2010, and concluded that leakage from the natural gas
 1513 distribution infrastructure in the basin is the most likely source of excess atmospheric CH₄.
 1514 Their study did not rule out natural gas seeps or industrial emissions as significant potential
 1515 sources. *Peischl et al.* [2013] examine CH₄ enhancement ratios to C₂ through C₅ alkanes
 1516 (ethane, propane, and the isomers of butane and pentane, Fig. F2) and utilized the geographic
 1517 distribution of airborne samples taken during CalNex to exclude traffic, dairy feedlots, landfills,
 1518 and wastewater treatment plants as significant sources of the unaccounted CH₄ emissions in the
 1519 LA basin. They attribute the missing methane to leaks from natural gas extraction, production,
 1520 and distribution, based on the observed correlations with the light alkanes. *Santoni et al.* [2013]
 1521 use an inverse model constrained by the WP-3D aircraft data and calculate emissions in the LA
 1522 basin of 0.39 Tg CH₄/year, consistent with an assumed leak rate of 2.5% from the natural gas
 1523 delivery infrastructure in the basin. Thus, these CalNex analyses implicate larger-than-expected
 1524 CH₄ emissions from the oil and gas sector in Los Angeles as the emissions missing from the
 1525 inventory, but differ on the root cause. Spatially-resolved measurements in Los Angeles,
 1526 possibly including CH₄ stable isotope data [*Townsend-Small et al.*, 2012] both in atmospheric
 1527 samples and in direct samples of potential source emissions, are needed for more detailed
 1528 identification and attribution of the excess CH₄ that appears to be a consistent feature of Los
 1529 Angeles' atmosphere.

1530 ***Finding F2b: Methane emissions from landfills and dairies in the SoCAB are accurately***
 1531 ***estimated in the inventories developed by CARB.***

1532 From crosswind plume transects flown by the NOAA P-3 aircraft downwind of the two largest
 1533 landfills in the basin, *Peischl et al.* [2013] determine CH₄ fluxes that are consistent with the 2008
 1534 CARB GHG inventory values, which total 164 Gg CH₄/yr emitted from all landfills in the South
 1535 Coast Air Basin. NOAA P-3 aircraft data were also used to determine CH₄ emission fluxes from
 1536 Chino-area dairies in the eastern L.A. basin. Flux estimates from these dairies ranged from $24 \pm$
 1537 12 to 87 ± 44 Gg CH₄/yr, and the average flux (49 ± 25 Gg CH₄/yr) is consistent with a revised
 1538 bottom-up inventory (31.6 Gg CH₄/yr,) derived from the methods compiled by *Salas et al.* [2008],
 1539 and with another previous inventory estimate of (76 Gg CH₄/yr,) [*Wennberg et al.*, 2012]. The
 1540 aircraft based flux determinations do vary by more than a factor of three, which is outside the



1541

Figure F2. **a)** Estimate of seven trace gas emissions from six sources in the SoCAB. The thick black line represents the estimated total annual emission for each of seven alkanes (CH₄ and C₂–C₅). The colored bars represent the fraction of the total contributed by each of the six sources. CH₄ emissions are written above the bar. **b)** Pie charts for the data in (a) showing the relative contributions from each source for each alkane, colored as in (a). The white region in the *i*-butane pie chart represents the 11% shortfall between the source attribution and the estimated total emissions. The total emission of each alkane in the SoCAB is given to the right of each pie chart. (Figure taken from *Peischl et al.* [2013]).

1542 expected uncertainties of the estimates. This variation suggests real day-to-day variability in the
 1543 dairy CH₄ fluxes, which may be associated with manure management practices. Further
 1544 investigation of this variability may provide guidance for reducing these CH₄ emissions.

1545 ***Finding F2c: Annual average methane emissions from rice agriculture are factors of 2 to 3***
 1546 ***greater than in the CARB inventory.***

1547 Data from two flights of the NOAA P-3 aircraft in CalNex were used to investigate the spatial
 1548 consistency of CH₄ emissions from rice paddies during the growing season in the Sacramento
 1549 Valley [Peischl *et al.*, 2012]. This paper demonstrated that rice emissions dominated other
 1550 potential sources of CH₄ in the region, including oil and gas development, dairy farms, and
 1551 wastewater treatment facilities. The analysis showed that earlier long-term measurements of
 1552 CH₄ and CO₂ at a single paddy [McMillan *et al.*, 2007] were generally representative of
 1553 emissions from rice cultivation throughout the Sacramento Valley in California. Peischl *et al.*
 1554 [2012] further note the annual average CH₄ emissions from rice in McMillan *et al.* [2007] are
 1555 factors of 2 to 3 greater than in the CARB annual inventory, and attribute this inventory
 1556 discrepancy to the lack of accounting for changes in residual crop management following a 2001
 1557 ban on most rice straw burning in the Sacramento Valley. Inverse modeling results reported by
 1558 Santoni *et al.* [2013] are also consistent with a low bias, by about a factor of three, in the CARB
 1559 inventory of CH₄ emissions from rice in the Sacramento Valley.

1560 ***Finding F3: Analyses of CalNex nitrous oxide measurements suggest that inventory***
 1561 ***improvements are needed to correct a potential low bias and improve the spatial and***
 1562 ***seasonal patterns of emissions.***

1563 *Analysis: This material is taken from Ryerson et al. (2013).*

1564 Xiang *et al.* [2012] used a 3-D mesoscale meteorological model coupled with a Lagrangian
 1565 particle dispersion model to link N₂O concentrations observed from the P-3 aircraft to source
 1566 emission areas, and concluded that fertilizer application in the Central Valley was the largest
 1567 source of N₂O during the study period. High-resolution surface emission maps derived from
 1568 their inversion analysis showed a different spatial pattern of N₂O emissions in the Central Valley
 1569 than expected from the EDGAR 4.0 inventory. This conclusion is consistent with a recent
 1570 inverse modeling study based on long-term tall tower N₂O observations [Miller *et al.*, 2012] of
 1571 agricultural N₂O emissions derived using top-down methods.

1572 The global total of N₂O emissions is thought to be well known; however, individual source terms
 1573 in inventories are uncertain. The potential low bias in agricultural N₂O inventories, potentially
 1574 coupled with poor spatial [Xiang *et al.*, 2012] and seasonal [Miller *et al.*, 2012] representations,
 1575 may handicap scientifically sound GHG emissions control strategies and ozone layer protection
 1576 based on N₂O emissions reductions. These uncertainties further complicate accurate projections
 1577 of future N₂O emissions under potential climate mitigation or adaptation strategies. These
 1578 conclusions suggest that improved quantification of agricultural N₂O sources in California may
 1579 help the State meet the GHG reduction timelines spelled out in AB32.

1580 ***Finding F4: Top-down assessments of anthropogenic halocarbon emissions are generally***
 1581 ***consistent with the CARB emission inventory.***

1582 *Analysis: This material is taken from Ryerson et al. (2013).*

1583 Halocarbon emissions patterns, trends, and seasonality in California have been previously
 1584 reported [Barletta *et al.*, 2011; Gentner *et al.*, 2010]. These compounds were measured at a

1585 variety of sites during CalNex (Appendix A). *Barletta et al.* [2013] used whole-air samples
 1586 acquired in the Central Valley and the Los Angeles basin from the NOAA WP-3D flights during
 1587 CalNex to show that the 2008 CARB inventory is generally consistent with their top-down
 1588 assessment of anthropogenic emissions of halocarbons HFC-134a, HFC-152a, HCFC-22, HCFC-
 1589 124, HCFC-141b, and HCFC-142b in California.

1590 **Finding F5: Top-down assessments of the CO emissions in 2010 are within 15% of the**
 1591 **CARB 2008 emission inventory.**

1592 The top-down method of *Brioude et al.* [2013] discussed in Finding F1 also provided estimates
 1593 of anthropogenic CO emissions based on NOAA P-3 aircraft flights. These estimates are within
 1594 15% of the CARB 2008 inventory for both LA County and the SoCAB, but average about 40%
 1595 lower than EPA's NEI 2005 inventory [US Environmental Protection Agency, 2010]. Urban CO
 1596 concentrations are dominated by on-road emissions from gasoline-fueled passenger vehicles and
 1597 have been steadily decreasing over time throughout the U.S. [Parrish et al., 2002] in response to
 1598 control strategies. CO in California shows a similar trend, recently demonstrated by a
 1599 study using atmospheric CO measurements and the radiocarbon composition of tree
 1600 rings in the Los Angeles basin as a record of atmospheric CO₂ from fossil fuel
 1601 [Djuricin et al., 2010]. Since the emissions of CO over time are thought to
 1602 be accurately known, CO serves as a conserved tracer, a utility that has been
 1603 exploited in several CalNex studies to calculate mass emissions of other species
 1604 of interest, either co-emitted with CO [Barletta et al., 2013; Pollack et al., 2012;
 1605 Warneke et al., 2012] or emitted from different sources but sufficiently mixed
 1606 following emission such that their atmospheric variability becomes correlated
 1607 with CO [Nowak et al., 2012; Peischl et al., 2013; Peischl et al., 2012].

1618 **Finding F6: Top-down assessments of NO_x emissions are in good agreement**
 1619 **with the CARB emission inventory.**
 1620

1621 *McDonald et al.* [2012] use a fuel-based approach to estimate NO_x emissions from
 1622 gasoline and diesel-powered on-road vehicles in the SoCAB and the SJVAB (Fig.
 1623 F3) as well as for California and the entire nation from 1990 to 2010. They compare

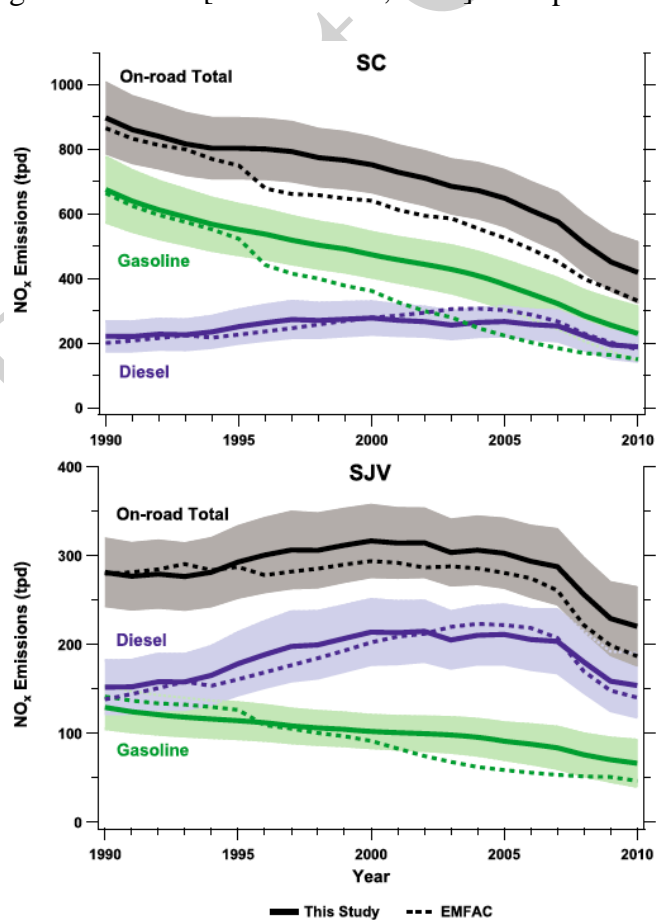


Figure F3. Trends in NO_x emissions from on-road vehicles in the South Coast air basin (SC) and SJV. Shaded areas represent uncertainties of estimates. Dotted lines show estimates from EMFAC (Figure taken from *McDonald et al.* [2013]).

1627 their results with emission inventories, including EMFAC. To quantify total NO_x emissions, the
 1628 on-road emission estimates were combined with estimates for other anthropogenic sources and
 1629 compared with satellite and ground-based observations.

1630 Growth in on-road diesel fuel consumption outpaced that of gasoline from 1990 to 2007,
 1631 followed by a decrease in the consumption of both, which is attributed to the economic
 1632 downturn. The ratio of NO_x emission factors for heavy-duty diesel versus light-duty gasoline
 1633 engines grew from ~3 in 1990 to ~8 in 2010, which is attributed to the near universal deployment
 1634 of catalytic converters on gasoline engines. In contrast, NO_x emission factors for heavy-duty
 1635 diesel trucks showed little change during the 1990s, and have decreased only gradually since
 1636 then. The NO_x emission changes shown in Fig. F3 result from the combination of changing fuel
 1637 consumption, both in total amount and apportionment between gasoline and diesel, and the NO_x
 1638 emission factors. The impact of the economic recession after 2007 is clear in the estimated NO_x
 1639 emissions.

1640 The top-down method of *Brioude et al.* [2013] discussed in Finding F1 also provided estimates
 1641 of anthropogenic NO_x emissions based on NOAA WP-3D aircraft flights. Their observation-
 1642 based estimate for NO_x emissions in Los Angeles County in 2010 is lower than the CARB 2008
 1643 inventory by 6% on weekdays and 17% during weekends, differences within the uncertainty
 1644 range of their inversion method. In the entire SoCAB region, a similar difference was seen on
 1645 weekdays, but only a 2% difference during weekends. However, their derived spatial
 1646 distribution of NO_x emissions in SoCAB was significantly different from the CARB 2008
 1647 inventory. The NEI 2005 inventory did not compare as well with the results of *Brioude et al.*
 1648 [2013], which were lower by 32%±10% in LA County and by 27%±15% in the SoCAB than in
 1649 the NEI 2005 inventory.

1650 Weekday-weekend NO_x emissions differences, and their trends over time, are documented from
 1651 1990 through the CalNex study in 2010 [*Pollack et al.*, 2012]. *Pollack et al.* [2012] used
 1652 ambient measurements to show significant weekend decreases of the NO_x to CO emission ratio,
 1653 between one-third to one-half of the characteristic weekday ratio, have been a consistent feature
 1654 of the South Coast Air Basin since at least the mid-1990s.

1655 ***Finding F7: Top-down assessments of VOC emissions indicate some discrepancies with***
 1656 ***inventories, but they are not sufficiently large to appreciably affect results of air quality***
 1657 ***modeling.***

1658 *Borbon et al.* [2013] used the CalNex Pasadena ground site data to derive top-down emissions
 1659 estimates of many VOCs relative to CO and acetylene in vehicular exhaust; they find that
 1660 individual VOC to CO emission ratios can disagree by a factor of 4 or more with the ratios
 1661 derived from NEI 2005 and CARB 2008 emission inventories. Nevertheless, the difference
 1662 between measurements and inventory in terms of the overall OH reactivity is within 15% of that
 1663 from the CARB inventory, and the potential to form secondary organic aerosols (SOA) agrees
 1664 within 35% (see discussion in response to Question G). *de Gouw et al.* [2012] used the CalNex
 1665 measurements to show that ethanol has become significantly enriched in U.S. urban atmospheres
 1666 in the last decade due to its increasing use as a biofuel amendment to gasoline (see discussion in
 1667 response to Question B).

1668 **References**

1669 Barletta, B., P. Nissenson, S. Meinardi, D. Dabdub, F. S. Rowland, R. A. VanCuren, J. Pederson,
 1670 G. S. Diskin, and D. R. Blake (2011), HFC-152a and HFC-134a emission estimates and

- 1671 characterization of CFCs, CFC replacements, and other halogenated solvents measured
 1672 during the 2008 ARCTAS campaign (CARB phase) over the South Coast Air Basin of
 1673 California, *Atmos. Chem. Phys.*, *11*, 2655-2669, doi:10.5194/acp-11-2655-2011.
- 1674 Barletta, B. et al. (2013), Emission estimates of HCFCs and HFCs in California from the 2010
 1675 CalNex study, *J. Geophys. Res. Atmos.*, *118*, 2019–2030, doi:10.1002/jgrd.50209.
- 1676 Borbon, A., et al. (2013), Emission ratios of anthropogenic volatile organic compounds in
 1677 northern mid-latitude megacities: Observations versus emission inventories in Los Angeles
 1678 and Paris, *J. Geophys. Res. Atmos.*, *118*, 2041–2057, doi:10.1002/jgrd.50059.
- 1679 Brioude, J., et al. (2013), Top-down estimate of surface flux in the Los Angeles Basin using a
 1680 mesoscale inverse modeling technique: Assessing anthropogenic emissions of CO, NO_x and
 1681 CO₂ and their impacts, *Atmos. Chem. Phys.*, *13*, 3661-3677, doi:10.5194/acp-13-3661-2013.
- 1682 CARB (2008), Climate Change Scoping Plan: A Framework for Change, pursuant to AB 32, the
 1683 California Global Warming Solutions Act of 2006, report, 133 pp., available at:
 1684 http://www.arb.ca.gov/cc/scopingplan/document/adopted_scoping_plan.pdf
- 1685 CARB (2011), California Greenhouse Gas Emission Inventory: 2000–2009, report, 32 pp.,
 1686 available at: [http://www.arb.ca.gov/cc/inventory/pubs/reports/ghg_inventory_00-](http://www.arb.ca.gov/cc/inventory/pubs/reports/ghg_inventory_00-09_report.pdf)
 1687 [09_report.pdf](http://www.arb.ca.gov/cc/inventory/pubs/reports/ghg_inventory_00-09_report.pdf).
- 1688 de Gouw, J. A., J. B. Gilman, A. Borbon, C. Warneke, W. C. Kuster, P. D. Goldan, J. S.
 1689 Holloway, J. Peischl, and T. B. Ryerson (2012), Increasing atmospheric burden of ethanol in
 1690 the United States, *Geophys. Res. Lett.*, *39*(L15803), doi:10.1029/2012GL052109.
- 1691 Djuricin, S., D. E. Pataki, and X. Xu (2010), A comparison of tracer methods for quantifying
 1692 CO₂ sources in an urban region, *J. Geophys. Res. Atmos.*, *115*(D11303),
 1693 doi:10.1029/2009JD012236.
- 1694 Gentner, D. R., A. M. Miller, and A. H. Goldstein (2010), Seasonal variability in anthropogenic
 1695 halocarbon emissions, *Environ. Sci. Technol.*, *44*(14), 5377-5382, doi:10.1021/es1005362.
- 1696 Gurney, K. R., Mendoza, D. L., Zhou, Y., Fischer, M. L., Miller, C. C., Geethakumar, S., and de
 1697 la Rue du Can, S. (2009), High resolution fossil fuel combustion CO₂ emission fluxes for the
 1698 United States, *Environ. Sci. Technol.*, *43*, 5535–5541, doi:10.1021/es900806c.
- 1699 McDonald, B. C., T. R. Dallmann, E. W. Martin, and R. A. Harley (2012), Long-term trends in
 1700 nitrogen oxide emissions from motor vehicles at national, state, and air basin scales, *J.*
 1701 *Geophys. Res. Atmos.*, *117*, D00V18, doi:10.1029/2012JD018304.
- 1702 McMillan, A. M. S., M. L. Goulden, and S. C. Tyler (2007), Stoichiometry of CH₄ and CO₂ flux
 1703 in a California rice paddy, *J. Geophys. Res. Atmos.*, *112*(G01008),
 1704 doi:10.1029/2006JG000198.
- 1705 Miller, S. M., et al. (2012), Regional sources of nitrous oxide over the United States: Seasonal
 1706 variation and spatial distribution, *J. Geophys. Res. Atmos.*, *117*(D06310),
 1707 doi:10.1029/2011JD016951.
- 1708 Nowak, J. B., J. A. Neuman, R. Bahreini, A. M. Middlebrook, J. S. Holloway, S. A. McKeen, D.
 1709 D. Parrish, T. B. Ryerson, and M. Trainer (2012), Ammonia sources in the California South
 1710 Coast Air Basin and their impact on ammonium nitrate formation, *Geophys. Res. Lett.*,
 1711 *39*(L07804), doi:10.1029/2012GL051197.

- 1712 Parrish, D. D., M. Trainer, D. Hereid, E. J. Williams, K. J. Olszyna, R. A. Harley, J. F. Meagher,
 1713 and F. C. Fehsenfeld (2002), Decadal change in carbon monoxide to nitrogen oxide ratio in
 1714 U.S. vehicular emissions, *J. Geophys. Res. Atmos.*, 107(D12), doi:10.1029/2001JD000720.
- 1715 Peischl, J., et al. (2012), Airborne observations of methane emissions from rice cultivation in the
 1716 Sacramento Valley of California, *J. Geophys. Res. Atmos.*, 117, D00V25,
 1717 doi:10.1029/2012JD017994.
- 1718 Peischl, J., et al. (2013), Quantifying sources of methane using light alkanes in the Los Angeles
 1719 basin, California, *J. Geophys. Res. Atmos.*, 118, 4974–4990, doi:10.1002/jgrd.50413.
- 1720 Pollack, I. B., et al. (2012), Airborne and ground-based observations of a weekend effect in
 1721 ozone, precursors, and oxidation products in the California South Coast Air Basin, *J.*
 1722 *Geophys. Res. Atmos.*, 117, D00V05, doi:10.1029/2011JD016772.
- 1723 Ryerson, T. B., et al. (2013), The 2010 California Research at the Nexus of Air Quality and
 1724 Climate Change (CalNex) field study, *J. Geophys. Res. Atmos.*, 118, 5830–5866,
 1725 doi:10.1002/jgrd.50331.
- 1726 Salas, W. A., et al. (2008), Developing and Applying Process-Based Models for Estimating
 1727 Greenhouse Gas and Air Emission From California Dairies, *California Energy Commission,*
 1728 *PIER Energy-Related Environmental Research, CEC-500-2008-093,*
 1729 <http://www.energy.ca.gov/2008publications/CEC-500-2008-093/CEC-500-2008-093.PDF>.
- 1730 Santoni, G. W., et al. (2013), California's methane budget derived from CalNex WP-3 aircraft
 1731 observations and a Lagrangian transport model, *J. Geophys. Res. Atmos.*, (in preparation).
- 1732 Townsend-Small, A., S. C. Tyler, D. E. Pataki, X. Xu, and L. E. Christensen (2012), Isotopic
 1733 measurements of atmospheric methane in Los Angeles, California, USA: Influence of
 1734 “fugitive” fossil fuel emissions, *J. Geophys. Res. Atmos.*, 117(D07308),
 1735 doi:10.1029/2011JD016826.
- 1736 US Environmental Protection Agency (2010), Technical support document: Preparation of
 1737 emissions inventories for the Version 4, 2005-based platform, report, Washington, DC, 73
 1738 pp., available at: [http://www.epa.gov/airquality/transport/pdfs/2005 emissions tsd](http://www.epa.gov/airquality/transport/pdfs/2005%20emissions%20tsd%2007jul2010.pdf)
 1739 [07jul2010.pdf](http://www.epa.gov/airquality/transport/pdfs/2005 emissions tsd 07jul2010.pdf).
- 1740 Warneke, C., J. A. de Gouw, J. S. Holloway, J. Peischl, T. B. Ryerson, E. Atlas, D. Blake, M.
 1741 Trainer, and D. D. Parrish (2012), Multi-year trends in volatile organic compounds in Los
 1742 Angeles, California: five decades of improving air quality, *J. Geophys. Res.*, 117, (D00V17),
 1743 doi:10.1029/2012JD017899.
- 1744 Wennberg, P. O., et al. (2012), On the sources of methane to the Los Angeles atmosphere,
 1745 *Environ. Sci. Technol.*, 46, 9282-9289, doi:10.1021/es301138y.
- 1746 Wunch, D., P. O. Wennberg, G. C. Toon, G. Keppel-Aleks, and Y. G. Yavin (2009), Emissions
 1747 of greenhouse gases from a North American megacity, *Geophys. Res. Lett.*, 36(L15810),
 1748 doi:10.1029/2009GL039825.
- 1749 Xiang, B., et al. (2013), Nitrous oxide (N₂O) emissions from California based on 2010 CalNex
 1750 airborne measurements, *J. Geophys. Res. Atmos.*, 118, 2809–2820, doi:[10.1002/jgrd.50189](https://doi.org/10.1002/jgrd.50189).
- 1751
- 1752

1753 **Synthesis of Results - Emissions**1754 **Response to Question G**1755 **QUESTION G**1756 **Do the VOC measurements provide any new insights into emission sources?**1757 **BACKGROUND**

1758 Patterns of measured ambient concentrations of VOCs provide indications of the important
1759 emission sources of these species to the atmosphere. There have been a wide variety of source
1760 apportionment techniques applied to data sets of VOC measurements in attempts to determine
1761 the VOC sources responsible for those ambient concentrations. However, many of these
1762 techniques give questionable results [e.g., Yuan, *et al.*, 2012] since reactions of VOCs within the
1763 atmosphere change the concentration patterns from those emitted. Parrish *et al.* [2009] identify
1764 similarities in the VOC emission patterns in urban areas throughout the world and suggest that in
1765 all urban areas, including Los Angeles, VOC emissions are dominated by mobile emission
1766 sources. Emissions from industrial processes and use of consumer products and biogenic
1767 emissions are additional sources that may be important in some urban areas.

1768 **POLICY RELEVANCE**

1769 Effective policies for improving air quality require accurate knowledge of emission sources of
1770 important VOC precursors of ozone and aerosols. Ambient VOC measurements can help to
1771 identify and quantify specific VOC sources (e.g. use of a particular solvent) that may be cost-
1772 effective control targets.

1773 **FINDINGS**

1774 ***Finding G1: Ambient VOC concentrations in the SoCAB have decreased by a factor of***
1775 ***approximately 50 in the past five decades, but the ambient relative concentrations have***
1776 ***remained remarkably constant, indicating that mobile emissions have remained the***
1777 ***predominant source over this entire period.***

1778 *Warneke et al.* [2012] summarize ambient VOC measurements in the SoCAB from 1960-2010
1779 (Fig. G1); they find that concentrations decreased by a factor of approximately 50 over that
1780 period, despite an approximate three-fold increase in fuel sales in the region. During these five
1781 decades the relative concentrations among the VOCs have remained remarkably constant, which
1782 is attributed to continuing dominance of mobile emissions, particularly the on-roadway vehicle
1783 fleet, throughout this period. This constant VOC pattern persisted through the introduction of
1784 catalytic converters in exhaust systems and also reformulated and oxygenated gasoline. There
1785 are some exceptions to this consistency. The relative concentrations of the light alkanes (ethane,
1786 propane) have increased to the point that by 2010 they have the highest concentrations of the
1787 species plotted in Fig. G1. This change is attributed to the growing relative importance of
1788 natural gas emissions in the SoCAB (see discussion in Finding F2a). *Pollack et al.* [2013] also
1789 note that concentrations of the biogenic hydrocarbon isoprene have not changed significantly
1790 over the last two decades.

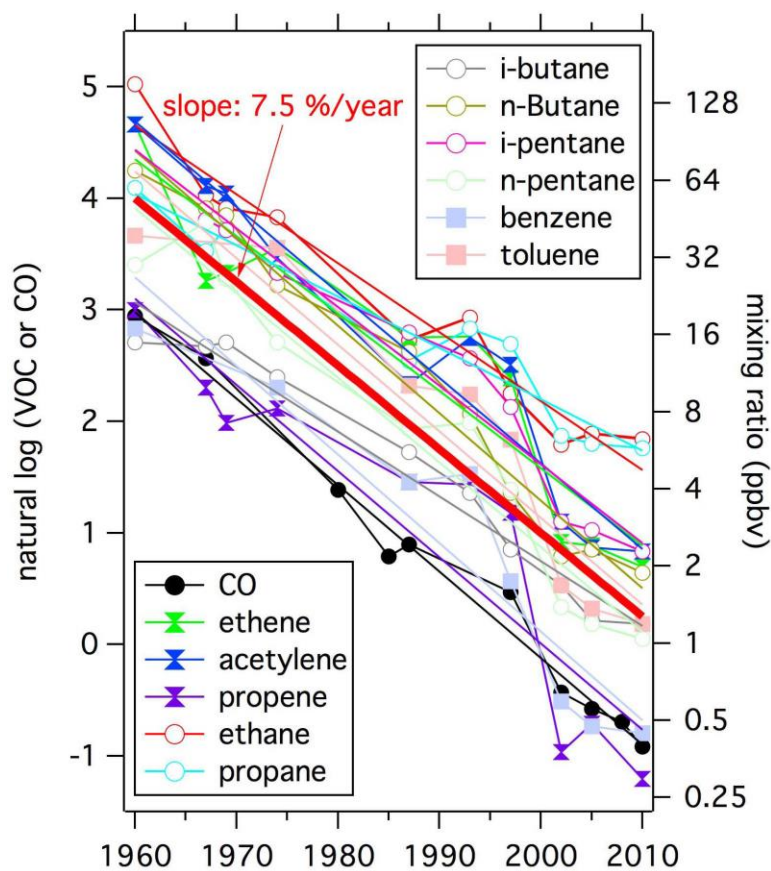


Figure G1. Typical mixing ratios estimated from published data from various field campaigns conducted near downtown Los Angeles together with linear fits to the logarithm of the data the left axis. The solid red line indicates a 7.5%/year decrease, which equates to a 98% reduction in concentrations during the last 50 years. Figure reproduced from *Warneke et al. (2012)*.

Similar anthropogenic VOC concentrations patterns are observed in urban areas throughout North America and in Asia [*Parrish et al., 2009*] and in Europe [*Borbon et al., 2013*]. Deviations from the common pattern can lead to conclusions regarding important characteristics

1800 of local sources. For example, *Borbon et al. [2013]* compared ambient VOC concentrations in
 1801 France to those observed in the SoCAB during CalNex. They found that the emission ratios for
 1802 C7–C9 aromatics in Paris are higher by a factor of 2–3 compared to the U.S. and other French
 1803 and European Union urban areas, and traced the cause to the greater aromatic content of gasoline
 1804 sold in the Paris region. A second example is ambient ethanol concentrations in the SoCAB,
 1805 which have greatly increased in recent years due to the rapid increase in the ethanol content of
 1806 gasoline (see more discussion in Finding B1.)

1807 **Finding G2: The individual VOC to CO emission ratios observed in the SoCAB can**
 1808 **disagree by a factor of four or more with the ratios derived from NEI 2005 and CARB 2008**
 1809 **emission inventories. The agreement is particularly poor for oxygenated VOCs.**
 1810 **Nevertheless, the difference between measurements and inventory in terms of the overall**
 1811 **OH reactivity is within 15% of that from the CARB inventory, and the potential to form**
 1812 **secondary organic aerosols (SOA) agrees within 35%.**

1813 The urban emission ratios (ERs) of individual VOCs relative to CO generally agree within a
 1814 factor of four (4) in the SoCAB (Figure G2a). The inventory ERs generally fall below the 1:1
 1815 line, particularly for the NEI 2005 [*US Environmental Protection Agency, 2010*], which is
 1816 consistent with the inventory overestimate of CO emissions discussed in Finding F5. When
 1817 comparing the ERs relative to acetylene (Figure G2b) and differences between the NEI 2005
 1818 inventory and observations are reduced by a factor of two (2) for most of the compounds. Figure
 1819 G2c reports the ERs relative to CO color coded by the VOC groups. The largest discrepancies
 1820 are for the three oxygenated VOCs (OVOCs) specifically identified in the figure.

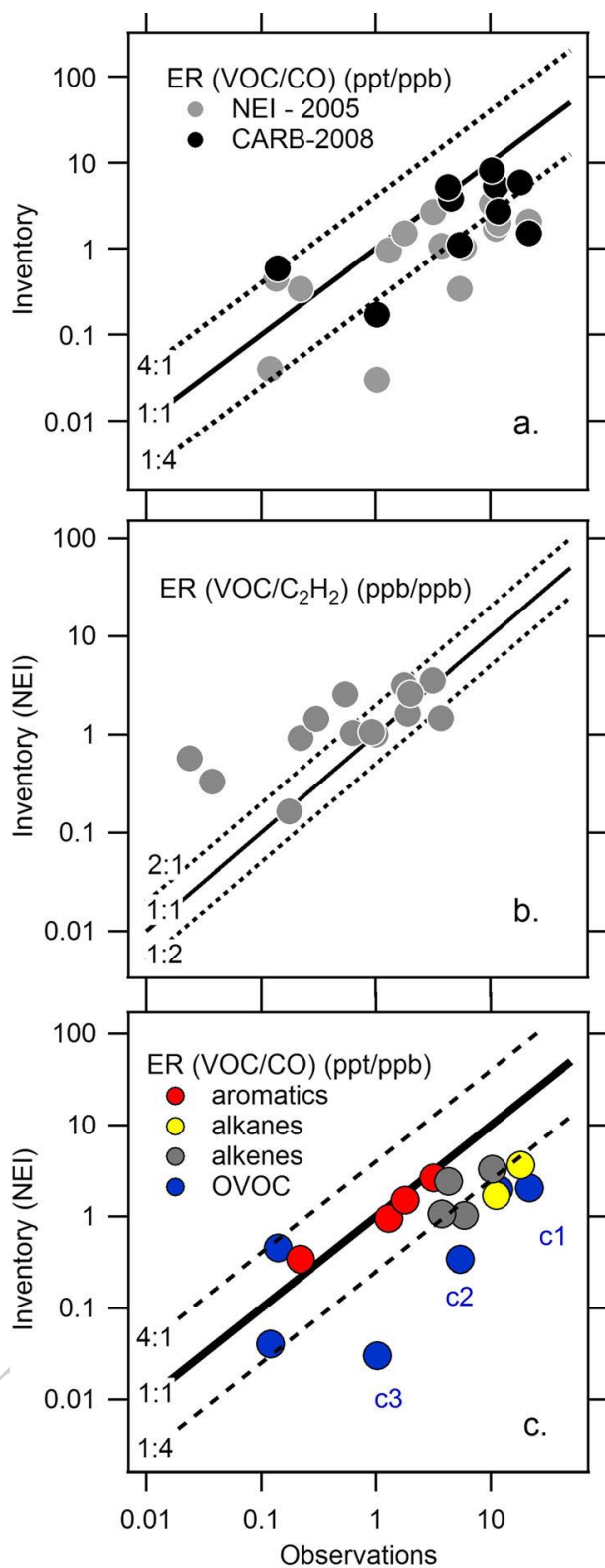


Figure G2. Comparison of measured emission ratios of VOCs relative to (a and c) CO and (b) acetylene to the ratios in two VOC emission inventories (NEI 2005 and CARB 2008) for the SoCAB. Abbreviations identifying specific species are: c1, methanol; c2, acetaldehyde; and c3, benzaldehyde. Figure reproduced from *Borbon et al.* [2013].

Two metrics can be used to test how well the emission database reproduces the potential of sampled air masses to form ozone and secondary organic aerosol (SOA): OH reactivity and the SOA formation potential. The OH reactivity is calculated by multiplying each compound's concentration by its OH rate coefficient, and summing over all individual VOCs included in the comparison, although this comparison is limited by the speciation in the inventory. Despite the large discrepancies between the individual ERs (Figure G2), the overall OH reactivity of the measured VOCs and the reactivity of the same compounds in the regional emission database per molecule of CO emitted agree within 15% (Figure G3, left panels) for the CARB 2008 inventory, but is in significantly greater disagreement with the NEI 2005 inventory. The OH reactivity is dominated by contributions from alkenes and aromatics, which are both well represented by the CARB 2008 inventory. The underestimate of OVOCs by the inventory primarily accounts for the underestimate of the total OH reactivity.

The secondary organic aerosol potential (SOAP) reflects the ability of each organic compound to form SOA on an equal mass emitted basis relative to toluene set to 100.

As a class, the aromatics exhibit the

1853 greatest propensity to form SOA. The potential of SoCAB anthropogenic VOC emissions to
 1854 form SOA (Figure G3, right panels) shows good agreement for the aromatics with an
 1855 underestimate for the OVOCs, in this case primarily benzaldehyde.

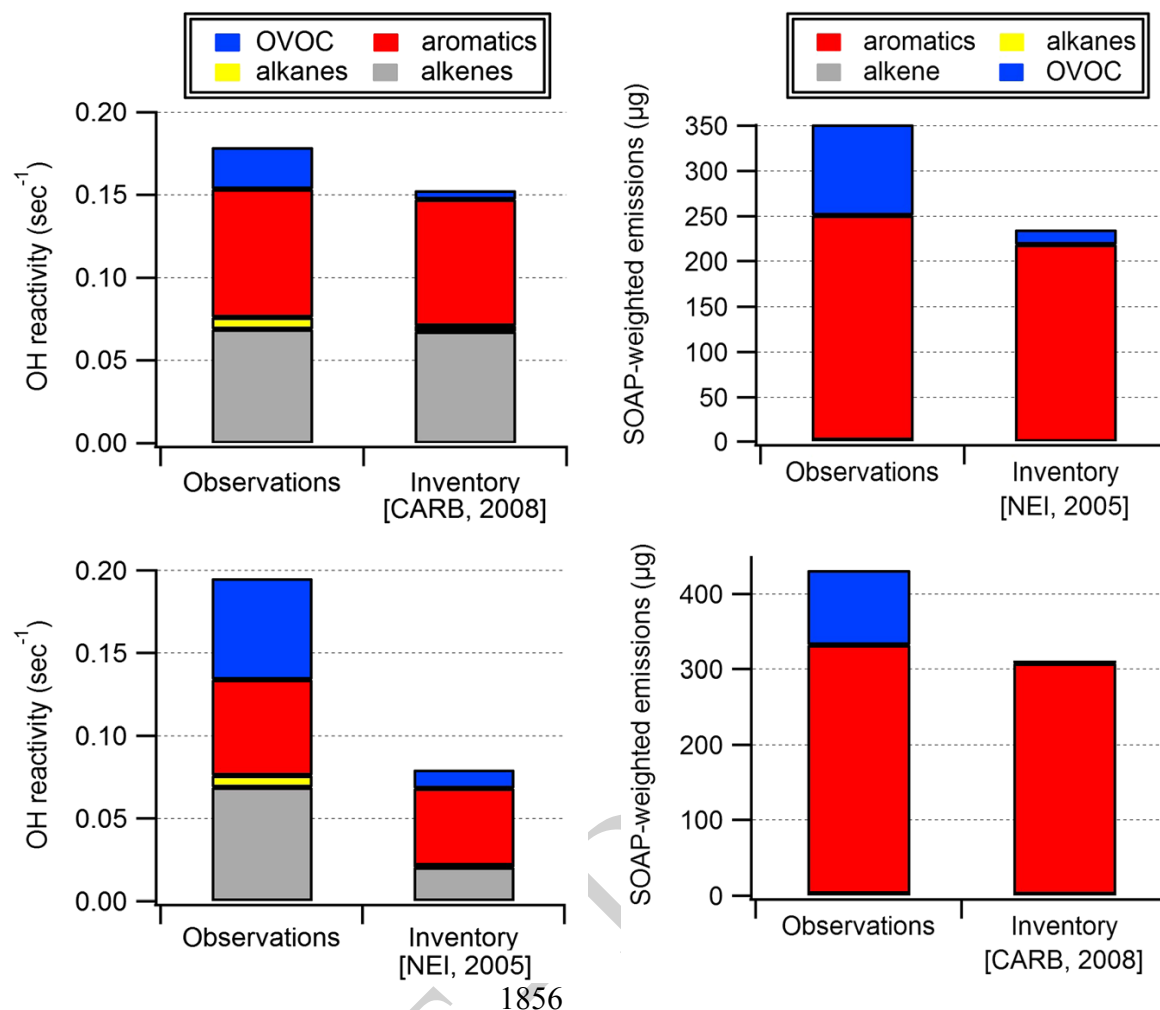


Figure G3. Sum of VOC reactivity with OH (left panel) and secondary organic aerosol formation potential (SOAP) (right panel) calculated from the emission ratios of anthropogenic VOCs and a CO enhancement of 100 ppb in the Los Angeles basin. Observed reactivity and SOAP (left-hand bars) are compared with the different emission database results (right-hand bars). The number and nature of the VOCs used in the comparisons are different depending on the speciation available in each inventory. Figure reproduced from *Borbon et al.* [2013].

1857 **Finding G3: Ambient benzene concentrations in the SoCAB have decreased more rapidly**
 1858 **than concentrations of other VOCs, which is primarily attributed to efforts to remove**
 1859 **benzene from gasoline due to its recognized toxicity.**

1860 In the early 1990s California implemented its Reformulated Gasoline Program. One goal of this
 1861 program was to reduce the amount of benzene in gasoline, as it is a recognized air toxic. From
 1862 1960 to 2010 ambient benzene concentrations have decreased about twice as much (by a factor
 1863 of ≈ 65) as the concentrations of other aromatics (factors of ≈ 32 and ≈ 37 for toluene and
 1864 ethylbenzene, respectively). This difference is believed to reflect a success of California's
 1865 Reformulated Gasoline Program, and is consistent with nationwide changes documented by
 1866 *Fortin et al.* [2005].

1867 **References**

- 1868 Borbon, A., et al. (2013), Emission ratios of anthropogenic volatile organic compounds in
1869 northern mid-latitude megacities: Observations versus emission inventories in Los Angeles
1870 and Paris, *J. Geophys. Res. Atmos.*, *118*, 2041–2057, doi:10.1002/jgrd.50059.
- 1871 CARB (2008), available at <http://www.arb.ca.gov/ei/maps/basins/abscmap.htm>.
- 1872 Fortin, T.J., B.J. Howard, D.D. Parrish, P.D. Goldan, W.C. Kuster, E.L. Atlas, and R.A. Harley
1873 (2005), Temporal changes in U.S. benzene emissions inferred from atmospheric
1874 measurements, *Environ. Sci. Technol.*, *39*, 1403-1408.
- 1875 Parrish, D.D., W.C. Kuster, M. Shao, Y. Yokouchi, Y. Kondo, P.D. Goldan, J.A. de Gouw, M.
1876 Koike and T. Shirai (2009), Comparison of air pollutant emissions among mega-cities,
1877 *Atmos. Environ.*, *43*, 6435-6441.
- 1878 Pollack, I. B., T. B. Ryerson, M. Trainer, J. A. Neuman, J. M. Roberts, and D. D. Parrish (2013),
1879 Trends in ozone, its precursors, and related secondary oxidation products in Los Angeles,
1880 California: A synthesis of measurements from 1960 to 2010, *J. Geophys. Res. Atmos.*, *118*,
1881 5893–5911, doi:10.1002/jgrd.50472.
- 1882 US Environmental Protection Agency (2010), Technical support document: Preparation of
1883 emissions inventories for the Version 4, 2005-based platform, report, Washington, DC, 73
1884 pp., available at: http://www.epa.gov/airquality/transport/pdfs/2005_emissions_tsd_07jul2010.pdf.
- 1886 Warneke, C., J. A. de Gouw, J. S. Holloway, J. Peischl, T. B. Ryerson, E. Atlas, D. Blake, M.
1887 Trainer, and D. D. Parrish (2012), Multi-year trends in volatile organic compounds in Los
1888 Angeles, California: five decades of improving air quality, *J. Geophys. Res.*, *117*, (D00V17),
1889 doi:10.1029/2012JD017899.
- 1890 Yuan, B., et al. (2012), Volatile organic compounds (VOCs) in urban air: How chemistry affects
1891 the interpretation of positive matrix factorization (PMF) analysis, *J. Geophys. Res.*, *117*,
1892 D24302, doi:10.1029/2012JD018236.
- 1893
- 1894
- 1895

1896 **Synthesis of Results - Emissions**1897 **Response to Question H**1898 **QUESTION H**1899 **Can emission estimates from area sources be improved with the CalNex measurements?**1900 **BACKGROUND**

1901 In general, area sources are defined as all stationary sources of air pollutants that are not
 1902 identified as major point sources. This category excludes large industrial and power generation
 1903 point sources, vehicle fleets, and natural sources, but includes all other sources. Though
 1904 emissions from individual area sources are often relatively small, collectively their emissions can
 1905 be of concern - particularly where large numbers of sources are located in heavily populated
 1906 areas. Area sources thus include many broad categories of industrial, commercial and
 1907 agricultural facilities.

1908 **POLICY RELEVANCE**

1909 The highly variable distribution, both spatially and temporally, of many pollutants makes
 1910 estimates of their emissions from area sources some of the most uncertain in the inventory.
 1911 Observation-based constraints on the quantification of these emissions are particularly valuable
 1912 for improving the accuracy of emission inventories, and hence the reliability of modeling based
 1913 upon these inventories.

1914 Some area source emissions have already been discussed in the response to Question F. These
 1915 emissions include methane and other small alkanes from the natural gas distribution system and
 1916 oil and gas production in the SoCAB (see Finding F2a), methane from landfills and dairies in the
 1917 SoCAB (see Finding F2b), methane and nitrous oxide from agricultural activities in the Central
 1918 Valley (see Findings F2c and F3), and halocarbon emissions in the SoCAB (see Finding F4).

1919 **FINDINGS**

1920 ***Finding H1: Gaseous elemental mercury emissions from a variety of California sources***
 1921 ***were estimated, and these estimates generally agreed with inventoried emissions. An***
 1922 ***exception is that emissions from the Los Angeles urban area were much larger than those***
 1923 ***in the inventory; reemission of mercury accumulated over the industrialized history of Los***
 1924 ***Angeles could account for this discrepancy.***

1925 *Weiss-Penzias et al.* [2013] measured gaseous elemental mercury (GEM) in the atmosphere
 1926 during the R/V *Atlantis* cruise between San Diego and San Francisco. GEM was quantified in
 1927 urban outflow, the Port of Los Angeles and associated shipping lanes, areas of high primary
 1928 productivity in coastal upwelling, the San Francisco Bay and the Sacramento ship channel.
 1929 Mean GEM for the whole cruise was $1.41 \pm 0.20 \text{ ng m}^{-3}$, indicating that background
 1930 concentrations were predominantly observed. When Los Angeles urban outflow was sampled
 1931 GEM displayed significantly higher concentrations that correlated with CO. Given the
 1932 inventoried CO emissions for the region, the correlation slope suggests a LA urban GEM source
 1933 of 1500 kg annually, which is about a factor of 10 larger than the total mercury emissions form

1934 the SoCAB estimated by the 2008 California Air Resources Board inventory. A contributing
1935 factor to this disagreement could be reemission of GEM from land and vegetation surfaces of
1936 anthropogenic mercury accumulated over the industrialized history of Los Angeles.

1937 Emissions from a local waste incinerator in the Port of Long Beach were measured during several
1938 encounters of its emission plume. GEM emissions from this source estimated in these plume
1939 encounters varied widely, suggesting that mercury-containing material was variable in the waste
1940 stream at this facility. A plume encounter from a large cargo ship allowed the estimation of
1941 GEM emissions from ocean ships worldwide of roughly 14 Mg y^{-1} , which is a minor contributor
1942 to global emissions ($< 1\%$ global anthropogenic sources), but may be an important local source
1943 in ports. GEM concentrations in the Carquinez Straits, where many large oil refineries are
1944 located, were rarely significantly elevated above the background. In an area where observed
1945 NO_x to SO_2 ratios indicated impacts refineries, the observed GEM concentrations were less than
1946 those predicted based on the 2008 California Air Resources Board inventory, indicating that
1947 GEM emissions may have been reduced.

1948 In a region north of Monterey Bay known for upwelling and high primary productivity, GEM
1949 was positively correlated with dimethyl sulfide (DMS) in seawater and the atmosphere. Using
1950 the observed GEM/DMS relationship and an estimate of the DMS flux in areas of high primary
1951 productivity, a flux of GEM of $0.017 \pm 0.009 \mu\text{mol m}^{-2} \text{ d}^{-1}$ was estimated. This flux is on the
1952 upper end of previously reported GEM ocean-air fluxes, suggesting that more data are needed to
1953 understand the potential for extremely high GEM fluxes in regions affected by coastal upwelling.

1954 **References**

1955 Weiss-Penzias, P. S., E. J. Williams, B. M. Lerner, T. S. Bates, C. Gaston, K. Prather, A.
1956 Vlasenko, and S. M. Li (2013), Shipboard measurements of gaseous elemental mercury along
1957 the coast of Central and Southern California. *J. Geophys. Res. Atmos.*, *118*, 208–219,
1958 doi:10.1029/2012JD018463.

1959
1960

1961

1962

1963

1964 **Synthesis of Results - Emissions**1965 **Response to Question I**1966 **QUESTION I**

1967 **What are the relative roles and impacts of NH₃ emissions from motor vehicles and dairy**
 1968 **farms?**

1969 **BACKGROUND**

1970 Ammonium nitrate (NH₄NO₃) aerosol is a major, and often the primary, contributor to
 1971 atmospheric PM_{2.5} concentrations in California. It is semi-volatile and continuously partitions
 1972 between the gas and aerosol phase. The distribution of total ammonium (NH₃ + NH₄⁺) and total
 1973 nitrate (NO₃⁻ + HNO₃) between the gas and aerosol phases is sensitive to meteorological factors
 1974 such as temperature and relative humidity. Major sources of ammonia in California are livestock
 1975 operations including dairies, agricultural fertilizers, waste management facilities, and motor
 1976 vehicles, while HNO₃ is an oxidation product of NO_x, primarily emitted by mobile sources.

1977 **POLICY RELEVANCE**

1978 PM_{2.5} currently exceeds ambient air quality standards in California. Development of effective
 1979 strategies for controlling the nitrate contribution to PM_{2.5} depends upon determining whether
 1980 available NH₃ or HNO₃ limits the amount of NH₄NO₃ that can be formed, and what are the major
 1981 sources of the limiting reactant.

1982 **FINDINGS**

1983 ***Finding II:* Within the SoCAB, conditions observed downwind of the dairy facilities were**
 1984 **always thermodynamically favorable for NH₄NO₃ formation due to high NH₃ mixing ratios**
 1985 **from those concentrated sources. Although automobile emissions of NH₃ were of**
 1986 **approximately the same magnitude as the dairies, they were more dispersed and thus**
 1987 **generated lower NH₃ mixing ratios. However, they are sufficiently high that they can**
 1988 **thermodynamically favor NH₄NO₃ formation. Reducing the dairy NH₃ emissions would**
 1989 **have a larger impact on reducing SoCAB NH₄NO₃ formation than would reducing**
 1990 **automobile NH₃ emissions.**

1991 *Nowak et al.* [2012] used airborne measurements from the NOAA WP-3D to quantify NH₃
 1992 emissions from both automobile and dairy facility sources in the LA basin. This analysis
 1993 compared these two emission sources to state and federal emission inventories, and assessed the
 1994 impact of these NH₃ sources on particulate ammonium nitrate (NH₄NO₃) formation. The
 1995 estimated NH₃ emissions from automobiles (62±24 metric tons per day) were similar in
 1996 magnitude to those from the dairy facilities (estimates from two flights were 33±16 and 176±88
 1997 metric tons per day). CARB's 2012 PM_{2.5} SIP inventory shows significantly lower NH₃
 1998 emission estimates for the SoCAB: 19 metric tons per day from on-road vehicles and 12 metric
 1999 tons per day for dairies. It must be noted that the CARB estimate for dairy emissions are based
 2000 on a winter emission factor; a summer emission factor would probably yield higher estimates.
 2001 The high emission rates from the spatially concentrated dairy facilities led to a larger impact on
 2002 NH₄NO₃ particle formation, with the calculated gas-particle equilibrium favoring the particle
 2003 phase in plumes downwind of the dairy facilities (points above black line in Figure I1). This

2004 paper suggested that NH_3 control strategies addressing dairy rather than automobile emissions
 2005 would have the larger effect on reducing particulate NH_4NO_3 formation in the Los Angeles
 2006 basin.

2007 To simulate atmospheric concentrations of gas- and aerosol-phase species in the SoCAB during
 2008 the CalNex study period, *Ensberg et al.* [2013] applied a detailed CMAQ three-dimensional
 2009 chemical transport model with boundary conditions extracted from a nested global-scale GEOS-
 2010 Chem model. Comparison of the simulation with observations at ground and sites and from
 2011 aircraft corroborated the conclusions of *Nowak et al.* [2012], but also showed that NH_3 mixing
 2012 ratios can be under-predicted by factors as high as 100 to 1000. Severe under-prediction of NH_3
 2013 emissions from dairy facilities is identified as the dominant source of measurement/model
 2014 disagreement in the eastern Los Angeles basin.

2015 The cause of the day-to-day variability in dairy farm NH_3 emissions seen in the two P-3 flights
 2016 [*Nowak et al.*, 2012] is not fully understood. Understanding variability of the magnitude
 2017 suggested by the WP-3D data may result in an improved ability to address NH_3 emissions, and
 2018 thus particulate ammonium nitrate formation in the LA basin, via dairy farm management
 2019 practices. These sources may be a good target for a longer-term, ground-based emissions
 2020 monitoring effort to better quantify and understand the drivers for such variability. *Ensberg et*
 2021 *al.* [2013] suggest that adding gas-phase NH_3 measurements and size-resolved measurements, up
 2022 to 10 μm , of nitrate and various cations (e.g. Na^+ , Ca^{2+} , K^+ , Mg^{2+}) to routine monitoring stations
 2023 in the L.A. basin would greatly facilitate interpreting day-to-day fluctuations in fine and coarse
 2024 inorganic aerosol.

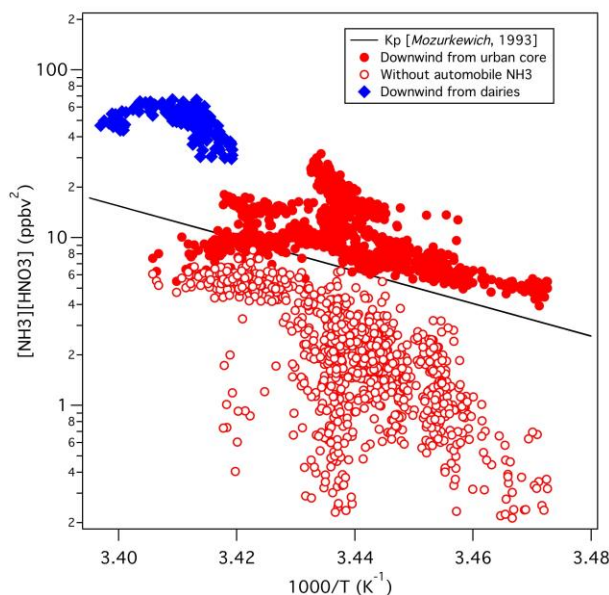


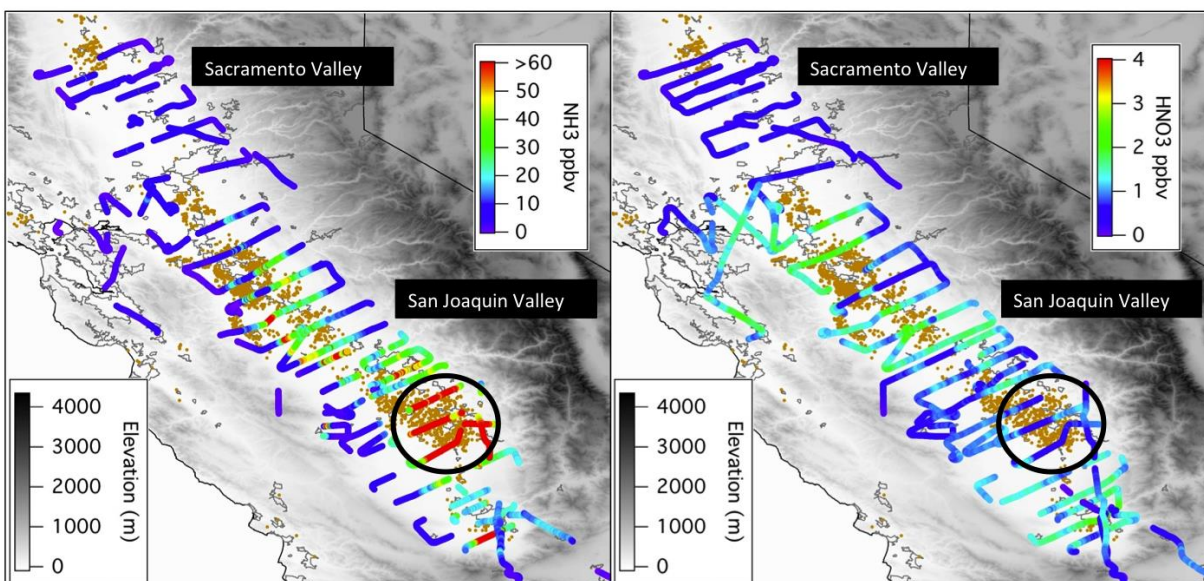
Figure 11. The theoretical solid NH_4NO_3 dissociation constant (K_p) (black line), the observed urban core NH_3 and HNO_3 partial pressure product (solid circles), the estimated urban core NH_3 and HNO_3 partial pressure product without automobile NH_3 emissions (open circles), and the observed NH_3 and HNO_3 partial pressure product in the dairy plumes (blue diamonds) for the 14 May flight plotted as a function of ambient temperature. Formation of particulate NH_4NO_3 is favored when points are above the line, and the gas-phase NH_3 and HNO_3 when points are below the line. The range of the abscissa corresponds to 14 °C on the right and 22 °C on the left.

2025
 2026

2027 ***Finding I2a:*** Within the San Joaquin Valley, despite large concentrations of NH_3 (often
 2028 many 100's of ppbv) associated with dairies, measured NH_4NO_3 concentrations were
 2029 relatively low (≤ 1 ppbv) due to low HNO_3 concentrations resulting from low NO_x
 2030 emissions.

2031 ***Finding I2b:*** Within the San Joaquin Valley NH_3 emissions are underestimated in the
 2032 inventories by about a factor of three.

2033 *Analysis: J.B. Nowak (presentation at ACS National Meeting, August 2012, Philadelphia)*
 2034 A limited number of WP-3D flights in the Central Valley during CalNex provided an initial look
 2035 at NH_3 emissions and subsequent NH_4NO_3 formation in the spring (i.e. May). Figure I2 presents
 2036 the observed concentrations of the NH_4NO_3 precursors, NH_3 and HNO_3 . NH_3 concentrations
 2037 were much higher (up to 100's of ppbv) in the San Joaquin Valley (SJV) than in SoCAB, but
 2038 NH_4NO_3 concentrations were not particularly elevated (maximum ≈ 1 ppbv), and were lower
 2039 than the maximum concentrations observed in SoCAB (≈ 3 ppbv). The concentrations of
 2040 NH_4NO_3 formed were limited by relatively small NO_x emissions in SJV, and by the magnitude
 2041 of NH_3 emissions in SoCAB.



2042
 2043 **Figure I2.** Flight tracks of the NOAA WP-3D aircraft in the Central Valley within the planetary
 2044 boundary layer during CalNex (May 7, 11, and 12). The color-coding indicates the measured
 2045 ammonia (left panel) and nitric acid (right panel) mixing ratios. The small orange circles indicate
 2046 livestock facilities.

2047 Measurements from the Bakersfield surface site are generally consistent with the WP-3D aircraft
 2048 results [Murphy, 2012]. The NH_3 concentrations and the $(\text{NH}_3 + \text{NH}_4^+)/\text{NO}_y$ ratio were much
 2049 higher than seen in the SoCAB, and NH_3 sources were clearly dominated by area emissions from
 2050 agricultural activities. The correlation between NH_3 and CO was weak indicating a relatively
 2051 small contribution of mobile NH_3 emissions in the SJV.

2052 References

2053 Ensberg, J. J., et al. (2013), Inorganic and black carbon aerosols in the Los Angeles Basin during
 2054 CalNex, *J. Geophys. Res. Atmos.*, 118, doi:10.1029/2012JD018136.
 2055 Murphy, J., (2012), personal communication, University of Toronto.
 2056 Nowak, J. B., J. A. Neuman, R. Bahreini, A. M. Middlebrook, J. S. Holloway, S. A. McKeen, D.
 2057 D. Parrish, T. B. Ryerson, and M. Trainer (2012), Ammonia sources in the California South
 2058 Coast Air Basin and their impact on ammonium nitrate formation, *Geophys. Res. Lett.*, 39,
 2059 L07804, doi:10.1029/2012GL051197.

2060

2061 **Synthesis of Results - Emissions**

2062 **Response to Question J**

2063 **QUESTION J**

2064 **Are there significant differences between emissions in the San Joaquin Valley Air Basin (SJVAB) and the South Coast Air Basin (SoCAB)?**
 2065

2066 **BACKGROUND**

2067 By some metrics, the improvement of air quality in the SoCAB has been faster than in the
 2068 SJVAB (e.g., see Fig. 1 in the Introduction). One possible cause of this difference may be due to
 2069 a different mix of emissions between the two regions.

2070 **POLICY RELEVANCE**

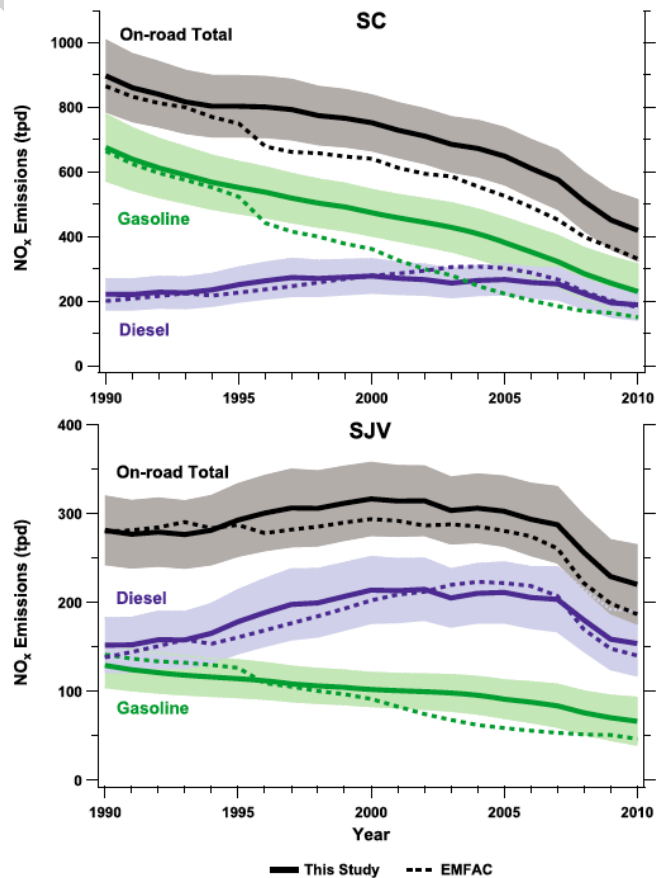
2071 Most emission controls are applied uniformly across California. However, there are indications
 2072 that the response of pollutant concentrations to these emission controls may differ among regions
 2073 of the State. When there are important regional differences in emissions, then regional/local
 2074 emphasis of area and stationary emission controls may more effectively reduce pollutant
 2075 concentrations.

2076 **FINDINGS**

2077 ***Finding J1:* NO_x emissions from the on-**
 2078 **road vehicle fleet have decreased more**
 2079 **rapidly in the SoCAB than in the**
 2080 **SJVAB.**

2081 *McDonald et al.* [2012] show that total
 2082 NO_x emissions from gasoline and diesel-
 2083 powered on-road vehicles in the SoCAB
 2084 and the SJVAB have differed in their time
 2085 response between 1990 and 2010 (Fig. J1,
 2086 also included in this report as Fig. F3). In
 2087 the SoCAB NO_x emissions decreased
 2088 continuously by more than a factor of 2
 2089 through the period, while in the SJV NO_x
 2090 emissions initially increased, reaching a
 2091 peak near 2000, and only dropping below
 2092 the 1990 level at the start of the recession

Figure J1. Trends in NO_x emissions from on-road vehicles in the South Coast Air Basin (SC) and the SJV. Shaded areas represent uncertainties of estimates. Dotted lines show estimates from EMFAC (Figure taken from *McDonald et al.* [2012]).

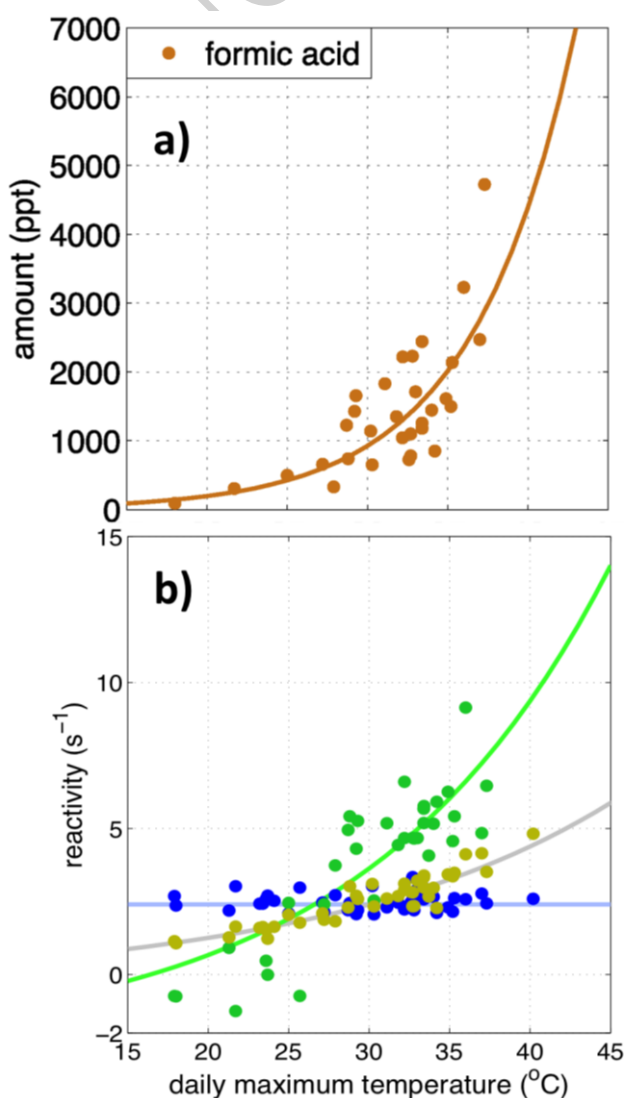


2093 in 2008. This is largely caused by differences in the vehicle fleets, with diesel vehicles
 2094 dominating in the SJV, and gasoline vehicles dominating in the SoCAB. The time variation of
 2095 the emissions from these two vehicle classes has differed markedly in California. Diesel NO_x
 2096 emissions increased between 1990 and 1997, stabilized between 1997 and 2007, and decreased
 2097 since 2007, while gasoline NO_x emissions decreased steadily, by 65% overall between 1990 and
 2098 2010. A secondary cause of this regional difference is a slower decrease of NO_x emissions from
 2099 gasoline vehicles due to larger percentage population increase in the SJVAB than in SoCAB.

2100 **Finding J2: There is evidence that temperature dependent VOC emissions from an**
 2101 **unidentified source, perhaps associated with agricultural activities and petroleum**
 2102 **operations, are important in the SJVAB but absent in the SoCAB.**

2103 Analysis of historical data from the SJVAB [Pusede and Cohen, 2012; Pusede et al., 2013]
 2104 shows that the NO_x versus VOC sensitivity of the O₃ photochemistry changes markedly with
 2105 ambient temperature, becoming much more NO_x sensitive on the hottest days, which are also the
 2106 days that lead to most O₃ exceedances in this air basin. CalNex measurements from the
 2107 Bakersfield site (Fig. J2) have been analyzed to identify the cause of this change in
 2108 photochemical regime as a particular VOC source that is rich in oxygenated VOCs [Pusede et
 2109 al., 2013]. The temperature dependence of the
 2110 ambient concentrations of some oxygenated
 2111 VOCs (Fig. J2a illustrates one example)
 2112 provides some of the support for this
 2113 identification; their rapid increase with
 2114 temperature provides more photochemical fuel
 2115 and larger VOC to NO_x ratios on hot days. In
 2116 addition, the measured reactivity of OH
 2117 radicals with VOCs (an indication of the
 2118 photochemical regime) shows a similar rapid
 2119 increase with temperature (Fig. J2b). Notably,
 2120 at lower temperatures, the measured OH
 2121 reactivity agrees with that calculated from the
 2122 measured VOC concentrations, indicating that
 2123 all VOCs important for O₃ production at those
 2124 temperatures are measured. However, at
 2125 higher temperatures the measured VOCs can

Figure J2. Temperature dependence of **a)** formic acid concentrations and **b)** reactivity of organic compounds with OH radicals at the Bakersfield site during CalNex 2010. Panel **b)** shows daily average reactivity (with fits) for sum of temperature-independent organic species (blue), sum of temperature-dependent organic species (yellow), and the directly measured OH reactivity with the contributions from inorganic and temperature-independent organic species subtracted (green). Figure **a)** taken from Cohen et al., [2013], and figure **b)** adapted from Pusede et al. [2013].



2126 account for only about half of the measured OH reactivity, pointing to the importance of
 2127 unmeasured VOCs. The reactivity contribution of these unmeasured VOCs is equal to the
 2128 difference between the green and yellow fits in Fig. J1b.

2129 The measured reactivity of OH radicals with VOCs behaves very differently in the SoCAB
 2130 compared to the SJV (Fig. J2) as evidenced by the measurements from the Pasadena ground site
 2131 [Stevens, 2013]. First, at all temperatures the measured OH reactivity agrees well (generally
 2132 about 20% greater) with that calculated from the measured VOC concentrations, and second the
 2133 relatively small difference between the measured reactivity and that calculated from the
 2134 measured VOC concentrations does not vary significantly with temperature. Evidently the
 2135 important, temperature dependent source of VOC emissions in the SJV is not present in the
 2136 SoCAB.

2137 The source of the oxygenated VOCs in the SJV has not been firmly established. The intense
 2138 agricultural activity in the SJVAB that is not present in the SoCAB may indicate that this source
 2139 leads to a significant difference in emissions between the air basins. However, our
 2140 understanding of the source of these species is not sufficient to design a strategy aimed at
 2141 controlling these VOC emissions in the southern SJVAB. Thus, NO_x controls are currently the
 2142 only option for reducing high temperature violations of the O₃ standard in the SJVAB. The
 2143 analysis of *Pusede and Cohen* [2012] and *Pusede et al.* [2013] indicates that such NO_x controls
 2144 would be effective. Indeed, they conclude that widespread NO_x reductions are approaching the
 2145 point where O₃ reductions will be a direct consequence of NO_x emission reductions throughout
 2146 the SJVAB. The effectiveness has been and will be dependent on temperature; at the highest
 2147 temperatures, where violations of state and federal standards are most frequent, NO_x controls
 2148 will be most effective.

2149 *Gentner et al.* [2013] find that at Bakersfield, petroleum and dairy operations each comprised 22-
 2150 23% of anthropogenic non-methane organic carbon and were each responsible for ~12% of
 2151 potential precursors to ozone, but their impacts as potential SOA precursors were estimated to be
 2152 minor. A rough comparison with the *CARB* [2010] emission inventory supports the
 2153 quantification of the relative emissions of reactive organic gases provided by the inventories.
 2154 The SoCAB does receive emissions from oil and gas production [*Peischl, et al.*, 2013], but of a
 2155 much smaller magnitude.

2156 ***Finding J3: The relative amounts of ammonia and NO_x emissions are such that formation***
 2157 ***of ammonium nitrate aerosol (the major component of PM_{2.5} during many exceedance***
 2158 ***episodes) is ammonia-limited in the SoCAB and NO_x-limited in the SJVAB.***

2159 *Analysis: This material is taken from Nowak et al. (2012a,b).*

2160 As fully discussed in the Response to Question I, the relatively large NO_x emissions from the
 2161 vehicle fleet and the relative small ammonia emissions from dairies and vehicles in the SoCAB
 2162 causes the formation of ammonium nitrate aerosol to be NH₃-limited. In the SJVAB the intense
 2163 agricultural activities and smaller vehicle emissions causes the relative emission magnitudes to
 2164 be reversed so that the formation of ammonium nitrate aerosol is NO_x-limited.

2165 References

- 2166 Cohen, R. C., et al. (2013), SJV Air Quality: Insights from CalNex 2010, ARB Chair's Research
 2167 Seminar, 22 April 2013 (<http://www.arb.ca.gov/research/seminars/cohen3/cohen3.pdf>).
- 2168 Gentner, D.R., et al. (2013), Emissions of organic carbon and methane from petroleum and dairy
 2169 operations in California's San Joaquin Valley, *Atmos. Chem. Phys. Disc.*, submitted.

- 2170 McDonald, B. C., T. R. Dallmann, E. W. Martin, and R. A. Harley (2012), Long-term trends in
2171 nitrogen oxide emissions from motor vehicles at national, state, and air basin scales, *J.*
2172 *Geophys. Res.*, *117*, D00V18, doi:10.1029/2012JD018304.
- 2173 Nowak, J. B., J. A. Neuman, R. Bahreini, A. M. Middlebrook, J. S. Holloway, S. A. McKeen, D.
2174 D. Parrish, T. B. Ryerson, and M. Trainer (2012a), Ammonia sources in the California South
2175 Coast Air Basin and their impact on ammonium nitrate formation, *Geophys. Res. Lett.*, *39*,
2176 L07804, doi:10.1029/2012GL051197.
- 2177 Nowak, J. B. (2012b), Ammonia Emissions from Agricultural Sources and their Implications for
2178 Ammonium Nitrate Formation in California, presentation at ACS National Meeting, August
2179 2012, Philadelphia, PA.
- 2180 Peischl, J., et al. (2013), Quantifying sources of methane using light alkanes in the Los Angeles
2181 basin, California, *J. Geophys. Res. Atmos.*, *118*, 4974–4990, doi:10.1002/jgrd.50413.
- 2182 Pusede, S. E., and R. C. Cohen (2012), On the observed response of ozone to NO_x and VOC
2183 reactivity reductions in San Joaquin Valley California 1995–present, *Atmos. Chem. Phys.*, *12*,
2184 8323–8339, doi:10.5194/acp-12-8323-2012.
- 2185 Pusede, S. E., et al. (2013), On the temperature dependence of organic reactivity, ozone
2186 production, and the impact of emissions controls in San Joaquin Valley California, *Atmos.*
2187 *Chem. Phys. Disc*, submitted.
- 2188 Stevens, P., (2013), personal communication, Indiana University.
- 2189

2190 **Synthesis of Results - Emissions**2191 **Response to Question K**2192 **QUESTION K**

2193 **What are the significant sources of sulfur in southern California that contribute to**
 2194 **enhanced sulfate (SO₄²⁻) concentrations in SoCAB?**

2195 Sulfate constitutes a significant fraction of ambient PM_{2.5} concentrations in the SoCAB, an air
 2196 basin that exceeded the NAAQS on an estimated 8 to 19 days in each of the years 2008-2012.
 2197 The sulfate contribution is particularly large in summer, when the highest PM_{2.5} concentrations
 2198 generally are recorded in SoCAB (see Fig. C2).

2199 **POLICY RELEVANCE**

2200 Due to ongoing control efforts, SO_x emissions and corresponding sulfate concentrations have
 2201 decreased in the SoCAB. An understanding of Southern California's remaining sulfur sources is
 2202 necessary to formulate effective policies to further reduce this PM_{2.5} constituent.

2203 California has made substantial efforts to reduce sulfur emissions from point sources, from the
 2204 on-road vehicle fleet by reducing the sulfur content of gasoline and diesel fuel, and from
 2205 commercial marine vessels by requiring use of low-sulfur fuel and low-speed operation within
 2206 Regulated California Waters (up to 24 nautical miles of the California coastline). The 2008
 2207 CARB emission inventory estimates that total SO_x emissions in the SoCAB decreased from 51.2
 2208 tons in 2000 to 38.0 tons in 2008.

2209 During CalNex, sulfur dioxide (SO₂, the primary sulfur species emitted by anthropogenic
 2210 sources) and dimethylsulfide (DMS, a major sulfur species released by natural sources) were
 2211 measured throughout the SoCAB by the WP-3D aircraft and at the Pasadena ground site; the R/V
 2212 *Atlantis* also measured SO₂ in California ports and coastal waters.

2213 **FINDINGS**

2214 ***Finding K1: No significant sources of sulfur beyond those included in the CARB inventory***
 2215 ***can be identified from the CalNex 2010 data.***

2216 The measurements in Fig. K1 illustrate emissions from the two major SO₂ source classes
 2217 impacting the SoCAB that could be identified from the CalNex 2010 data: point source industrial
 2218 emissions in the vicinity of the Port of Long Beach and commercial marine vessels. Although it
 2219 is not possible to quantify the Long Beach point source emissions from the WP-3D aircraft data,
 2220 it is clear that the emissions in 2010 were significantly reduced from those observed in 2002,
 2221 qualitatively consistent with the reductions included in the CARB inventory. The ship emission
 2222 data included in Fig. K2 are those collected by the WP-3D reported by *Lack et al.* [2011] while
 2223 the marine vessel was operating on high sulfur fuel. The slope of the line (10.6 ± 0.5 ppbv SO₂ /
 2224 ppmv CO₂) is consistent with the 3.1% sulfur fuel content reported by the vessel. These
 2225 emissions represent marine vessel operation outside of the Regulated California Waters. When
 2226 the vessel switched to low-sulfur fuel and low-speed operation, sulfur emissions dropped by 96%
 2227 [*Lack et al.*, 2011], indicating that the marine vessel regulations are highly effective.

2228 Within the urban areas of the SoCAB, it
 2229 was not possible to identify and quantify
 2230 emissions from the on-road vehicle fleet.
 2231 At the Pasadena ground site, both surface
 2232 measurements and DOAS measurements at
 2233 elevated altitudes through the boundary
 2234 layer [Ryerson *et al.*, 2013] generally found
 2235 low concentrations (average \pm standard
 2236 deviation = 0.3 ± 0.3 ppbv), with only
 2237 occasional peaks increasing to a maximum
 2238 of 3.4 ppbv. Any on-road vehicle emissions
 2239 could not be differentiated from small
 2240 contributions from point source plumes
 2241 transported to Pasadena from industrial
 2242 facilities or marine vessels.

2243 DMS emissions from oceanic sources do
 2244 not make a significant contribution to the
 2245 sulfate burden in the SoCAB. DMS
 2246 measurements at Pasadena were very low
 2247 (average \pm standard deviation = $0.010 \pm$
 2248 0.016 ppbv, with a maximum of 0.13 ppbv).
 2249 The WP-3D aircraft measured within the
 2250 SoCAB and over coastal waters, but did not
 2251 encounter any concentrations greater than
 2252 0.4 ppbv. With a lifetime on the order of a
 2253 day, the DMS contribution to the SoCAB
 2254 sulfate burden cannot be large (average
 2255 roughly estimated as less than $0.1 \mu\text{g}/\text{m}^3$).

2256 References

2257 Lack, D. A., et al. (2011), Impact of fuel quality regulation and speed reductions on shipping
 2258 emissions: Implications for climate and air quality, *Environ. Sci. Technol.*, 45, 9052–9060,
 2259 doi:10.1021/es2013424.

2260 Ryerson, T.B., et al. (2013), The 2010 California Research at the Nexus of Air Quality and
 2261 Climate Change (CalNex) field study, *J. Geophys. Res. Atmos.*, 118, 5830–5866,
 2262 doi:10.1002/jgrd.50331.

2263

2264

2265

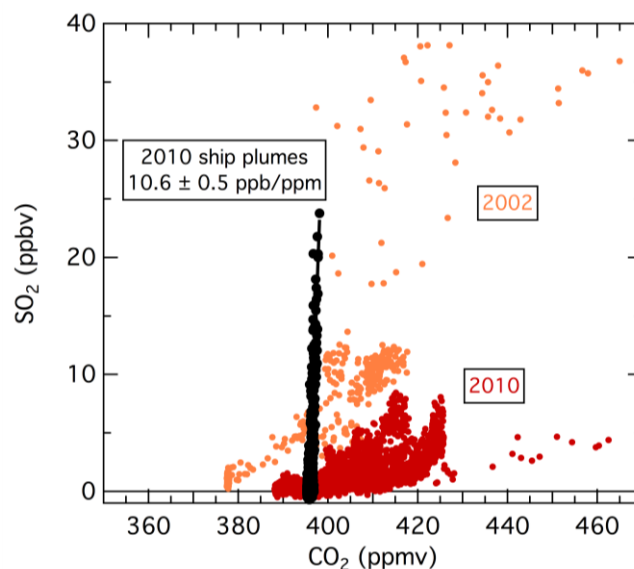


Figure K1. Dependence of SO₂ on CO₂ in the Long Beach area and in offshore ship plumes. The WP-3D aircraft collected the Long Beach data during a single flight in 2002 (orange symbols) and four flights in 2010 (red symbols). The ship plume data (black symbols) were collected in the ship emission study reported by *Lack et al.* [2011] outside Regulated California Waters. The black line indicates the linear least squares fit to the ship plume data, with the slope annotated. (Figure from *J. Holloway*, NOAA)

2266 **Synthesis of Results - Emissions**2267 **Response to Question L**2268 **QUESTION L**2269 **What is the impact of biogenic emissions, especially in foothills of the Sierra Nevada?**2270 **BACKGROUND**

2271 On a global scale, emissions of VOCs from vegetation are estimated to be an order of magnitude
 2272 greater than those anthropogenic sources [Guenther *et al.*, 1995]. In forested rural environments
 2273 [Trainer *et al.*, 1987] and even in some urban areas [Chameides *et al.*, 1988] biogenic VOCs
 2274 have been shown to dominate over anthropogenic VOCs in photochemical O₃ production. They
 2275 are also thought to play a major role in SOA formation, a role that may involve interaction
 2276 between biogenic VOCs and anthropogenic NO_x emissions [e.g., Hoyle *et al.*, 2011].

2277 Quantifying the impact of biogenic species on O₃ and SOA production is difficult because the
 2278 emissions are highly variable, dependent upon vegetation density and plant species as well as a
 2279 variety of meteorological parameters including temperature, sunlight intensity and drought stress.
 2280 Up to the present time, isoprene (primarily from deciduous vegetation) and monoterpenes
 2281 (primarily from coniferous trees) are the biogenic species that have received the most attention in
 2282 atmospheric chemistry research, but it is suspected that there are many more biogenic species
 2283 whose emissions may be important [e.g., Goldstein and Galbally, 2007], including those from
 2284 agricultural sources [e.g., Fares *et al.*, 2012].

2285 **POLICY RELEVANCE**

2286 Biogenic emissions of VOCs represent a natural source of fuel for photochemical production of
 2287 O₃ and SOA formation, a source that largely cannot be regulated. It is important to quantify the
 2288 emissions and the roles of these VOCs in order to accurately evaluate the effectiveness of policy-
 2289 mandated reductions of emissions of anthropogenic VOCs.

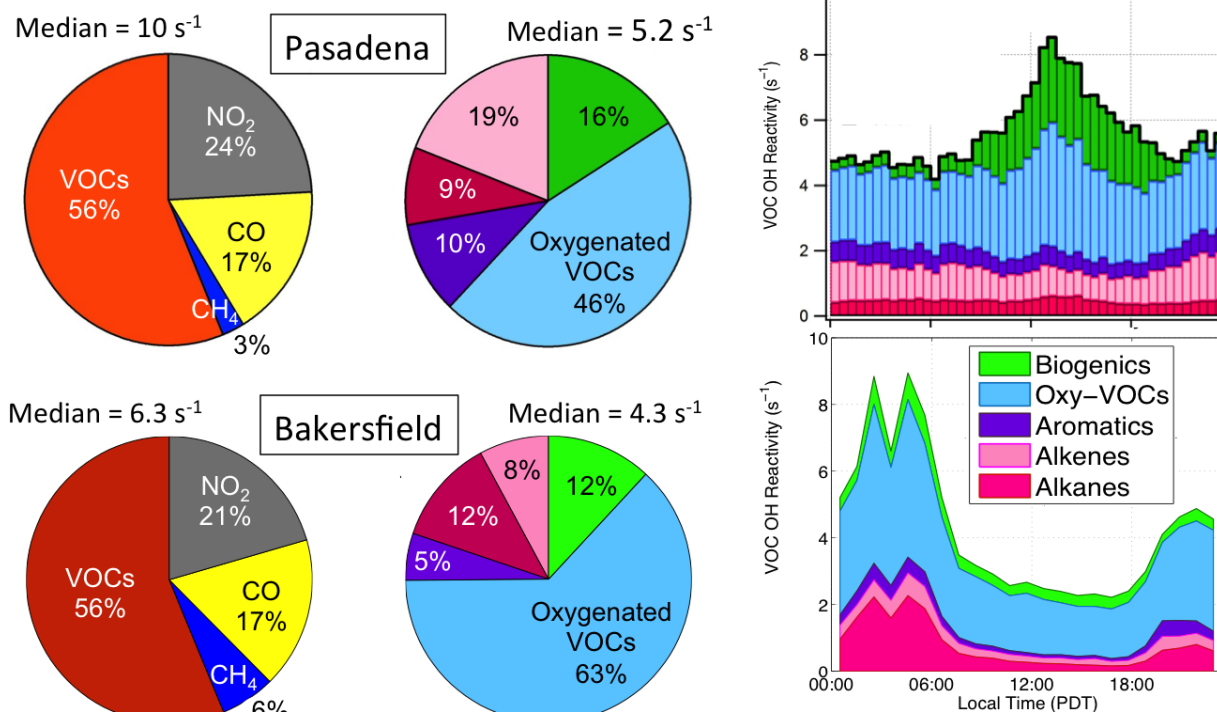
2290 **FINDINGS**

2291 ***Finding L1a: Photochemical O₃ formation in the SoCAB is dominated by anthropogenic***
 2292 ***VOCs rather than biogenic VOCs; this was true in 2010 despite very substantial reductions***
 2293 ***in anthropogenic VOC emissions over past decades.***

2294 ***Finding L1b: Considering only the individually measured VOCs, photochemical O₃***
 2295 ***formation in the SJVAB is also dominated by anthropogenic VOCs. However, on the***
 2296 ***hotter days in the SJVAB there is evidence that unmeasured VOCs make an important***
 2297 ***contribution to O₃ formation, and this contribution well may be of biogenic origin.***

2298 The OH reactivity of organic species provides a measure of the O₃ photochemical formation
 2299 potential of ambient pollutant concentrations. Figure L1 compares the OH reactivity for species
 2300 measured at the Pasadena and Bakersfield sites during CalNex 2010. Considering all species
 2301 (with all VOCs considered together), the relative contributions of the different species (left
 2302 panels in Fig. L1) are quite similar at the two sites, although the median total reactivity was
 2303 about 60% higher in Pasadena.

2304 The measured biogenic VOCs (green segments in the four plots to the right) account for a
 2305 relatively small and similar fraction of the total organic OH reactivity at each site. However, at
 2306 Pasadena, the biogenic contribution peaked at midday (upper right panel in Fig. L1), when O₃
 2307 production is at its maximum, while at Bakersfield the biogenic contribution remained
 2308 approximately constant throughout the day and night (lower right panel in Fig. L1). Thus, the
 2309 directly measured biogenic species make a larger contribution to photochemical O₃ production at
 2310 the Pasadena site compared to the Bakersfield site. However it is important to consider the
 2311 difference between the total, directly measured OH reactivity at the Bakersfield site and the
 2312 reactivity calculated from the sum of the individually measured VOCs. *Pusede and Cohen*
 2313 [2012] and *Pusede et al.* [2013] show that there is a large contribution to total VOC reactivity
 2314 due to unmeasured VOCs, especially on the hotter days (see more detailed discussion in the
 2315 Response to Question J). If these unmeasured species are of biogenic origin, such as dairy
 2316 emissions or other biogenic sources, then the importance of biogenic VOCs would be
 2317 underestimated by the analysis in Fig. L1. Importantly, at the Pasadena a similar difference was
 2318 not observed between total OH reactivity and that calculated from the individually measured
 2319 VOCs.



2320 **Figure L1.** OH reactivity for all species (left) and organic species only (middle) at the Pasadena
 2321 (top) and Bakersfield (bottom) sites, based on the median measured concentrations throughout the
 2322 day. The diurnal variability of the VOC reactivity and its speciation is shown on the right. The
 2323 color code for the VOC species are annotated in lower right panel. Biogenic species include
 2324 isoprene, MVK and MACR. Oxygenated species include ethanol, formaldehyde and
 2325 acetaldehyde; the latter two may include a contribution produced from the oxidation of isoprene.
 2326 (Figure from *J. Gilman, NOAA and S. Pusede, Univ. Cal., Berkeley*)
 2327

2328

2329 **Finding L2: Biogenic VOCs play significant roles in SOA formation in the SJVAB during**
 2330 **both daytime and nighttime; the different processes important during light and dark**
 2331 **periods both involve interactions between biogenic VOCs and anthropogenic emissions.**

2332 *Rollins et al.* [2013] identified substantial secondary organic aerosol (SOA) production at night
 2333 at the Bakersfield site. SOA was produced from the reaction of the NO₃ radical (a nighttime
 2334 oxidation product of anthropogenic NO_x emissions) with unsaturated VOCs of biogenic origin.
 2335 At this site, SOA concentrations peaked during the night, a situation different from most urban
 2336 areas, which experience daytime SOA maxima. This analysis of *Rollins et al.* [2013] is
 2337 discussed more completely in Finding N4.

2338 Research conducted as part of the Carbonaceous Aerosols and Radiative Effects Study (CARES)
 2339 field campaign has identified enhanced SOA formation in the transported Sacramento plume,
 2340 when the anthropogenic emissions mixed with isoprene-rich air in the Sierra Nevada foothills
 2341 [*Setyan et al.*, 2012; *Shilling et al.*, 2013]. These results indicate that the presence of
 2342 anthropogenic emissions increase SOA formation from biogenic VOCs.

2343 Two studies [*Liu et al.*, 2012; *Zhao et al.*, 2013] based upon different instrumental measurement
 2344 techniques and utilizing different analysis approaches reach similar conclusions regarding
 2345 sources of organic aerosol (OA) at the Bakersfield site. SOA accounts for 70-90% of the OA,
 2346 while the SOA formed from biogenic VOCs account for only about ~10% of the total OA. This
 2347 biogenic contribution is a maximum at night, consistent with the conclusions of *Rollins et al.*
 2348 [2013].

2349 Both the nighttime mechanism in the southern SJV and the daytime mechanism in the
 2350 Sacramento plume produce significant amounts of SOA, but it has not yet been possible to
 2351 provide a budget of the contributions of different VOC sources to the atmospheric burden of
 2352 SOA. Development of such a budget must account for the interactions of biogenic VOCs with
 2353 anthropogenic emissions. However, as pointed out by *Rollins et al.* [2013], it is clear that
 2354 reductions in NO_x emissions should reduce the concentration of organic aerosol, at least in
 2355 Bakersfield and the southern SJV region.

2356 **Finding L3: Biogenic VOCs play a significant, but minor role in SOA formation in the**
 2357 **SoCAB.**

2358 Several lines of reasoning indicate that biogenic VOCs make a significant but minor contribution
 2359 to SOA formation in the SoCAB. First, Figure L1 shows that biogenic VOCs account for only a
 2360 small fraction of total organic OH reactivity, and oxidation of the species responsible for the
 2361 reactivity (isoprene, MVK and MACR) are generally believed to have small yields of SOA.
 2362 Second, glyoxal is believed to be an important secondary product of biogenic VOC oxidation
 2363 that is particularly important for SOA formation. However, *Washfelder et al.* [2011] show that
 2364 glyoxal contributes no more than 0.2 μg m⁻³ or 4% of the SOA mass at the Pasadena site in the
 2365 SoCAB. *Williams et al.* [2010] present an analysis of SOA measurements from the 2005
 2366 Study of Organic Aerosol at Riverside (SOAR). They find that the sources SOA appear
 2367 to be mostly from the oxidation of anthropogenic precursor gases, but that one SOA
 2368 component had contributions from oxygenated biogenics. *Hayes et al.*, [2013] analyze SOA
 2369 sources at the Pasadena site during CalNex, and find that biogenic sources do influence the
 2370 measured OA. They also note that ¹⁴C measurements for selected days during CalNex show that
 2371 in the early morning hours when low-volatility oxygenated organic aerosol (LV-OOA) is
 2372 dominant (compared to other OA components and elemental carbon), about 50% of total carbon
 2373 is nonfossil (e.g., from modern presumably biogenic sources) [P. Zotter et al., manuscript in

2374 preparation, 2012; Bahreini et al., 2012]. However, the mass of the nonfossil aerosol component
2375 does not increase during the day when SOA is primarily formed in the SoCAB.

2376 References

- 2377 Bahreini, R., et al. (2012), Gasoline emissions dominate over diesel in formation of secondary
2378 organic aerosol mass, *Geophys. Res. Lett.*, *39*, L06805, doi:10.1029/2011GL050718.
- 2379 Chameides, W. L., et al. (1988), The role of biogenic hydrocarbons in urban photochemical
2380 smog: Atlanta as a case study, *Science*, *241*, 1473–1475.
- 2381 Fares, S., J-H. Park, D.R. Gentner, R. Weber, E. Ormeño, J. Karlik, and A.H. Goldstein (2012),
2382 Seasonal cycles of biogenic volatile organic compound fluxes and concentrations in a
2383 California citrus orchard, *Atmos. Chem. Phys.*, *12*, 9865-9880, doi:10.5194/acp-12-9865-
2384 2012.
- 2385 Goldstein, A. H., and I. E. Galbally (2007), Known and unexplored organic constituents in the
2386 earth's atmosphere, *Environ. Sci. Technol.*, *41*(5), 1514-1521.
- 2387 Guenther, A., et al. (1995), A Global Model of Natural Volatile Organic Compound Emissions,
2388 *J. Geophys. Res. Atmos.*, *100*, 8873–8892.
- 2389 Hayes, P. L., et al. (2013), Organic aerosol composition and sources in Pasadena, California
2390 during the 2010 CalNex campaign, *J. Geophys. Res. Atmos.*, *118*, 9233–9257,
2391 doi:10.1002/jgrd.50530.
- 2392 Hoyle, C. R., et al. (2011), A review of the anthropogenic influence on biogenic secondary
2393 organic aerosol *Atmos. Chem. Phys.*, *11*, 321–343.
- 2394 Liu, S., et al. (2012), Secondary organic aerosol formation from fossil fuel sources contribute
2395 majority of summertime organic mass at Bakersfield, *J. Geophys. Res.*, *117*, D00V26,
2396 doi:10.1029/2012JD018170.
- 2397 Pusede, S. E., and R. C. Cohen (2012), On the observed response of ozone to NO_x and VOC
2398 reactivity reductions in San Joaquin Valley California 1995–present, *Atmos. Chem. Phys.*, *12*,
2399 8323–8339, doi:10.5194/acp-12-8323-2012.
- 2400 Pusede, S. E., et al. (2013), On the temperature dependence of organic reactivity, ozone
2401 production, and the impact of emissions controls in San Joaquin Valley California, *Atmos.*
2402 *Chem. Phys. Disc*, submitted.
- 2403 Rollins, A. W., E. C. Browne, K.-E. Min, S. E. Pusede, P. J. Wooldridge, D. Gentner, A. H.
2404 Goldstein, S. Liu, D. A. Day, L. M. Russell, and R. C. Cohen (2012) Evidence for NO_x
2405 Control over Nighttime SOA Formation, *Science*, *337*, 1210-1212,
2406 doi:10.1126/science.1221520.
- 2407 Setyan, A., et al. (2012) Characterization of submicron particles influenced by mixed biogenic
2408 and anthropogenic emissions using high-resolution aerosol mass spectrometry: results from
2409 CARES, *Atmos. Chem. Phys.*, *12*, 8131-8156, doi:10.5194/acp-12-8131-2012.
- 2410 Shilling, J. E. (2013) Enhanced SOA formation from mixed anthropogenic and biogenic
2411 emissions during the CARES campaign, *Atmos. Chem. Phys.*, *13*, 2091-2113,
2412 doi:10.5194/acp-13-2091-2013.

- 2413 Trainer, M., Williams, E. J., Parrish, D. D., Buhr, M. P., Allwine, E. J., Westberg, H. H.,
2414 Fehsenfeld, F. C., and Liu, S. C. (1987), Models and observations of the impact of natural
2415 hydrocarbons on rural ozone, *Nature*, 329, 705–707.
- 2416 Washenfelder, R. A., et al. (2011), The glyoxal budget and its contribution to organic aerosol for
2417 Los Angeles, California, during CalNex 2010, *J. Geophys. Res.*, 116, D00V02,
2418 doi:10.1029/2011JD016314.
- 2419 Williams, B. J., A. H. Goldstein, N. M. Kreisberg, S. V. Hering, D. R. Worsnop, I. M. Ulbrich,
2420 K. S. Docherty, and J. L. Jimenez (2010), Major components of atmospheric organic aerosol
2421 in southern California as determined by hourly measurements of source marker compounds,
2422 *Atmos. Chem. Phys.*, 10 (23), 11577-11603.
- 2423 Zhao, Y., et al. (2013), Sources of organic aerosol investigated using organic compounds as
2424 tracers measured during CalNex in Bakersfield, *J. Geophys. Res. Atmos.*, 118,
2425 doi:10.1002/jgrd.50825.
- 2426
- 2427

DRAFT - Do Not Cite

2428 **Synthesis of Results - Climate Processes/Transformation**2429 **Response to Question M**2430 **QUESTION M**2431 **How does the atmospheric chemistry vary spatially and temporally?**2432 **BACKGROUND**

2433 California has a great diversity of lands, from seashore to high mountains, from densely
 2434 populated urban areas through sparsely populated rural areas to wilderness areas, and from rich
 2435 agricultural areas to deserts. A great spatial variation in the emissions of reactive species to the
 2436 atmosphere accompanies this diversity of land types and uses. Within all of these areas, these
 2437 emissions vary widely on time scales of hours with changing solar radiance, days as synoptic
 2438 scale meteorological systems pass, days of the week in response to human activities, seasons
 2439 (with all of the accompanying changes in temperature, humidity, vegetation activity, etc.), years
 2440 in response to interannual variability, and decades in response to changing climate. These spatial
 2441 and temporal variations influence the chemical processing of pollutants in the atmosphere.

2442 **POLICY RELEVANCE**

2443 Developing effective policies for air quality improvement in California is challenging, as they
 2444 must account for the spatial and temporal variation in emissions and atmospheric chemistry.
 2445 Further, our knowledge of this chemistry and its variation is incomplete and continually
 2446 advancing. The CalNex study has added to this knowledge of atmospheric processes, which can
 2447 help guide and increase confidence in policy development.

2448 Temporally, the CalNex field study provides only a single point on annual to decadal time scales,
 2449 and so the results represent the particular conditions of 2010 within the uncertainties of
 2450 interannual variations and changing climate. Some aspects of the relationship of the CalNex
 2451 measurements to those of earlier years and decades are discussed in the responses to Questions
 2452 A, B and E. The CalNex sampling season was late spring to early summer and the results are
 2453 directly relevant to that season only; how the results relate to other seasons is addressed in the
 2454 response to Question C. The CalNex field study was primarily limited to two months, May and
 2455 June 2010, with most platforms and sites active for only a portion of that period. Hence,
 2456 statistical sampling of the synoptic scale meteorological and weekly scale changes is limited in
 2457 the CalNex results; the response to Question P addresses temporal variations on a weekly time
 2458 scale. In this response we primarily examine variations in atmospheric chemistry with time of
 2459 day.

2460 Spatially, the CalNex field study focused on southern California, particularly the SoCAB and the
 2461 SJV, where the two major field sites were established. The mobile platforms (four aircraft and a
 2462 research vessel) and CalNex's and California's statewide monitoring networks allowed some of
 2463 California's spatial variability to be probed. For example, the NOAA WP-3D aircraft conducted
 2464 several flights into the Sacramento Valley and SJV, and the Research Vessel Atlantis sailed up
 2465 the coast from Los Angeles to San Francisco, and up the Sacramento River to Sacramento.
 2466 Appendix A gives details of networks and mobile platform deployments.

2467 In the response to this question, we concentrated on two areas where the CalNex results have
 2468 significantly advanced our understanding of atmospheric chemistry: nighttime atmospheric
 2469 processing and the relative contributions of different radical sources to photochemistry during
 2470 the day. Other advances in our understanding of atmospheric chemistry and its spatial variability
 2471 include the formation of secondary organic aerosols (see Response to Question N), and what has
 2472 been learned from studies of the ozone weekend effect (see Response to Question P).

2473 In the ambient atmosphere, the NO_3 radical is formed when NO_2 (one of the components of
 2474 NO_x) reacts with O_3 . NO_3 only accumulates to significant concentrations at night because
 2475 during the day it is rapidly photolyzed by sunlight and reacts with NO to reform NO_2 . NO_3 is an
 2476 important species because it reacts rapidly with unsaturated VOCs and because it can combine
 2477 with NO_2 to form N_2O_5 , which is potentially a source for nitrate aerosol and a sink for NO_x when
 2478 it is incorporated into particulate matter. If that particulate matter contains significant chloride
 2479 ion (e.g. from sea salt aerosol) N_2O_5 can release ClNO_2 , which can then accumulate in the
 2480 nighttime atmosphere. ClNO_2 is important because at sunrise it photolyzes to release NO_2 and
 2481 produce a chlorine atom; thus, NO_2 is returned to the NO_x reservoir where it can take part in
 2482 daytime photochemistry and chlorine atoms are radicals that can help to drive that
 2483 photochemistry.

2484 Radicals formed by sunlight are the active agents that drive atmospheric photochemistry.
 2485 Traditional photochemical modeling considers photolysis of O_3 (with subsequent reaction of the
 2486 $\text{O}(^1\text{D})$ product with water) and photolysis of carbonyls, particularly formaldehyde, as the primary
 2487 radical sources. Photolysis of ClNO_2 , formed during the night as outlined above, and photolysis
 2488 of nitrous acid (HONO) are also radical sources that can affect daytime photochemistry. HONO
 2489 can be directly emitted (e.g., from on-road vehicles) and is also formed from NO_2 and water in
 2490 the ambient environment.

2491 FINDINGS

2492 ***Finding M1: Nighttime atmospheric chemistry plays multiple important air quality roles***
 2493 ***including interconversion of reactive oxidized nitrogen species, formation of gas phase***
 2494 ***chlorine species, and formation of aerosol nitrate. It is important that these processes are***
 2495 ***accurately included in the air quality models from which air quality policy and regulations***
 2496 ***are generally developed.***

2497 In-situ measurements of NO_3 , N_2O_5 , ClNO_2 , aerosol chloride and relevant ancillary species were
 2498 made at the Pasadena ground site and/or aboard the NOAA WP-3D aircraft (a comprehensive list
 2499 of measurements is included in Appendix A) to better understand the complex interaction
 2500 between emissions, chemistry, and transport that determine the balance between sources and
 2501 sinks of the highly reactive nocturnal nitrogen oxides. Measurements of N_2O_5 , ClNO_2 ,
 2502 molecular chlorine (Cl_2), and aerosol chloride (Cl^-) on the *Atlantis* provided additional key data
 2503 with which to examine chemistry involving N_2O_5 -mediated chlorine release from aerosol
 2504 particles. In-situ ClNO_2 , aerosol chloride, and long-path DOAS measurements of NO_3 , NO_2 , and
 2505 O_3 were made from the Pasadena site to simultaneously constrain the chemistry as well as the
 2506 vertical distribution of the nocturnal nitrogen oxides.

2507 *Meilke et al.* [2013] concluded from the Pasadena ground site data that nocturnal nitrogen oxides
 2508 constitute a significant reservoir for NO_x at night, with ClNO_2 alone contributing 21% on
 2509 average to the total budget of NO_x oxidation products measured at the site during the CalNex
 2510 study. They further calculated that photolysis of ClNO_2 during the study added a median of 0.8

2511 ppbv of Cl radicals and NO₂ to the Pasadena boundary layer following sunrise. Stable isotopic
 2512 measurements of aerosol nitrate made from the R/V *Atlantis* suggested significant differences in
 2513 aerosol sources to the inshore marine boundary layers of the southern and central coasts of
 2514 California [Vicars *et al.*, 2013]. This analysis concluded that nocturnal nitrogen oxide chemistry
 2515 in continental outflow is an important source of aerosol nitrate to the South Coast marine layer,
 2516 while daytime oxidation of NO₂ by the hydroxyl radical OH was the principal source for aerosol
 2517 nitrate in the Central Coast marine layer. Hayes *et al.* [2013] noted the sea salt aerosol measured
 2518 at the Pasadena ground site was substantially depleted in chloride due to atmospheric processing,
 2519 presumably in part due to nocturnal oxidation chemistry involving reactive uptake of N₂O₅; they
 2520 further noted a parallel increase in supermicron aerosol nitrate. Young *et al.* [2012] used altitude
 2521 profiles from the NOAA P-3 aircraft to report the first vertically-resolved measurements of
 2522 ClNO₂, and noted different source terms led to very different vertical profiles of ClNO₂ and
 2523 HONO after dark.

2524 Measurements inland at the Bakersfield ground site during CalNex showed that roughly 30% of
 2525 nighttime increases in organic particle mass were due to particulate organic nitrates (pΣANs)
 2526 [Rollins *et al.*, 2012], demonstrating that their production after dark via NO₃-initiated chemistry
 2527 was a major source of SOA mass. These results are described in more detail in the response to
 2528 Question N.

2529 ***Finding M2: ClNO₂ and HONO are significant primary radical sources in SoCAB,***
 2530 ***particularly in early morning when they were the dominant radical source near the surface***
 2531 ***between sunrise and 09:00 PDT. However, it is important that vertical gradients of radical***
 2532 ***precursors be taken into account in radical budgets, particularly with respect to HONO.***

2533 Young *et al.* [2012] used the Pasadena ground site measurements to construct a primary radical
 2534 budget (Fig. M1), and showed that contributions from HONO photolysis would be overestimated
 2535 without proper accounting for significant decreases in the vertical, due to its strong surface
 2536 source. At ground level, total daytime radical formation calculated from nighttime-accumulated
 2537 HONO and ClNO₂ was about the same for the two radical sources. Incorporating the different
 2538 vertical distributions by integrating through the boundary and residual layers demonstrated that
 2539 nighttime-accumulated ClNO₂ produced nine times as many radicals as nighttime-accumulated
 2540 HONO. A comprehensive radical budget at ground level demonstrated that nighttime radical
 2541 reservoirs accounted for 8% of total radicals formed and that they were the dominant radical
 2542 source between sunrise and 09:00 Pacific daylight time (PDT). Importantly, these data show that
 2543 vertical gradients of radical precursors must be taken into account in radical budgets, particularly
 2544 with respect to HONO.

2545 Radicals that are formed in early morning can contribute to radical propagation through the
 2546 formation of O₃ early in the day, which will act as a radical source, via O₃ photolysis, to produce
 2547 more O₃ later in the day. Thus, early morning radical sources may have an overall greater
 2548 impact on chemistry that occurs throughout the day. It should be noted that photolysis of ClNO₂
 2549 produces chlorine atoms, while photolysis of HONO produces hydroxyl radicals. The impacts of
 2550 these two radicals are not equal, as they react differently with VOCs, affecting their propensity to
 2551 form O₃ and aerosols. For example, Cl radicals are reactive toward all VOC classes, including
 2552 alkanes, whereas aromatics, oxygenates, and alkenes tend to dominate OH reactivity. Thus, the
 2553 absolute number of radicals produced by each nighttime radical reservoir may not represent their
 2554 full atmospheric influence. A complete comparison of Cl to OH requires consideration of the
 2555 particular VOC mixture, its variation over time, and relative reactivities of each radical. Further,
 2556 it is noted that recent observations of daytime HONO concentrations have indicated that

2557 additional daytime sources must exist with a rate of formation more rapid than the nighttime
 2558 source, though the mechanism for these sources remains highly uncertain. This daytime source
 2559 would increase the HONO contribution to primary radical formation.

2560 *Riedel et al.* [2012] used data from the R/V *Atlantis* to show that photolysis of ClNO₂ following
 2561 sunrise dominates the morning-time source of reactive Cl atoms. They noted that Cl atoms from
 2562 ClNO₂ photolysis dominate the early-morning oxidation of alkanes in the polluted coastal marine
 2563 boundary layer, resulting in increased O₃ production in the LA basin. Full 3-dimensional
 2564 chemical-transport modeling incorporating the CalNex ClNO₂ observations has not been
 2565 published to date. Earlier results using the CMAQ model suggest that chemistry involving
 2566 ClNO₂ could increase monthly mean 8-hour O₃ averages in Los Angeles by 1-2 ppbv, but could
 2567 cause larger increases, up to 13 ppbv of O₃, in isolated episodes [*Sarwar et al.*, 2012].

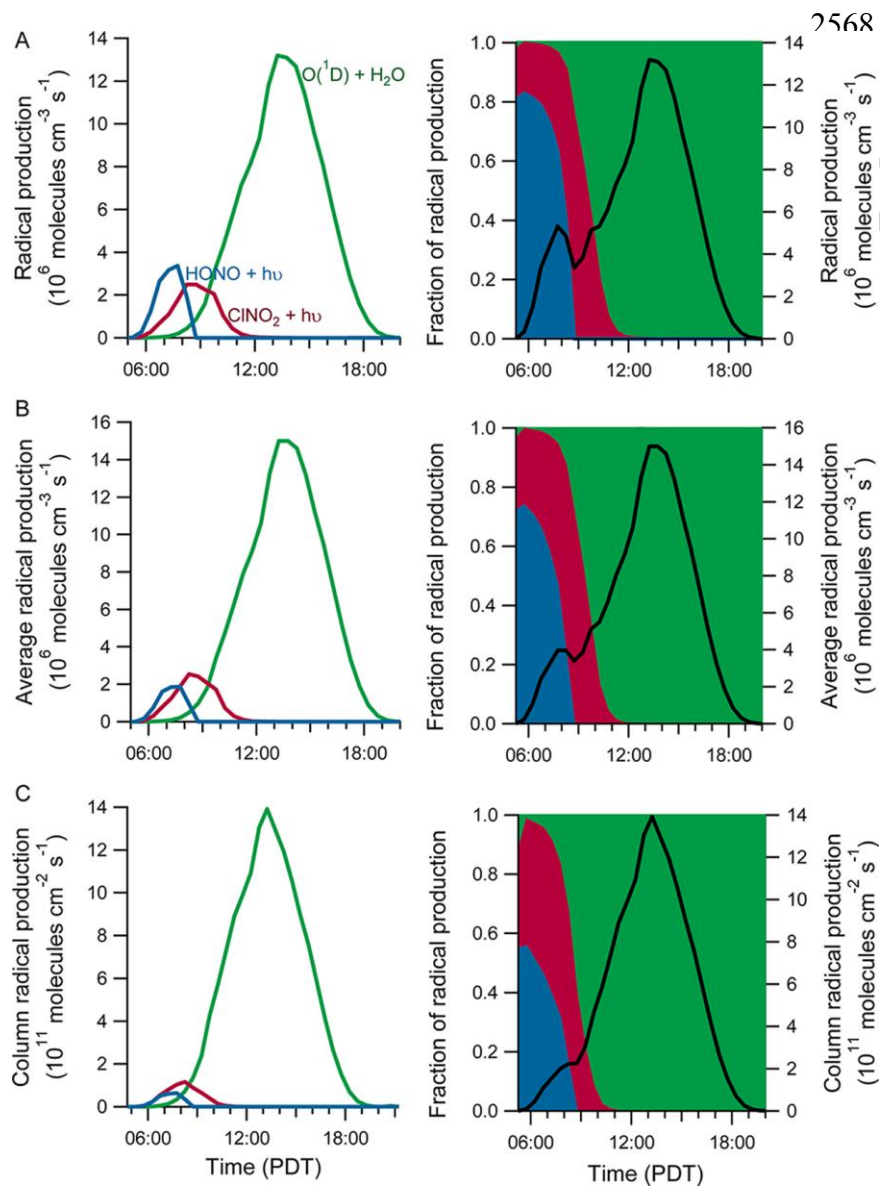


Figure M1. Comparison of absolute and fractional radical production for HONO photolysis (blue), ClNO₂ photolysis (red), reaction of O(¹D) plus water (green), and total radical production of the three processes (black) under different conditions: (a) ground level (10 m); (b) average through the boundary layer; and (c) integrated through the boundary and residual layers. (Figure reproduced from Young *et al.*, 2012)

2582 Gas-phase chlorine chemistry was recently added to the SAPRC07 chemical mechanism, which
 2583 is used in regional air quality models. However, the default versions of air quality models like
 2584 CMAQ, do not include the ClNO₂ formation from aqueous phase chemistry involving N₂O₅.

2585 The findings above confirm the importance of including these chemical processes in future
2586 model development and applications in California.

2587 **Finding M3: The propensity of Cl for radical propagation yielding second-generation OH**
2588 **radicals indicates that the relative contributions of Cl and OH to tropospheric oxidation**
2589 **are not accurately captured through simple radical budgets.**

2590 *Young et al.* [2013] used a box model constrained by observations at the Pasadena site to
2591 examine Cl and OH chemistry as a function of NO_x and secondary radical production. The
2592 model results show that second-generation OH production resulting from Cl oxidation of VOCs
2593 is strongly influenced by NO_x, and that this effect can greatly amplify the importance of Cl as a
2594 primary oxidant.

2595 **References**

- 2596 Hayes, P. L., et al. (2013), Organic aerosol composition and sources in Pasadena, California
2597 during the 2010 CalNex campaign, *J. Geophys. Res. Atmos.*, *118*, 9233–9257,
2598 doi:10.1002/jgrd.50530.
- 2599 Mielke, L. H., et al. (2013), Heterogeneous formation of nitryl chloride and its role as a nocturnal
2600 NO_x reservoir species during CalNex-LA 2010, *J. Geophys. Res. Atmos.*, *118*,
2601 doi:10.1002/jgrd.50783.
- 2602 Riedel, T. P., et al. (2012), Nitryl chloride and molecular chlorine in the coastal marine boundary
2603 layer, *Environ. Sci. Technol.*, *46*, 10463-10470, doi:10.1021/es204632r.
- 2604 Rollins, A. W., et al. (2012), Evidence for NO_x control over nighttime SOA formation, *Science*,
2605 *337*(6099), 1210-1212, doi:10.1126/science.1221520.
- 2606 Sarwar, G., H. Simon, P. Bhawe, and G. Yarwood (2012), Examining the impact of
2607 heterogeneous nitryl chloride production on air quality across the United States, *Atmos.*
2608 *Chem. and Phys.*, *12*, 6455-6473, doi:10.5194/acp-12-6455-2012.
- 2609 Vicars, W. C., et al. (2013), Spatial and diurnal variability in reactive nitrogen oxide chemistry
2610 as reflected in the isotopic composition of atmospheric nitrate: Results from the CalNex 2010
2611 field study, *J. Geophys. Res. Atmos.*, *118*, doi:10.1002/jgrd.50680.
- 2612 Young, C. J., et al. (2012), Vertically resolved measurements of nighttime radical reservoirs in
2613 Los Angeles and their contribution to the urban radical budget, *Environ. Sci. Technol.*, *46*,
2614 10965-10973, doi:10.1021/es302206a.
- 2615 Young, C.J., et al. (2013), Evaluating the role of chlorine in tropospheric oxidation using
2616 observations and models in a coastal, urban environment, *Atmos. Chem. Phys.*
2617 *Discuss.*, *13*, 13685-13720.

2618

2619

2620

2621

2622

Synthesis of Results - Climate Processes/Transformation

2623

Response to Question N

2624

QUESTION N

2625

What are the major contributors to secondary organic aerosol (SOA)? What are the

2626

relative magnitudes of SOA compared with primary organic aerosols in different areas?

2627

BACKGROUND

2628

In many environments, including California as exemplified in Fig. N1, organic aerosol (OA)

2629

composes a large fraction (~50%) of the submicron aerosol mass (PM₁) in the troposphere. This

2630

is true in all seasons (c.f., Fig. C2), although the OA contribution is less in winter at many sites.

2631

The sources, composition, and chemical processing of OA are not well-understood. Generally,

2632

OA is composed of thousands of individual compounds that are either directly emitted into the

2633

atmosphere ('primary' OA or 'POA') or are formed through chemical reactions involving gas

2634

phase precursors ('secondary' OA or 'SOA'). The multiple sources and complexity of molecular

2635

composition represent major challenges for understanding and predicting OA properties. During

2636

CalNex extensive investigations of OA were conducted at the Pasadena and Bakersfield ground

2637

sites, aboard the NOAA WP-3D and CIRPAS Twin Otter aircraft, and aboard the R/V *Atlantis*.

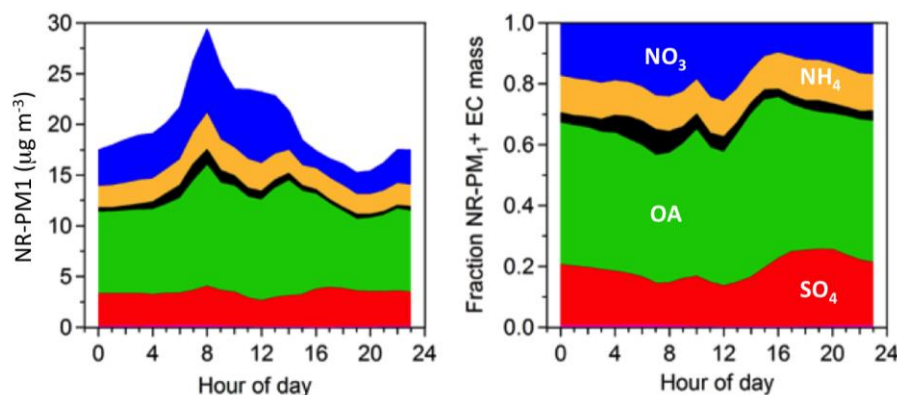


Figure N1. Diurnal profiles of non-refractory (NR) PM₁ aerosol species and elemental carbon (black) measured during the 2005 summertime Study of Organic Aerosols at Riverside (SOAR) field study in Riverside CA [Figure modified from Docherty *et al.*, 2011].

2638

2639

POLICY RELEVANCE

2640

Many areas of California do not attain health-based ambient air quality standards for PM_{2.5}.

2641

Organic aerosol is a major contributor to ambient PM_{2.5} concentrations. To effectively address

2642

the reduction of this contribution, it is necessary to identify the emission sources responsible for

2643

primary organic aerosol, determine the processes that form SOA, and identify the emission

2644

sources of the precursors of this SOA.

2645

Caution must be exercised when comparing the CalNex aerosol measurements made for research

2646

purposes with regulatory measurements of PM_{2.5}. Most of the CalNex research measurements

2647

are of sub-micron (PM₁) aerosol. Comparisons of PM₁ and PM_{2.5} measurements at Pasadena

2648

[Jimenez *et al.*, 2013] indicate that less than about 20% of the OA mass and negligible sulfate

2649

mass is above 1 µm, but that a substantial amount of nitrate mass (about 35%) is present above 1

2650

µm. The super-micron nitrate is at least partially composed of sodium nitrate from chemical

2651

aging of sea salt by nitric acid although some super-micron ammonium nitrate may be present as

2652

well. In addition, there are systematic differences between PM_{2.5} measured by air quality

2653 networks and by research instrumentation. These differences arise at least partially from loss of
 2654 semi-volatile components of PM_{2.5}, such as NH₄NO₃ and OA components [e.g., Tortajada-
 2655 Genaro and Borrás, 2011]. Consequently the OA contribution found in research measurements
 2656 is often larger than that found with regulatory air quality monitoring methods.

2657 FINDINGS

2658 **Finding N1: SOA contributions to OA at Pasadena could be identified from 1) their diurnal**
 2659 **cycles and their correlations with photochemical ozone production, and 2) an increase in**
 2660 **SOA concentration with increasing photochemical processing of urban air.**

2661 *Analysis: This material is taken from Hayes et al. [2013]*

2662 At the Pasadena site the total organic contribution was 41% of total sub-micron aerosol.
 2663 Analysis of ambient aerosol by AMS (aerosol mass spectrometer) provides an effective means to
 2664 quantify various contributions to this organic fraction. Five contributions to OA were identified
 2665 from the Pasadena data set. The two oxygenated OA (OOA) contributions were identified as
 2666 SOA (SV-OOA and LV-OOA). Figure N2 shows the total measured SOA and total
 2667 photochemical ozone produced (approximated by O_x, the sum of the measured O₃ and NO₂ to

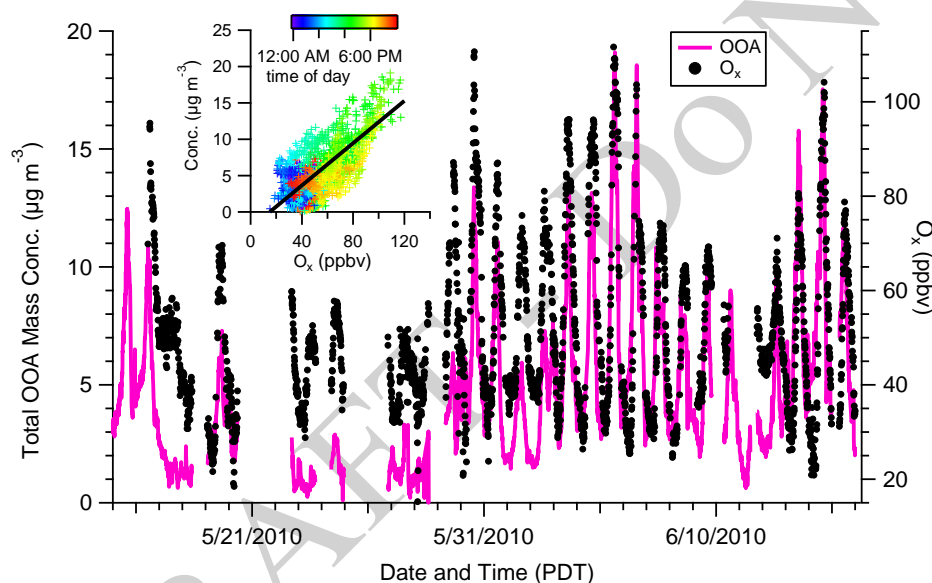


Figure N2. Time series for OOA (the sum of SV-OOA and LV-OOA), and O_x (the sum of O₃ and NO₂). **(Inset)** Correlation plot of OOA versus O_x with linear fit and colored by time-of-day. The best-fit slope is 0.146 ($R^2 = 0.53$). [Figure from Hayes et al., 2013].

2668 account for O₃ lost through reaction with NO emitted by local sources) at the Pasadena site
 2669 during the CalNex study. The measured SOA and O_x follow similar diurnal cycles ($R^2 = 0.53$),
 2670 with afternoon maxima indicating that photochemical processes in the atmosphere form both.
 2671 The magnitude of the SOA and O_x maxima are also correlated, each depending upon the
 2672 changing photochemical environment. The correlation between the two species is stronger
 2673 during the more polluted periods of high OOA concentration in June ($R^2 = 0.72$ for the June 2nd
 2674 through 6th). At the Pasadena site the regression slope for OOA versus O_x is $0.146 \pm 0.001 \mu\text{g m}^{-3}$
 2675 ppbv^{-1} (Figure N2 inset). The slopes of identical analyses for Riverside, CA and Mexico City
 2676 (0.142 ± 0.004 and $0.156 \pm 0.001 \mu\text{g m}^{-3} \text{ppbv}^{-1}$, respectively) are similar to the Pasadena ground
 2677 site. This similarity suggests similar SOA and O_x formation chemistries on average, in these
 2678 different urban environments.

2679 To evaluate the timescales and efficiency of SOA formation in Pasadena, the evolution of OA
 2680 relative to CO (OA/ Δ CO) as a function of photochemical age is plotted in Figure N3. Here Δ CO

2681 is the CO concentration enhancement above its background concentration, which is taken as 105
 2682 ppbv based on CO measurements taken aboard the NOAA WP-3D aircraft off the LA coastline.
 2683 The CO enhancement is assumed to be a conservative tracer of urban combustion emissions that
 2684 are also a source of aerosols and aerosol precursors, and thus, normalizing the OA concentration
 2685 to CO will remove the effect of dilution. The photochemical age is a semi-quantitative measure
 2686 of the degree of photochemical processing of a sampled air mass. For the air masses sampled at
 2687 the Pasadena site, photochemical age was calculated by two different methods. First, using the
 2688 ratio of 1,2,4-trimethylbenzene to benzene, and second, by defining the photochemical age as $-\log_{10}(\text{NO}_x/\text{NO}_y)$.
 2689 Both photochemical ages were calculated using a standard OH radical

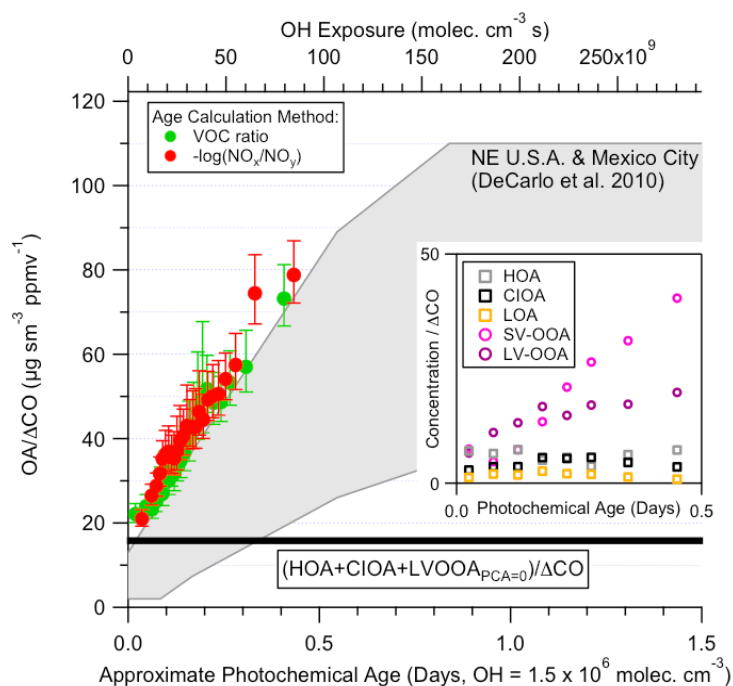


Figure N3. Evolution of OA/ Δ CO versus photochemical age at the Pasadena site during CalNex. The measured ratios are averaged into 25 bins according to photochemical age. The enhanced CO (Δ CO) is the ambient CO minus the estimated background CO (105 ppbv). Error bars representing the uncertainty in the ratio are shown. The gray region represents the evolution of OA/ Δ CO observed in the northeastern United States and the Mexico City area. The black horizontal line is the ratio of (HOA + CIOA + 'background LVOOA') to Δ CO. **Inset:** Evolution of the OA component concentrations normalized to Δ CO versus photochemical age. Data are binned according to photochemical age. [Figure from Hayes *et al.*, 2013].

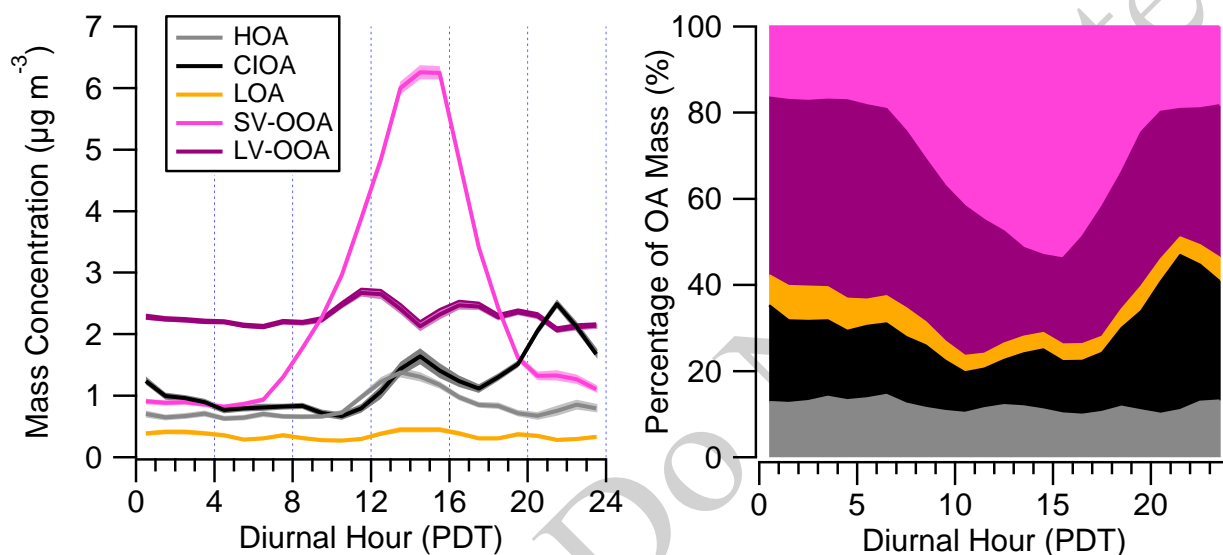
2690 concentration of 1.5×10^6 molecules cm^{-3} . For reference,
 2691 the daily OH radical concentrations averaged for the whole campaign at the Pasadena site was
 2692 1.3×10^6 molecules cm^{-3} . The diurnal cycles of the two photochemical age estimates show
 2693 generally good agreement.

2694 In Figure N3, the Pasadena OA/ Δ CO increases markedly with photochemical age, a clear
 2695 indication of SOA production during photochemical processing of urban air within the Los
 2696 Angeles basin. The Pasadena results follow the upper limit of the range of values previously
 2697 reported for Mexico City and the northeastern United States (grey region in the figure), which
 2698 suggests a common, dominant source of SOA precursors in these urban areas. The inset in
 2699 Figure N2 shows the variation with photochemical age of the five contributors to OA identified
 2700 in the analysis of the Pasadena AMS data. Both of the contributions identified as SOA (SV-
 2701 OOA and LV-OOA) increase with photochemical age, while the other three contributors remain
 2702 constant, which is consistent with their identification as POA contributions from different
 2703 sources.

2704 **Finding N2:** Averaged over the entire CalNex study, the 24-hour average SOA contribution
 2705 ($\approx 66\%$) to total OA at the Pasadena site was about twice that of primary organic aerosols.

2706 *Analysis:* This material is taken from Hayes *et al.* (2013)

2707 Figure N4 shows the diurnal cycle of the five aerosol components identified at the Pasadena site.
 2708 *Hayes et al.* [2013] take the total of the two OOA components as a surrogate for SOA, and the
 2709 sum of HOA, CIOA, and LOA is taken as a surrogate for POA. On average the total OA mass
 2710 for the measurement period is composed of 66% OOA (SV-OOA + LV-OOA), a percentage that
 2711 lies between that observed for a selection of ‘urban’ and ‘urban downwind’ sites [*Zhang et al.*,
 2712 2007]. This percentage is also similar to previous results from measurements based in Pasadena;
 2713 *Hersey et al.* [2011] reported that, during the PACO campaign in May/June 2009, 77% of OA
 2714 was classified as OOA, and *Turpin et al.* [1991] reported that SOA contributed roughly half of
 2715 the OA mass during the summer of 1984.



2716 **Figure N4.** Diurnal profiles of the SOA components in concentrations (left) and by
 2717 percent mass (right). [Figure from *Hayes et al.*, 2013].

2718 ***Finding N3: Analysis of ambient OA measurements in SoCAB indicate that gasoline***
 2719 ***emissions dominate over diesel in formation of secondary organic aerosol mass; however,***
 2720 ***an analysis (based on liquid fuel composition) indicated that diesel dominates over gasoline***
 2721 ***for the formation of SOA in the southern SJV.***

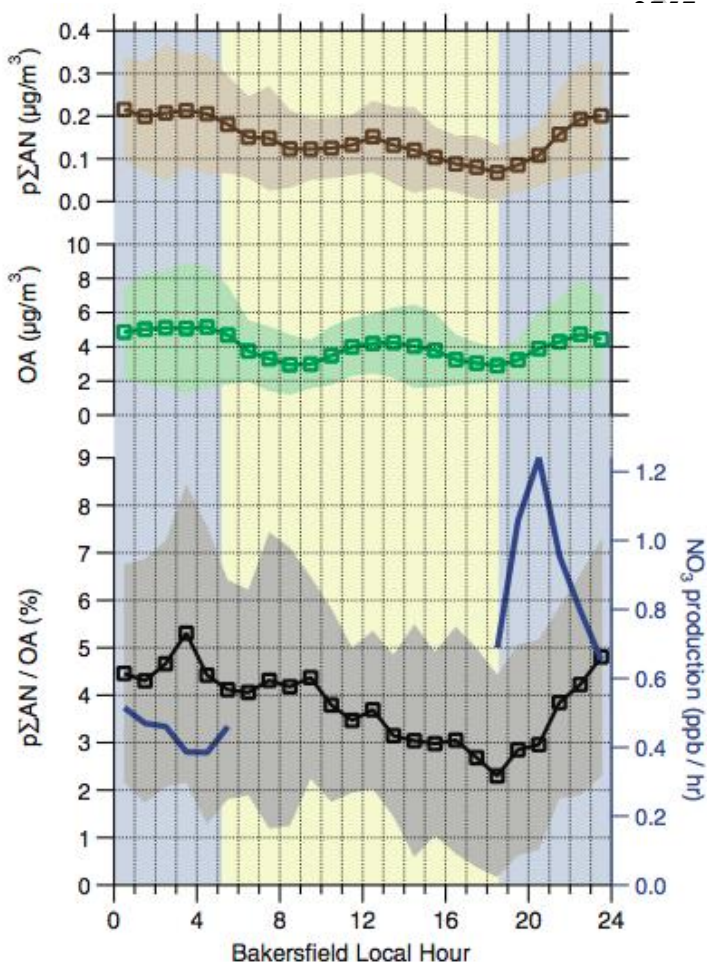
2722 On weekends compared to weekdays, daily total heavy-duty diesel truck traffic decreases in the
 2723 SoCAB, but light-duty gasoline vehicle traffic remains relatively constant (although the spatial
 2724 and temporal patterns change). As a consequence, NO_x and black carbon emissions decrease by
 2725 almost 50%, while CO and VOCs, which are predominantly from gasoline exhaust, remain
 2726 nearly constant (see *Pollack, et al.*, [2012] and discussion in response to Question P). However,
 2727 *Bahreini et al.* [2012] show that concentrations of OA do not significantly decrease on
 2728 weekends. Two separate top-down analyses of CalNex data utilized the lack of a weekend effect
 2729 in OA mass in the Los Angeles basin, under the assumption that vehicular emissions dominate
 2730 urban SOA, to conclude that gasoline emissions dominate over diesel emissions in the formation
 2731 of SOA [*Bahreini et al.*, 2012; *Hayes et al.*, 2013], providing support for SOA control strategies
 2732 that target gasoline-fueled vehicular emissions. However, a bottom-up approach using detailed
 2733 fuel chemical composition information, estimates of the SOA formation potential of individual
 2734 species, and regional fuel sales data [*Gentner et al.*, 2012] concluded that diesel fuel is
 2735 responsible for 60-90% of the SOA, depending on the diesel fraction of total fuel sales (ranging
 2736 in California from ~10% in some urban areas to ~30% in some rural areas). A resolution of the

2737 contradiction between these studies may be provided by smog chamber studies of SOA
 2738 formation from evaporated gasoline and diesel fuel and from exhaust from these two classes of
 2739 vehicles. *Chirico et al.* [2010] find very little primary or secondary OA from diesel engines, at
 2740 least when equipped with a diesel oxidation catalyst and diesel particulate filter. *Gordon et al.*
 2741 [2013] find that the SOA formed from exhaust of newer gasoline vehicles, greatly exceeds that
 2742 formed from vaporized gasoline, and conclude that the mix of organic vapors emitted by newer
 2743 vehicles appear to be more efficient (higher yielding) in producing SOA than the emissions from
 2744 older vehicles. This suggests that while tighter emission standards are clearly reducing primary
 2745 PM emissions from light duty gasoline vehicle exhaust, they may not be as effective at reducing
 2746 SOA formation. ARB is now investigating this issue for SULEV vehicles, which were not a
 2747 focus of the work cited above.

2748 **Finding N4: At the Bakersfield site, most nighttime SOA formation is due to the reaction of**
 2749 **the NO₃ radical (a product of anthropogenic NO_x emissions) with unsaturated, primarily**
 2750 **biogenic VOCs.**

2751 *Analysis; This material is taken from Rollins et al. (2012)*

2752 Instruments at the Bakersfield site measured the total alkyl and multifunctional nitrates in the
 2753 aerosol phase (pΣAN) as well as total OA and many aerosol precursors, including a wide suite of
 2754 VOCs. OA concentrations exceeding 10 µg/m³ were frequently observed at night. The pΣAN
 2755 and pΣAN/OA ratio were observed to increase at night (Figure N5), which suggests not only that
 2756 NO₃ chemistry is important for SOA production at night, but also that the organic nitrate tracers



of this chemistry contribute appreciably to the total OA. Over the 5-hour time period after sunset (18:30 to 23:30), the average total OA increase was 1.54 µg/m³. The added mass of nitrate functional groups alone accounted for 0.13 µg/m³ (8.4%) of this total mass. That this ratio increased continuously for five hours after sunset (a period of predominately northwesterly winds) while Bakersfield is only 1 to 2 hours upwind suggests that the production process has somewhat of a regional character.

Rollins et al. [2012] further interpret

Figure N5. Diurnal trends (means shown with $\pm 1\sigma$ ranges in shading) in pΣAN (brown), OA (green), pΣAN/OA (black), and NO₃ production rate (blue). Blue shading indicates nighttime (solar zenith angle > 85°), and yellow indicates daytime. [Figure from *Rollins et al.*, 2012]

- 2773 the observed relationship of particulate organic nitrates with NO₂ measured at the site, and
 2774 suggest that this major source of particulate mass would be effectively addressed by targeted
 2775 NO_x emissions reductions in the Central Valley. While the carbon source of this newly
 2776 quantified nighttime source can be biogenic in origin, the product SOA must be considered
 2777 anthropogenic, since its formation is critically dependent on anthropogenic NO_x emissions
 2778 driving the NO₃ radical chemistry after dark.
- 2779 From the nitrate content of the aerosol, *Rollins et al.* [2012] calculate that 27 to 40% of the OA
 2780 growth was due to molecules with nitrate functionalities. This fraction of OA molecules that are
 2781 nitrates is similar to the nitrate yields from a number of NO₃ plus biogenic VOC reactions. Thus,
 2782 these numbers do not preclude all of the nighttime SOA production, including non-nitrates, being
 2783 a result of NO₃ chemistry.
- 2784 **References**
- 2785 Bahreini, R., et al. (2012), Gasoline emissions dominate over diesel in formation of secondary
 2786 organic aerosol mass, *Geophys. Res. Lett.*, 39(L06805), doi:10.1029/2011GL050718.
- 2787 Chirico, R., et al. (2010) Impact of aftertreatment devices on primary emissions and secondary
 2788 organic aerosol formation potential from in-use diesel vehicles: results from smog chamber
 2789 experiments, *Atmos. Chem. Phys.*, 10, 11545–11563, doi:10.5194/acp-10-11545-2010
- 2790 DeCarlo, P. F., et al. (2010), Investigation of the sources and processing of organic aerosol over
 2791 the Central Mexican Plateau from aircraft measurements during MILAGRO, *Atmos. Chem.*
 2792 *Phys.*, 10(12), 5257-5280.
- 2793 Docherty, K. S., et al. (2011), The 2005 Study of Organic Aerosols at Riverside (SOAR-1):
 2794 instrumental intercomparisons and fine particle composition, *Atmos. Chem. Phys.*, 11, 12387-
 2795 12420, doi:10.5194/acp-11-12387-2011.
- 2796 Gentner, D. R., et al. (2012), Elucidating secondary organic aerosol from diesel and gasoline
 2797 vehicles through detailed characterization of organic carbon emissions, *roc. Natl. Acad. Sci.*,
 2798 109(45), 18318-18323, doi:10.1073/pnas.1212272109.
- 2799 Gordon, T.D. (2013), Secondary Organic Aerosol Formed from Gasoline Powered Light Duty
 2800 Vehicle Exhaust Dominates Primary Particulate Matter Emissions, *manuscript in*
 2801 *preparation*.
- 2802 Hayes, P.L., et al. (2013), Aerosol Composition and Sources in Los Angeles during the 2010
 2803 CalNex Campaign, *J. Geophys. Res.-Atmos.*, doi: 10.1002/jgrd.50530.
- 2804 Hersey, S. P., J. S. Craven, K. A. Schilling, A. R. Metcalf, A. Sorooshian, M. N. Chan, R. C.
 2805 Flagan, and J. H. Seinfeld (2011), The Pasadena Aerosol Characterization Observatory
 2806 (PACO): chemical and physical analysis of the Western Los Angeles basin aerosol, *Atmos.*
 2807 *Chem. Phys.*, 11(15), 7417-7443.
- 2808 Jimenez, J.-L., W.H. Brune, P.L. Hayes, A.M. Ortega and M.J. Cubison (2013), Characterization
 2809 of Ambient Aerosol Sources and Processes during CalNex 2010 with Aerosol Mass
 2810 Spectrometry, Final Report Contract 08-319, California Air Resources Board.
- 2811 Pollack, I.B., et al. (2012), Airborne and ground-based observations of a weekend effect in
 2812 ozone, precursors, and oxidation products in the California South Coast Air Basin, *J.*
 2813 *Geophys. Res.*, 117, D00V05, doi:10.1029/2011JD016772.
- 2814 Rollins, A. W., E. C. Browne, K.-E. Min, S. E. Pusede, P. J. Wooldridge, D. Gentner, A. H.
 2815 Goldstein, S. Liu, D. A. Day, L. M. Russell, and R. C. Cohen (2012) Evidence for NO_x

- 2816 Control over Nighttime SOA Formation, *Science*, 337, 1210-1212,
2817 doi:10.1126/science.1221520.
- 2818 Tortajada-Genaro, L.-A., and E. Borrás (2011), Temperature effect of tapered element oscillating
2819 microbalance (TEOM) system measuring semi-volatile organic particulate matter, *J. Environ.*
2820 *Monit.*, 13, 1017-1026.
- 2821 Turpin, B. J., J. J. Huntzicker, S. M. Larson, and G. R. Cass (1991), Los-Angeles Summer
2822 Midday Particulate Carbon - Primary And Secondary Aerosol, *Environ. Sci. Technol.*,
2823 25(10), 1788-1793.
- 2824 Zhang, Q., et al. (2007), Ubiquity and Dominance of Oxygenated Species in Organic Aerosols in
2825 Anthropogenically-Influenced Northern Hemisphere Mid-latitudes, *Geophys. Res. Lett.*, 34,
2826 L13801.
- 2827
- 2828
- 2829
- 2830
- 2831
- 2832

DRAFT - Do Not Cite

2833 **Synthesis of Results - Climate Processes/Transformation**2834 **Response to Question O**2835 **QUESTION O**

2836 **How do layers of enhanced ozone concentrations form aloft and how do they impact**
 2837 **ground-level ozone concentrations?**

2838 **BACKGROUND**

2839 Compared to surface concentrations, over most areas of the Earth layers of enhanced ozone
 2840 concentrations aloft are quite common [e.g., *Newell et al.*, 1999]. The troposphere is filled with
 2841 such layers for two reasons. First, ozone concentrations on average increase with altitude from
 2842 the surface through the depth of the troposphere up to the tropopause, which marks the bottom of
 2843 the stratosphere. (Ozone concentrations increase much more rapidly still with increasing altitude
 2844 in the lower stratosphere.) Second, above the convective boundary layer (CBL, the near surface
 2845 layer of the troposphere that is rapidly mixed by surface-based convection) the troposphere is
 2846 quite stable, limiting vertical mixing. Vertical wind shear causes air at different altitudes to
 2847 move in different directions, much as a deck of cards can slide horizontally with respect to each
 2848 other. This transport effectively produces atmospheric layers. As a result of differing sources
 2849 and sinks of O₃ among the layers, different O₃ concentrations generally mark different layers.

2850 Following sunrise, solar heating of the Earth's surface causes the CBL to grow through turbulent
 2851 mixing, thereby mixing higher atmospheric layers to the surface. On average, in unpolluted
 2852 regions, this mixing down of higher layers increases surface O₃ concentrations. Even in polluted
 2853 regions (e.g., the Los Angeles basin) where the surface layer often has O₃ concentrations
 2854 exceeding those in most layers aloft, the growth of the CBL and the concomitant mixing of air
 2855 from aloft will yield a higher net O₃ concentration within the growing CBL than would mixing of
 2856 an equal amount of clean air from near the surface (e.g., inflow from the marine boundary layer
 2857 over the Pacific Ocean in the case of Los Angeles basin). The entrainment of layers aloft will
 2858 have a greater impact in locations where the CBL typically grows to higher altitudes, e.g. in
 2859 inland air basins compared to coastal air basins where the more pronounced marine influence
 2860 limits CBL growth.

2861 **POLICY RELEVANCE**

2862 Mixing of air layers aloft that contain enhanced O₃ concentrations down to the surface can
 2863 increase surface concentrations within an air basin. This O₃ source is potentially not subject to
 2864 local controls. Understanding the origin and the impact of this mixing is important for
 2865 formulating effective air quality control policies. Further, if a particular episode can be shown to
 2866 originate from mixing down of an elevated layer containing O₃ of stratospheric origin, it may be
 2867 excluded from regulatory determinations related to violations of the U.S. NAAQS, since these
 2868 naturally occurring "exceptional events" are not controllable by state agencies [*U.S. EPA*, 2007].

2869 The response to this question discusses some of the evidence for the formation of layers of
 2870 enhanced O₃ and the mechanism by which they impact ground-level O₃ concentrations. The
 2871 Response to Question T quantifies the magnitude of this impact.

2872 **FINDINGS**

2873 ***Finding O1:* Layers of enhanced O₃ concentrations aloft over California reflect the**
 2874 **interleaving of layers of air affected by differing O₃ sources. Enhanced O₃ concentrations**
 2875 **arise from descent of upper tropospheric air with O₃ of stratospheric origin, long-range**
 2876 **transport of anthropogenic emissions (e.g., from Asia), and lofted aged regional pollution**
 2877 **(e.g., from California urban areas).**

2878 Several CalNex modeling and measurement studies investigated the vertical structure of O₃
 2879 concentrations above California, and identified layers of enhanced O₃. Figure O1 shows one
 2880 example when an atmospheric layer with O₃ of stratospheric origin at concentrations greater than
 2881 100 ppbv was transported to within 1 km of the surface. This layer was being actively entrained
 2882 into the CBL at the time of the sonde measurement [Langford *et al.*, 2012].

2883 *Neuman et al.* [2012] studied the
 2884 chemical composition, origin, and
 2885 transport of air upwind and over Los
 2886 Angeles, California, using
 2887 measurements of carbon monoxide
 2888 (CO), O₃, reactive nitrogen species and
 2889 meteorological parameters from the
 2890 WP-3D aircraft during CalNex.
 2891 Measurements in 32 vertical profiles
 2892 were used to characterize air masses in
 2893 the free troposphere over the LA basin,
 2894 in order to determine the source of
 2895 enhanced O₃ observed above the CBL.
 2896 Four primary air mass influences were
 2897 observed regularly between
 2898 approximately 1 and 3.5 km altitude:
 2899 descent of upper tropospheric air
 2900 carrying O₃ of stratospheric origin,
 2901 long-range transport of anthropogenic
 2902 emissions (e.g., from Asia), lofting of
 2903 aged regional emissions (i.e., from
 2904 California), and lofting of marine air.
 2905 The first three air mass types accounted
 2906 for 89% of the free troposphere
 2907 observations, each with similarly
 2908 enhanced average (± 1 standard
 2909 deviation) O₃ concentrations: 71 (± 8) ppbv in upper tropospheric air, 69 (± 6) ppbv in air affected
 2910 by long-range emission transport, and 65 (± 4) ppbv in air with aged regional emissions. Marine
 2911 air had lower average O₃ concentrations: 53 (± 10) ppbv. *Langford et al.* [2010] provide detailed
 2912 documentation of one episode of lofting of aged regional pollution when a layer with O₃
 2913 concentrations in excess of 100 ppbv was observed at an altitude of about 4 km above the Los
 2914 Angeles basin.

2915 It is useful to note that O₃ concentrations in layers from two of the three sources of enhanced O₃
 2916 are expected to have evolved over the past decades above California. Emissions of O₃ precursors
 2917 have decreased substantially in California (see Response to Question E), but increased in Asia

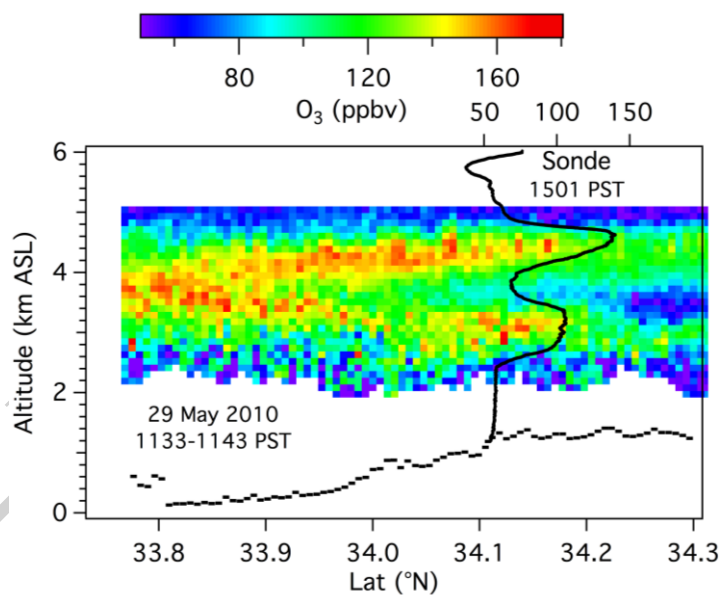


Figure O1. Latitude-height curtain plot of ozone measured along a N-S transect ~10 km west of Joshua Tree National Park by the airborne ozone lidar aboard the NOAA Twin Otter aircraft. The solid black curve shows the concentration profile observed by the ozonesonde. The dashed line along the bottom shows the surface elevation. (Figure based on *Langford et al.*, 2012.)

2918 [e.g., *Ohara et al.*, 2007]. Consequently, it is expected that O₃ enhancements in layers of lofted
 2919 regional emissions have decreased markedly, while they have increased in layers affected by
 2920 long-range transport from Asia.

2921 ***Finding O2: Layers of enhanced ozone concentrations aloft are entrained into the***
 2922 ***convective boundary layer, thereby enhancing surface level ozone concentrations.***

2923 *Neuman et al.* [2012] examined correlations between O₃ and CO and between O₃ and nitric acid
 2924 from WP-3D aircraft observations over the Los Angeles basin. These correlations demonstrate
 2925 that mixing of three different air masses affect O₃ concentrations across the LA basin: clean
 2926 marine air with low concentrations of all three species, dry air with increased O₃ and decreased
 2927 CO characteristic of the upper troposphere, and photochemically-processed Los Angeles basin
 2928 air with enhanced O₃, CO and nitric acid. This observation-based study is complemented by
 2929 studies that incorporate both measurements and model calculations.

2930 *Langford et al.* [2012] utilized principal component analysis (PCA) to quantify the influence of
 2931 air from the upper troposphere/lower stratosphere (UT/LS) on surface O₃; they find that ~13% of
 2932 the variance in the maximum daily 8-hour average O₃ between May 10 and June 19, 2010 was
 2933 associated with changes of 2–3 day duration linked to the passage of upper-level troughs.
 2934 Vertical profiles of O₃ measured by balloon borne instruments above Joshua Tree National Park
 2935 and by airborne lidar over the Los Angeles basin (see Fig. O1) show that these changes
 2936 coincided with the appearance of intrusions descending from the UT/LS to just above the CBL
 2937 over southern California. The Lagrangian particle dispersion model FLEXPART reproduced
 2938 most of these intrusions, and supports the conclusion from the PCA that significant transport to
 2939 the surface of UT/LS air did occur.

2940 To explore baseline O₃ (i.e., O₃ not affected by local and regional emissions) entering California
 2941 throughout the latitude expanse of the state, an ozonesonde network was implemented during
 2942 spring 2010, including four launch sites along the California coast. *Cooper et al.* [2011]
 2943 determined that the vertical and latitudinal variation in free tropospheric baseline O₃ is partly
 2944 explained by polluted and stratospheric air masses descending along the west coast. Above 3 km
 2945 altitude, the dominant pollution sources of O₃ precursors were China and international shipping,
 2946 while international shipping was the greatest source below 2 km. Within California, the major
 2947 surface impact of baseline O₃ transported ashore above 2 km is on the high elevation terrain of
 2948 eastern California. Baseline O₃ below 2 km has its strongest impact on the low elevation sites
 2949 throughout the state.

2950 Analysis of ozonesondes, lidar, and surface measurements over the western U.S. from April to
 2951 June 2010 show that a global high-resolution (~50 x ~50 km²) chemistry-climate model (GFDL
 2952 AM3) successfully reproduced the observed sharp O₃ gradients above California, including the
 2953 interleaving and mixing of Asian pollution and stratospheric air associated with complex
 2954 interactions of midlatitude cyclone air streams. The model results show that from April to June
 2955 2010 thirteen stratospheric intrusions enhanced total daily maximum 8-hour average (MDA8) O₃
 2956 at surface sites [*Lin et al.*, 2012a]. O₃ due to long-range transport of anthropogenic emissions
 2957 from Asia was also identified in the CalNex data set and quantified in the model simulations [*Lin*
 2958 *et al.*, 2012b]. Asian pollution descends behind cold fronts. The maximum O₃ enhancement
 2959 from Asian pollution occurs at about 2 km AGL over the southwestern U.S., including the
 2960 densely populated Los Angeles basin. This layer can be entrained into the CBL and impact
 2961 surface concentrations.

2962 Although the higher spatial resolution of the model utilized by *Lin et al.* [2012a;b] improved
 2963 model performance over earlier model calculations, concern remains that the model does not
 2964 perform as well as desired over California with its complex meteorology and terrain. Their work
 2965 has significantly increased our understanding of upper level impacts on surface O₃ in the
 2966 southwest U.S. However, because of the difficulty of modeling California (especially in coastal
 2967 areas such as the Los Angeles basin), the model-derived impacts of upper-level O₃ sources are
 2968 better interpreted heuristically than quantitatively.

2969 **References**

- 2970 Cooper, O. R., et al. (2011), Measurement of western U.S. baseline ozone from the surface to the
 2971 tropopause and assessment of downwind impact regions, *J. Geophys. Res.*, *116*, D00V03,
 2972 doi:10.1029/2011JD016095.
- 2973 Langford, A. O., C. J. Senff, R. J. Alvarez II, R. M. Banta, and R. M. Hardesty (2010),
 2974 Long- range transport of ozone from the Los Angeles Basin: A case study, *Geophys. Res.*
 2975 *Lett.*, *37*, L06807, doi:10.1029/2010GL042507.
- 2976 Langford, A. O., J. Brioude, O. R. Cooper, C. J. Senff, R. J. Alvarez II, R. M. Hardesty, B. J.
 2977 Johnson, and S. J. Oltmans (2012), Stratospheric influence on surface ozone in the Los
 2978 Angeles area during late spring and early summer of 2010, *J. Geophys. Res.*, *117*(D00V06),
 2979 doi:10.1029/2011JD016766.
- 2980 Lin, M., A. M. Fiore, O. R. Cooper, L. W. Horowitz, A. O. Langford, H. Levy II, B. J. Johnson,
 2981 B. Naik, S. J. Oltmans, and C. J. Senff (2012a), Springtime high surface ozone events over
 2982 the western United States: Quantifying the role of stratospheric intrusions, *J. Geophys. Res.*,
 2983 *117*(D00V22), doi:10.1029/2012JD018151.
- 2984 Lin, M., et al. (2012b), Transport of Asian ozone pollution into surface air over the western
 2985 United States in spring, *J. Geophys. Res.*, *117*(D00V07), doi:10.1029/2011JD016961.
- 2986 Neuman, J. A., et al. (2012), Observations of ozone transport from the free troposphere to the
 2987 Los Angeles basin, *J. Geophys. Res.*, *117*(D00V09), doi:10.1029/2011JD016919.
- 2988 Newell R.E., V. Thouret, J.Y.N. Cho, P. Stoller, A. Marenco and H.G. Smit (1999), Ubiquity of
 2989 quasi-horizontal layers in the troposphere, *Nature*, *398*, 316-319.
- 2990 Ohara, T., H. Akimoto, J. Kurokawa, N. Horii, K. Yamaji, X. Yan and T. Hayasaka (2007), An
 2991 Asian emission inventory of anthropogenic emission sources for the period 1980-2020.
 2992 *Atmos. Chem. Phys.* *7*, 4419-4444.
- 2993 U.S. Environmental Protection Agency (U.S. EPA) (2007), Treatment of data influenced by
 2994 exceptional events, *Fed. Regist.*, *72*(55), 13,560–13,581.
- 2995
- 2996
- 2997

2998 **Synthesis of Results - Climate Processes/Transformation**2999 **Response to Question P**3000 **QUESTION P**

3001 **What is the prevalence and spatial extent of the ozone weekend effect? What are the**
 3002 **contributing factors?**

3003 **BACKGROUND**

3004 The O₃ weekend effect is a phenomenon documented since the 1970s [Cleveland *et al.*, 1974;
 3005 Levitt and Chock, 1976] in which ambient, daytime surface O₃ concentrations in some urban
 3006 areas tend to be higher on weekends than on weekdays. An O₃ weekend effect in the SoCAB has
 3007 been extensively studied, and decreased concentrations of NO_x emissions on weekends are
 3008 considered to be the dominant cause of increased weekend O₃ concentrations [Marr and Harley,
 3009 2002a; b; Yarwood *et al.*, 2008]. A large decrease in on-road diesel-fueled vehicle activity on
 3010 weekends accounts for the significant reductions in weekend NO_x (and BC) emissions. Reduced
 3011 NO_x emissions on weekends can affect O₃ concentrations via two processes: 1) decreased O₃
 3012 loss by titration by freshly emitted NO and 2) increased O₃ production due to an increase in the
 3013 ratio of VOCs to NO_x. The more recent studies [Marr and Harley, 2002a; b; Yarwood *et al.*,
 3014 2008] indicate that the second process, increased photochemical production of O₃, plays a
 3015 significant role in increased weekend O₃ concentrations in and downwind of urban areas in
 3016 California.

3017 **POLICY RELEVANCE**

3018 The changes in ambient ozone concentrations that are observed to occur in response to emission
 3019 changes between weekdays and weekends can provide insights regarding the efficacy of NO_x
 3020 emission reduction policies. However, a comprehensive understanding of the day-of-week
 3021 variations in ozone concentrations is necessary for this phenomenon to provide reliable guidance
 3022 regarding long-term emission control strategies.

3023 The O₃ weekend effect has been investigated using airborne and ground-based measurements
 3024 from the CalNex field study conducted in May and June 2010. It must be noted that this is a
 3025 statistically limited period with only a few weekends, which may have been on average warmer
 3026 than the weekdays. Efforts have been made to compare the analysis of the CalNex data with
 3027 analyses of more extensive data sets, such as the data from the South Coast Air Quality
 3028 Management District monitoring network for the entire 2010 O₃ season and for other years.

3029 **FINDINGS**

3030 ***Finding P1: In the SoCAB, NO_x emissions are reduced by nearly half on weekends, while***
 3031 ***VOC emissions remain approximately constant. As a result, weekend hydroxyl radical***
 3032 ***concentrations are greater, giving 65%–75% faster photochemical processing. In addition,***
 3033 ***ozone production efficiency is 20%–50% higher. These effects yield 8-16 ppbv higher***
 3034 ***average midday ozone concentrations on weekends than on weekdays.***

3035 *Pollack et al.* [2012] analyze the O₃ weekend effect by examining a wide variety of data sets
 3036 collected in the SoCAB over many years. Consistent with previous work, they show that NO_x
 3037 emissions are significantly reduced (by approximately half) on weekends (Fig. P1) while no
 3038 change could be discerned in CO, CO₂ and VOC emissions. Reduced diesel truck traffic on the
 3039 weekends has been identified as the cause of the reduced NO_x emissions; *Pollack et al.* [2012]
 3040 further support this identification by showing that black carbon emissions (primarily due to
 3041 diesel-fueled vehicles) are also reduced by approximately half on weekends. These NO_x
 3042 emission reductions lead to average increases of 48±8% and 43±22% in the weekend VOC/NO_x
 3043 ratio as determined from the CalNex 2010 airborne and ground-based measurements,
 3044 respectively.

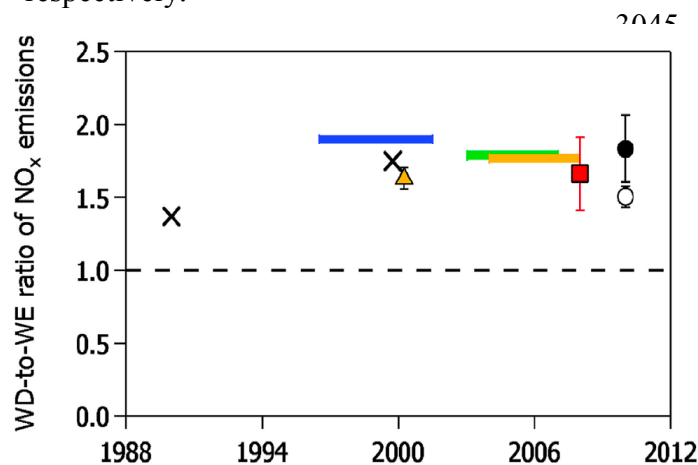
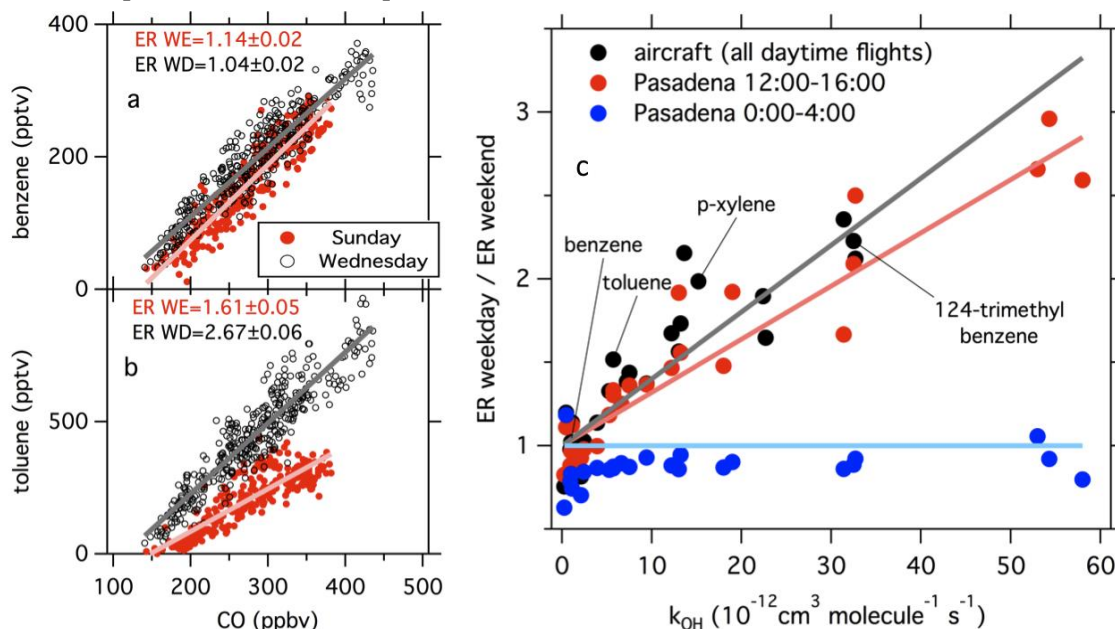


Figure P1. Weekday-to-weekend-day ratios of NO_x emissions derived for the LA basin from CalNex airborne (solid black circle) and ground-based (open circle) measurements, CARB flights of ARCTAS (red square), roadside/tunnel studies (crosses), ground-based network measurements (orange triangle), and satellite measurements from GOME (blue bar), SCIAMACHY (orange bar), and OMI (green bar). (Figure based on *Pollack et al.*, 2012).

3059 Reaction with NO₂ is the major sink for the hydroxyl radical (OH) in the Los Angeles
 3060 atmosphere. Thus, one consequence of reduced NO_x emissions on weekends is an increased
 3061 concentration of OH radicals. Since these radicals initiate the oxidation of VOCs, atmospheric
 3062 photochemistry proceeds more rapidly on weekends. Figure P2 demonstrates this faster
 3063 photochemistry by examining the relationships between VOCs and CO. The slope of the linear
 3064 correlation of each VOC with respect to CO is defined as the enhancement ratio (ER) of the
 3065 VOC to CO. CO is unreactive on the timescale of transport of pollutants out of the Los Angeles
 3066 basin. In the absence of photochemical loss of the VOC, the ER is equal to the ratio of emissions
 3067 of that VOC to CO. The same enhancement ratio is observed on weekdays and on weekends for
 3068 VOCs that react only slowly (on a timescale of days), such as benzene in Fig. P2a, while smaller
 3069 enhancement ratios are observed on weekends for more reactive VOCs, such as toluene in Fig.
 3070 P2b. The decrease in ERs on weekends is due to faster removal of the reactive VOCs due to the
 3071 higher OH concentrations. Figure P2c demonstrates that ERs are the same at night on weekends
 3072 and on weekdays, showing that the emission ratios are the same throughout the week. However,
 3073 the ERs are higher during weekday afternoons than on weekends by a factor that correlates with
 3074 the reaction rate constant of the VOC with OH radicals. This behavior indicates that average
 3075 daytime OH concentrations are larger on weekends by 65%–75% [*Warneke et al.*, 2013].

3076 As a result of the lower NO_x emissions and the higher OH concentrations on weekends, NO_x is
 3077 oxidized more rapidly and the O₃ formation efficiency per unit NO_x oxidized are both enhanced
 3078 on weekends. Figure P3 shows the fraction of emitted NO_x that had not been oxidized to other
 3079 NO_y species at the time of measurement; this fraction is significantly smaller on weekends,
 3080 demonstrating the faster weekend NO_x oxidation rate. Figure P4 shows the relationship between
 3081 O₃ formed and NO_x oxidized in the airborne and ground-based measurements. Here O_x, which
 3082 equals O₃ + NO₂, rather than O₃ is plotted on the ordinate to avoid the influence of reaction of

3083 ambient O₃ with fresh emissions of NO. The slopes of these plots, which approximate the
 3084 number of O₃ molecules formed per NO_x oxidized (i.e. the O₃ formation efficiency), are higher
 3085 on weekends. These two effects are the fundamental cause of the higher O₃ concentrations on
 3086 weekends [Pollack *et al.*, 2012].



3087 **Figure P2.** Correlation of **a)** benzene and **b)** toluene with CO measured during NOAA WP-3D
 3088 flights on a weekday (black symbols) and a weekend day (red symbols). Linear least square fits are
 3089 shown and the slopes with confidence limits are annotated. Each slope defines an enhancement ratio
 3090 (ER) of the VOC with respect to CO. **c)** Ratio of weekday to weekend ERs measured on all daytime
 3091 NOAA WP-3D flights (black symbols) and at the Pasadena ground site during the afternoon (red
 3092 symbols) and during nighttime (blue symbols). The lines of the respective colors indicate linear
 3093 least square fits forced to an intercept of unity. (Figure based on Warneke *et al.*, 2013).
 3094

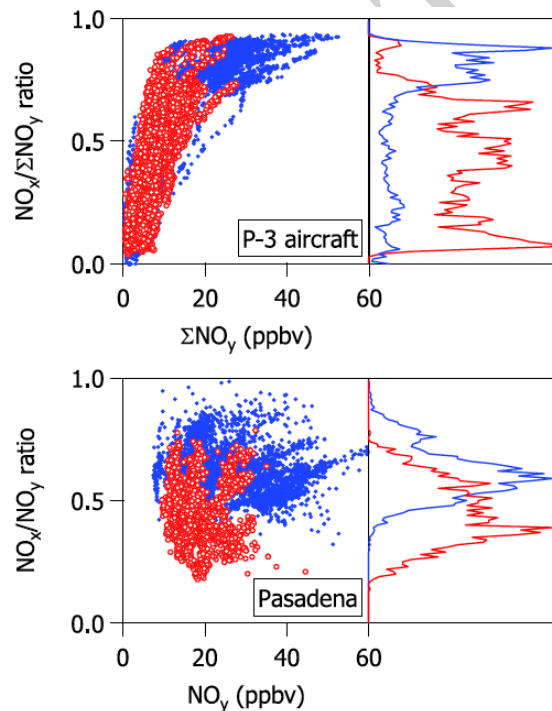
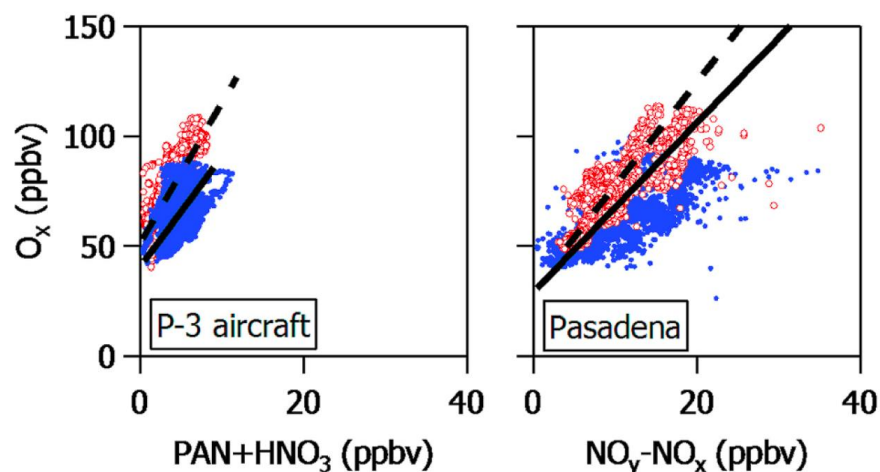


Figure P3. Plots of NO_x/ΣNO_y ratio versus ΣNO_y (left) and histogram (right) of the corresponding ratio on weekdays (blue) and weekends (red). Top plots are airborne observations over SoCAB, and bottom plots are ground-based measurements from the CalNex Pasadena site. (Figure from Pollack *et al.*, 2012.)



3115 **Figure P4.** Plots of (left) airborne observations of O_x versus PAN+HNO₃ and (right) ground-
 3116 based measurements of O_x versus NO_y-NO_x on weekdays (blue dots, solid lines) and weekends
 3117 (red circles, dashed lines). (Figure from *Pollack et al.*, 2012).

3118 ***Finding P2: The weekend reduction of NO_x emissions, and the concomitant changes in the***
 3119 ***photochemical environment in the SoCAB, provides an opportunity to investigate certain***
 3120 ***aspects of urban photochemistry such as secondary aerosol formation.***

3121 *Bahreini et al.* [2012] compare the formation of secondary organic aerosol in the SoCAB on
 3122 weekdays with weekends. Even though diesel truck traffic is reduced by about a factor of two on
 3123 weekends, SOA concentrations are about the same throughout the week in air masses with
 3124 similar degrees of photochemical processing. This result indicates that the contribution to SOA
 3125 formation from diesel emissions is zero within the uncertainties of their analysis. This work is
 3126 discussed more fully in the Response to Question N.

3127 ***Finding P3: Investigation of the history of the weekend O₃ effect in the San Joaquin Valley***
 3128 ***suggests that NO_x emissions reductions are already effective for reducing maximum O₃***
 3129 ***concentrations, or are poised to become so, in the southern and central SJV.***

3130 *Pusede and Cohen* [2012] describe the effects of NO_x and organic reactivity reductions on the
 3131 frequency of high O₃ days in the SJV. They use sixteen years of observations of O₃, NO_x, and
 3132 temperature at sites upwind, within, and downwind of three cities located along the axis of the
 3133 Valley to assess the probability of exceeding the California 8-h average O₃ standard of 70.4 ppb
 3134 at each location. They show that reductions in organic reactivity have been very effective in the
 3135 central and northern regions of the SJV but less so in the southern region, and present evidence
 3136 for two distinct categories of organic reactivity sources: one source that has decreased and
 3137 dominates at moderate temperatures, and a second source that dominates at high temperatures,
 3138 particularly in the southern SJV, and has not changed over the last twelve years. They conclude
 3139 that NO_x emissions reductions are already effective for reducing maximum O₃ concentrations, or
 3140 are poised to become so, in the southern and central SJV. These are the regions of the SJV
 3141 where O₃ violations are most frequent, and where conditions are transitioning to NO_x-limited
 3142 chemistry on the days when air temperatures are hottest and high O₃ concentrations are most
 3143 probable.

3144
 3145
 3146

3147 **References**

- 3148
- 3149 Bahreini, R., et al. (2012), Gasoline emissions dominate over diesel in formation of secondary
3150 organic aerosol mass, *Geophys. Res. Lett.*, 39(L06805), doi:10.1029/2011GL050718.
- 3151 Cleveland, W. S., et al. (1974), Sunday and workday variations in photochemical air-pollutants
3152 in New Jersey and New York, *Science*, 186(4168), 1037–1038,
3153 doi:10.1126/science.186.4168.1037.
- 3154 Levitt, S. B., and D. P. Chock (1976), Weekday-weekend pollutant studies of Los Angeles Basin,
3155 *J. Air Pollut. Control Assoc.*, 26(11), 1091–1092.
- 3156 Marr, L. C., and R. A. Harley (2002a), Modeling the effect of weekday-weekend differences in
3157 motor vehicle emissions on photochemical air pollution in central California, *Environ. Sci.*
3158 *Technol.*, 36(19), 4099–4106, doi:10.1021/es020629x.
- 3159 Marr, L. C., and R. A. Harley (2002b), Spectral analysis of weekday-weekend differences in
3160 ambient ozone, nitrogen oxide, and non-methane hydrocarbon time series in California,
3161 *Atmos. Environ.*, 36(14), 2327–2335, doi:10.1016/S1352-2310(02)00188-7.
- 3162 Pollack, I. B., et al. (2012), Airborne and ground-based observations of a weekend effect in
3163 ozone, precursors, and oxidation products in the California South Coast Air Basin, *J.*
3164 *Geophys. Res.*, 117(D00V05), doi:10.1029/2011JD016772.
- 3165 Pusede, S. E. and R. C. Cohen (2012), On the observed response of ozone to NO_x and VOC
3166 reactivity reductions in San Joaquin Valley California 1995–present, *Atmos. Chem. Phys.*, 12,
3167 8323–8339.
- 3168 Warneke, C., et al. (2013), Photochemical aging of volatile organic compounds in the Los
3169 Angeles basin: weekday - weekend effect, *J. Geophys. Res. Atmos.*, 118, 5018–5028,
3170 doi:10.1002/jgrd.50423.
- 3171 Yarwood, G., et al. (2008), Modeling weekday to weekend changes in emissions and ozone in
3172 the Los Angeles basin for 1997 and 2010, *Atmos. Environ.*, 42(16), 3765–3779,
3173 doi:10.1016/j.atmosenv.2007.12.074.
- 3174
- 3175

3176 **Synthesis of Results - Climate Processes/Transformation**3177 **Response to Question Q**3178 **QUESTION Q**3179 **How do the different aerosol compositions in different areas influence radiative balances?**3180 **BACKGROUND**

3181 Aerosols affect climate through their direct and indirect interactions with radiation in the
 3182 atmosphere. Aerosols can directly scatter and absorb short-wave (i.e., visible and near
 3183 ultraviolet wavelengths) radiation and can emit long-wave (i.e., infrared) radiation. Aerosols can
 3184 also affect cloud radiative properties by altering the cloud droplet number and size, and by
 3185 changing cloud lifetime and extent. These properties in part determine the scattering and
 3186 absorption of radiation by clouds.

3187 It is recognized that these aerosol climate effects are likely large and represent primarily a net
 3188 climate cooling, but that they are only poorly quantified [e.g. *IPCC*, 2007]. While it is important
 3189 that earth-system models accurately simulate these effects, cloud-aerosol interactions are
 3190 complex and nonlinear, leading to large uncertainties in estimates of indirect climate forcing.
 3191 The CalNex field study included measurements of many aerosol properties, and these
 3192 measurements have been analyzed from a variety of perspectives. The following material
 3193 summarizes some of the results of these analyses.

3194 **POLICY RELEVANCE**

3195 Informed climate change mitigation policies must understand aerosol influences on climate,
 3196 which arise primarily from aerosol effects on the radiative balance of the atmosphere. These
 3197 effects are poorly understood and thus modeling results are uncertain. The CalNex
 3198 measurements and analyses provide information to improve this understanding and provide
 3199 benchmarks to which modeling results can be compared.

3200 **FINDINGS**

3201 ***Finding Q1: Climate models need more detailed treatment of direct radiative effects***
 3202 ***related to black carbon absorption enhancements and also of ammonium nitrate***
 3203 ***partitioning between aerosol and gas phases.***

3204 *Cappa et al.* [2012; 2013] compared direct measurements of black carbon absorption
 3205 enhancements from two different regions in California to show that the mixing state of aerosol
 3206 BC enhances its ability to absorb solar radiation by relatively small factors of ~1.06 at 532 nm
 3207 and ~1.13 at 405 nm. This analysis used the contrast between measurements made offshore from
 3208 the R/V Atlantis during CalNex with those made in Sacramento, CA during the concurrent
 3209 CARES project [*Zaveri et al.*, 2012], and concluded that climate models that use absorption
 3210 enhancement dependence of up to a factor of two may produce significant overestimates of
 3211 warming by BC under some conditions. The observed BC in these two data sets was dominated
 3212 by diesel emissions [*Cappa et al.*, 2012]. *Adachi, et al.* [2013] conclude that the ways in which
 3213 BC mixes with other particles explains why these observations of light amplification by BC coatings

3214 are smaller than optical model calculations produce. In contrast, a recent study [Lack *et al.*, 2012]
 3215 measured the effect of coatings on absorption in biomass burning plumes and found that coatings
 3216 of organic and inorganic material on BC enhanced absorption by up to a factor of 1.7 at 532 nm
 3217 and up to a factor of three at 405 nm. The Lack *et al.* [2012] analysis also concluded that while
 3218 absorption at 532 nm by particulate organic matter (POM) was very weak, significant variability
 3219 of absorption at 404 nm was important in determining the overall mass absorption efficiency of
 3220 POM at low wavelengths in the visible range. Taken together, the Cappa *et al.* [2012] and Lack
 3221 *et al.* [2012] analyses suggest sufficiently large differences between the radiative effects of BC,
 3222 and internal mixtures with BC, from anthropogenic and biomass sources to warrant their separate
 3223 treatment in climate models.

3224 LeBlanc *et al.* [2012] used spectral irradiance measurements taken on board the WP-3D aircraft
 3225 when above and below an aerosol layer to estimate the aerosol direct radiative forcing. The
 3226 observations were compared, using relative forcing efficiency, to direct radiative forcing from
 3227 other field missions in different parts of the world. The CalNex relative forcing efficiency
 3228 spectra agreed with earlier studies that found this parameter to be constrained at each wavelength
 3229 within 20% per unit of aerosol optical thickness at 500 nm, and was found to be independent of
 3230 aerosol type and location. The diurnally averaged below-layer forcing integrated over the
 3231 wavelength range of 350-700 nm for CalNex was estimated to be 59 ± 14 W/m² of cooling at the
 3232 surface per unit optical depth.

3233 Langridge *et al.* [2012] used WP-3D aircraft data to track the evolution of aerosol radiative
 3234 properties during transport within and downwind of the Los Angeles basin. They documented
 3235 that changes in aerosol hygroscopicity, secondary organic carbon content, and ammonium nitrate
 3236 mass occurring during transport over the time scale of hours had significant effects on the
 3237 aerosol extinction. In particular, they found that the semi-volatile partitioning of ammonium
 3238 nitrate with gas phase ammonia and nitric acid was strongly affected by temperature and plume
 3239 dilution, in accordance with thermodynamic models. They noted that the small spatial and
 3240 temporal scales of variability of aerosol hygroscopicity require explicit, high-resolution
 3241 treatment for accurate representation of aerosol direct radiative forcing in regional and large-
 3242 scale climate models.

3243 Zhang *et al.* [2011] analyzed water-soluble organic carbon (WSOC) aerosol data from the
 3244 Pasadena ground site to show that nitroaromatics contribute significantly to the brown SOA in
 3245 Los Angeles. They use aerosol radiocarbon (¹⁴C) measurements to conclude that anthropogenic
 3246 carbon dominated the aerosol budget in Los Angeles, in contrast to measurements in Atlanta, GA
 3247 showing a minimal anthropogenic component to the water-soluble SOA.

3248 ***Finding Q2: The hygroscopicity of particles in the Central Valley is consistent with the***
 3249 ***emerging global picture of a limited range of hygroscopicities, which may simplify the***
 3250 ***treatment of indirect aerosol effects in global climate models. However, considerable***
 3251 ***variability was found in aerosol hygroscopicity in the Los Angeles basin, which may***
 3252 ***complicate the treatment of this issue in regional climate models.***

3253 Measurements of cloud condensation nuclei (CCN) concentrations throughout the boundary
 3254 layer in the Los Angeles basin and Central Valley varied by two orders of magnitude ($\sim 10^2$ - 10^4
 3255 cm⁻³ @ STP), and represented a substantial fraction of the total submicron particle concentration
 3256 ($\sim 10^3$ - 10^5 cm⁻³ @ STP). Organic species and fully-neutralized sulfate were found to constitute
 3257 more than 75% of the particle mass in all regions, on average, with higher organic fractions
 3258 observed in the Central Valley than in the Los Angeles basin. Despite this variation, large

3259 changes in the regionally-averaged CCN-derived aerosol hygroscopicity were not observed, and
 3260 most CCN were found to activate between 0.2-0.4% supersaturation ($\kappa \sim 0.1-0.4$) [Moore *et al.*,
 3261 2012], where κ is the hygroscopicity parameter [Petters and Kreidenweis, 2007].
 3262 Hygroscopicities in this range reflect the dominance of inorganic and oxygenated organic species
 3263 (particularly in the Central Valley) and are consistent with the emerging global picture of a
 3264 continental aerosol hygroscopicity of $\kappa \sim 0.3$ [e.g., Andreae and Rosenfeld, 2008; Pringle *et al.*,
 3265 2010].

3266 More significant compositional variation was observed within the Los Angeles basin than in the
 3267 Central Valley, resulting in a more complex picture with regard to aerosol hygroscopicity. For
 3268 example, Langridge *et al.* [2012] attributed measured changes in humidified aerosol optical
 3269 extinction to gas-aerosol partitioning of organic and nitrate species as the urban LA plume
 3270 moved inland into the warmer, eastern part of the basin. The gas-to-particle partitioning of SOA
 3271 precursors and the evaporation of semi-volatile ammonium nitrate resulted in an overall decrease
 3272 in hygroscopicity of the aging aerosol. This trend is consistent with Hersey *et al.* [2013], who
 3273 also observed a decrease from west to east in the Los Angeles basin (from $\kappa=0.4$ to $\kappa=0.2$) in
 3274 sub-saturated aerosol hygroscopicity for 150-250 nm aerosol measured aboard the CIRPAS Twin
 3275 Otter. Meanwhile, concurrent CCN measurements aboard the CIRPAS Twin Otter showed the
 3276 opposite trend, with supersaturated aerosol hygroscopicity increasing with plume photochemical
 3277 age ($\kappa=0.2$ to $\kappa=0.4$) at 0.73% supersaturation. This discrepancy likely reflects size-dependent
 3278 changes in aerosol composition during plume aging – a conclusion that is supported by particle
 3279 time-of-flight mass spectrometry compositional data [Hersey *et al.*, 2013]. This sort of size-
 3280 dependent chemistry was also observed in measurements of a biomass-burning (BB) plume
 3281 sampled by the CIRPAS Twin Otter in the Los Angeles basin, emphasizing the role of BB as a
 3282 source of CCN even while being effectively non-hygroscopic at relative humidities less than
 3283 100%.

3284 References

- 3285 Adachi, K., and P. R. Buseck (2013), Changes of ns-soot mixing states and shapes in an urban
 3286 area during CalNex, *J. Geophys. Res. Atmos.*, *118*, 3723–3730, doi:10.1002/jgrd.50321.
- 3287 Andreae, M. O., and D. Rosenfeld (2008), Aerosol-cloud-precipitation interactions. Part 1. The
 3288 nature and sources of cloud-active aerosols, *Earth Sci. Rev.*, *89*, 13–41,
 3289 doi:10.1016/j.earscirev.2008.03.001.
- 3290 Cappa, C. D., et al. (2012), Radiative absorption enhancements due to the mixing state of
 3291 atmospheric black carbon, *Science*, *337*, 1078-1081, doi:10.1126/science.1223447.
- 3292 Cappa, C. D.; et al. (2013), Response to Comment on 'Radiative absorption enhancements due to
 3293 the mixing state of atmospheric black carbon'., *Science*, *339*, 393-c, doi:
 3294 10.1126/science.1230260.
- 3295 Hersey, S. P., et al. (2013), Composition and hygroscopicity of the Los Angeles Aerosol:
 3296 CalNex, *J. Geophys. Res.*, *118*, 3016–3036, doi:10.1002/jgrd.50307.
- 3297 IPCC, Intergovernmental Panel on Climate Change: Climate Change 2007: The Physical Science
 3298 Basis. Contribution of Working Group I to the Fourth Assessment, Report of the
 3299 Intergovernmental Panel on Climate Change [Solomon, S., D. Qin, M. Manning, Z. Chen, M.
 3300 Marquis, K.B. Averyt, M. Tignor and H.L. Miller (eds.)]. Cambridge University Press,
 3301 Cambridge, United Kingdom and New York, NY, USA, 996 pp, 2007.

- 3302 Lack, D. A., J. M. Langridge, R. Bahreini, C. D. Cappa, A. M. Middlebrook, and J. P. Schwarz
3303 (2012), Brown carbon and internal mixing in biomass burning particles, *Proceedings of the*
3304 *National Academy of Sciences*, 109(37), 14802-14807, doi:10.1073/pnas.1206575109.
- 3305 Langridge, J. M., et al. (2012), Evolution of aerosol properties impacting visibility and direct
3306 climate forcing in an ammonia-rich urban environment, *J. Geophys. Res.*, 117(D00V11),
3307 doi:10.1029/2011JD017116.
- 3308 LeBlanc, S. E., K. S. Schmidt, P. Pilewskie, J. Redemann, C. Hostetler, R. Ferrare, J. Hair, J. M.
3309 Langridge, and D. A. Lack (2012), Spectral aerosol direct radiative forcing from airborne
3310 radiative measurements during CalNex and ARCTAS, *J. Geophys. Res.*, 117(D00V20),
3311 doi:10.1029/2012JD018106.
- 3312 Moore, R. H., K. Cerully, R. Bahreini, C. A. Brock, A. M. Middlebrook, and A. Nenes (2012),
3313 Hygroscopicity and composition of California CCN during summer 2010, *J. Geophys. Res.*,
3314 117(D00V12), doi:10.1029/2011JD017352.
- 3315 Petters, M. D., and S. M. Kreidenweis (2007), A single parameter representation of hygroscopic
3316 growth and cloud condensation nucleus activity, *Atmos. Chem. Phys.*, 7, 1961-1971,
3317 doi:10.5194/acp-8-6273-2008.
- 3318 Pringle, K. J., H. Tost, A. Pozzer, U. Pöschl, and J. Lelieveld (2010), Global distribution of the
3319 effective aerosol hygroscopicity parameter for CCN activation, *Atmos. Chem. Phys.*, 10, 5241-
3320 5255, doi:10.5194/acp-10-5241-2010.
- 3321 Zaveri, R. A., et al. (2012), Overview of the 2010 Carbonaceous Aerosols and Radiative Effects
3322 Study (CARES), *Atmos. Chem. Phys.*, 12, 7647-7687, doi:10.5194/acp-12-7647-2012.
- 3323 Zhang, X., Y.-H. Lin, J. D. Surratt, P. Zotter, A. S. H. Prévôt, and R. J. Weber (2011), Light-
3324 absorbing soluble organic aerosol in Los Angeles and Atlanta: A contrast in secondary
3325 organic aerosol, *Geophys. Res. Lett.*, 38(L21810), doi:10.1029/2011GL049385.
- 3326
3327
3328
3329
3330

3331 **Synthesis of Results - Atmospheric Transport**3332 **Response to Question R**3333 **QUESTION R**3334 **Is there evidence of pollutant transport between air basins or states?**

3335

3336 **POLICY RELEVANCE**

3337 Several regions within California have significant air quality challenges, and the emission
 3338 sources throughout the State vary widely in magnitude and species emitted. Pollutants emitted in
 3339 one region and transported to other regions may add significantly to the impact of the local
 3340 emissions within the receptor regions. This transport may affect the effectiveness of air quality
 3341 control measures taken within a particular receptor region.

3342 **BACKGROUND**

3343 California is a large state with several distinct regions, the more populated of which generally
 3344 face air quality challenges. Air quality within each region (for example, Southern California) has
 3345 been studied extensively. However, less attention has been given to understanding the impacts
 3346 of transport of air pollutants from one region to another. Previous studies showed that pollution
 3347 produced in the Los Angeles area can be transported eastward to the deserts [see for example,
 3348 *Langford et al.*, 2010; *Riley et al.*, 2008; *White and Macias*, 1990] and similarly, pollutants from
 3349 the San Francisco Bay Area (SFBA) can affect the Central Valley and the foothills of the Sierra
 3350 Nevada [see for example, *Bao et al.*, 2008; *Beaver and Palazoglu*, 2009; *Michelson and Bao*,
 3351 2008; *Riley et al.*, 2008]. Other possible interregional impacts are from Southern California and
 3352 the San Francisco Bay Area to the coastal waters and from the Central Valley to the mountains,
 3353 deserts, and Southern California. Transport between and within regions can take place in the
 3354 free troposphere as well as in the boundary layer [*Neuman et al.*, 2012]. The CalNex field study
 3355 included analysis of some of the transport patterns that were observed during that period;
 3356 however this period was limited, so these findings must be considered in context of previous
 3357 work (some referenced above).

3358 The focus of the response to this question is on transport between California's Air Basins and
 3359 between Mexico and California across the southern border of California. The Response to
 3360 Question T briefly discusses transport from California to other states.

3361 **FINDINGS**

3362 ***Finding R1a:* San Francisco Bay Area pollutants are transported efficiently to the Central**
 3363 **Valley. Automotive CO emitted in the Bay Area is a significant fraction of total CO found**
 3364 **in the San Joaquin Valley.**

3365 ***Finding R1b:* Agricultural emissions (as well as emissions from other sources) in the**
 3366 **Central Valley can be transported aloft to the Southern California Bight.**

3367 ***Finding R1c:* Southern California emissions are typically transported to less-populated**
 3368 **areas to the east.**

3369 *Angevine et al.* [2013] apply WRF/FLEXPART Lagrangian particle dispersion model
 3370 simulations to determine the amounts of gaseous tracers that are transported within and among
 3371 four regions: Southern California, the San Francisco Bay Area (SFBA), the Central Valley, and
 3372 the rest of the state. They consider two completely inert tracers, whose emissions are set equal to
 3373 those of carbon monoxide (CO) and ammonia (NH₃) to represent emissions from anthropogenic
 3374 and agricultural sources, respectively. These species have quite different spatial emissions
 3375 patterns throughout the State. The concentrations of the tracers from the simulations of the
 3376 particle dispersion model are compared to airborne and ground-based measurements. The age of
 3377 the tracers in each location is also presented. Vertical profiles and diurnal cycles are analyzed to
 3378 help clarify important transport processes. The simulations cover the period of CalNex studies
 3379 (May and June of 2010). So the analysis presented here applies only to the time period simulated
 3380 (primarily early June). This period is expected to be representative of summer in general. The
 3381 transport patterns could be quite different in other seasons of the year, particularly in winter.

3382 The simulations of pollutant transport in May and June 2010 are illustrated in Figures R1 and
 3383 R2. They conform to the basic picture developed over several decades of research (see
 3384 references above). Southern California emissions are transported to the east and affect the desert
 3385 areas. The SFBA emissions are an important source of pollutants in the San Joaquin Valley.
 3386 Central Valley automobile emissions affect their local areas (e.g., Sacramento and Bakersfield)
 3387 and the Sierra Nevada.

3388 *Angevine et al.* [2013] also see some novel, or at least easily-visualized, results from the
 3389 simulations. The Southern California Bight (i.e., the part of the Pacific Ocean bounded by the
 3390 curved coastline of Southern California from Point Conception to San Diego including the
 3391 Channel Islands) is filled with a mixture of aged CO tracer from Southern California and the
 3392 SFBA, with the two sources dominating at different times of day and locations within the Bight.
 3393 The SFBA emissions are transported through the San Jose area and into and beyond the valleys
 3394 through the coastal mountains, where they join the offshore flow. The SFBA tracer is
 3395 transported down the coast by the prevailing northwesterly winds, introduced into the western
 3396 edge of the Bight, and then recirculated by the “Catalina” eddy. The Southern California tracer
 3397 drifts out to Santa Monica Bay on the nocturnal land breeze and joins in the eddy circulation.
 3398 Overall CO tracer mixing ratios are low. Air over the Bight is also affected by the Central
 3399 Valley emissions represented by the NH₃ tracer (Figure R2).

3400 In these simulations, there is no indication of transport from Southern California to the Central
 3401 Valley. Emissions from the Central Valley do make their way to Southern California, as shown
 3402 by the NH₃ tracer, but the contribution of automobile emissions from the Central Valley to
 3403 Southern California is negligible compared to the region’s large emissions from automobile
 3404 sources.

3405 ***Finding R2: The primary direction of transport of Mexican emissions in the border area***
 3406 ***(as exemplified by Tijuana emissions) was to the east or southeast. Under most conditions***
 3407 ***during May and June of 2010, the transport of emissions from the Mexican border regions***
 3408 ***into the San Diego area was not an important influence.***

3409 The Cal-Mex 2010 Field Study is a US-Mexico collaborative project to investigate cross-border
 3410 transport of emissions in the California-Mexico border region, which took place from May 15 to
 3411 June 30, 2010, and was loosely coordinated with CalNex. *Bei et al.* [2012] present an overview
 3412 of the meteorological conditions and plume transport patterns during the study period based on

3413 the analysis of surface and vertical measurements (radiosonde, ceilometers and tethered balloon)
 3414 conducted in Tijuana, Mexico and the modeling output using the WRF/FLEXPART model.
 3415 Based on simulations with particles released in Tijuana in the morning, four representative plume
 3416 transport patterns are identified as “plume-southeast”, “plume-southwest”, “plume-east” and
 3417 “plume-north”, indicating the direction of plume transport. Most of the days during May and
 3418 June are classified as plume-east and plume-southeast days, showing that the plumes in Tijuana
 3419 are mostly carried to the southeast and east of Tijuana within the boundary layer during daytime,
 3420 although some may trickle over the US-Mexico border near the eastern edge of California. This
 3421 general transport pattern is consistent with the back trajectory simulations of *Takahama et al.*
 3422 [2013], who found that under mean wind conditions, much of the oxygenated organic aerosol
 3423 observed in Tijuana may have come from the Southern California Air Basin. On a subset of days
 3424 considered by *Shores et al.* [2013], forward trajectory analysis using meteorological fields
 3425 generated by *Baker et al.* [2013] indicates that transport from Tijuana into the US was common,
 3426 often entering in a northeasterly direction east of San Diego-Tijuana and sometimes as far east
 3427 as Imperial County at the eastern edge of California.

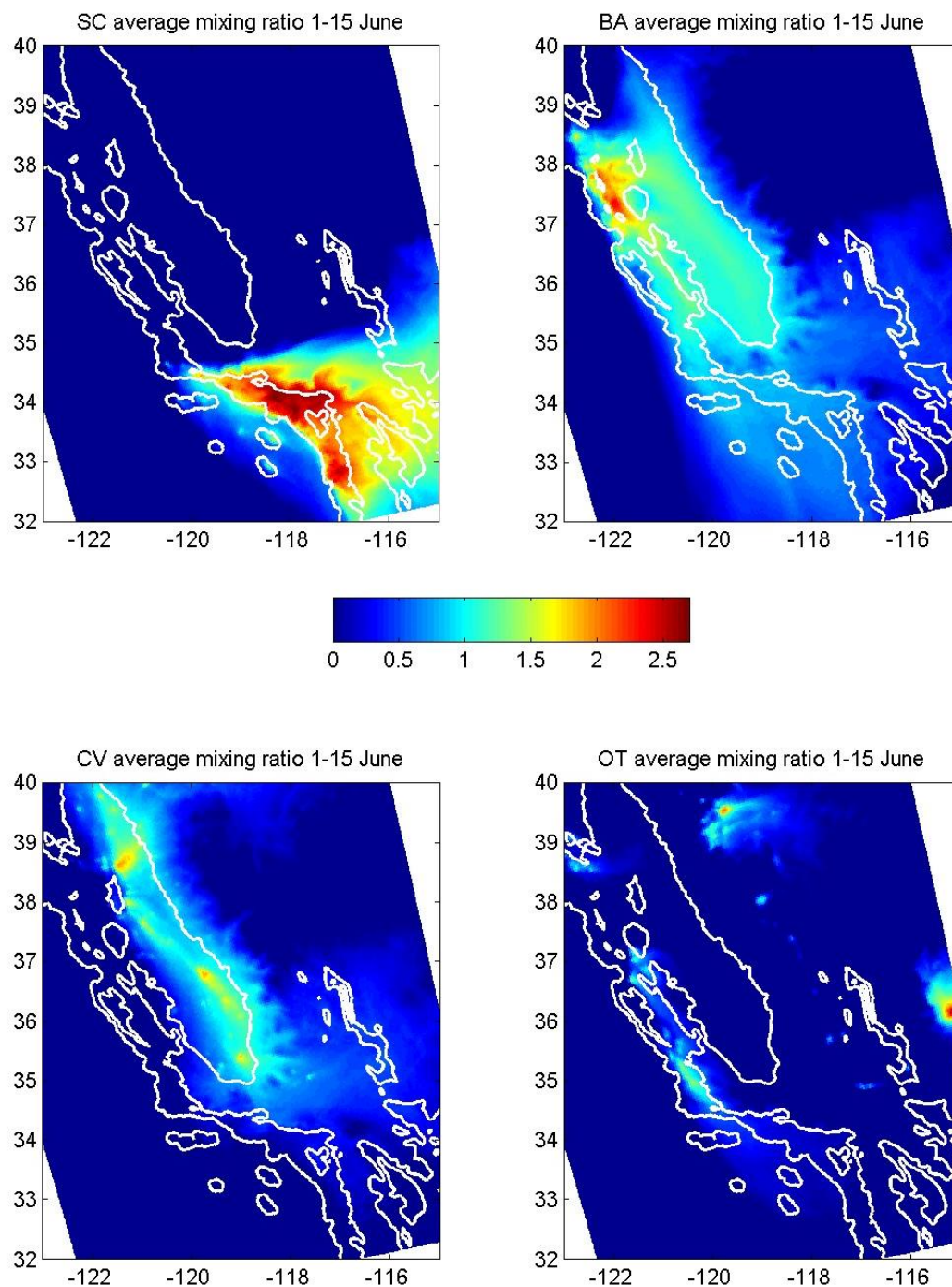
3428 **References**

- 3429 Angevine, W. M., et al. (2013), Pollutant transport among California regions, *J. Geophys. Res.*
 3430 *Atmos.*, *118*, 6750–6763, doi:10.1002/jgrd.50490.
- 3431 Baker, K. R., et al. (2013), Evaluation of surface and upper air fine scale WRF meteorological
 3432 modeling of the May and June 2010 CalNex period in California, *Atmos. Environ.*, *80*, 299-
 3433 309, doi: 10.1016/j.atmosenv.2013.08.006.
- 3434 Bao, J. W., S. A. Michelson, P. O. G. Persson, I. V. Djalalova, and J. M. Wilczak (2008),
 3435 Observed and WRF-simulated low-level winds in a high-ozone episode during the Central
 3436 California Ozone Study, *J. Appl. Meteorol. Clim.*, *47*(9), 2372–2394.
- 3437 Beaver, S., and A. Palazoglu (2009), Influence of synoptic and mesoscale meteorology on ozone
 3438 pollution potential for San Joaquin Valley of California, *Atmos. Environ.*, *43*(10), 1779–
 3439 1788.
- 3440 Bei, N., et al. (2012), Meteorological overview and plume transport patterns during Cal-Mex 2010,
 3441 *Atmos. Environ.* *70*, 477–489, doi:10.1016/j.atmosenv.2012.01.065.
- 3442 Langford, A. O., C. J. Senff, R. J. Alvarez II, R. M. Banta, and R. M. Hardesty (2010), Long-
 3443 range transport of ozone from the Los Angeles Basin: A case study, *Geophys. Res. Lett.*, *37*,
 3444 L06807, doi:10.1029/2010GL042507.
- 3445 Michelson, S. A., and J.-W. Bao (2008), Sensitivity of low-level winds simulated by the WRF
 3446 model in California’s Central Valley to uncertainties in the large-scale forcing and soil
 3447 initialization, *J. Appl. Meteorol. Clim.*, *47*, 3131–3149.
- 3448 Neuman, J. A., et al. (2012), Observations of ozone transport from the free troposphere to the
 3449 Los Angeles basin, *J. Geophys. Res.*, *117*, D00V09, doi:10.1029/2011JD016919.
- 3450 Riley, W. J., D. Y. Hsueh, J. T. Randerson, M. L. Fischer, J. G. Hatch, D. E. Pataki, W. Wang,
 3451 and M. L. Goulden (2008), Where do fossil fuel carbon dioxide emissions from California
 3452 go? An analysis based on radiocarbon observations and an atmospheric transport model, *J.*
 3453 *Geophys. Res.*, *113*, G04002, doi:10.1029/ 2007JG000625.
- 3454 Shores, C.A., et al. (2013), Sources and transport of black carbon at the California-Mexico
 3455 border, *Atmos. Environ.*, *70*, 490-499.

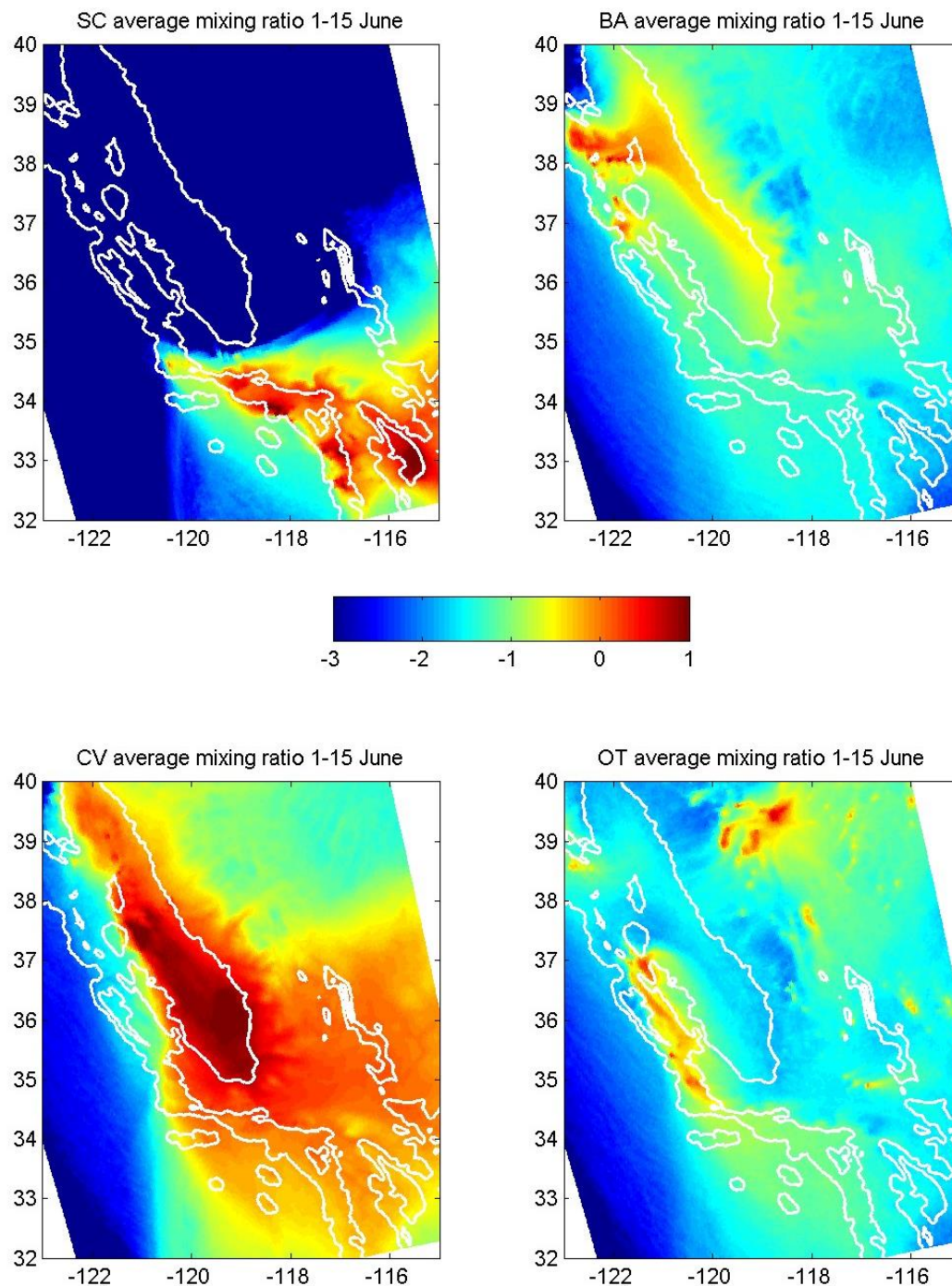
- 3456 Takahama, S., et al. (2013), Submicron organic aerosol in Tijuana, Mexico, from local and
3457 Southern California sources during the CalMex campaign, *Atmos. Environ.*, *70*, 500–512.
- 3458 White, W. H., and E. S. Macias (1990), Regional transport of the urban workweek:
3459 Methylchloroform cycles in the Nevada-Arizona desert, *Geophys. Res. Lett.*, *17*, 1081–1084,
3460 doi:10.1029/GL017i008p01081.
3461

DRAFT - Do Not Cite

3462



3463 **Figure R1:** Average near-surface mixing ratios of each CO tracer (log₁₀ (ppbv)) for all hours of 1-15
 3464 June, 2010. Log (base 10) scale is used to make small concentrations visible. The maps span from the
 3465 Sacramento Valley in the northwest to the California-Mexico border in the southeast; the white lines
 3466 show the 1 m and 500 m elevation contours. In the model calculation, a background CO concentration of
 3467 120 ppbv is assumed, but that background is not added in this figure. The tracers are identified according
 3468 to their emission region: Southern California (SC), San Francisco Bay Area (BA), Central Valley (CV)
 3469 and other regions of the state (OT). [Figure from *Angevine et al.*, 2013].



3470 **Figure R2:** Average of near-surface mixing ratios (\log_{10} (ppbv)) of NH_3 , used as a tracer of agricultural
 3471 emissions from four source regions. All hours of 1-15 June 2010 are included. The log (base 10) scale is
 3472 used to make small concentrations visible. The figure is in the same format as in Figure R1. [Adapted
 3473 from *Angevine et al.*, 2013].

3474

3475

3476

3477 **Synthesis of Results - Atmospheric Transport**3478 **Response to Question S**3479 **QUESTION S**

3480 **Is there evidence of pollutant recirculation, particularly in the South Coast Air Basin**
 3481 **(SoCAB)?**

3482 **POLICY RELEVANCE**

3483 Air quality models are required to formulate and evaluate air pollution control strategies as well
 3484 as to demonstrate attainment of air quality goals included in the State Implementation Plan (SIP).
 3485 The ability of a model to reproduce situations where yesterday's pollution is recirculated within
 3486 an air basin to contribute to today's concentration levels, as opposed to being dispersed by the
 3487 prevailing winds between days, is a critical measure of model performance. Observational
 3488 evidence of recirculation that can be compared to results from air quality models provides critical
 3489 guidance in their development as regulatory tools.

3490 **BACKGROUND**

3491 California is a state with complex topographic features that interact with synoptic-scale
 3492 meteorological patterns and can contribute to strong temperature gradients, both horizontal (e.g.,
 3493 between the ocean and land) and vertical (e.g., radiative, marine, subsidence inversions). These
 3494 interactions and temperature gradients generate complex airflow that transports pollutants in
 3495 complicated patterns - some of which can recirculate aged emissions back to their source area.

3496 The response to this question discusses recirculation of pollutants within the SoCAB; related
 3497 material is given in responses to other questions. Questions R and T discuss transport between
 3498 air basins and transport of pollutants from upwind sources into California, respectively; both of
 3499 these transport discussions have some relation to the transport mechanisms responsible for the
 3500 recirculation of pollutants.

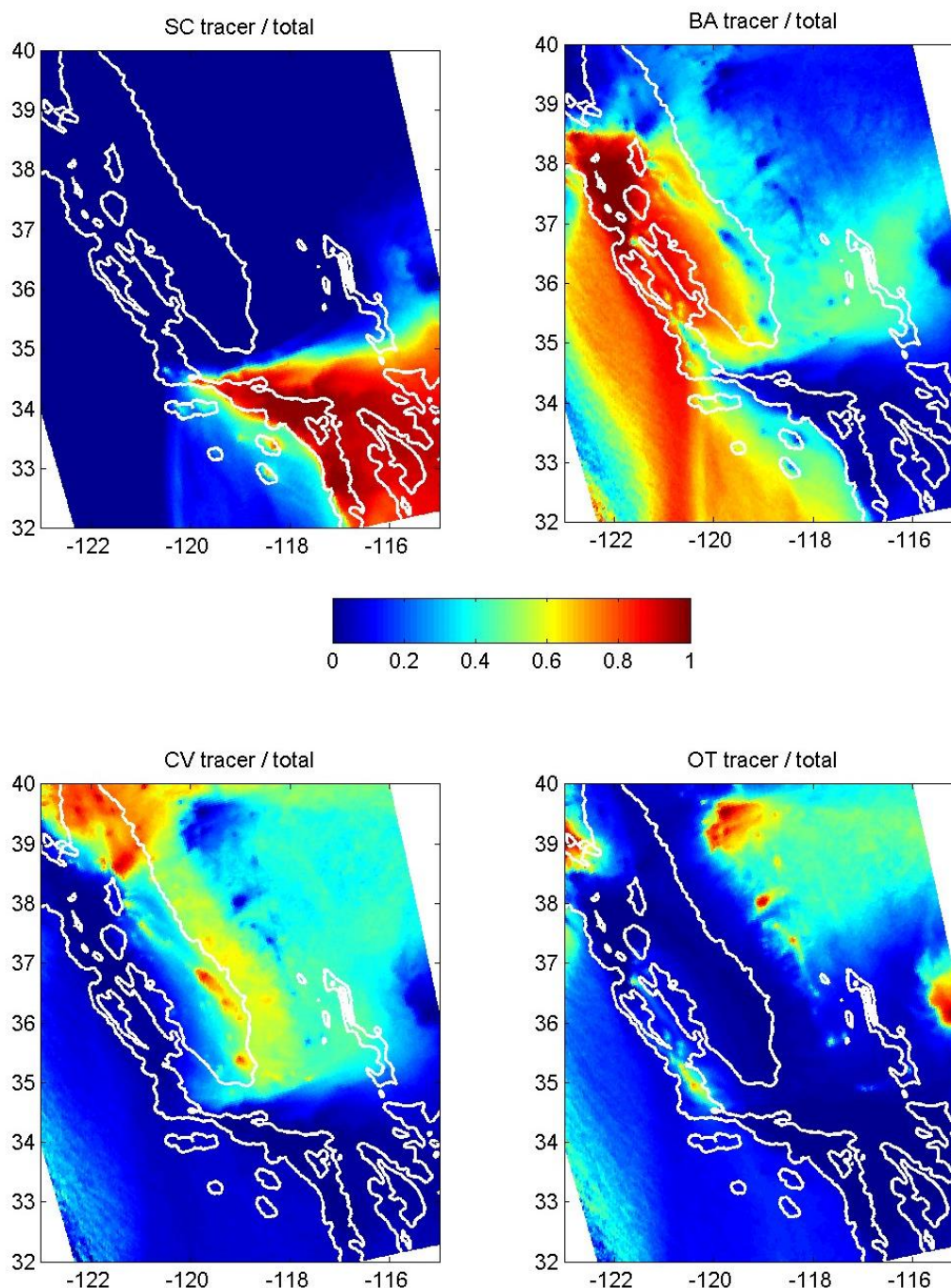
3501 **FINDINGS**

3502 ***Finding S1: Pollutants from the SoCAB can be recirculated within the Catalina Eddy in***
 3503 ***the boundary layer over the Southern California Bight. In the process, they can be***
 3504 ***combined with pollutants from the San Francisco Bay Area, which can be transported***
 3505 ***down the coast. Concentrations from San Francisco Bay Area sources coming onshore in***
 3506 ***the southern part of the Los Angeles metropolitan area and Orange County are generally***
 3507 ***small.***

3508 *Angevine et al.* [2013] applied a Lagrangian particle dispersion model to determine the amounts
 3509 of tracers that are transported within regions of the State, including southern California (see more
 3510 complete description in Response to Question R). They selected carbon monoxide (CO)
 3511 emissions from automobiles as a tracer to represent anthropogenic urban emissions and
 3512 separately tracked the CO tracer emitted from four regions of the State: Southern California, San
 3513 Francisco Bay Area, Central Valley and all other regions of the State. The simulations cover

3514 May and June 2010, the CalNex field measurement period, and are likely only applicable to
 3515 similar seasonal conditions. Tracer patterns in winter could be quite different.

3516 The regional to total ratio of the CO tracers (Fig. S1) shows the predominate source of the tracer
 3517 in a particular area, regardless of how much tracer is present. The Southern California tracer is



3518 **Figure S1:** Ratios of near-surface mixing ratios of CO regional tracers for 1-15 June 2010. Each
 3519 tracer is summed over all hours and divided by the sum over all tracers and all hours. The maps span
 3520 from the Sacramento Valley in the northwest to the California-Mexico border in the southeast; the
 3521 white lines show the 1 m and 500 m elevation contours. The tracers are identified according to their
 3522 emission region: southern California (SC), San Francisco Bay Area (BA), Central Valley (CV) and
 3523 other regions of the state (OT). [Figure from *Angevine et al.*, 2013].

3524 confined entirely to Southern California, with no detectable influence north of the mountains that
 3525 mark the northern edge of the Los Angeles basin, except very small ratios very far to the east. Its
 3526 influence is also present in the near-shore Southern California Bight. The most widely
 3527 distributed tracer is from the San Francisco Bay Area (SFBA). It dominates over the coastal
 3528 waters and the Coastal Ranges south of the SFBA, as well as the western part of the Southern
 3529 California Bight. It also dominates the San Joaquin Valley except for those areas with strong
 3530 emissions of the CV tracer. *Angevine et al.*, [2013] show that the tracer is aged over the water in
 3531 the Southern California Bight, with the oldest tracer material present near the coastline.
 3532 *Angevine et al.* [2012] attribute this effect to the “Catalina” eddy, which circulates aged
 3533 Southern California emissions (seen in their study as fresh tracer in Santa Monica Bay at 0400
 3534 LST) around and combines them with aged SFBA emissions brought down the coast. This air is
 3535 returned ashore to the Los Angeles basin, but the concentrations are small as evidenced by the
 3536 diminishing influence of the SFBA tracer inland from the coast. *Angevine et al.* [2013] caution
 3537 that their findings are subject to errors in the meteorological model and in the emissions
 3538 inventory.

3539 ***Finding S2: The direction that emissions originating from Los Angeles exit from the basin***
 3540 ***varies with time of day. From late morning to early evening most emissions exit to the east,***
 3541 ***while during the rest of the day significant flux exits to the west and south in shallow layers***
 3542 ***over the ocean. Both the sea-land breeze circulation and the Catalina Eddy flow over the***
 3543 ***Southern California Bight force emissions that had exited the LA basin to the west and***
 3544 ***south back into the source region. For NO_y, total inflow from upwind sources and this***
 3545 ***return flux equals 40% of that emitted within the basin when averaged over May of 2010.***

3546 *Analysis: S.A. McKeen, unpublished*

3547 An Eulerian, regional-scale air quality model, WRF/Chem [*Ahmadov et al.*, 2012], has been
 3548 applied to the May-July 2010 time period over the western U.S. (12 km x 12 km resolution), and
 3549 over the southern two-thirds of California at 4 km x 4 km resolution in support of field
 3550 measurement analysis and emission validation studies. *Angevine et al.* [2012] have shown that
 3551 the WRF model adequately characterized meteorology in the Los Angeles region during the
 3552 study period, thus allowing model results to be used for identifying transport and conversion
 3553 pathways for several key gas-phase and aerosol-phase pollution constituents. Here, a 4-week
 3554 period of emission fluxes (NO_y is taken as the tracer) during May is used to demonstrate the
 3555 mean diurnal pattern of in-flow and recirculation of O₃ precursors through an imaginary cylinder
 3556 (Fig. S2) placed over Los Angeles.

3557 A 4-week average of NO_y fluxes was derived from the 12 km x 12 km resolution model
 3558 simulations described in *Brioude et al.* [2013]. This simulation included marine vessel emissions
 3559 from within the Long Beach and Los Angeles harbors, but not over the ocean. Figure S2 shows
 3560 the location of the cylindrical surface (36 km radius) through which the vertical and angular
 3561 distribution of NO_y flux was calculated. Figure S3 illustrates that flux for three specific hours of
 3562 the day.

3563 Figure S3a shows the transport before sunrise (5:00 am LDT). The land breeze carries NO_y
 3564 away from Los Angeles in a 200-meter layer heading west (over LAX) and a smaller flux into
 3565 the area from the southeast (Anaheim direction). Downslope flow from the San Gabriel
 3566 Mountains also brings a dilute NO_y flux into the cylinder. At noon (7 hours later, Fig. S3b), the
 3567 sea breeze and mountain upslope flow have reversed the transport, with a return flux from the
 3568 west over LAX and from over Long Beach. This oceanic inflow comes at a critical time for O₃

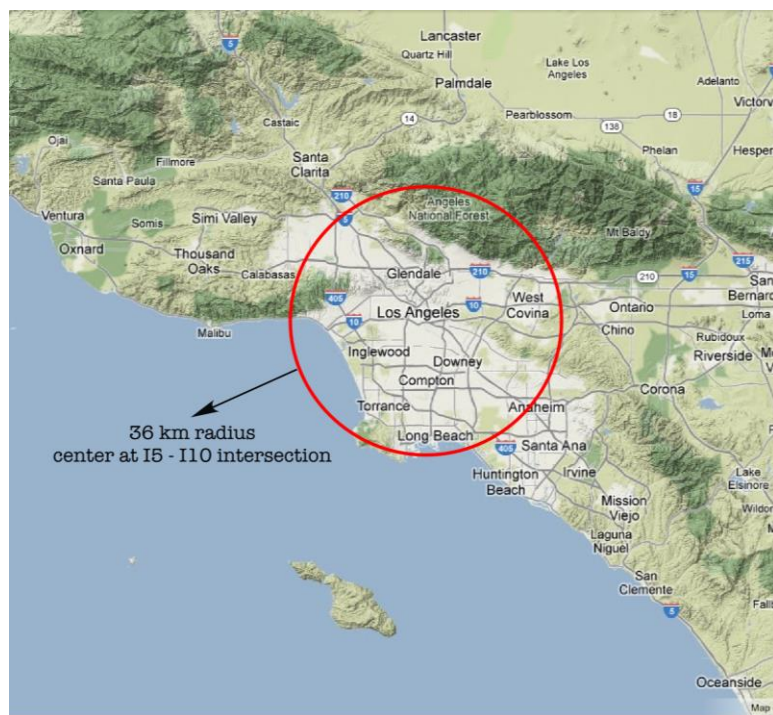


Figure S2. Base of imaginary cylinder (red circle) placed over Los Angeles for the purpose of calculating fluxes of pollutant emissions through the wall of the cylinder.

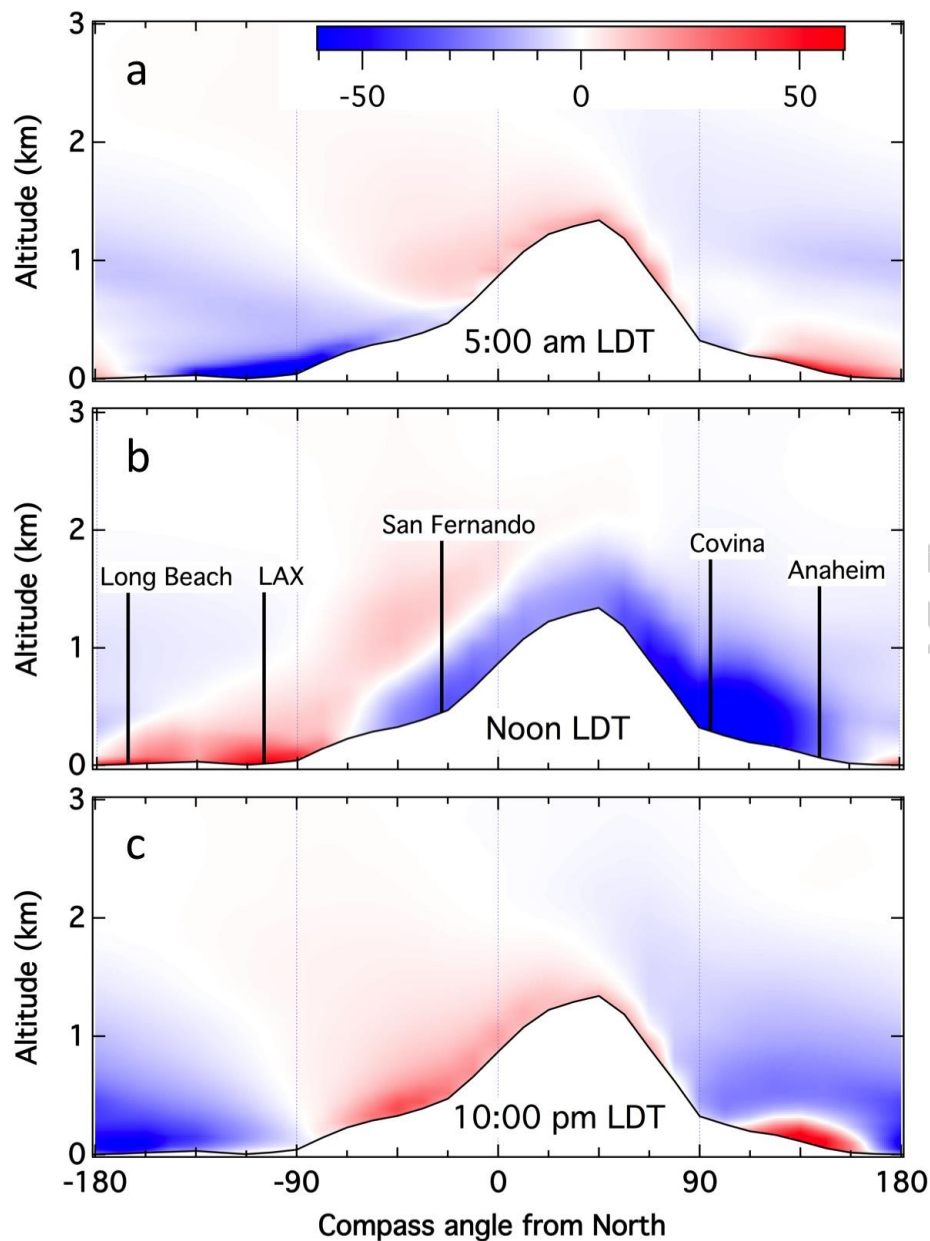
pollution over the LA basin, between sunrise and early afternoon when photolysis of NO_Y species can occur and contribute to O_3 formation. This onshore inflow is accompanied by large fluxes out of the basin both to the north over the San Gabriel Mountains and to the east-southeast through Covina and Anaheim. At 10:00 pm LDT, Figure S3c shows a southward NO_Y flux extending through a deep layer. Imbedded within this broad

southerly outward flow is a sharp gradient in NO_Y flux with a low-level, 200-meter layer of inflow. At the surface, the strong southward outflow is just over and west of Long Beach, while just east of Long Beach, the inflow flux is strongly to the northwest along the southwestern flanks of the Santa Ana Mountains and Chino Hills. This inflow to the LA basin, attributable to the Catalina Eddy circulation, continues until sunrise (Fig. S3a), combining the recirculated NO_Y with fresh Orange County emissions.

A vertically integrated (0-1.2km) budget analysis of emissions and outbound and inbound fluxes of NO_Y within the cylinder defined in Fig. S2 concluded that inbound NO_Y fluxes are 40% of the NO_Y emitted within the cylinder, and a majority of this inbound flux is attributed to recirculated pollution.

References

- Ahmadov, R., et al. (2012), A volatility basis set model for summertime secondary organic aerosols over the eastern United States in 2006, *J. Geophys. Res.*, 117, D06301, doi:10.1029/2011JD016831.
- Angevine, W. M., L. Eddington, K. Durkee, C. Fairall, L. Bianco, and J. Brioude (2012), Meteorological model evaluation for CalNex 2010, *Monthly Weather Review*, doi:10.1175/MWR-D-12-00042.1
- Angevine, W. M., et al. (2013), Pollutant transport among California regions, *J. Geophys. Res. Atmos.*, 118, 6750–6763, doi:10.1002/jgrd.50490.
- Brioude, J., et al. (2013), Top-down estimate of surface flux in the Los Angeles Basin using a mesoscale inverse modeling technique: Assessing anthropogenic emissions of CO , NO_x and CO_2 and their impacts, *Atmospheric Chemistry and Physics*, 13, 3661–3677, doi:10.5194/acp-13-3661-2013.



3605
 3606 **Figure S3.** 28-day (4-31 May 2010) average NO_y fluxes normal to the cylinder walls defined in
 3607 Figure S2 at three hours during the day. Red (positive) signifies a flux into the cylinder, and blue
 3608 signifies out of the cylinder. Fluxes are in units of $\text{mol/hr}/\Delta\text{angle}/\text{meter}$ (vertical), where $\Delta\text{angle} =$
 3609 11.25° . The flux magnitude is indicated in the color bar in a). For orientation, the directions of 5
 3610 landmarks are indicated in b). In each panel, the black line with white below indicates the
 3611 intersection of the cylinder wall with ground level.

3612

3613
3614

Synthesis of Results - Atmospheric Transport Response to Question T

3615 **QUESTION T**

3616 **Is there evidence of long-range transport during CalNex? What were the relative**
3617 **contributions of the various sources outside the control of emissions within California (i.e.,**
3618 **policy-relevant background ozone)?**

3619 **BACKGROUND**

3620 The Response to Question D discusses "background" (better termed "baseline") concentrations
3621 observed during CalNex. Transport of these baseline concentrations into California provides the
3622 largest contributions to degraded air quality within the state that are outside the control of
3623 California. As discussed in that Response, important species are limited to O₃, PM, CO and
3624 peroxyacetyl nitrate (PAN). Transport of CO and PAN contribute O₃ precursors of importance
3625 in California, but the CalNex analyses thus far have not addressed these species beyond the
3626 discussion in the Response to Question D; their importance will not be discussed further here.
3627 PM is a pollutant whose long-range transport is primarily limited to extraordinary episodic
3628 events; causes of these events include large wildfires, extensive agricultural burning and dust
3629 storms. Each such event must be considered separately, and no such event was observed during
3630 CalNex. Hence, the response to this question is limited to the long-range transport of O₃. Within
3631 California's atmospheric boundary layer, local O₃ formation and destruction are rapid. These
3632 rapid processes combined with the strong non-linear dependence of O₃ formation on precursor
3633 concentrations make it difficult to accurately quantify the influence of long-range transport.

3634 **POLICY RELEVANCE**

3635 Transport of ozone into California from upwind regions is beyond the control of California
3636 policies. The fractional contribution from this transport to the state's ozone concentrations is
3637 growing as baseline ozone concentrations rise and local precursor emissions decrease.
3638 Particularly intense episodes of stratospheric O₃ may constitute "exceptional events" that can be
3639 excluded from regulatory consideration.

3640 Quantification of source contributions to observed surface O₃ concentrations is a complicated
3641 bookkeeping issue that has significant subtleties. A useful concept is "policy-relevant
3642 background" or PRB O₃ concentration [*McDonald-Buller et al., 2011*], which is defined as the
3643 concentrations that would exist in the United States in the absence of anthropogenic emissions in
3644 continental North America (i.e., the U.S., Canada, and Mexico). PRB O₃ is purely a model
3645 concept; it cannot be directly observed anywhere at anytime. Models are imperfect, but even if
3646 PRB O₃ could be accurately calculated, the difference between observed O₃ concentrations and
3647 the PRB O₃ cannot simply be attributed to anthropogenic O₃ formation, due to the non-linear
3648 character of tropospheric photochemistry. For example, local anthropogenic emissions of NO_x
3649 tend to increase the ambient concentrations of hydroxyl radicals, which leads to faster
3650 photochemical destruction of O₃, thereby reducing the PRB contribution. Higher PRB O₃
3651 concentrations also increase radical concentrations, which leads to faster production of O₃ from
3652 anthropogenic precursors. The following discussion presents results of various analyses aimed
3653 to quantify the influence of long-range transport of O₃. No consistent bookkeeping system has
3654 been employed so subtleties remain in their interpretation. Since California is on the west coast

3655 of North America and the prevailing winds are onshore, the focus of this work excludes transport
 3656 from other regions of North America. These analyses focus on the 2010 late spring, early
 3657 summer period of CalNex. This season is near the maximum of long-range transport for both
 3658 Asian pollution and stratospheric intrusions, and 2010 was a particularly active year for both.
 3659 Consequently, the results may be biased high to some extent.

3660 Intense episodes of stratospheric O₃ transport are of particular policy relevance. The current
 3661 guidelines from the U.S. Environmental Protection Agency (EPA) state that air quality
 3662 monitoring data influenced by an extreme stratospheric O₃ intrusion may be excluded from
 3663 regulatory determinations related to violations of the U.S. National Ambient Air Quality
 3664 Standard (NAAQS) for ground-level O₃, since these naturally occurring “exceptional events” are
 3665 not controllable by state agencies [U.S. EPA, 2007].

3666 FINDINGS

3667 ***Finding T1: Transport of baseline O₃ can enhance surface O₃ concentrations to such an***
 3668 ***extent that the margin for local and regional O₃ production before exceeding the NAAQS is***
 3669 ***greatly reduced or potentially eliminated, even in California's urban areas.***

3670 *Langford et al.* [2012] used
 3671 principal component analysis
 3672 and FLEXPART particle
 3673 trajectory analysis to quantify
 3674 the episodic contribution of
 3675 transport of stratospheric O₃ to
 3676 the surface of the greater Los
 3677 Angeles area during the CalNex
 3678 period (Fig. T1). The May 29–
 3679 30 episode (Fig. T1; also

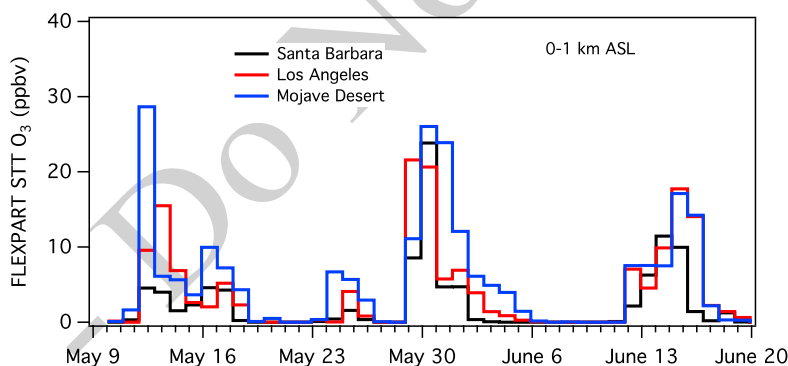


Figure T1. Time series of the contribution of stratospheric O₃ to surface concentrations at three sites in the greater Los Angeles area as calculated by the FLEXPART particle dispersion model. (Figure based on *Langford et al.*, 2012).

3680 illustrated in Fig. O1) led to a peak
 3681 1-hour O₃ concentration of 88 ppbv
 3682 at Joshua Tree National Park, and
 3683 widespread entrainment of upper
 3684 tropospheric air into the CBL
 3685 increased local background O₃
 3686 concentrations over the entire greater Los Angeles area to ~55 ppbv. This background was 10–
 3687 15 ppbv higher than the O₃ concentrations in marine air transported ashore from the Pacific
 3688 Ocean. When combined with locally produced O₃, several exceedances of the current NAAQS
 3689 occurred on the following day.

3690 *Lin et al.* [2012a,b] compare model results with surface measurements in order to quantify the
 3691 impact of transported baseline O₃ on surface concentrations over the western U.S. They utilize a
 3692 new global high-resolution chemistry-climate model (GFDL AM3) with full stratosphere-
 3693 troposphere chemistry nudged to reanalysis winds, which is expected to give much more
 3694 accurate results than earlier models. They find that AM3 successfully reproduces observed sharp
 3695 ozone gradients above California, including the interleaving and mixing of Asian pollution and
 3696 stratospheric air associated with complex interactions of mid-latitude cyclone air streams.
 3697 Particular emphasis is placed on quantifying transport of stratospheric O₃ [*Lin et al.*, 2012a] and
 3698 Asian O₃ pollution [*Lin et al.*, 2012b] into California. Figure T2 shows results for the population
 3699 centers of Southern California and Las Vegas from April to June 2010. In these areas transport

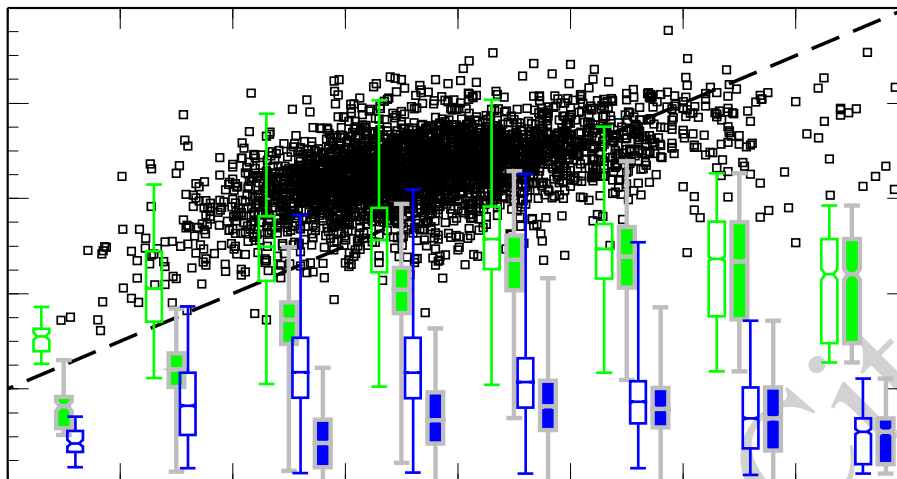


Figure T2. Model versus observed MDA8 surface O₃ for April–June 2010 at polluted sites in the densely populated regions of the Central Valley, Southern California, and Las Vegas, Nevada. The box-and-whisker plots (minimum, 25th, 50th, 75th percentiles, and maximum) concentrations give statistics of the PRB O₃ (green) and the stratospheric contribution (blue) for every 10-ppbv bin of observed O₃. Points greater than 80 ppbv are merged in the 70–80 ppbv range. The filled boxes are bias-corrected. The dashed line indicates the 1:1 relationship. (Figure based on *Lin et al*, 2012a).

3700 of baseline O₃ to the surface can mix with high levels of locally produced O₃ pollution. The
 3701 model calculates that stratospheric intrusions (solid blue symbols in Fig. T2) can episodically
 3702 increase surface maximum daily 8-hour average (MDA8) O₃ concentrations by 20 to 40 ppbv,
 3703 including on days when observed O₃ concentrations exceed the NAAQS threshold. In these
 3704 areas, PRB O₃ (solid green symbols in Fig. T2) and its stratospheric component peak when
 3705 observed O₃ is in the 60–80 ppbv range, and both tend to decline by 2–5 ppbv when observed O₃
 3706 increases to higher values. The PRB O₃ elevated by stratospheric intrusions reached maxima as
 3707 high as 60–75 ppbv.

3708 At high-elevation western U.S. sites, the model successfully reproduces the observed O₃ values
 3709 in excess of 60 ppbv, and estimates a total PRB contribution of 83% and a North American
 3710 anthropogenic contribution of 17%. The 25th–75th percentile of the stratospheric contribution is
 3711 15–25 ppbv when observed MDA8 ozone is 60–70 ppbv, and increases to ~17–40 ppbv for the
 3712 70–85 ppbv range. These estimates, which are up to 2–3 times greater than previously reported,
 3713 indicate a major role for stratospheric intrusions in contributing to springtime high-O₃ events
 3714 over the high-altitude western U.S. The stratospheric contribution and Asian pollution account
 3715 for 39% and 8% of the total, respectively. The dominant contribution from stratospheric O₃, and
 3716 larger impacts with increasing O₃, indicates an important role for stratospheric intrusions in
 3717 driving springtime surface high-O₃ events at western U.S. high-elevation sites.

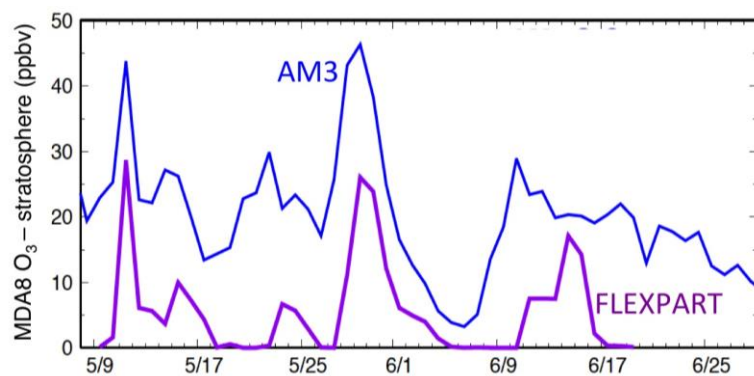


Figure T3. Time series of the contribution of stratospheric O₃ to MDA8 surface O₃ concentrations over the Mojave Desert calculated by the AM3 and FLEXPART models. (Figure based on *Lin et al.*, 2012a).

3718 Figure T3 compares the stratospheric impacts on surface O₃ over the Mojave Desert as calculated
 3719 by the AM3 [*Lin et al.*, 2012a] and FLEXPART models [*Langford et al.*, 2012 and Fig. T1]. The
 3720 significantly larger impact from the AM3 calculation is more realistic, because it reflects the
 3721 influence of the stratospheric impact on O₃ from all stratospheric intrusions in the northern
 3722 hemisphere over the past months. In contrast, FLEXPART, as implemented for CalNex, directly
 3723 treated transport of stratospheric O₃ from intrusions that occurred over only the North Pacific
 3724 Ocean during the previous ten days. Hence, the O₃ contributions illustrated in Fig. T1 represent
 3725 lower limits for the total stratospheric impact.

3726 ***Finding T2: Transport of baseline ozone accounts for a majority of surface ozone***
 3727 ***concentrations in California at urban as well as rural locations, both on average and***
 3728 ***during many exceedance events. Only in the most intense exceedance events does local and***
 3729 ***regional photochemical production contribute a majority.***

3730 To quantify ozone production within California, *Cooper et al.* [2011] compared inland ozone
 3731 concentrations to baseline concentrations. Median values of lower tropospheric baseline O₃ are
 3732 equal to more than 80% of the median O₃ measured within the daytime mixed layer above
 3733 California's Central Valley. Similar comparisons across the polluted regions of southern
 3734 California show that baseline O₃ is equal to 63–76% of the measured O₃ above Joshua Tree
 3735 National Park and the LA basin.

3736 The model calculations of *Lin et al.* [2012a,b] agree well with this observation-based estimate of
 3737 *Cooper et al.* [2011]. Fig. T2 shows that the median contribution of PRB O₃ (middle of solid
 3738 green symbols) averages more than 50% of the observed MDA8 surface O₃ throughout the
 3739 observed range, dropping to near 50% only at surface O₃ concentrations of 90 ppbv or greater.
 3740 The observation-based analysis of *Parrish et al.* [2010] suggests that free tropospheric baseline
 3741 O₃ transported to the surface of the northern Central Valley explains most of this region's O₃
 3742 variability, a conclusion generally consistent with the transport analysis presented by *Cooper et*
 3743 *al.* [2011].

3744 ***Finding T3: In addition to being a receptor of long-range pollutant transport, California is***
 3745 ***also a source of transport to downwind areas.***

3746 Airborne lidar measurements of ozone above the Los Angeles Basin on 17 July 2009 during a
 3747 "pre-CalNex" deployment of the NOAA Twin Otter aircraft show orographic lifting of ozone
 3748 from the surface to the free troposphere by the San Gabriel Mountains. Mixing ratios in excess
 3749 of 100 ppbv were measured ~4 km above mean sea level. These observations are in excellent
 3750 agreement with published model studies, confirming that boundary layer venting by the so called
 3751 "mountain chimney effect" is a potentially important pathway for removal of pollutants from the
 3752 Los Angeles basin. The lofting of ozone and other pollutants into the free troposphere greatly

3753 increases the potential for long-range transport from the basin, and trajectory calculations
3754 suggest that some of this ozone was transported ~1000 km to eastern Utah and western Colorado
3755 [Langford *et al.*, 2010].

3756 **References**

3757 Cooper, O. R., et al. (2011), Measurement of western U.S. baseline ozone from the surface to the
3758 tropopause and assessment of downwind impact regions, *J. Geophys. Res.*, 116, D00V03,
3759 doi:10.1029/2011JD016095.

3760 Langford, A. O., C. J. Senff, R. J. I. Alvarez, R. M. Banta, and R. M. Hardesty (2010),
3761 Long- range transport of ozone from the Los Angeles Basin: a case study, *Geophys. Res.*
3762 *Lett.*, 37(L06807), doi:10.1029/2010GL042507.

3763 Langford, A. O., J. Brioude, O. R. Cooper, C. J. Senff, R. J. Alvarez II, R. M. Hardesty, B. J.
3764 Johnson, and S. J. Oltmans (2012), Stratospheric influence on surface ozone in the Los
3765 Angeles area during late spring and early summer of 2010, , *J. Geophys. Res.*, 117(D00V06),
3766 doi:10.1029/2011JD016766.

3767 Lin, M., A. M. Fiore, O. R. Cooper, L. W. Horowitz, A. O. Langford, H. Levy II, B. J. Johnson,
3768 B. Naik, S. J. Oltmans, and C. J. Senff (2012a), Springtime high surface ozone events over
3769 the western United States: Quantifying the role of stratospheric intrusions, , *J. Geophys. Res.*,
3770 117(D00V22), doi:10.1029/2012JD018151.

3771 Lin, M., et al. (2012b), Transport of Asian ozone pollution into surface air over the western
3772 United States in spring, , *J. Geophys. Res.*, 117(D00V07), doi:10.1029/2011JD016961.

3773 McDonald-Buller, E.C., D.T. Allen, N. Brown, D.J. Jacob, D. Jaffe, C.E. Kolb, A.S. Lefohn, S.
3774 Oltmans, D.D. Parrish, G. Yarwood and L. Zhang (2011), Establishing Policy Relevant
3775 Background (PRB) Ozone Concentrations in the United States, *Environ. Sci. Technol.*,
3776 45(22), 9484-9497, doi:10.1021/es2022818.

3777 Parrish, D. D., K. C. Aikin, S. J. Oltmans, B. J. Johnson, M. Ives, and C. Sweeny (2010), Impact
3778 of transported background ozone inflow on summertime air quality in a California ozone
3779 exceedance area, *Atmos. Chem. Phys.*, 10, 10,093–10,109, doi:10.5194/acp-10-10093-2010.

3780 U.S. EPA (2007), Treatment of data influenced by exceptional events, *Fed. Regist.*, 72(55),
3781 13,560–13,581.

3782

3783

3784 **Synthesis of Results - Modeling**3785 **Response to Question U**3786 **QUESTION U**

3787 **How well did the meteorological and air quality forecast models perform during CalNex?**
 3788 **What weaknesses need attention?**

3789 **BACKGROUND**

3790 *Angevine et al.* [2012] provide meteorological fields for interpretation of chemical and aerosol
 3791 measurements taken during the CalNex field campaign. The simulations have been used to
 3792 support inverse modeling to improve estimates of emissions in the Los Angeles area and the
 3793 Central Valley [*Brioude et al.*, 2013; *Kim et al.*, 2013], to understand transport and chemical
 3794 evolution in the Los Angeles area and beyond [e.g., *Cooper et al.*, 2011; *Angevine et al.*, 2013]
 3795 and to explore the characteristics and impact of marine stratocumulus clouds. For those
 3796 purposes, *Angevine et al.* [2012] focus on boundary layer structure, clouds, and winds in the
 3797 coastal zone of Southern California, the Los Angeles basin, and the San Joaquin Valley.

3798 During the CalNex intensive period, results from seven real-time air quality forecast models
 3799 were provided to NOAA/ESRL/CSD by four institutions: Environment Canada, NOAA/NCEP,
 3800 NOAA/ESRL/GSD, and Baron Advanced Meteorological Services (BAMS). An additional real-
 3801 time ensemble forecast based on four of the forecast models was also available to study
 3802 participants. A graphical archive of the 24 and 48-hour forecasts from May 1 through July 18,
 3803 2010 is available at: <http://www.esrl.noaa.gov/csd/groups/csd4/modelevel>.

3804

3805 **POLICY RELEVANCE**

3806 In air quality applications, meteorological fields from mesoscale models are used to drive
 3807 Lagrangian or Eulerian transport and chemistry models. We need to understand the accuracy
 3808 and uncertainty of the meteorological fields in order to know what confidence to place in the air
 3809 quality modeling results. In a real sense, the transport and chemistry models are a synthesis of
 3810 our understanding of the atmosphere, and provide our only means of evaluating emission control
 3811 scenarios.

3812

3813 **FINDINGS**

3814 ***Finding U1:* Evaluation of different meteorological models against CalNex measurements**
 3815 **shows that details of model configuration (physics, initialization, resolution) can impact**
 3816 **performance for specific processes and regions. Particular attention needs to be paid to**
 3817 **land surface and soil parameters and to clouds offshore. Significant but poorly**
 3818 **characterized biases (for example, high wind speeds and weak land breeze) remain in the**
 3819 **best available simulations.**

3820 *Angevine et al.* [2012] evaluate the performance of mesoscale meteorological models for the
 3821 coastal zone and Los Angeles area of Southern California, and for the San Joaquin Valley.
 3822 Several configurations of the Weather Research and Forecasting Model (WRF) with differing

3823 grid spacing, initialization, planetary boundary layer (PBL) physics, and land surface models are
 3824 compared. One configuration of the Coupled Ocean–Atmosphere Mesoscale Prediction System
 3825 (COAMPS) model is also included, providing results from an independent development and
 3826 process flow. Specific phenomena of interest for air quality studies are examined. All model
 3827 configurations are biased toward higher wind speeds than observed. The diurnal cycle of wind
 3828 direction and speed (land–sea-breeze cycle) as modeled and observed by a wind profiler at Los
 3829 Angeles International Airport is examined. Each of the models shows different biases in
 3830 reproducing the cycle. Soundings from San Nicolas Island, a case study involving the Research
 3831 Vessel (R/V) Atlantis and the NOAA P3 aircraft, and satellite images are used to evaluate
 3832 simulation performance for cloudy boundary layers. In a case study, the boundary layer structure
 3833 over the water is poorly simulated by all of the WRF configurations except one with the total
 3834 energy–mass flux boundary layer scheme and ECMWF reanalysis. The original WRF
 3835 configuration had a substantial bias toward low PBL heights in the San Joaquin Valley, which is
 3836 improved in the final configuration. WRF runs with 12-km grids have larger errors in wind
 3837 speed and direction than those present in the 4-km grid runs.

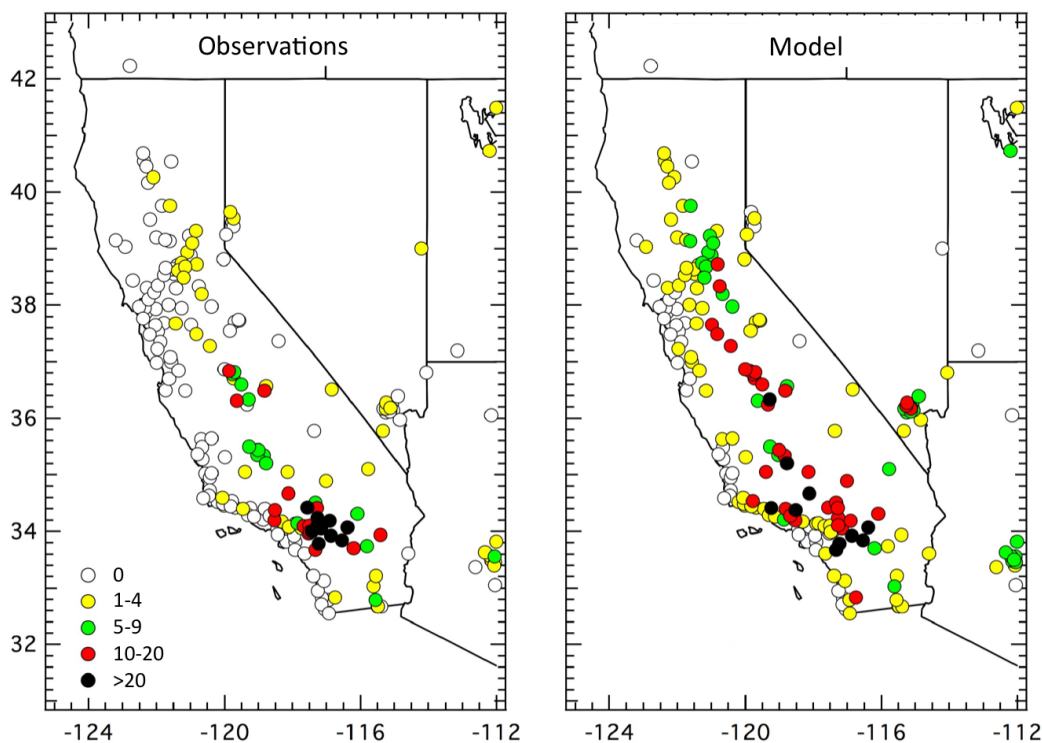
3838 ***Finding U2a: Evaluation of several different real-time air quality forecasts against O₃ and***
 3839 ***PM_{2.5} observations show that none of the models perform statistically better than the***
 3840 ***persistence forecast (i.e., predicting that tomorrow’s air quality will be exactly the same as***
 3841 ***today’s air quality). All models show temporal correlations for maximum 8-hr O₃ that beat***
 3842 ***persistence, but model biases and poor spatial correlations limit over-all forecast skill.***

3843 ***Finding U2b: Incorporation of the RAQMS global forecast [Pierce et al., 2003] to modify***
 3844 ***lateral boundary conditions improved temporal skill for O₃ forecasts but increased model***
 3845 ***bias.***

3846 *Analysis: S.A. McKeen, unpublished*

3847 The focus of this evaluation is a comparison of predicted maximum 8-hr average O₃, and 24-hr
 3848 average PM_{2.5} with those observed. For example, Figure U1 shows AIRNow O₃ monitor
 3849 locations, and compares observations with the NOAA/NCEP forecast (without incorporation of
 3850 boundary conditions from the RAQMS global forecast) for the number of occurrences when
 3851 maximum 8-hr average O₃ is greater than 75 ppbv. The forecast model tends to over-predict the
 3852 number of occurrences throughout the sample area, except for the under-predictions east of the
 3853 LA basin. Analysis attributes the overall O₃ over-prediction to NO_x emissions being too high,
 3854 and the behavior east of the LA basin to titration effects from the resulting high NO_x in that
 3855 region.

3856 The performance of each of the seven forecast models was evaluated through several statistical
 3857 comparisons of the model output with observations. For example, the overall r-correlation and
 3858 median bias between the model predictions and the measurements are evaluation measures that
 3859 cover both space and time. The benchmark selected for evaluating model performance is the
 3860 same statistical comparison of the persistence forecast with observations, whereby tomorrow's
 3861 forecast is simply taken to be today’s observations. It is found that none of the models for
 3862 forecasting O₃ can outperform persistence forecasting in terms of correlation, and that all but one
 3863 model are biased high.



3864 **Figure U1.** Number of days with maximum 8-hr average O₃ concentration ≥ 75 ppbv from 19
 3865 May to 15 July 2010. Observations are shown on the left and results from a model forecast are
 3866 shown on the right.

3867 All models do have more than 50% of their points with better temporal correlation than
 3868 persistence. The inclusion of the RAQMS global forecast to provide lateral boundary conditions
 3869 for the NCEP model significantly improves the O₃ r-correlation, but also significantly increases
 3870 the positive bias of the model. The RAQMS forecast includes real-time assimilation of upper-
 3871 tropospheric satellite O₃ data, which has the largest impact on high elevation stations and the
 3872 eastern part of California.

3873 For PM_{2.5}, like O₃, none of the models can outperform the persistence forecast in terms of
 3874 correlation or root mean square error. With a median observed average PM_{2.5} concentration of
 3875 10 $\mu\text{g}/\text{m}^3$, all but two models display low absolute bias. Unlike the O₃ forecasting, inclusion of
 3876 the RAQMS global forecast for PM_{2.5} has a negative impact in terms of the correlation
 3877 measures. Retrospective runs tested the impact of assimilating the global GOCART aerosol
 3878 transport model into one of the WRF/Chem models; this approach improved forecast predictions
 3879 over the base model, but r-correlation skill still remained less than that for the persistence
 3880 forecast.

3881 It should be noted that the use of persistence as a statistical reference puts the forecast models at
 3882 a distinct disadvantage when applied to California in the summertime. Correlations of the
 3883 persistence forecast are noticeably higher for California, when compared to the rest of the U.S.
 3884 for the same time period, particularly for O₃. Thus, individual model performance for California
 3885 should not be extrapolated to other parts of the U.S. and Canada.

3886

3887 **References**

- 3888 Angevine, W. M., L. Eddington, K. Durkee, C. Fairall, L. Bianco, and J. Brioude (2012),
3889 Meteorological model evaluation for CalNex 2010, *Monthly Weather Review*,
3890 doi:10.1175/MWR-D-12-00042.1
- 3891 Angevine, W. M., et al. (2013), Pollutant transport among California regions, *J. Geophys. Res.*
3892 *Atmos.*, *118*, 6750–6763, doi:10.1002/jgrd.50490.
- 3893 Brioude, J., et al. (2013), Top-down estimate of surface flux in the Los Angeles Basin using a
3894 mesoscale inverse modeling technique: Assessing anthropogenic emissions of CO, NO_x and
3895 CO₂ and their impacts, *Atmos. Chem. Phys.*, *13*, 3661–3677, doi:10.5194/acp-13-3661-2013.
- 3896 Cooper, O. R., et al. (2011), Measurement of western U.S. baseline ozone from the surface to the
3897 tropopause and assessment of downwind impact regions, *J. Geophys. Res.*, *116*(D00V03),
3898 doi:10.1029/2011JD016095.
- 3899 Kim, S.W., et al. (2013), Evaluation of NO_x emission inventories in California using multi-
3900 satellite data sets, in-situ airborne measurements, and regional model simulations during
3901 CalNex 2010, *J. Geophys. Res.*, in preparation.
- 3902 McKeen, S.A., G. Grell, S. Peckham, E.-Y. Hsie, W. Gong, S. Ménard, H. Landry, J. McQueen,
3903 Y. Tang, J. McHenry, D. Olerud, 2010-12-14: Evaluation of Real-time Air Quality Model
3904 Forecasts and Their Emissions During the CalNex-2010 Field Campaign. *American*
3905 *Geophysical Union, Fall Meeting*, San Francisco, CA, USA.
- 3906 Pierce, R. B., *et al.*, 2003, Regional Air Quality Modeling System (RAQMS) predictions of the
3907 tropospheric ozone budget over east Asia, *J. Geophys. Res.*, *108*, 8825,
3908 doi:10.1029/2002JD003176, D21.
3909
3910

3911 **Synthesis of Results - Climate and Air Quality Nexus**3912 **Response to Question V**3913 **QUESTION V**3914 **What pollution control efforts are likely to result in “win-win” or “win-lose” situations?**3915 **BACKGROUND**

3916 The California Research at the Nexus of Air Quality and Climate Change (CalNex) 2010 field
 3917 project was undertaken to provide improved scientific knowledge for emissions control strategies
 3918 to simultaneously address the two interrelated issues of air quality and climate change. Air
 3919 quality and climate change issues are linked because in many cases, the agents of concern are the
 3920 same and the sources of the agents are the same or intimately connected. Examples include
 3921 tropospheric ozone, which is both an air pollutant and a greenhouse gas, and atmospheric
 3922 particulate matter, which has effects on the radiative budget of the atmosphere as well as human
 3923 and ecosystem health, visibility degradation, and acidic deposition. Efforts to address one of
 3924 these issues can be beneficial to the other ("win-win" situations), but in some cases, policies
 3925 addressing one issue without additional consideration can have unintended detrimental impacts
 3926 on the other ("win-lose" situations). The goal of CalNex 2010 is to improve and advance the
 3927 science needed to support continued and effective air quality and climate management policy for
 3928 the State of California and the Nation as a whole.

3929 **POLICY RELEVANCE**

3930 Policies to address climate change and air quality degradation are more effective when both
 3931 issues are considered together so that policies positively impact both issues ("win-win"
 3932 situations) rather than improving one, but worsening the other ("win-lose" situations).

3933 One clear example of a “win-win” control strategy is reduction in emissions of light-absorbing or
 3934 black carbon (BC) aerosol. This material is emitted with widely varying emission factors from a
 3935 variety of combustion processes, including heavy-duty diesel engines and biomass burning. It is
 3936 a component of PM that is suspected to be particularly important in the negative health effects
 3937 associated with aerosols [*Jansen et al.*, 2005], and thus constitutes an important air quality issue.
 3938 It also acts as a warming agent in the atmosphere [*Bond et al.*, 2013] due to its light-absorbing
 3939 properties, and thus constitutes an equally important climate change issue. Light absorbing
 3940 aerosols like black carbon also generally act to reduce cloudiness [*Ackerman et al.*, 2000; *Koren*
 3941 *et al.*, 2005], further warming the atmosphere. Thus, reducing BC emissions will create a “win-
 3942 win” situation for both climate change and air quality in California.

3943 It is also worth emphasizing here that any pollutant control effort that increases efficiency of
 3944 energy use (e.g., increased fuel mileage of on-road vehicles, or increased use of mass transport to
 3945 replace personal vehicle usage) is a "win-win" change for air quality and climate change. Less
 3946 fuel burned implies both smaller air pollutant emissions and less CO₂ released to the atmosphere.

3947

3948 **FINDINGS**

3949 The data set collected during the CalNex fieldwork provides a wide range of measurements that
 3950 allow air quality and climate change policies to be developed with a full appreciation of the ways
 3951 in which the policies will impact both issues. Until now, relatively few studies have considered
 3952 both issues together. However, the following are two specific examples.

3953 ***Finding V1: Cessation of burning crop residue from rice agriculture (a "win" for air***
 3954 ***quality) increased methane emissions (a "lose" for climate).***

3955 Peischl et al. [2012] analyzed airborne measurements of methane (CH₄) and carbon dioxide
 3956 (CO₂) taken over the rice growing region of California's Sacramento Valley in the late spring of
 3957 2010 and 2011. From these and ancillary measurements, they show that CH₄ mixing ratios were
 3958 enhanced in the planetary boundary layer above the Sacramento Valley during the rice growing
 3959 season than they were before it, which they attribute to emissions from rice paddies. They derive
 3960 daytime emission fluxes of CH₄ between 0.6 and 2.0% of the CO₂ taken up by photosynthesis on
 3961 a per carbon, or mole-to-mole, basis. They also use a mixing model to determine an average
 3962 CH₄/CO₂ flux ratio of ~0.6% for one day early in the growing season of 2010. They conclude
 3963 the CH₄/CO₂ flux ratio estimates from a single rice field in a previous study [McMillan et al.,
 3964 2007] are representative of rice fields in the Sacramento Valley. If generally true, the CARB
 3965 greenhouse gas inventory emission rate [Franco, 2002, which is consistent with CARB's current
 3966 on-line GHG inventory (http://www.arb.ca.gov/app/ghg/2000_2011/ghg_sector_data.php)] of 2.7
 3967 x 10¹⁰ g CH₄/yr is approximately three times lower than the range of probable CH₄ emissions
 3968 (7.8–9.3 x 10¹⁰ g CH₄/yr) from rice cultivation derived in this study. They attribute this
 3969 difference to decreased burning of the residual rice crop since 1991, which leads to an increase in
 3970 CH₄ emissions from rice paddies in succeeding years, but which is not accounted for in the
 3971 CARB inventory.

3972 ***Finding V2: Marine vessel emissions changes due to fuel sulfur reductions and speed***
 3973 ***controls result in a net warming effect (a "lose" for climate), but have substantial positive***
 3974 ***impacts on local sulfur and primary PM emissions (a "win" for air quality).***

3975 *Lack et al.* [2011] demonstrate the efficacy of California's shipping fuel quality regulation and
 3976 vessel speed reduction (VSR) program in reducing emission factors and absolute emissions of
 3977 SO₂, sulfate, and (somewhat unexpectedly) particulate organic matter (POM) and black carbon
 3978 (BC). (See Response to Question E for more complete discussion.) The emission factors of N_{Tot}
 3979 (total particle number) appear to increase due to the regulations, although these are small
 3980 particles that will likely quickly condense or coagulate with existing particles. On an absolute
 3981 scale (per kilometer of travel), mass reductions of SO₂, sulfate, and PM are in excess of 96%; BC
 3982 and POM reductions are 75% and 88% respectively, and CO₂ reductions are 58%. The
 3983 regulations significantly alter the direct climate cooling impacts of the emitted PM by reducing
 3984 the sulfate that forms just after emission and through secondary formation from SO₂ oxidation.
 3985 In areas where low sulfur fuel is used, significant reductions in the number of cloud condensation
 3986 nuclei (CCN) as well as reductions in particle size will decrease the indirect cooling impacts
 3987 associated with enhanced cloud formation, particularly in regions sensitive to inputs of CCN
 3988 from shipping, such as at ~30° N. This reduced cooling is partially offset by a concurrent
 3989 decrease in the climate warming impact of BC and CO₂ emissions. Their observations suggest
 3990 that air quality benefits from the fuel quality regulation and the VSR program are likely to be
 3991 substantial, although these air-quality benefits are likely to occur concurrently with a reduction in
 3992 the anthropogenic cooling effect that results from shipping PM. If it is determined that air

3993 pollution (i.e., human health and welfare) goals can be met through near-coast regulation, then
3994 the implementation of a more nuanced location-dependent global fuel quality regulation may be
3995 worthy of consideration. Possible reductions in BC emissions due to fuel quality changes might
3996 suggest a consideration of more refined fuels for future Arctic shipping.

3997 **References**

- 3998 Ackerman, A.S., O.B. Toon, D.E. Stevens, A.J. Heymsfield, V. Ramanathan, and E.J. Welton
3999 (2000), Reduction of tropical cloudiness by soot, *Science*, 288, 1042-1047.
- 4000 Bond, T. C., et al. (2013), Bounding the role of black carbon in the climate system: A scientific
4001 assessment, *J. Geophys. Res. Atmos.*, 118, 5380–5552, doi: 10.1002/jgrd.50171.
- 4002 Franco, G. (2002), Inventory of California greenhouse gas emissions and sinks: 1990–1999,
4003 Report 600–02–001F, Calif. Energy Comm., Sacramento.
- 4004 Jansen, K. L., T. V. Larson, J. Q. Koenig, T. F. Mar, C. Fields, J. Stewart and M. Lippmann
4005 (2005), Associations between Health Effects and Particulate Matter and Black Carbon in
4006 Subjects with Respiratory Disease, *Environ. Health Perspect.*, 113(12), 1741–1746, doi:
4007 10.1289/ehp.8153.
- 4008 Koren, I., Y.J. Kaufman, D. Rosenfeld, L.A. Remer, and Y. Rudich (2005), Aerosol invigoration
4009 and restructuring of Atlantic convective clouds, *Geophys. Res. Lett.*, 32, L14828,
4010 doi:10.1029/2005GL023187.
- 4011 Lack, D. A., et al. (2011), Impact of fuel quality regulation and speed reductions on shipping
4012 emissions: Implications for climate and air quality, *Environ. Sci. Technol.*, 45, 9052-9060,
4013 doi:10.1021/es2013424.
- 4014 McMillan, A. M. S., M. L. Goulden, and S. C. Tyler (2007), Stoichiometry of CH₄ and CO₂ flux
4015 in a California rice paddy, *J. Geophys. Res.*, 112, G01008, doi:10.1029/2006JG000198.
- 4016 Peischl, J., et al. (2012), Airborne observations of methane emissions from rice cultivation in the
4017 Sacramento Valley of California, *J. Geophys. Res.*, 117(D00V25),
4018 doi:10.1029/2012JD017994.
- 4019

4020 **Synthesis of Results - Climate and Air Quality Nexus**4021 **Response to Question W**4022 **QUESTION W**

4023 **Could the same pollutant control efforts in different air basins (i.e., SJVAB and SoCAB)**
4024 **have different results with respect to changes in air quality and climate (i.e., move toward**
4025 **different nexus quadrants in the figure on the front page of this report)?**

4026 **BACKGROUND**

4027 There are some circumstances where the same control efforts have markedly different effects on
4028 air quality. A well known example is the work of *Chameides et al.* [1988] who showed that
4029 control of anthropogenic VOC emissions is effective in reducing ambient O₃ concentrations in
4030 many urban areas, but much less effective in some urban areas (such as Atlanta, Georgia) that
4031 have large emissions of biogenic hydrocarbons. Such hydrocarbons are generally highly reactive
4032 and thus effective O₃ precursors. Consequently, their concentrations do not accumulate greatly
4033 in the ambient atmosphere despite their major role in photochemical O₃ production. In regions
4034 with large emissions of biogenic hydrocarbons, reduction of NO_x emissions may be a more
4035 effective control strategy than reduction of anthropogenic VOC emissions.

4036 In California, the air basins with the most difficult air quality issues (i.e., SJVAB and SoCAB)
4037 are not thought to have large emissions of the biogenic hydrocarbons that are important in
4038 forested regions, although biogenic emissions in downslope flow from the Sierra Mountains
4039 contribute to nighttime formation of aerosols in the southern SJVAB [*Rollins et al.*, 2012]. In
4040 other air basins (e.g., the Mountain Counties), biogenic emissions may be important but such
4041 areas generally experience only modest ambient O₃ concentrations (due to limited NO_x
4042 emissions) unless O₃ is transported there from regions with large anthropogenic emissions.
4043 However, within either SJVAB or SoCAB, other unrecognized sources of reactive VOCs could
4044 possibly affect the efficacy of pollutant control efforts; such possible sources deserve
4045 investigation. The possible role of agricultural emissions in the SJVAB is a topic of increasing
4046 concern.

4048 **POLICY RELEVANCE**

4049 Many of California's air quality regulations, such as mobile source controls, are applicable
4050 throughout the entire State. However, other regulations address the individual needs of a specific
4051 region, as different air basins (e.g., SJVAB, and SoCAB) have important differences in the mix
4052 of air quality relevant emissions. It is important to understand this emission mix in developing
4053 appropriate control strategies

4054 **FINDINGS**

4055 ***Finding W1:* The southern SJVAB has an unidentified, temperature dependent VOC**
4056 **emission source that dominates O₃ production on the hottest days when the highest O₃**
4057 **concentrations occur. As a consequence, NO_x emission controls are expected to be more**
4058 **effective for reducing O₃ in the southern SJVAB than in the SoCAB.**

4059 As more thoroughly discussed in the Response to Question J, *Pusede and Cohen* [2012] and
4060 *Pusede et al.* [2013] show that the NO_x versus VOC sensitivity of the O₃ photochemistry in the
4061 SJVAB changes markedly with ambient temperature, becoming much more NO_x sensitive on the
4062 hottest days, which are also the days that lead to most O₃ exceedances in this air basin. CalNex
4063 measurements from the Bakersfield site (Fig. J2) have been analyzed to identify the cause of this
4064 change in photochemical regime as a particular VOC source that is rich in oxygenated VOCs. A
4065 similar analysis indicates that such a temperature dependent VOC source is not present in the
4066 SoCAB. As a consequence, NO_x emission controls are expected to be more effective in the
4067 SJVAB than in the SoCAB, and indeed may be required for further reduction of the highest O₃
4068 levels in the southern SJVAB.

4069 ***Finding W2a: In the SJVAB ammonia is in large excess compared to nitric acid;***
4070 ***consequently NH₄NO₃ PM concentrations in the SJVAB will be more responsive to NO_x***
4071 ***emissions reductions compared to ammonia emissions reductions.***

4072 ***Finding W2b: In the SoCAB the response of NH₄NO₃ PM concentrations to emission***
4073 ***reductions will depend upon meteorological conditions, other aerosol components, and the***
4074 ***regional distribution of NH₃ and NO_x emissions.***

4075 Ammonia (NH₃) is the dominant gas-phase base in the troposphere. Anthropogenic emissions of
4076 NO_x are oxidized in sunlight to form nitric acid (HNO₃), which can react in the atmosphere to
4077 form ammonium nitrate (NH₄NO₃) particulate matter (PM). In the SJVAB two major NH₃
4078 sources from agricultural activity, animal waste and crop fertilization, are particularly important.
4079 In general, in both the SoCAB and the SJVAB agricultural activity (i.e., dairy farms and other
4080 livestock operations) and urban centers (i.e., Fresno, Los Angeles) are sources of ammonium
4081 nitrate gas-phase precursors. As more thoroughly discussed in the Response to Question I and J,
4082 *Nowak et al.* [2012a,b] utilize airborne measurements of NH₃, HNO₃, and particle composition
4083 made aboard the NOAA WP-3D aircraft to quantify NH₃ emissions from agricultural and vehicle
4084 sources, describe the vertical structure and transport of NH₃ from these sources, examine their
4085 impact on ammonium nitrate formation, and contrast the SoCAB and the SJVAB.

4086 In the SJVAB during CalNex, ambient NH₃ concentrations were quite large, much larger on
4087 average than observed by the WP-3D aircraft in any other location; nevertheless NH₄NO₃
4088 concentrations were relatively small. The amount of NH₄NO₃ that can be formed is limited by
4089 the amount of HNO₃ that can be formed from the relatively small NO_x emissions in the SJVAB.
4090 Consequently, ambient NH₄NO₃ concentrations will be much more responsive to NO_x emissions
4091 reductions compared to NH₃ emissions reductions.

4092 The CalNex data were collected in late spring-early summer, but NH₄NO₃ concentrations are
4093 much larger in winter in the SJVAB. Since NO_x emissions are not expected to have a large
4094 seasonal variation, sensitivities to NO_x and NH₃ emissions reductions are expected to be similar
4095 throughout the year. Data collected during the Discover-AQ campaign in the Central Valley
4096 during January and February 2013 may provide a means to verify this expectation for winter.

4097 The situation in the SoCAB is quite different. The relatively large NO_x emissions from the
4098 vehicle fleet and the relative small NH₃ emissions from dairies and vehicles cause the formation
4099 of ammonium nitrate aerosol to depend on many variables. Meteorological conditions
4100 (temperature, humidity and sunlight) will affect the thermodynamics and kinetics of NH₄NO₃
4101 formation as well as the rate of conversion of NO_x to HNO₃. The regional distribution of NH₃
4102 and NO_x emissions will determine which of the reactants is in excess at any particular location.

4103 Additionally, the formation of NH_4NO_3 will also be affected by preexisting aerosol. Judging the
 4104 most effective control strategy for NH_4NO_3 PM in the SoCAB must consider all of these
 4105 variables.

4106 ***Finding W3a: In both the SoCAB and the SJVAB, anthropogenic VOCs are believed to be***
 4107 ***the primary precursors of secondary organic aerosol; thus in both basins organic aerosol***
 4108 ***concentrations will be sensitive to VOC emissions control.***

4109 ***Finding W3b: Biogenic VOCs oxidized in the presence of NO_x provides additional sources***
 4110 ***of secondary organic aerosol that are important for the SJVAB, but less so in the SoCAB.***
 4111 ***Thus, NO_x emissions reductions will be effective for controlling this source of organic***
 4112 ***aerosol in the SJVAB, but will have less impact in the SoCAB.***

4113 As more thoroughly discussed in the Response to Questions L, anthropogenic VOCs are the
 4114 primary precursors of secondary organic aerosol (SOA) in both the SoCAB and the SJVAB.
 4115 Consequently, control of the emissions of these species is the obvious approach to reducing the
 4116 SOA contribution to ambient PM concentrations in both air basins. Additionally, as discussed
 4117 with regard to *Finding L2*, there are nighttime and daytime mechanisms involving NO_x that lead
 4118 to additional SOA formation from the oxidation of biogenic VOCs. These mechanisms are more
 4119 important in the SJVAB than the SoCAB. The nighttime mechanism directly involves NO_x , as
 4120 the NO_3 radical is the biogenic VOC oxidant [Rollins et al., 2012]. NO_x is also believed to play
 4121 a role in the daytime mechanism, where urban plumes are transported into the biogenic VOC rich
 4122 environment of the Sierra foothills. Thus, this component of SOA formation from biogenic
 4123 VOCs is expected to be sensitive to NO_x emission controls.

4124 **References**

- 4125 Chameides, W.L., R.W. Lindsay, J. Richardson and C.S. Kiang (1988), The role of biogenic
 4126 hydrocarbons in urban photochemical smog: Atlanta as a case study, *Science*, 241, 1473-
 4127 1475.
- 4128 Nowak, J. B., J. A. Neuman, R. Bahreini, A. M. Middlebrook, J. S. Holloway, S. A. McKeen, D.
 4129 D. Parrish, T. B. Ryerson, and M. Trainer (2012a), Ammonia sources in the California South
 4130 Coast Air Basin and their impact on ammonium nitrate formation, *Geophys. Res. Lett.*, 39,
 4131 L07804, doi:10.1029/2012GL051197.
- 4132 Nowak, J. B. (2012b), Ammonia Emissions from Agricultural Sources and their Implications for
 4133 Ammonium Nitrate Formation in California, presentation at ACS National Meeting, August
 4134 2012, Philadelphia, PA.
- 4135 Pusede, S. E. and R. C. Cohen (2012), On the observed response of ozone to NO_x and VOC
 4136 reactivity reductions in San Joaquin Valley California 1995–present, *Atmos. Chem. Phys.*, 12,
 4137 8323–8339.
- 4138 Pusede, S. E., et al. (2013), On the temperature dependence of organic reactivity, ozone
 4139 production, and the impact of emissions controls in San Joaquin Valley California, *Atmos.*
 4140 *Chem. Phys. Disc.*, submitted.
- 4141 Rollins, A. W., et al. (2012), Evidence for NO_x control over nighttime SOA formation, *Science*,
 4142 337(6099), 1210-1212, doi:10.1126/science.1221520.
- 4143

4144 **Acknowledgments**

4145 The California Air Resources Board (CARB) and the National Oceanic and Atmospheric
 4146 Administration (NOAA) gratefully acknowledge significant contributions to the success of the
 4147 CalNex field research campaign by the many different organizations listed below. These
 4148 contributions include significant financial and in-kind organizational support as well as the time
 4149 and creative energy of individual scientists, engineers, post-doctoral fellows, and graduate
 4150 students who joined in this collaborative enterprise.

4151 These contributions include:

- 4152 • Defining the objectives of CalNex,
- 4153 • Instrumenting the various atmospheric measurement platforms and sites,
- 4154 • Implementing and quality assuring the myriad field measurements during the course of
 4155 the study,
- 4156 • Completing the analysis, interpretation, and intercomparison of research results, and
- 4157 • Publishing and reporting the research findings, so that they can be used for policy
 4158 purposes by CARB and other stakeholders.

4159 **Cooperating State Government Organizations**

4160 California Air Resources Board
 4161 Research Division
 4162 Atmospheric Processes Research Section
 4163 Planning and Technical Support Division
 4164 California Energy Commission

4165 **Cooperating California Local Government Organizations**

4166 Sacramento Metropolitan Air Quality Management District
 4167 San Joaquin Valley Air Pollution Control District
 4168 San Luis Obispo County Air Pollution Control District
 4169 South Coast Air Quality Management District

4170 **Cooperating Federal Government Agencies**

4171 Centre National de la Recherche Scientifique (Toulouse, France), Laboratoire d'Aérodologie
 4172 Department of Energy (DOE)
 4173 Brookhaven National Laboratory (BNL)
 4174 Pacific Northwest National Laboratory (PNNL)
 4175 Environment Canada (EC)
 4176 Air Quality Research Division, Science and Technology Branch
 4177 Meteorological Service of Canada
 4178 Lawrence Berkeley National Laboratory
 4179 Chemical Sciences Division
 4180 Environment and Energy Technologies Division
 4181 Meteorological Research Institute (Ibaraki, Japan)
 4182 National Aeronautics and Space Administration (NASA)
 4183 Goddard Institute for Space Studies
 4184 Headquarters Science Mission Directorate, Tropospheric Chemistry Program
 4185 Langley Research Center (LRC)
 4186 National Oceanic and Atmospheric Administration (NOAA)
 4187 Air Resources Laboratory (ARL)

- 4188 ESRL Chemical Sciences Division
 4189 ESRL Global Monitoring Division
 4190 ESRL Physical Sciences Division
 4191 Geophysical Fluid Dynamics Laboratory
 4192 Health of the Atmosphere Program
 4193 National Centers for Environmental Prediction
 4194 Pacific Marine Environmental Laboratory (PMEL)
 4195 National Weather Service (NWS)
 4196 National Environmental Satellite Data and Information Service (NESDIS)
 4197 Office of Marine and Aviation Operations (OMAO)
 4198 National Park Service, Air Resources Division
 4199 National Science Foundation (NSF)
 4200 National Center for Atmospheric Research (NCAR)
 4201 Atmospheric Chemistry Division
 4202 Earth Observing Laboratory
 4203 Research Aviation Facility
 4204 University Corporation of Atmospheric Research
 4205 Research Centre Jülich GmbH (Jülich, Germany), Institute for Chemistry of the Polluted
 4206 Atmosphere
 4207 United States Environmental Protection Agency (USEPA), National Exposure Research
 4208 Laboratory
 4209 United States Navy (USN), Point Mugu Naval Air Warfare Center
- 4210 **Cooperating Research Universities**
 4211 Arizona State University
 4212 Department of Chemistry and Biochemistry
 4213 School of Earth and Space Exploration
 4214 Auburn University, School of Forestry and Wildlife Science
 4215 Baylor University, Department of Environmental Science
 4216 Boston College, Department of Chemistry
 4217 California Institute of Technology
 4218 Division of Chemistry and Chemical Engineering
 4219 Division of Engineering and Applied Science
 4220 Division of Geological and Planetary Sciences
 4221 Jet Propulsion Laboratory (JPL)
 4222 Keck Institute for Space Studies
 4223 California State Polytechnic University, Pomona, Department of Mechanical Engineering
 4224 Colorado State University, Cooperative Institute for Research in Atmospheres (CIRA)
 4225 Columbia University
 4226 Department of Earth and Environmental Sciences
 4227 Lamont-Doherty Earth Observatory
 4228 Georgia Institute of Technology
 4229 School of Earth and Atmospheric Sciences
 4230 School of Chemical and Biomolecular Engineering
 4231 Harvard University
 4232 Atmospheric and Environmental Chemistry
 4233 School of Engineering and Applied Sciences
 4234 Department of Earth and Planetary Sciences

4235 Indiana University
4236 Center for Research in Environmental Science
4237 Department of Chemistry
4238 School of Public and Environmental Affairs
4239 Massachusetts Institute of Technology
4240 Department of Civil and Environmental Engineering
4241 Department of Earth, Atmospheric and Planetary Sciences
4242 Molina Center for Energy and the Environment
4243 Naval Postgraduate School, Center for Interdisciplinary Remotely-Piloted Aircraft Studies
4244 (CIRPAS)
4245 North Carolina Agricultural and Technical State University, Interdisciplinary Scientific
4246 Environmental Technology Center (ISET)
4247 Paul Scherrer Institut (Villigen, Switzerland), Laboratory of Atmospheric Chemistry
4248 Peking University (Beijing, China)
4249 Pennsylvania State University
4250 Princeton University, Atmospheric and Oceanic Sciences
4251 Scripps Institution of Oceanography
4252 Seoul National University (Seoul, Republic of Korea), School of Earth and Environmental
4253 Sciences
4254 Texas Tech University, Department of Chemistry & Biochemistry
4255 Université Lille Nord de France (Lille, France)
4256 Université Paris Est Créteil (Créteil, France), Laboratoire Interuniversitaire des Systèmes
4257 Atmosphériques
4258 Université de Versailles Saint Quentin en Yvelines, (Gif-sur-Yvette, France), Laboratoire des
4259 Sciences du Climat et de l'Environnement,
4260 University of Alberta (Edmonton, Canada), Department of Mechanical Engineering
4261 University of Arizona, Chemical and Environmental Engineering
4262 University of Bern (Bern, Switzerland)
4263 Department of Chemistry and Biochemistry
4264 Oeschger Centre for Climate Change Research,
4265 University of Calgary (Calgary, Canada), Department of Chemistry
4266 University of California, Berkeley
4267 Department of Chemistry
4268 Department of Civil and Environmental Engineering
4269 Department of Earth and Planetary Sciences
4270 Department of Environmental Science, Policy, and Management
4271 Transportation Sustainability Research Center
4272 University of California, Davis
4273 Air Quality Research Center
4274 Department of Civil and Environmental Engineering
4275 University of California, Irvine
4276 Department of Chemistry
4277 Department of Mechanical and Aerospace Engineering
4278 University of California, Los Angeles, Department of Atmospheric and Oceanic Sciences
4279 University of California, San Diego, Department Chemistry and Biochemistry
4280 University of California, Santa Cruz, Department of Microbiology and Environmental
4281 Toxicology
4282 University of Colorado

4283 Cooperative Institute for Research in Environmental Science (CIRES)
 4284 Department of Atmospheric and Oceanic Sciences
 4285 Department of Chemistry and Biochemistry
 4286 Laboratory for Atmospheric and Space Physics
 4287 University of Colombia (Bogota, Colombia), Chemical Engineering and Environmental
 4288 Studies
 4289 University of Delaware, Department of Chemistry and Biochemistry
 4290 University of Helsinki (Helsinki, Finland), Department of Physics
 4291 University of Houston, Department of Earth and Atmospheric Sciences
 4292 University of Iowa, Center for Global and Regional Environmental Research
 4293 University of Manchester (Manchester, UK)
 4294 National Centre for Atmospheric Science
 4295 School of Earth, Atmospheric and Environmental Sciences
 4296 University of Maryland, Joint Center for Earth Systems Technology
 4297 University of Miami, Rosenstiel School of Marine and Atmospheric Science
 4298 University of North Carolina at Chapel Hill, Department of Environmental Sciences and
 4299 Engineering
 4300 University of Toronto (Toronto, Canada), Department of Chemistry
 4301 University of Virginia, Climate Change Research Center
 4302 University of Washington, Seattle
 4303 Department of Atmospheric Sciences
 4304 Department of Chemistry
 4305 University of Wisconsin Madison
 4306 Department of Chemistry
 4307 Environmental Chemistry and Technology
 4308 Virginia Tech, Department of Civil and Environmental Engineering
 4309 Washington State University, Department of Civil and Environmental Engineering
 4310 York University (Toronto, Canada), Centre for Atmospheric Chemistry

4311 **Cooperating Private Sector Organizations**

4312 Aerodyne Research Inc.
 4313 Aerosol Dynamics Inc.
 4314 Alion Science and Technology
 4315 Atmospheric and Environmental Research, Inc.
 4316 Baron Advanced Meteorological Services
 4317 Bay Area Environmental Research Institute
 4318 Maersk Line
 4319 RTI International

4320 **Other Cooperating Organizations**

4321 Wisconsin State Laboratory of Hygiene, Environmental Health Division
 4322
 4323
 4324
 4325

4326 **Appendix A - See separate document**

DRAFT - Do Not Cite